APPLICATIONS OF FERROCENE-PEPTIDE CONJUGATES: TOWARDS NEW BIOSENSORS AND MATERIALS

A Thesis Submitted to the College of
Graduate Studies and Research
in Partial Fulfillment of the Requirements
for the Degree of Doctorate of Philosophy
in the Department of Chemistry
University of Saskatchewan
Saskatoon

By

Khaled Ahmed Mahmoud

PERMISSION TO USE

Presenting this thesis in partial fulfillment of the requirements for a degree of Doctorate of Philosophy from the University of Saskatchewan, I agree that the libraries of this university may make it available for inspection. I further agree that permission for copying of this thesis in any manner, in whole or in part, for scholarly purposes may be granted by the professor or professors who supervised my thesis work or, in their absence, by the Head of the Department of Chemistry or the Dean of the College of Graduate Studies and Research. It is understood that any copying or publication or use of this thesis or parts thereof, for financial gain shall not be allowed without my written permission. It is also understood that due recognition shall be given to me and to the University of Saskatchewan in any scholarly use which may be made of any material in this thesis.

Requests for permission to copy or to make other use of material in this thesis in whole or part should be addressed to:

The Head
Department of Chemistry
University of Saskatchewan
Saskatoon, Saskatchewan,
S7K 5C9

ABSTRACT

Ferrocene-peptide conjugates represent a hybrid area between organometallic chemistry and biochemistry. In these bioconjugates, the ferrocene (Fc) moiety can serve as molecular scaffold, chromophore, sensitive probe, biological marker, redox active site, etc. Disubstituted Fc systems, in which both cyclopentadienyl rings are substituted, provide influence over the supramolecular structure of the assemblies, and serve as starting materials for the design of electronic biomaterials. Recently, 1'-amino-ferrocene-1-carboxylic acid (Fca) and 1,1'-diaminoferrocene $Fc[NH_2]_2$ were recognized as useful tools in bioorganometallic chemistry. This work sketches some novel preparative and structural aspects of Fc-peptide conjugates and explores their applications as biosensors and as polymeric materials.

First, I demonstrated that Fca invariably induces a turn-like structure, which is stable in solution and the solid state. The obtained results showed different behaviour for Fca peptides depending on the chirality and position of the attached amino acid. The axial chirality of the Fca is completely dependent on the chirality of the first amino acid attached to the amino terminal of the Fca group.

Second, I was able to develop a surface based sensor for the electrochemical detection of papain based on Fc-peptide conjugates. The idea was to place a surface-bound redox probe in close proximity to the electrode surface. In addition, the redox-active Fca label will be part of the recognition site but will not interfere with the recognition process. My sensor provides an attractive alternative for the electrochemical detection of non-labelled non-redox active proteins, which under current detection schemes remains a significant challenge.

This work represents a truly important proof of concept for establishing this novel bioorganometallic approach for the electrochemical detection of important biological targets.

Last, I was successful in developing a very convenient method to synthesize 1,1'-bis(*tert*-butoxycarbonylamino)ferrocene as a stable derivative of $Fc[NH_2]_2$. This new synthetic approach has circumvented the problems encountered with the explosive diazide usually used as a precursor in the conventional synthons of $Fc[NH_2]_2$. Building on this achievement, a series of novel peptide-like oligomeric and polymeric ferrocenyl-amides were synthesized and fully characterized. The electrochemical investigations on these polymers suggested unresolved or no electronic interaction between the ferrocene groups in all systems. These results may reveal the influence of the amide groups on suppressing the electronic interaction between the iron centers in my polymers.

Thus, my systematic work on Fc-peptide conjugates lays solid foundations in the fields of structural control, biosensors, and material science.

ACKNOWLEDGEMENTS

I would like to acknowledge everybody who showed interest in my work and supported me during this Ph.D. work. I would like to sincerely thank my supervisor, professor H.-B. Kraatz, for his patience, support, guidance and faith in me in the course of this study. His suggestions and constructive criticisms were extremely useful and necessary in the successful completion of this work.

I would like to thank with gratitude my Advisory Committee members: Dr. D. Ward, Dr. D. Sanders and Dr K. Mitchell for helping me in various ways during this project.

My appreciation also goes to Dr. Gabriele Schatte, Saskatchewan Structural Science Center, for Crystallographic data collections and solving the structures. The assistance given by Dr. K. Brown in performing NMR experiments and collecting mass spectral data by Mr. K. Thoms are really appreciated.

I sincerely thank the past and present members of our group for their help and suggestions in different stages during this work.

Financial support from NSERC, Department of Chemistry and University of Saskatchewan is gratefully acknowledged.

DEDICATION

This work is dedicated to my parents and my wife Kareman for their encouragement, supplications, and faith in me.

TABLE OF CONTENT Page No.

LIST OF FIGURES Page No.

LIST OF SCHEMES

LIST OF TABLES Page No.

LIST OF ABBREVIATIONS

A	absorption
Å	angstrom
Ala	alanine
Arg	arginine
Asn	aspartine
Asp	aspartic acid
Boc	*t*-butyloxycarbonyl
BOP	benzotriazol-1-yl-*N*-oxy-tris(dimethylamino)-phosphonium hexafluoro-phosphate
Bz	benzyl
CD	circular dichroism
COSY	correlation spectroscopy
Cp	cyclopentadiene
CSA	cystamine
CV	cyclic voltammetry
Cys	cystein
DCC	dicyclohexyl-carbodiimide
DCM	dichloromethane
DLS	Dynamic light scatternic
DMSO	dimethylsulfoxide
DPV	differential pulse voltammetry
DTT	±-threo-1,4-dimercapto-2,3-butanediol. L-1,4-dithiothreitol
E^0	standard potential
$E_{1/2}$	half-wave potential
EDC	1-Ethyl-3-(3-dimethylaminopropyl)-carbodiimide
EDTA	ethylenediamminetetraacetate
Et	ethyl
EtOAc	ethylacetate
FAB	fast atom bombardment
Fc	ferrocene
Fca	1-amino-1'-ferrocene carboxylic acid
FTIR	fourier transform infrared spectroscopy
Gln	glutamine
Glu	glutamic acid
Gly	glycine
HBTU	O-(benzotriazole-1-yl)-N,N,N',N'-tetramethylurionium hexafluorophosphate

His	histidine
HMBC	heteronuclear multiple bond correlation spectroscopy
HOBt	hydroxybenzotriazole
HOSu	1-hydroxysuccinimide
HPLC	high performance liquid chromatography
HRMS	high resolution mass spectrometry
Hz	hertz
Ile	Isoleucine
j	coupling constant
K	kelvin
K_i	inhibition constant
K_i'	apparent inhibition constant
K_m	Michaelis-Menten constant
Leu	leucine
LRMS	low resolution mass spectrometry
Lys	lysine
m	milli
Me	methyl
MeOH	methanol
Met	methionine
min.	minute
ml	millilitre
mM	millimolar
mmol	millimole
mol	mole
MS	mass spectrometry
MW	molecular weight
NMR	nuclear magnetic resonance
Phe	phenylalanine
ppb	parts per billion
ppm	parts per million
Pro	proline
r t	room temperature
Ser	serin
SPPS	solid phase peptide synthesis
SPR	surface plasmon resonance
Thc	thiostic acid

THF	tetrahydrofuran
TFA	trifluro acetic acid
Thr	threonine
TOCSY	total correlation spectroscopy
Trp	triptophan
Tyr	tyrosine
UV	ultra violet
Val	valine
ε	extinction coefficient
ΔEp	potential peak separation
ΔT	change of temperature
$\Delta\delta$	change of chemical shift
δ	chemical shift
λ	Wavelength

CHAPTER 1

GENERAL INTRODUCTION

The field of bioorganometallic chemistry, which is a hybrid area between biochemistry and organometallic chemistry has rapidly matured and has gained great interest over the past two decades and has allowed for the design of new organometallic bioconjugates which can be engaged in many important fields such as molecular recognition, biosensors, bioelectronics, and catalysis.[1-6] In addition, by choosing the appropriate organometallic group and peptide sequences it may be possible to control the supramolecular self-organization. Considerable efforts have focused on utilizing ferrocene (Fc) building blocks in supramolecular chemistry. These systems have been exploited as molecular scaffolds to control the organization of peptides secondary structures in order to have a better understanding of the factors affecting protein structure and stability, and to facilitate the rational design of useful drugs.[7-13]

Peptide-derived bioconjugates occupy a special position in that they offer the potential for biomolecular recognition and enable probing of biological processes.[14, 15] These systems are also of a more fundamental interest for the construction of well-defined scaffolds. The assembly of amino acids and peptides into extended supramolecular three-dimensional structures is controlled by the hydrogen bonding between individual molecules.[16, 17] The desire to control the properties of such assemblies has led to a considerable body of work focused on the design of secondary

structural elements,[18, 19] and on the design of new peptidic materials, ranging from peptide nanotubes[20-24] to peptide hydrogels.[25-27] Bioorganometallic peptide conjugates have allowed additional control over the structural properties by choosing the appropriate organometallic group. Fc is particularly useful in this regard.[28-32] Disubstituted Fc systems in which both cyclopentadienyl rings are substituted have allowed influence over the supramolecular structure of the assemblies by controlling the Cp-twist, as well as providing a starting point for the design of electronic biomaterials.[33] Recently, the artificial amino acid 1'-amino-ferrocene-1-carboxylic acid (Fca) was recognized as a useful tool in bioorganometallic chemistry. A series of peptides incorporating Fca have been synthesized by using solution phase methods.[34-36] Initial investigations show that Fca imposes specific secondary-structural elements onto the peptide.[34-36] Fca derivatives have also been employed as transition state analogues for formation of catalytic antibodies.[37] Electrochemical sensing of bimolecular interactions is one of the important applications of Fc chemistry. Our group has been interested in studying the interaction of Fc-peptide conjugates with papain. This interaction was readily monitored electrochemically.[38]

The following sections will provide an overview over the recent advances into the preparative and structural aspects of Fc-peptide conjugates. In particular, the focus is on the use of disubstituted Fc systems as templates in an effort to control the secondary structure, and the recent efforts of incorporating disubstituted Fc into oligo- and polyamides.

1.1. Preparation of Ferrocene Peptides Conjugates

Amide coupling methods provided the most extensively explored way to couple the Fc moiety to amino acids and peptides. The preparation of Fc-peptide conjugates was achieved by coupling of a Fc-carboxylic acid and the terminal amino group of the amino acid. The pre-activation of the carboxylic group is important in order to achieve efficient synthesis under mild conditions. Different activation strategies include the "acid chloride" , "active ester", and the oxazolone methods were developed.[39] The "acid chloride" method provides a fast and convenient rout for labeling peptides, which makes use of the reaction between Fc-acid chloride, prepared from Fc-carboxylic acid, and amino acids or peptides having an available amino terminus. Different organic bases can be used for capturing the formed HCl. The "active ester" method is based on the formation of an often-isolable Fc-CO-active ester. A variety of activating ester groups were used such as N-hydroxybenzotriazole (HOBt), 2-(1H-7-azabenzotriazol-1-yl)-1,1,3,3-tetramethyl uronium hexafluorophosphate (HATU), and 1-hydroxysuccinimide (HOSu).

These active esters can be used ether as stoichiometric Fc delivery reagent, as an intermediate in one pot reaction or used during solid phase peptide synthesis (SPPS). The Fc-CO-esters then react with the desired amino acid or peptide to give rise to Fc-conjugate **5** (see Scheme 1.1). This effective method has led to the preparation of a number of mono- and disubstituted Fc-peptide derivatives. Up to now, a large number of mono- and disubstituted Fc-peptide conjugates of defined structure have been reported. Some excellent comprehensive reviews on Fc-peptide conjugates were

published recently and can be used as a valuable source of references.[40, 41] The following section focuses on the bioorganometallic conjugates containing disubstituted Fc.

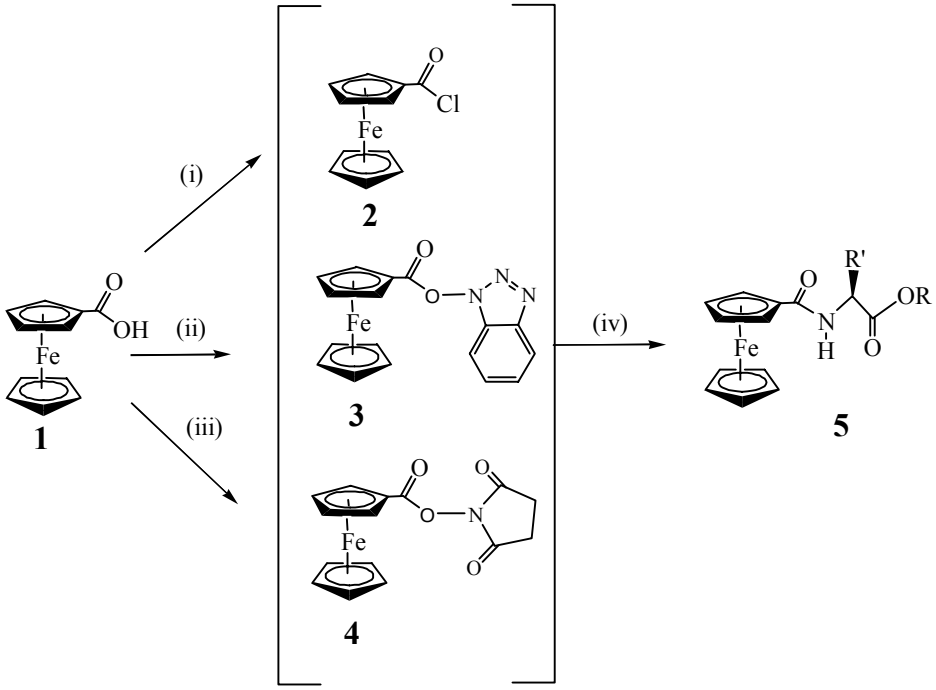

Scheme 1.1. Synthesis of ferrocenoyl amino acid esters (**5**) via the acid chloride and active ester methods: (i) $(COCl)_2$ or $SOCl_2$; (ii) carbodiimide such as DCC or EDC, HOBt; (iii) carbodiimide such as DCC or EDC, HOSu and (iv) peptide or amino acid and base.

1.1.1. 1,1'-Ferrocenedicarboxylic Acid Conjugates

A large number of bisamino acid and bispeptide substituted Fc-conjugates were synthesized by employing 1,1'-ferrocenedicarboxylic acid, $Fc[COOH]_2$ **6** as starting material.

Fc-active esters, initially employed by Degani and Heller for coupling the Fc-group to the ε-amino group of lysines in proteins,[42, 43] were successfully employed in the synthesis of symmetrical Fc-peptide-cystamines having two Fc groups linked to the two terminal amino groups. A series of 1,1'-oligoprolinoyl-Fc(s) **7-10** were obtained from $Fc[COOH]_2$ **6**, HOBt, EDC, and a series of oligoproline esters (Scheme 1.2).[44, 45]

The proline derivative **7** was first obtained by Herrick via the acid chloride route.[46] Importantly, this route also offers a way to introduce site differentiation between the two cyclopentadienyl (Cp) rings and in essence allows the formation of Fc-peptide conjugates, in which two different peptides can be attached to the two Cp rings. Using only one equivalent of peptide ester, ring-differentiated 1-oligoprolinoyl-1'-OBt-Fc derivatives **11-13** were obtained. This class of compounds is a convenient starting material for the synthesis of asymmetrically substituted ferrocenoyl derivatives, which may potentially have applications in proteomics and protein sensing. Erker and co-workers reported an unusual procedure for the synthesis of Fc[Val-OMe]$_2$ **15** from two equivalents of the Li-salt of a Cp-Val-OMe-conjugate with anhydrous $FeCl_2$ in THF (Scheme 1.3).[47]

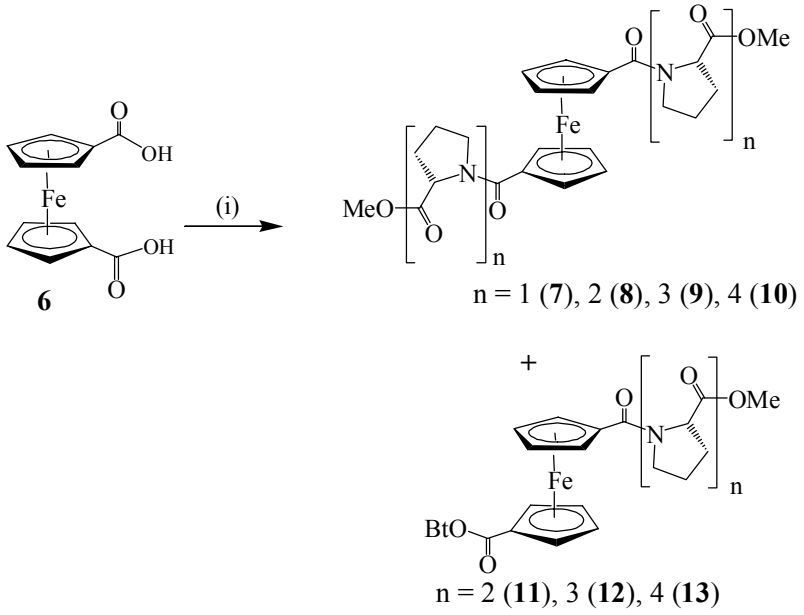

Scheme 1.2. Synthesis of 1,1'-bispeptide Fc derivatives peptides **7** – **13** via the HOBt/EDC protocol: (i) HOBt, EDC, CH_2Cl_2, H-Pro$_n$-OMe (n = 1-4).

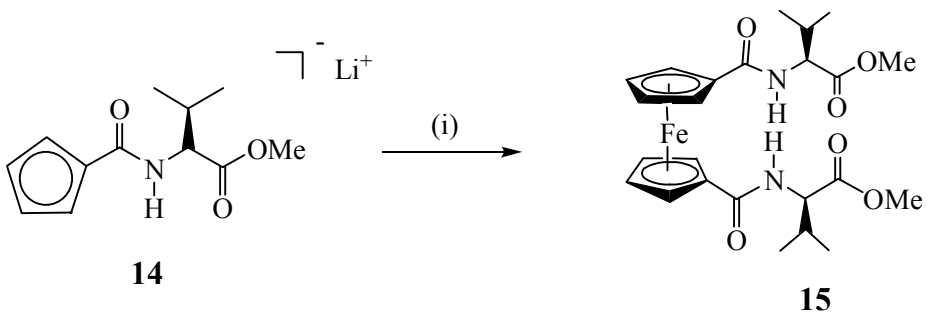

Scheme 1.3. Unusual synthesis of Fc[Val-OMe]$_2$ **15** from the Li salt of CP-Val-OMe **14** formed by the addition of isocyanate: (i) $FeCl_2$, THF, 60°C, 7d; (ii) $FeCl_2$/CpLi, 50 °C, THF, 7d.

Using the same procedure, the Fc-peptide macrocycles **25-29** were obtained in low to moderate yields by the reaction of Fc[COOH]$_2$ **6** with the appropriate amino acid-cystamine conjugates in the presence of carbodiimide and HOBt under high dilution conditions (Scheme 1.4). At concentrations above 2 mM in Fc[COOH]$_2$ **6** the yields were decreased significantly, as expected for the synthesis of macrocycles. Cheng reported on the synthesis of the related Fc-peptide-cystine-macrocycles using the acid chloride method starting from Fc-dicarboxylic acid chloride Fc(COCl)$_2$ **30**. In addition to the desired systems, a series of dimeric Fc-macrocycles was obtained (see Scheme 1.14).[48] Interestingly, the cystine macrocycles were able to coordinate alkali ions very effectively. Another series of such Fc-peptide conjugates were prepared by incorporating Gly, Ala, Val, and Leu. The cystamine disulfide was used as anchor group for the preparation of Fc-peptide films on gold substrates and their subsequent investigations of the electron transfer properties from the Fc group through the peptide spacer to the gold surface.[49]

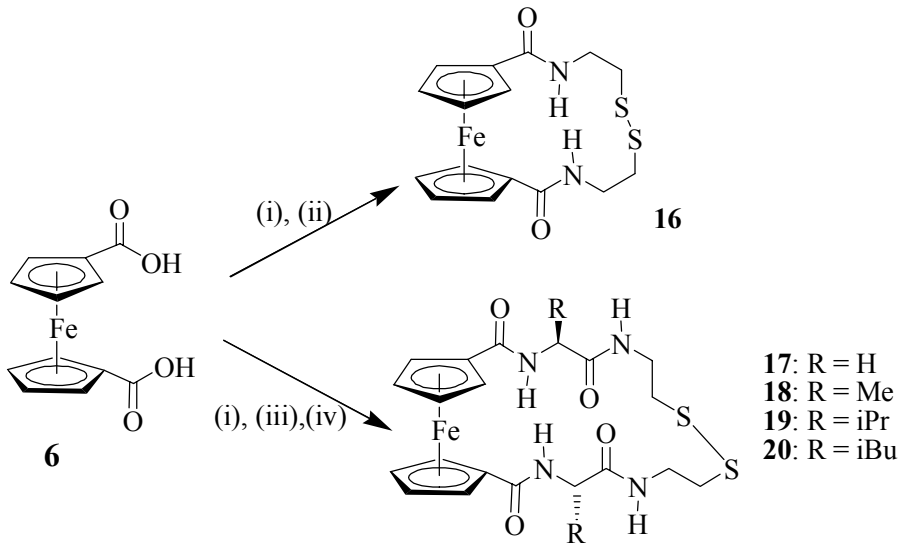

Scheme 1.4. Synthesis of redox active cyclopeptides : (i) EDC, HOBt, CH_2Cl_2; (ii) $(CSA)_2$• 2HCl, CH_2Cl_2; (iii) a) Boc-amino acid CSA dimer, TFA; b) Et_3N, CH_2Cl_2; (iv) dilution

Importantly, a fascinating macromolecular assembly can be produced by expansion of the ring by additional amino acids, in which the peptide macrocycles associate into "pseudo-β-barrels".[13] Fc[Gly-Val-CSA]$_2$ **21** has Gly as the first amino acid to be attached to the Fc group, giving maximum flexibility to the podant peptide chains, followed by Val, an amino acid with very high propensity to form β-sheets.[50]

1.1.2. 1'-Aminoferrocene-1-Carboxylic Acid Conjugates

While extensive studies have been focusing on Fc[COOH]$_2$ derivatives, fewer reports have utilized 1'-aminoferrocene-1-carboxylic acid (Fca) as starting material for making Fca-peptide conjugates. Modifying Fc with an amino group was always difficult and the product was often considered as unstable and sensitive to air and water. Nevertheless, different synthetic routes were described in an attempt to obtain Fca. In several of these synthetic procedures 1-bromo-1'-dilitioferrocene has been used as a key

precursor.[51-53] The resulting compound can be considered as promising monomer for the formation of the peptide-like Fc backbone polymers. However, the material is readily oxidizable and easily contaminated with butylated byproducts.[53]

Recently, Rapić and coworkers reported an alternative synthetic approach to full-protected derivative of Fca **23** as shown in Scheme 1.5. The compound showed good stability and can be readily coupled to amino acids and peptides in mild conditions. The removal of the protecting groups can be achieved easily to give the desired precursor. For example, deprotection of ester group can be performed by base hydrolysis in aqueous medium, and the Boc group can be removed by treatment with acid.[54] During the synthesis, the symmetrical Fc-substituted urea, dimethyl 1',1'-ureylenedi(1-ferrocenecarboxylate) **24** was formed as a by-product (Scheme 1.5).[55] The Fc groups linked through a urea group, which upon deprotection maybe used in condensation reactions.

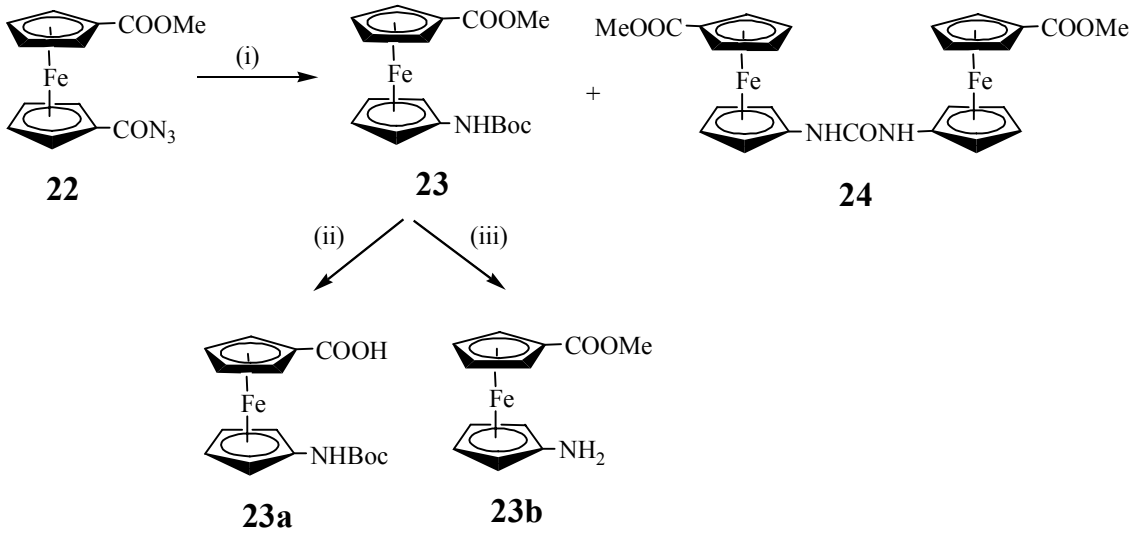

Scheme 1.5. Synthesis of Boc-protected 1'-aminoferrocene-1-carboxylic acid. (i) *t*-BuOH, reflux for 4 hours (ii) $NaOH/H_2O$, MeOH (iii) TFA/CH_2Cl_2.

Another convenient synthetic route starting from Fc to give the hydrochloride salt of Fca **27** was described by Heinze and coworkers.[56] Scheme 1.6 summarizes the reaction sequence. The key material in this synthesis was 1-aminoferrocene **24**, prepared from *N*-ferrocenylphthalimide. However, this route requires the synthesis of 1-haloferrocene or Fc boronic acid as precursors of *N*-ferrocenylphthalimide. In addition, the reaction is accompanied by the formation of biferrocenes due to a copper-mediated C-C coupling reaction, even in the presence of excess phthalimide.[57-59]

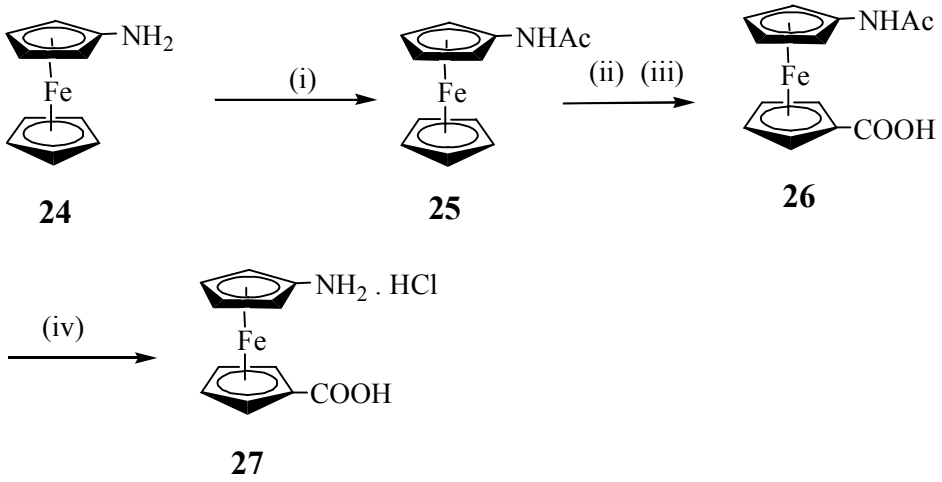

Scheme 1.6. Synthesis of Fc amino acid hydrochloride **27** according to Heinze: (i) *N*-acetylation with Ac_2O, (ii) selective Friedel-Crafts acylation with 2,6-dichlorobenzoyl chloride at the unsubstituted Cp ring; (iii) base hydrolysis; (iv) removal of the acetyl protection group with hydrochloric acid.

The first attempt for the preparation of Fca-peptide conjugate Boc-Ala-Fca-Ala-Ala-OMe **29** was reported by Rapić and Metzler-Nolte and is shown in Scheme 1.7.[35] They employed EDC/HOBt coupling protocol, starting from Fca derivative **23a** and coupled H-Ala-Ala-OMe to the C-terminal followed by coupling Boc-Ala-OH to the N-terminal.

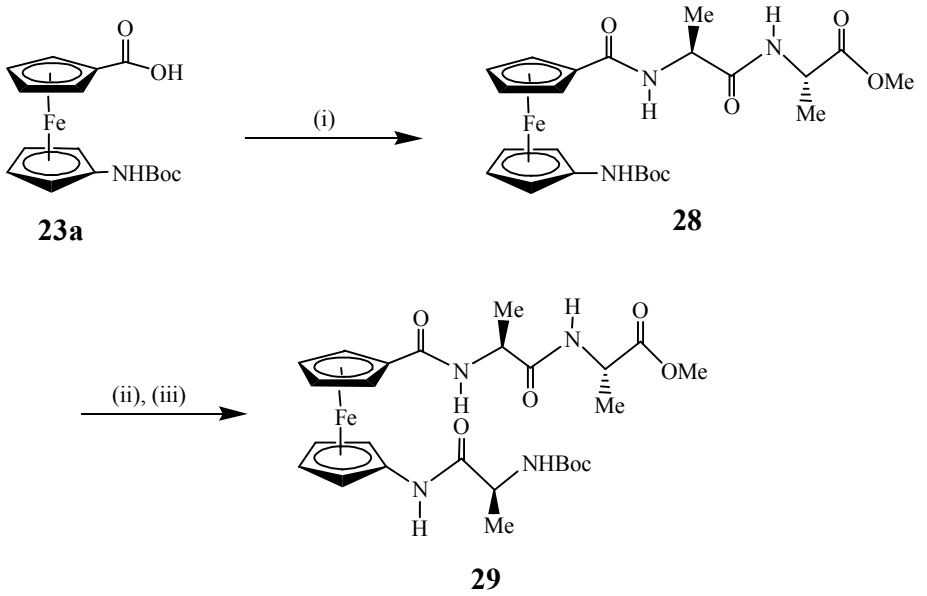

23a **28** **29**

Scheme 1.7. Synthesis of the tetrapeptide Boc-Ala-Fca-Ala-Ala-OMe **29** derived from 1'-Boc-aminoferrocene-1-carboxylic (Fca) **23a**: (i) + H-Ala-Ala-OMe, EDC/HOBt; (ii) HCl(g)/ AcOEt; + Boc-Ala-OH, EDC/HOBt.

Kraatz reported on the reactivity of Fca derivative **23b** with different alkylating agents such as $EtSCH_2CH_2Cl$ and $(CN)(EtO)_2P(O)$ which serve as chemical warfare agents mimic.[60] The successful preparation of compounds **30**-**33** has led to the novel idea of exploiting Fca as a redox active precursor towards developing an electrochemical sensor for the detection of chemical warfare agents. Summary of alkylation reactions of the amino group of **23b** is described in Scheme 1.8. This study was extended by preparing the cystamine conjugate of Fca which was then anchored to the gold surface in order to carry out surface reactions with simulants for chemical warfare agents.[61]

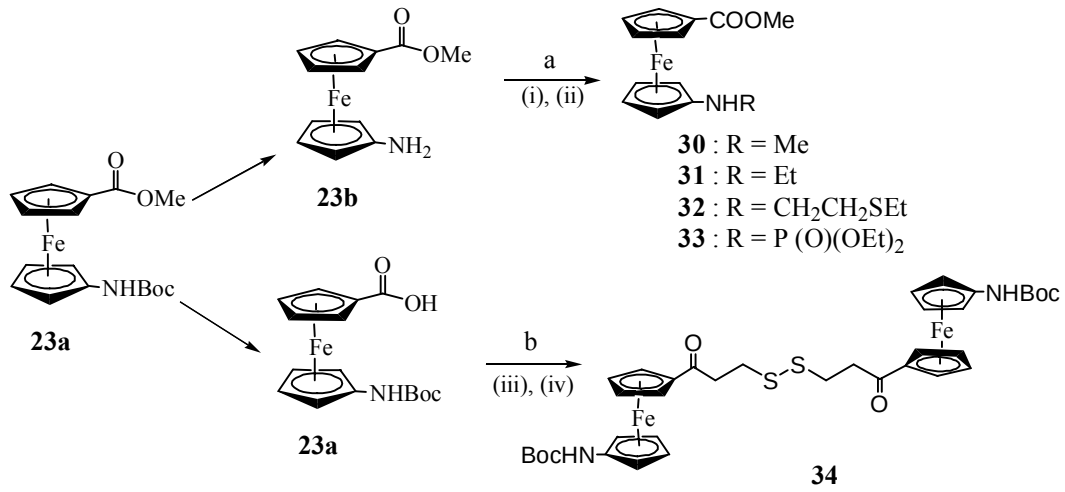

Scheme 1.8. (a) Reaction of **38b** with the alkylating reagents to form compounds **30-33** (b) synthesis of compound **34** from **23a** according to Khan et al. [60, 61] (i) EtOH (ii) Saturated $NaHCO_3$ (iii) HOBt, EDC (iv) Cystamine, Et_3N.

1.1. 3. 1,1'-Diaminoferrocene Conjugates

Over the past decade or so, little efforts have been made to synthesize Fc-amine compounds.[62-64] None of these methods appeared attractive because of poor overall yield and inconvenient reaction conditions. Since 1961, the first attempt to prepare 1,1'-diaminoferrocene **38** made by Knox et al,[65] very few studies have attempted to develop an improved synthetic route because of the explosive nature of the diazoferocene intermediate, also the products were unstable and very sensitive to air.[66] Therefore, peptide derivatives of 1,1'-diaminoferrocene were completely absent from the literature until recent date. An improved high-yield synthesis of diaminoferrocene was described by Arnold and coworkers.[66] They started from diazioferrocene using a modified Nesmeyanov procedure (Scheme 1.9). Catalytic reduction of the diazide with H_2-Pd/C in MeOH resulted in the formation of diaminoferrocene. Removal of the Pd/C catalyst and crystallization at -30 °C afforded diaminoferrocene in a good yield. However, an

extreme care should be exercised when handling solid diazidoferrocene, as it tends to explode if heated rapidly above 56 °C .[66]

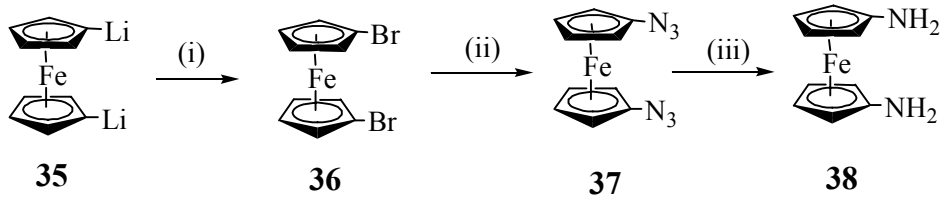

35 **36** **37** **38**

Scheme 1.9. Arnold's synthesis of 1,1'-diaminoferrocene involving the explosive diazidoferrocene: (i) $C_2H_2Br_4$, Et_2O, (ii) NaN_3, CuI, $EtOH/H_2O$, (iii) H_2, Pd/C, MeOH

Most recently, we have described a convenient synthon for 1,1'-.bis(*tert*-butoxycarbonylamino)ferrocene **40** as a stable Boc-protected form of 1,1'-diaminoferrocene **38**. This new synthetic approach has circumvented the problems encountered with the explosive diazide as described in Scheme 1.10. First, 1,1'-Bis(carbonylazido)ferrocene **39** was synthesized from $Fc[COOH]_2$ **6** by treatment with ethyl chloroformate, followed by reaction with sodium azide. The resulting carbonylazido 1,1'-Bis(carbonylazido)ferrocene **39** is then reacted with *tert*-butanol to give 1,1'-bis(*tert*-butoxycarbonylamino)ferrocene **40**.[67]

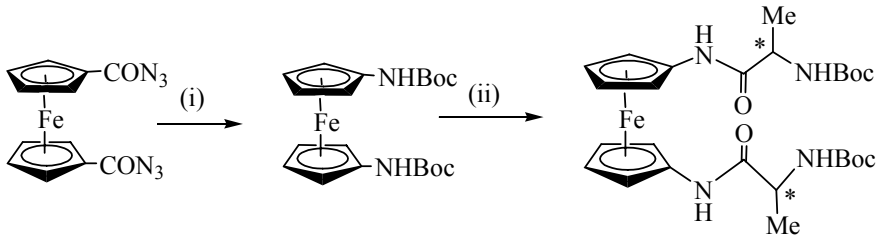

39 **40**

* L-Ala: **41a**
D-Ala: **41b**

Scheme 1.10. Synthesis of 1,1-bis(Boc-amino)ferrocene **40** via 1,1-bis(carbonylazido) Fc **39**, and its amino acid derivatives with L-Ala (**41a**) and D-Ala (**41b**). (i) Reflux in t-BuOH, 80 °C, 8 h; (ii) a) TFA, b) TEA, c) Boc-Ala-OH activated by EDC/HOBt.[67]

The compatibility of the bis-Boc derivative with the peptide synthesis protocol was successfully proved by the preparation of its first amino acid conjugates. The

syntheses of the L-Ala and D-Ala conjugates, 1,1'-bis(*tert*-butoxycarbonyl-L-alanine-amido)Fc (**41a**) and 1,1'-bis(*tert*-butoxycarbonyl-D-alanine-amido)Fc (**41b**) were readily achieved after deprotection of the amino group, followed by coupling with the corresponding Ala derivatives in the presence of a carbodiimide under inert atmosphere, to prevent the oxidation of the diaminoferrocene formed *in situ*.

1.2. Structural Studies of Ferrocene-Peptide Conjugates

In the structure of Fc the two Cp rings are separated by about 3.3Å, a distance suitable for forming a hydrogen bonding network for the attached peptide strands as observed in *β*-sheets. That gives Fc the ability to act as organometallic scaffold with a central reverse-turn unit. Moreover, by choosing the appropriate molecular assemblies and by utilizing chiral centers and H-bonding sites of conjugated peptide chains, it was possible to design highly ordered supramolecular systems. From these points of view, a variety of Fc–peptide bioconjugates have been designed to obtain a peptidomimetic basis for protein folding and to construct highly ordered molecular assemblies.

1.2.1. General Features

Some pertinent structural features for some Fc-amino acids and Fc-peptide conjugates are summarized in Table 1.1. In general, the two Cp rings of most structurally investigated Fc-amides are virtually co-planar[68] with a small angle θ and co-planarity between the amide and Cp planes (β) as defined in Scheme 1.11. In many cases, the two Cp rings are eclipsed.

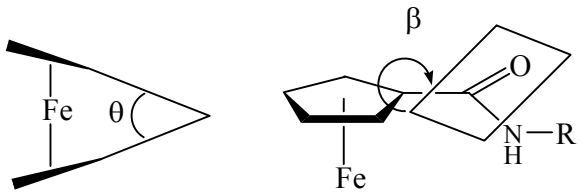

Scheme 1.11. Torsion angles in Fc-amino acids and peptides: θ = Cp bent and β = twist between amide and Cp planes

Table 1.1. Some common structural parameters for disubstituted ferrocenoyl amino acids and peptides

Compound	d(C-C)	<(O-C-N)	θ	β	d(C=O)	Ref.
$Fc[Gly\text{-}CSA]_2$ (**17**)	1.238(4) 1.235(5)	1.482(5) 1.477(6)	122.6(4) 122.9(4)	< 1		[9]
$Fc[Gly\text{-}Val\text{-}CSA]_2$ (**21**)	1.243(4) 1.243(4)	1.490(5) 1.483(5)	123.2(3) 122.8(4)	< 1		[13]
$Fc[Gly\text{-}OEt]_2$ (**42**)	1.235(5) 1.230(4)	1.482(5) 1.487(5)	121.1(3) 121.2(3)	1.8	14.1 15.2	[69]
$Fc[Gly\text{-}OH]_2$ (**43**)	1.246(2)	1.472(3)	121.1(2)	0.9	2.9	[69]
$Fc[Gly\text{-}NH_2]_2$ (**44**)	1.238(5)	1.478(5)	121.9(4)	0.1	6	[70]
$Fc[Pro\text{-}OMe]_2$ (**45**)	1.219(11) 1.227(11)	1.515(14) 1.481(14)	129.2(9) 120.1(9)	< 1		[46]
$Fc[AlaPro\text{-}OMe]_2$ (**46a**)	1.219(7)	1.506(9)	121.7(7)	0.53	3.77, 5.64	[71]
$Fc[AlaPro\text{-}OEt]_2$ (**46b**)	1.222(7)	1.478(8)	121.7 (6)	2.45	5.27	[72]
$Fc[AlaPro\text{-}OPr]_2$ (**46c**)	1.220(1)	1.47(1)	119.0(1)	1.75	1.70, 4.38	[73]
$Fc[AlaPro\text{-}OBz]_2$ (**46d**)	1.22(1)	1.51(1)	121.0(1)	2.60	2.64, 2.84	[73]
$Fc[Val\text{-}OMe]_2$ (**47**)	1.222(4)	1.488(5)	122.4(3)			[47]
$Fc[Phe\text{-}OMe]_2$ (**48**)	1.238(5) 1.232(6)	1.492(7) 1.498(7)	121.7(4) 123.0(5)	4.7	31.4, 15.1	[74]

The group attached to Fc moiety has a significant influence on the co-planarity of the Cp and amide planes. Steric interactions of the substituents with adjacent molecules may result in a loss of coplanarity of the Cp rings. Generally, the twist angle between the Cp and amide planes will increase with increasing size of the substituent (see Scheme 1.11), which will result in poor electronic coupling between Cp and amide

for large twist angles. In general, for all ferrocenoyl amino acids and peptides, the Cp bent angle is less than 1 - 4.5°, which is relatively small. However, extending the peptide sequence will result in increasing the angle due to the relief of steric pressures.[68]

The distances from the carbonyl carbon to the Cp rings for all structurally characterized Fc-peptides are well within established bond distances for a normal C-C single bond in Fc-amides (range d(C-C) = 1.43 – 1.507 Å).[68] Furthermore, the amide C(O)-N group is planar in all Fc-amino acids and –peptides and the carbonyl C=O distances compare well with simple Fc-amides. Similarly, the bond distances and angles of the Fc-moiety itself are well within established parameters for Fc derivatives.[68] With some exceptions in which larger twist angles are realized, the small cp-amide twists for most Fc-peptides allowed for significant electronic interaction between the π-systems of the Cp and the amide group, which will be discussed in the following section.

1.2.2. Hydrogen Bonding Properties of Disubstituted Ferrocene Peptide Conjugates

All Fc-peptides exhibit a fascinating array of intermolecular H-bonding interactions, which result in an ordered packing of the molecules in the solid state. It was observed in all structures investigated to date that the Fc-group does not interfere with the intrinsic ability of the peptides to assemble into larger aggregates via intermolecular H-bonding. The crystal structure of the two compounds $Fc[Gly\text{-}OEt]_2$ **42** and $Fc[Gly\text{-}OH]_2$ **43** are of particular interest where they display two completely different substitutional patterns as well as different H-bonding patterns (Figure 1.1).[69]

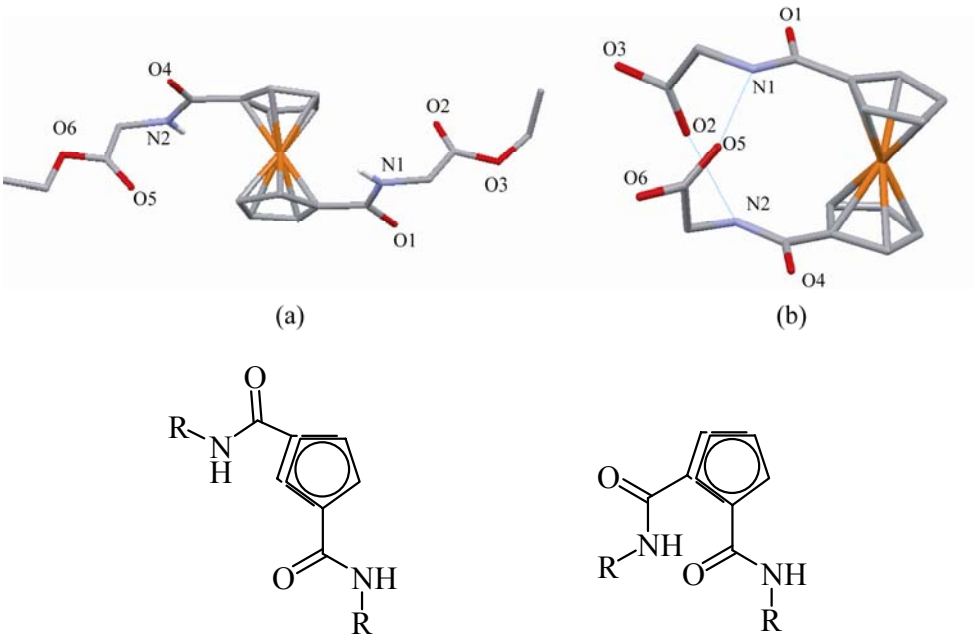

Figure 1.1. a) Molecular drawing of compound Fc[Gly-OEt]$_2$ **42** showing the 1,3'-substitution of the Fc group; (b) molecular drawing of the centrosymmetric Fc[Gly-OH]$_2$ **43** showing the 1,2'-substitution and the typical H-bonding pattern. Redrawn from Ref. [69]

In the case of Fc[Gly-OEt]$_2$ **42**, a 1,3'-substitution pattern is observed, which results in the formation of intermolecular H-bonding exclusively. Interestingly, the amide group on the other Cp ring is not involved in H-bonding and is well separated from other molecules (ca. 4 Å). This H-bonding pattern is reminiscent of that reported by Gallagher, Kenny and Hirao[71, 75, 76] with alternating up-down orientation of the individual H-bonded molecules. On the other hand, the free acid Fc[Gly-OH]$_2$ **43** adopts C_2 symmetry with a 1,2'-conformation which allows the formation of strong intramolecular H-bonding between the two podand substitutents (N…O(2A) and O(2)…N(A) = 2.875(3) Å). This pattern provides a rigid framework, in which the amide twist is reduced considerably (β = 1.8º) (see Table 1.1, Scheme 1.11). Mingos et al described a related amide Fc[Gly-NH$_2$]$_2$ **44**,[70] which was engages in intermolecular

interactions with adjacent molecules. Different 1,1'-disubstituted Fc-peptides, such as Fc[Pro-OMe]$_2$ **45** and Fc[Ala-Pro-OMe]$_2$ **46a** were reported by Herrick and Hirao.[46, 71]

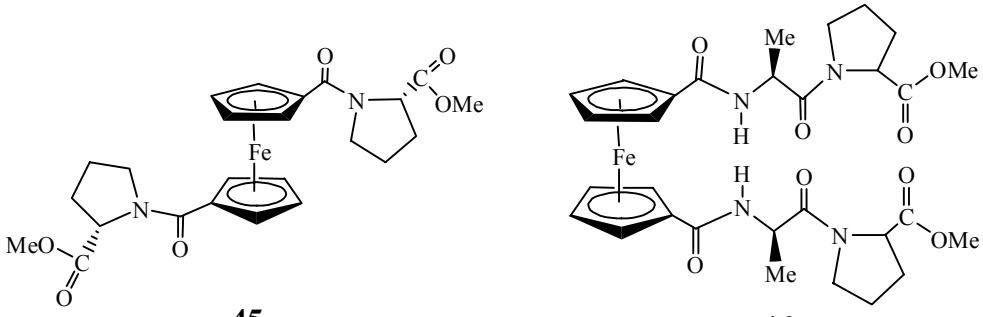

Figure 1.2. Molecular structure of 1,1'-Fc-prolinylmethylester **45** and 1,1'-Fc-bis(alanylprolinylesters) **46a**.

A series of related disubstituted Fc-dipeptides was studied by Hirao and coworkers.[71-73] It was shown that only intramolecular H-bonding is present in the C_2 symmetrical molecules Fc[Ala-Pro-OR]$_2$ (**46a-d**) forcing the two Cp rings into a 1,2'-conformation which has been observed frequently in other disubstituted Fc systems. Two strong intramolecular H-bonding interactions are present between the C=O of Ala of the Cp ring and the amide NH of Ala of another strand on the Cp' ring giving d(O···HN) distances of 1.88 and 2.15 Å (Figure 1.3).

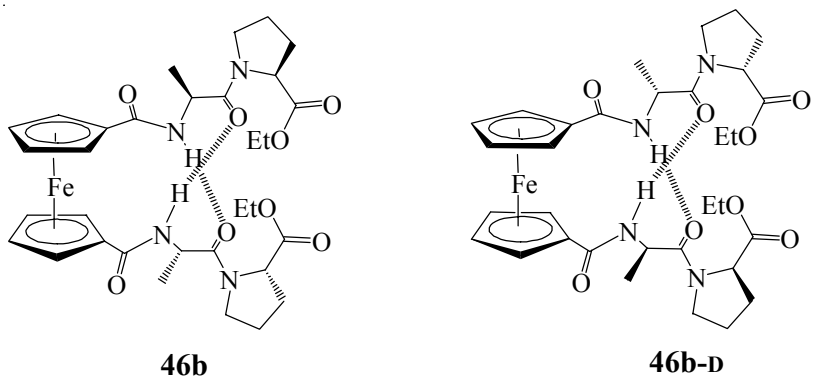

Figure 1.3. Molecular structure of Fc-[L-Ala-L-Pro-OEt]$_2$ **46b** and Fc-(D-Ala-D-Pro-OEt)$_2$ **46b-D**.[72]

It was found that the strong intramolecular H-bonding is the dominant factor, forcing the two amide planes to be co-planar to their respective Cp ring. In addition, the size of the peptide has very little effect on the structure. Changing the ester substituent in this series of compounds has virtually no effect on their molecular conformation.[72] Importantly, the intramolecular H-bonding is preserved in solution. Despite the lack of intermolecular H-bonding, these molecules assemble in a chirality-directed self-assembly into helical structures. The helicity of the super-structure depends on the chirality of the podant peptide. The L-Ala-L-Pro podant peptide chain will result in a helical arrangement, with the podant D-Ala-D-Pro giving the exact mirror image (Figure 1.3). Both helices have a pitch height of >14 Å and a distance between the Fc groups of approximately 4.5 Å. The related GlyPro and ProGly systems form related supramolecular arrangements in which intramolecular H-bonding determines the structure of the assembly.[77] Importantly, the helical chirality of the Fc core itself is preserved in solution.

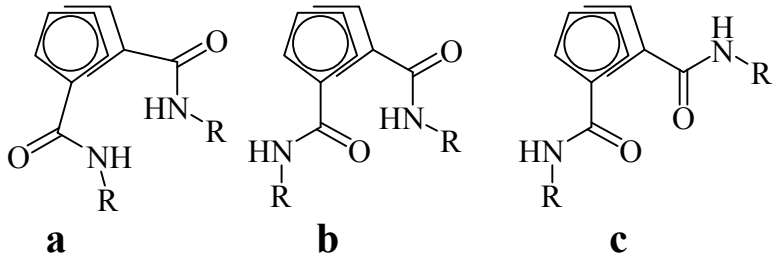

Scheme 1.12. Some of the possible orientations of the amino acid and peptide substituents. Structure a) is the most commonly found structural motif having the two C=O anti orientation.

In 1,2'-substituted Fc derivative, the two peptide substituents can adopt three different orientations with respect to each other shown in Scheme 1.12. The two Fc-CO

groups on the two Cp rings are pointing away from each other (**A**) allowing the remaining peptide chain to engage in intramolecular H-bonding interactions between the Fc-amide N-H and the amino acid or peptide carbonyl groups, resulting in the formation of two interstrand H-bonds. This is the typical "Herrick pattern", commonly observed in disubstituted Fc-peptide conjugates. For example, in Mingos' Fc[Gly-NH_2]$_2$ **44** two H-bonds are formed with N···O distances of 2.88 Å.[70] However, for the sterically more demanding isopropyl substituent in Erker's Fc[Val-OMe]$_2$ **47**, only very long N···O contacts of 3.247 Å are established. Metzler-Nolte[74] described the only case in which isomer **B** is observed. In Fc[Phe-OMe]$_2$ **48**, one of the carbonyl groups points inwards towards the amide group of the other amino acid substituent. As a consequence, only a single inter-strand C=O···H-N H-bond is formed with a N···O contact of 2.832 Å.

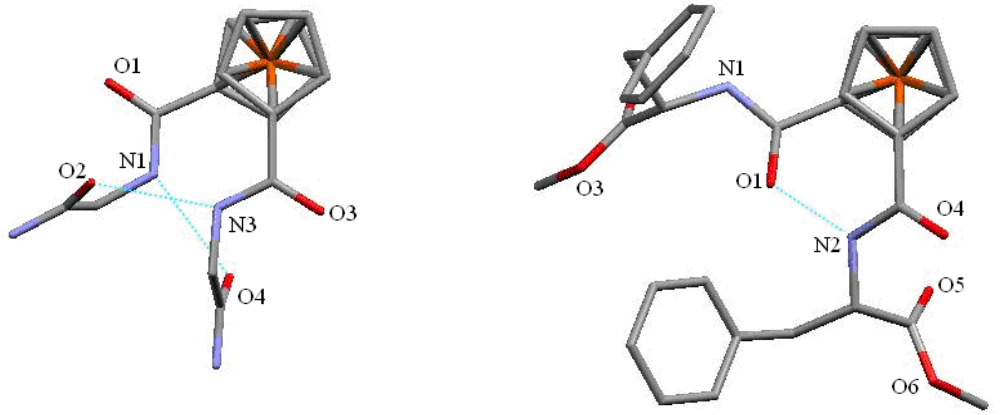

A **B**

Figure 1.4. 1,2'-substituted Fc systems showing the two different conformations of the amino acid substitutents: a) Conformation **A**: drawing of the molecular structure for Fc[Gly-NH_2]$_2$ **44** showing the two C=O pointing outwards, allowing the formation of interstrand H-bonding between the two amide C=O and N-H; b) Conformation **B**: drawing of the molecular structure of Fc[Phe-OMe]$_2$ **48**, showing one of the C=O pointing inwards the other pointing outwards, resulting in the formation of only a single H-bond. Redrawn from Refs.[70, 74]

The macrocyclic Fc[Gly-CSA]$_2$ **17** can be thought of as having the two podant Gly substituents clipped together with a cystamine linker.[9] Its structure is shown in Figure 1.5. The molecule is also achiral and like Fc[Gly-OH]$_2$ **43**, adopts a 1,2'-configuration, having both Fc-C=O pointing outwards. Both carbonyl groups and are engaged in intermolecular H-bonding interactions to adjacent molecules. Strong intramolecular H-bonding was observed as result of both amide NH contribution opposite peptide C=O across the ring (d(N(11)···O(22) = 2.862(4) Å, d(N(21)···O(12)) = 2.873(4) Å, d(N(31)···O(42) = 2.959(4)Å, d(N(41)···O(32)) = 2.815(4) Å).

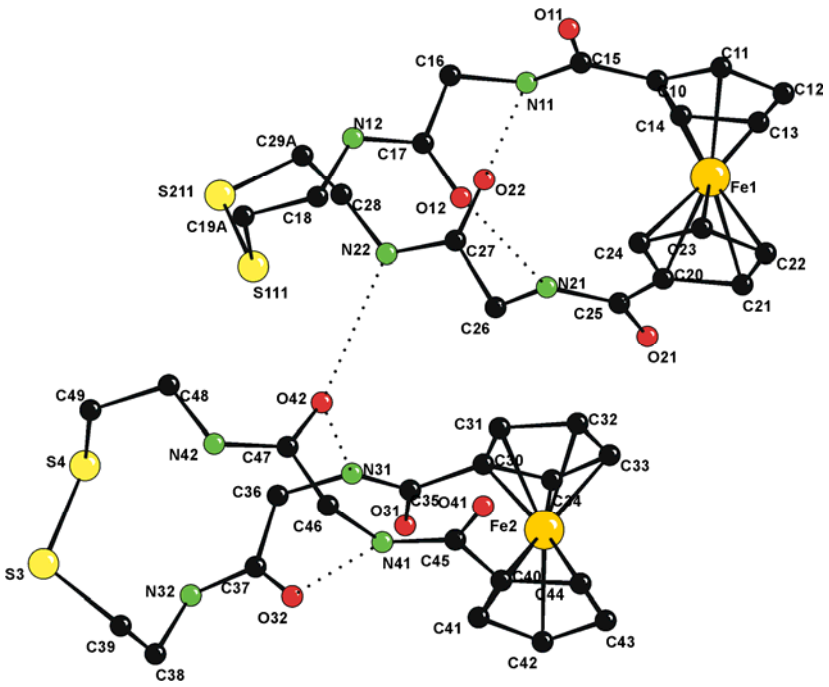

Figure 1.5. Molecular structure of the macrocyclic Fc[Gly-CSA]$_2$ (**17**) showing the intra- and intermolecular H-bonding interactions. The molecule has two diastereomers in the asymmetric unit.[9]

Interestingly, expansion of the ring by additional amino acids results in the formation of a fascinating macromolecular assembly, in which the peptide macrocycles associate into "pseudo-β-barrels".[13] Fc[Gly-Val-CSA]$_2$ **21** has Gly as the first amino acid to be attached to the Fc group, giving maximum flexibility to the podant peptide

chains, followed by Val, an amino acids with very high propensity to form β-sheets.[50] The Fc-system itself adopts a "Herrick conformation" and the cystamine acts as a structural restraint enabling additional H-bonding and establishing the appropriate H-bonding interface on the "exterior" of the macrocycle which allows β-sheet type interaction with adjacent molecules.[13]

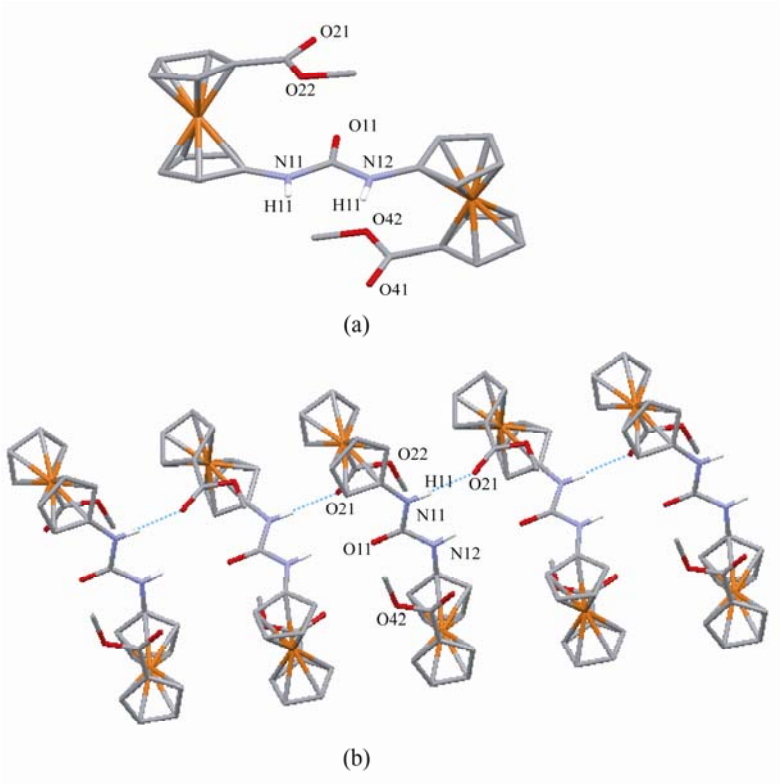

Figure 1.6. a) Structural drawing of dimethyl-1',1'-ureylenedi (1-ferrocenecarboxylate) **24** ; b) the crystal packing showing the intermolecular hydrogen bonding pattern. Redrawn from the original crystal structure.[55]

Figure 1.6 shows the single crystal structure of the urea compound **24**. In comparison to other urea compounds, the urea oxygen is not involved in intermolecular H-bonding. Instead, intermolecular H-bonding involves the methylester C=O and the urea N-H of an adjacent molecule resulting in a slight asymmetry of the urea group, resulting in the formation of a one-dimensional chain. However, on the molecular level,

this introduces a degree of asymmetry in the molecule which manifests itself in two different C-N bond lengths (N(11)-C(15) = 1.367(3) Å, N(12)-C(15) = 1.378(3) Å).

Interestingly, Rapić and Metzler-Nolte observed a turn-structure into their first Fca peptide conjugate **29** induced by this unnatural organometallic amino acid Fca with an anti-parallel motif. The solid state structure showed two intra-molecular H-bonds as shown in Figure 1.7. The N–H–O bond angle deviates only slightly from linearity, and N–O distances around 2.9 Å indicate strong hydrogen bonding. The angle ω between the substituents on the Cp rings is 60.7°, which confirm a typical 1,2'-conformation of the Fc system. The structure adopts a *P*-helical arrangement in the solid state and in solution which parallels work by Hirao and coworkers on peptide conjugates of $Fc[COOH]_2$ conjugates.[72] Additional studies show that amino acid and peptide conjugates of Fca in general adopt a β-turn-like structure in which the peptide strands are forced to adopt an antiparallel orientation with respect to each other.

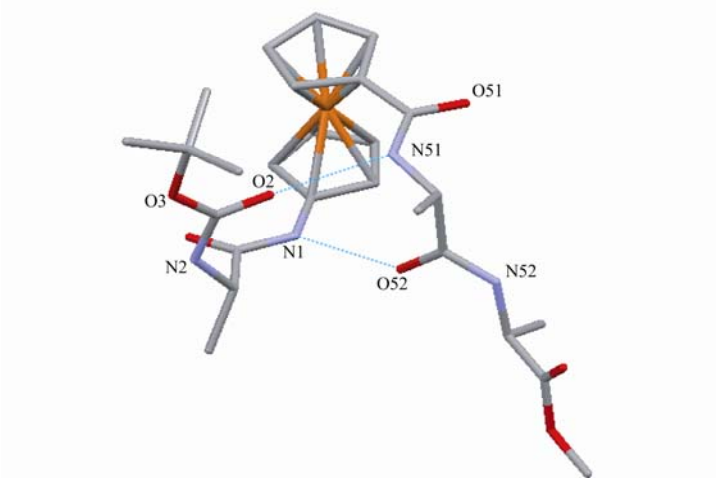

Figure 1.7. X-ray structure of the first Fca peptide conjugate **29** showing two intra-molecular hydrogen bonds. Selected hydrogen bond distances (Å) and angles (°): N1–O52 2.812(3), N51–O2 2.914(3), N1–H1N–O52 169(3), H51–H51N–O2 157(3). Redrawn from reference [35].

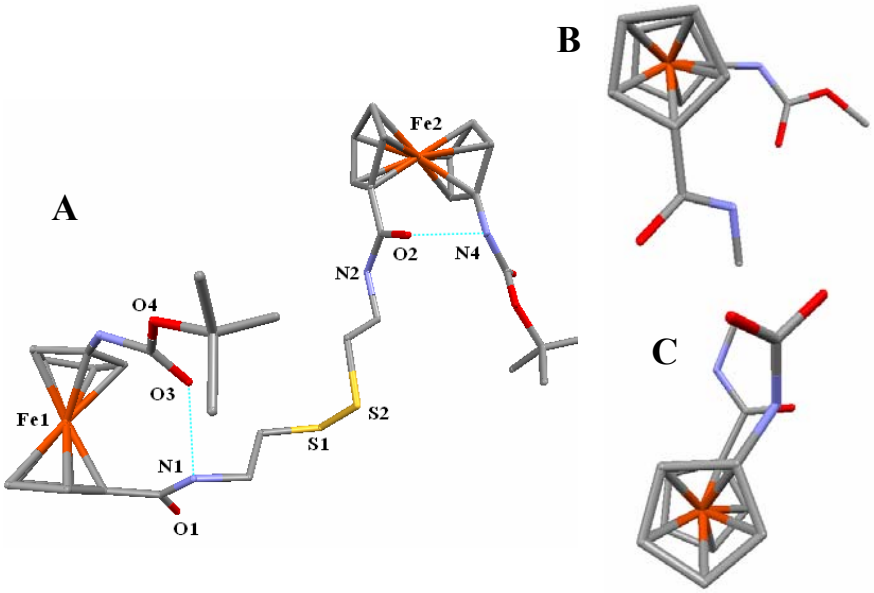

Figure 1.8. X-ray structure of $[BocNH(C_5H_4)Fe(C_5H_4)C(O)NHCH_2CH_2S]_2$ **43** (A) showing two intra-molecular hydrogen bonds. Selected hydrogen bond distances (Å) and angles (°) N1–O3 2.849(3) and N4–O2 2.989(3) Å. (B) 1,5' conformation of **Fc1**. (C) 1,1' conformation of **Fc2** with respect to the orientation of the substituents. Redrawn from reference [61].

Different conformations were observed for the two Fc units as was proposed by the solid state structure of **43**.[61] While Fc1 can be described as 1,5' with respect to the orientation of the substituents (Figure 1.8.B), Fc2 can be described as approximately 1,1' (Figure 1.8.C). These conformations were stabilized by intramolecular H-bonding interactions between N1 and O3 and N4 and O2. The intramolecular N(H)···O=C distances were 2.849(3) and 2.989(3) Å, respectively.[61]

Figure 1.9 shows a structural drawing of 1,1'-bis(Boc-amino)Fc **40**, in which several rotamers co-exist within the same material, due to the absence of strong intramolecular H-bonding, as encountered in Fc-peptide conjugates which stabilize a particular conformation. The Cp rings in both ferrocenoyl groups are co-planar (angle between Cp planes: 2.8(2)°). The amide and Cp rings are twisted by 18.9(2)°.

Importantly, the molecules maximize their H-bonding through formation of intermolecular and intramolecular N(H)···O=C bonding. Two intramolecular H-bonds (2.805(6) Å) are formed between the amide groups connected to the Cp rings and the adjacent carbonyl of the Boc causing *M*-helicity of the compound.

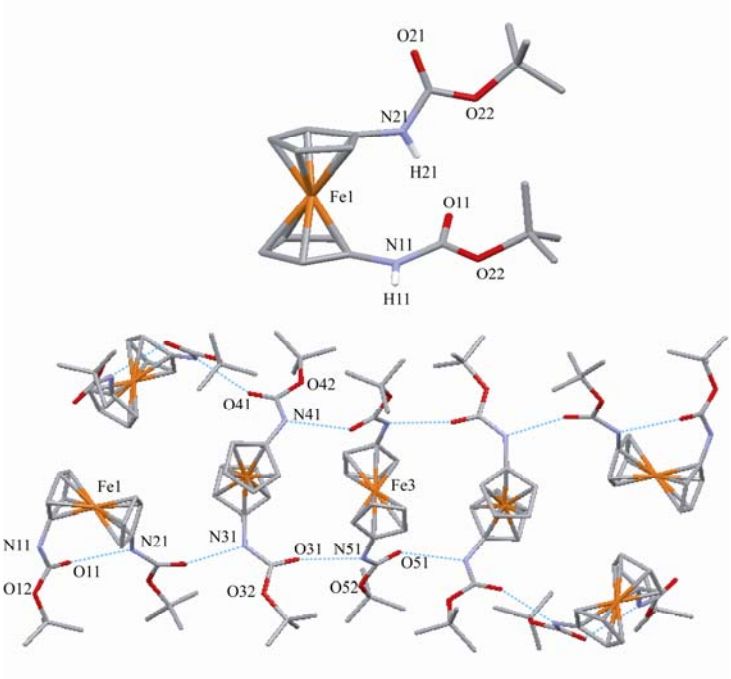

Figure 1.9. Structure of 1,1'-bis(tert-butoxycarbonylamino)ferrocene **40** showing three rotamers having the two substituents at different rotational angles with respect to the Cp-Fe-Cp vector with an approximate 1,2' (70º) and 1,3' (144º, 180º) conformation. All three rotamers are linked via intermolecular N(H)•••O=C bonding, redrawn from Reference [67].

Importantly, for amino acid conjugates the intramolecular NH···O=C H-bonding results in the formation of a previously unobserved 14-membered H-bonded ring, which is a new structural motif for Fc-peptide conjugates. [67] The resulting bioconjugates from the reaction of 1,1'-bis(tert-butoxycarbonylamino)ferrocene **40** with Me-protected D- and L-Ala showed a specific secondary structure through the involvement of strong intramolecular H-bonding in the solid state as well as in solution, forming a 14-

membered ring as is seen in antiparallel β-sheet peptides. The chirality of the amino acid is found to change the chiral organization of the peptide strands with respect to Fc center. To the best of our knowledge, this is the only available example of diaminoferrocene-labeled bioconjugates.

1.3. Oligomeric and Polymeric Ferrocene Amides

Fc-based organometallic polymers have received considerable attention since the first report of poly(vinylferrocene) by Arimoto and Haven in 1955.[28-30, 78-89] A large number of attempts to produce Fc-containing polymers, including polyalkenes, polyketones, polyesters, polyamines, polyamides, polyurethanes, and polyureas were reported.[84, 90] Polyamidoamine-based conjugates represent a class of polymere which can be readily ferrocenylated through amide-linked Fc in which the metallocene is linked to the side chain.[91] Early synthetic efforts have focused on the modification of the polymer side chains with Fc groups. In particular, ferrocenylalkylcarboxylic acids, Fc-$(CH_2)_n$-COOH (n = 0-3) were useful by allowing a facile conjugation to the polymer by a variety of methods.[78, 82, 92-96]

The preparation of polyamides having metallocenes incorporated into the backbone can be achieved by the use of bifunctional Fc derivatives, such as diacid chlorides or diamines. In the following, a few examples of such reactions are presented. In the early 1960's Knobloch and Rauscher reported the preparation of polyamides and polyesters by the reaction of 1,1'-ferrocenyldicarbonyl chloride **30** with several diamines and diols by interfacial polycondensation.[97]

Related work by Cuadrado and coworkers focused on the interfacial polycondensation protocol to prepare organosilicon polymer **50** in which the amid-linked ferrocenyl moieties are part of the main polymer chain as shown in Scheme 12.[98] The material was prepared by polycondensation of 1,1'-ferrocenyldicarbonyl chloride **30** with the siloxane **49** in the presence of triethylamine as base.

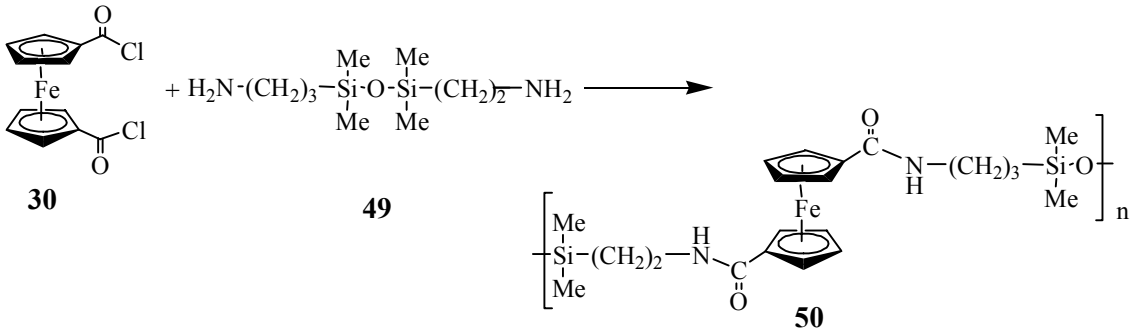

Scheme 1.13. Synthesis of the methylsiloxane polymer [-Si-$(CH_3)_2$-$(CH_2)_3$-NHC(O)-Fc-C(O)NH$(CH_2)_3$Si$(CH_3)_2$O-]$_n$ **50** having Fc in the backbone of the polymer chain

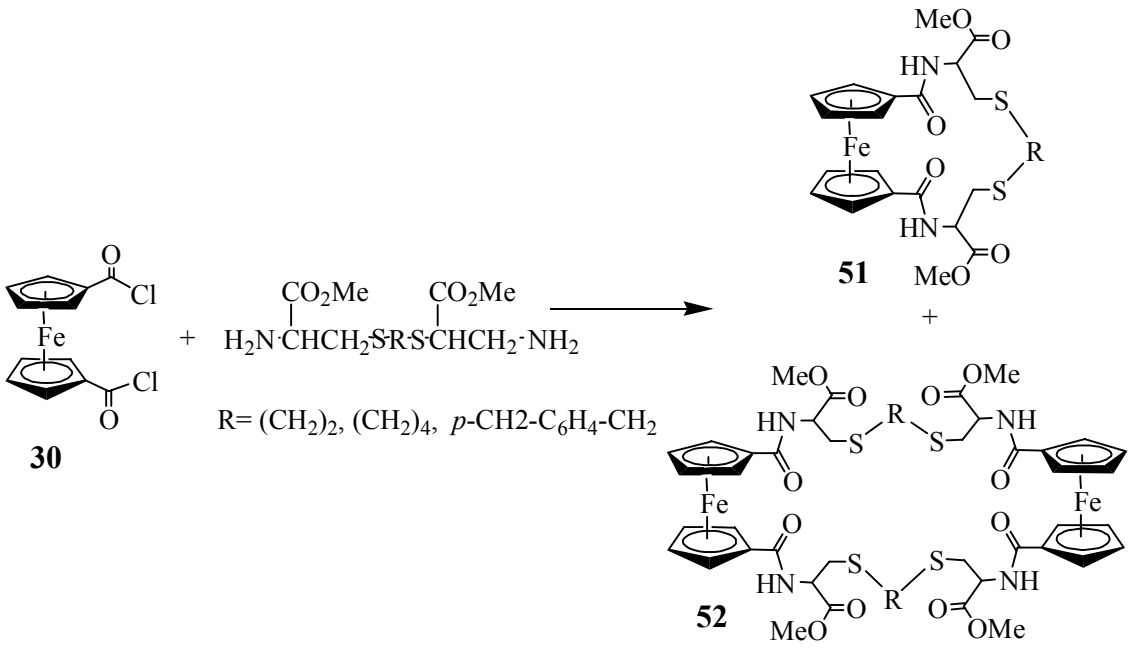

Scheme 1.14. Synthesis of cyclopeptides **51** and **52** by condensation of 1,1'-ferrocenyldicarbonyl chloride and bifunctional cystein derivatives.

Using $Fc[COCl]_2$, it should also be possible to prepare polypeptide conjugates, in which the Fc group is part of the polymer backbone and linked to the polypeptide through amide linkages. Han and coworkers were able to prepare 1,1'-ferrocenophane derivatives **51** as well as cyclodimers **52** and macrocyclic compounds from **30** and various cystein derivatives (Scheme 1.14).[99] Presumably, a non-defined polymer was also formed under the reaction conditions. This reaction is akin to the reaction leading to the formation of other Fc-peptide macrocycles discussed earlier (see Scheme 1.4).

Several other reports have considered the synthesis, solubility, and thermal properties of the formed polymers. For example, Khan et al.[61, 100, 101] recently prepared Fc-containing aromatic polyamides, by solution phase polycondensation of $Fc[COCl]_2$ with various aromatic diamines in solution at low temperature. The resulting polyaramides possess glass transition temperature above 350 °C. However, the polymers were only soluble in concentrated H_2SO_4, which limited their characterization significantly.

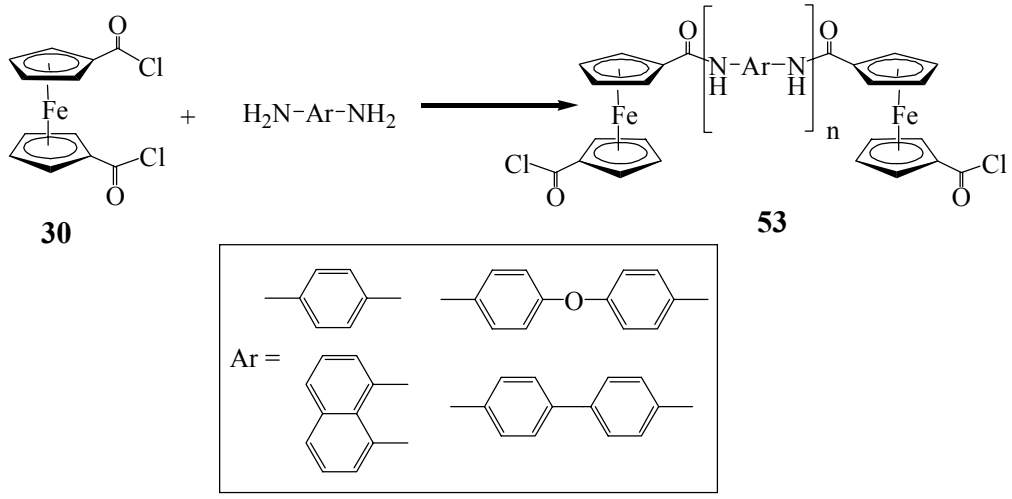

Scheme 1.15. Synthesis of some Fc-containing aromatic polyamides **53.**

In a similar fashion, Mehdipour-Ataei and coworkers attempted to improve the solubility of Fc-polyamides by introducing a flexible linker into the polymeric backbone though the synthesis of Fc-containing diamine decorated by ether and amide units **54** (Scheme 1.16).[102] The polymers showed improved solubility and good thermal stability.

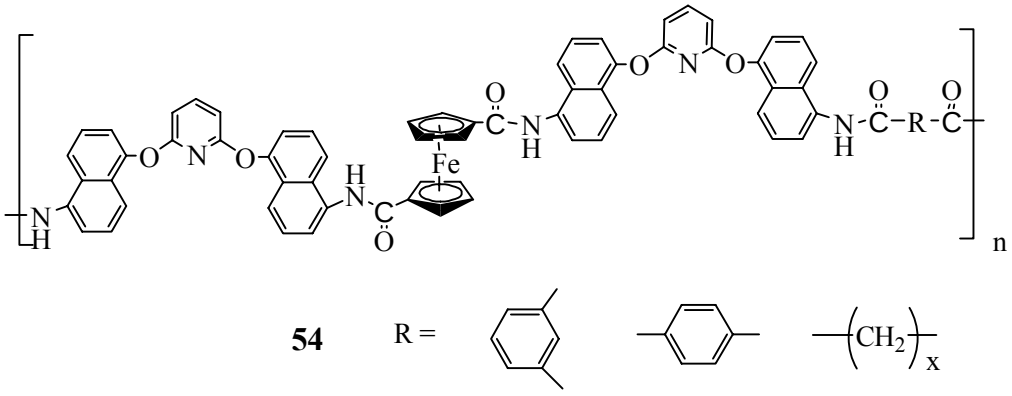

Scheme 1.16. Preparation of some Fc-based poly(amide ether amide)s **54**.

An interesting development is the use of Fca for the formation of a ferrocenylene polymer, in which the Fc groups are connected through amide linkages.[53] In essence, Fca polymers could be built up in a stepwise fashion using orthogonalized building blocks. Nakamura and Heinze presented good examples for this approach. Starting from a protected Fca derivative, Nakamura was able to obtain its amide dimer.[58] The structure was related to the symmetrical ferrocenyl-substituted urea, dimethyl 1',1'-ureylenedi(1-ferrocenecarboxylate) **24** (see Scheme 1.6).[55] Based on the structure of this Fc-amide dimer, Nakamura proposed a strongly H-bonded structure for the polymeric material (Scheme 15).

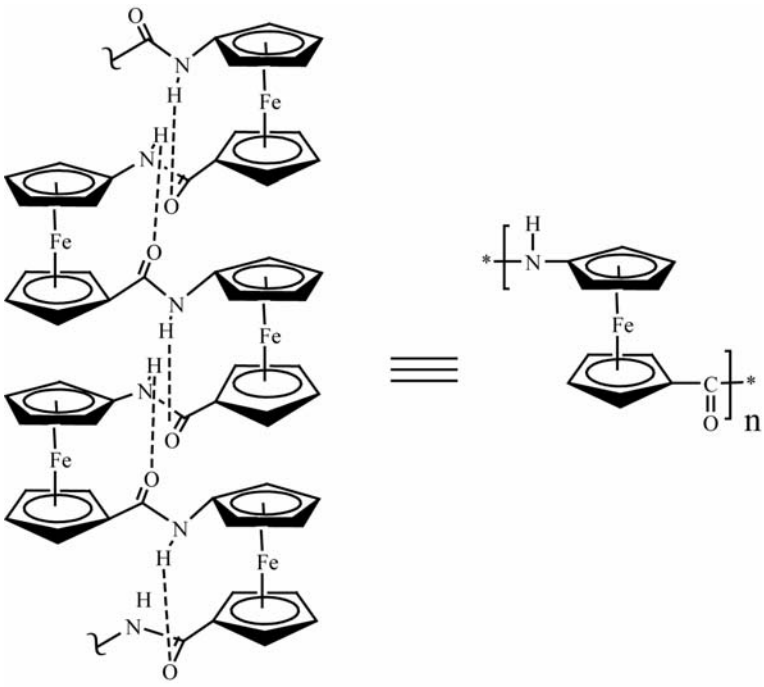

Scheme 1.17. Structure of the organometallic Fc-polypeptide proposed by Nakamura.[58]

Heinz prepared diferrocenyl diamide **68** from the reaction of ferrocenoyl 1-hydroxybenzotriazole ester **66** with aminoferrocene (Scheme 1.18).[56] She was able to make use of this flexible building block, which can be incorporated into a peptide backbone by solid phase synthesis.[103]

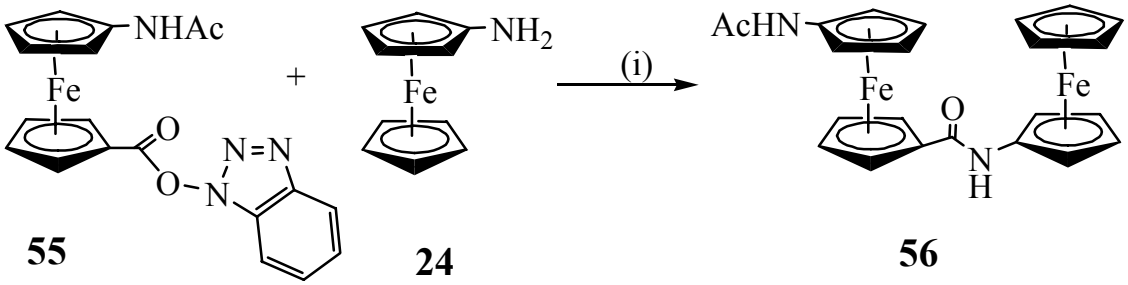

Scheme 1.18. Coupling of ferrocenoyl benzotriazole ester **55** with aminoferrocene **24** to give the diferrocenyl diamide **56**; (i) THF, 12 h.

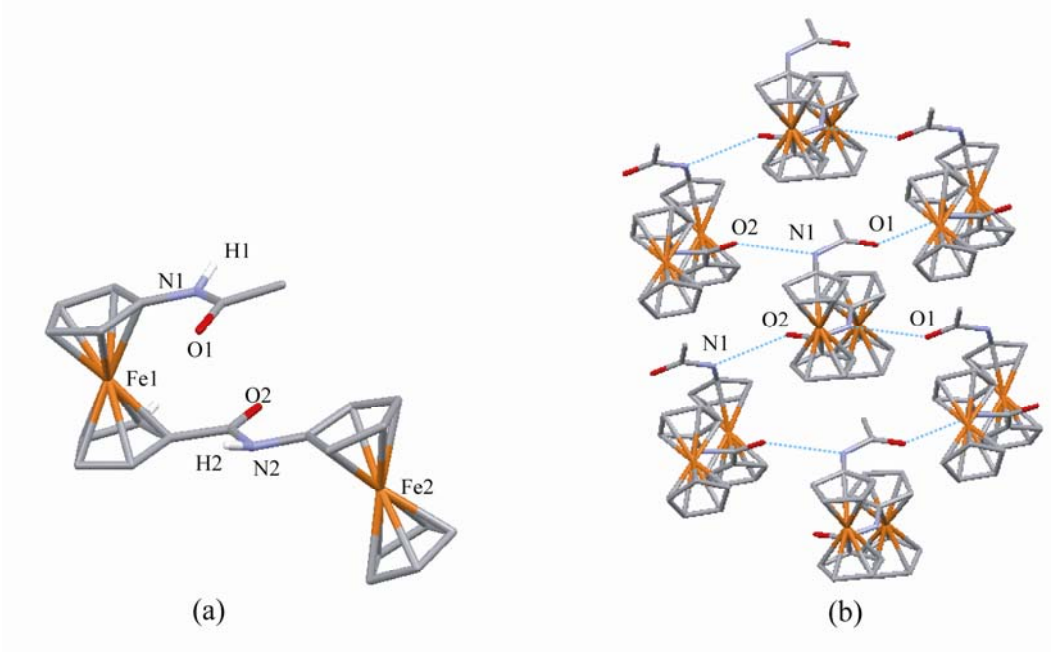

Figure 1.10. a) Molecular structure of the diferrocenyl peptide **56** in the solid state, b) hydrogen bonding pattern in the solid state. Redrawn from Reference.[56]

The crystal structure shows that the diferrocenyl dimer **56** possesses a conformation similar to Nakamura's dimer. In addition, the individual molecules are connected through intermolecular H-bonding between the NH-acetyl group and the amide C=O (N1···O2 distance: 3.04 Å) and between the NH-amide group and the C=O oxygen atom of the acetyl group (N2···O1 distance: 3.03 Å) resulting in a sheet-like structure (Figure 1.10).

Kraatz and coworkers have described the synthesis of a series of oligomeric and polymeric Fca-peptide conjugates based on D and L alanines.[104] They employed peptide-coupling strategies in solution to prepare the desired monomers Fca-L-alanine **30** and Fca-D-alanine **31**, their corresponding oligomers **32-37**, and poly(Fca-L-alanine) **38** (Scheme 1.19). A parallel β-sheet-like structure involving the amino acid residues

with 12-membered hydrogen-bonded rings was formed. By exploiting the turn-inducing ability of Fca they proposed a structure that shows some structural similarities to the β-helical motif found in naturally occurring proteins which may be employed as electrochemical screens for "β-breakers".

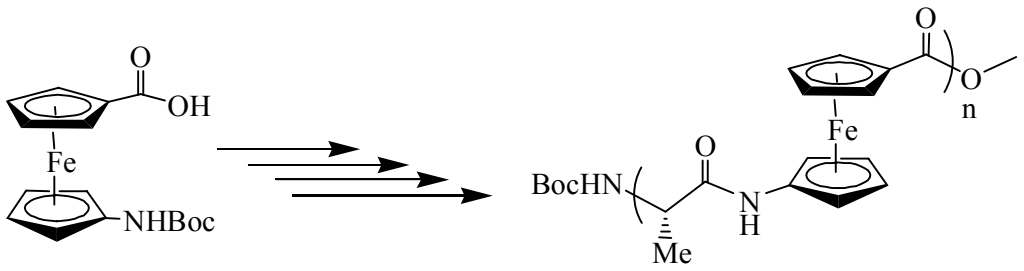

23a

n =1: **57** (S) ; **58** (R)
n =2: **59** (S) ; **60** (R)
n =3: **61** (S) ; **62** (R)
n =4: **63** (S) ; **64** (R)
polymer: **65** (S)

Scheme 1.19. Synthesis of P- and M-helical foldamers from the conjugates of Fca with L- and D-alanine resulted in the formation of the oligomers **57**-**64** and the polymer **65**.

In addition to the poly-Fc amide derived from $Fc[COCl]_2$ and Fca, very few reports described the synthesis of poly-Fc amides obtainable by the polycondensation ferrocenediamine derivatives. For example, the synthesis of elastomeric polyamides **68**, M_n = 10 000-18 000) in high yields was reported by Rausch and coworkers from 1,1'-bis(β-aminoethyl)ferrocene **67** and diacid chlorides (Scheme 1.20). The reaction with bis-isocyanates allows the formation of Fc-containing polyureas **69**.

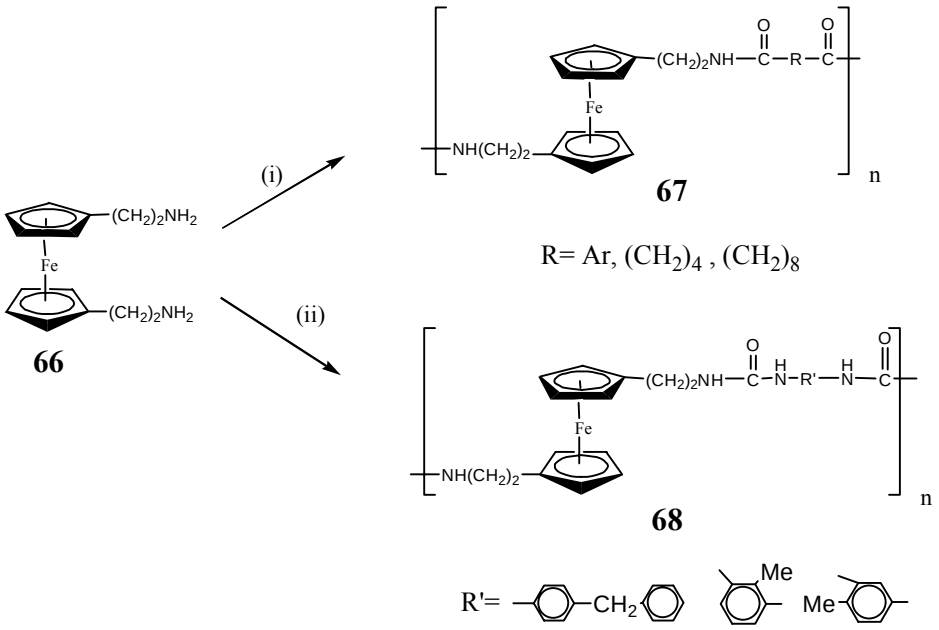

Scheme 1.20. Synthesis of elastomeric polyamides **67** and **68** from 1,1'-bis(β-aminoethyl) Fc **66** and diacid chlorides. (i) Cl-CO-R-CO-Cl; (ii) OCN-R'-NCO.

Frejd's 1,1'-ferrocenylbisalanine system[105-110] is another interesting bifunctional molecule for the synthesis of macrocyclic oligopeptides and potentially of Fc-containing polypeptides. The fully protected 1,1'-ferrocenylbisalanine derivative **69** contains orthogonal protecting groups, which allow their deprotection by hydrogenolysis, which is followed by cyclization in the presence of the peptide coupling reagent PyAOP.[105, 106, 110, 111] The obtained product was a mixture of the 1,1'-ferrocenophane **71** and two macrocyclic peptides, a cyclic "dimer" **72** and a cyclic "trimer" **73** (Scheme 1.21). Interestingly, poly-Fc amides obtained facial condensation of $Fc[NH_2]_2$ and $Fc[COCl]_2$ were completely missing from the literature.

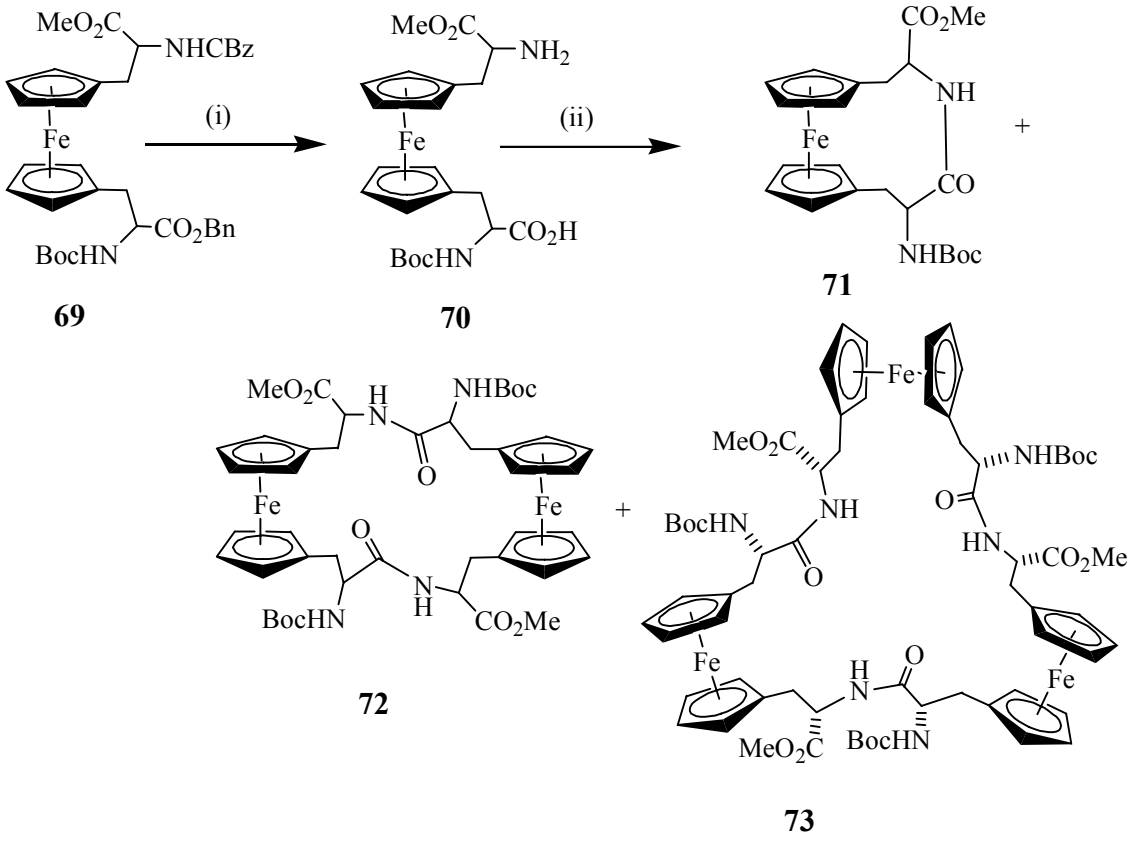

Scheme 1.21. Cyclization of **70** forming macrocyclic oligopeptides **71-73**: (i) H_2, Pd/C(5%),MeOH (ii) 7-azabenzotriazol-1-yloxytris(pyrrolidino)phosphonium hexafluoro phosphate (PyAOP), Dipea, DMF.

1.4. Objectives and Motivation

The objectives of this thesis are to explore the preparative and structural aspects of Fc-peptide conjugates and their potential applications as new biosensors and polymeric materials.

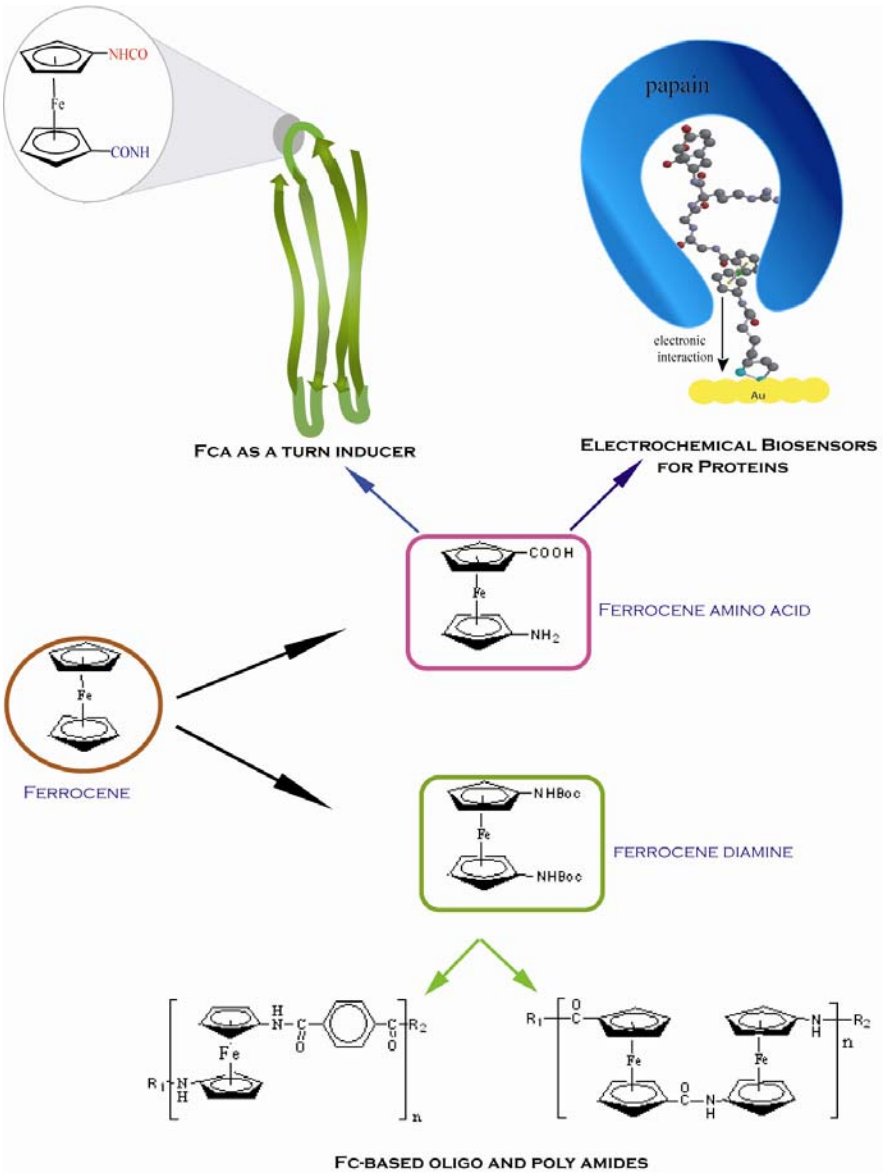

Scheme 1.22. Schematic representation summarizes the objectives of the study described in this thesis.

After surveying the literature we pointed out some challenges and scientific questions that were not answered or not properly addressed in the field of Fc-peptide conjugates and their applications in the fields of molecular recognition, biosensing and material science. First, the artificial amino acid 1'-amino-ferrocene-1-carboxylic acid (ferrocene amino acid, Fca) was recognized as a useful tool in bioorganometallic chemistry. Therefore, it was important to investigate the capability of this promising artificial amino acid to conjugate with amino acids and peptides, and study the structural properties of these conjugates. This will be addressed in Chapter 2.

Second, it is important to explore the influence Fca on the self-assembly abilities of the conjugates and investigate the supramolecular structure of the Fca-peptides. This will be addressed in Chapter 3.

Third, because of the interesting reversible redox properties and the suitable potential ranges of Fc, it was widely exploited as part of molecular recognition systems. Fc-peptide conjugates combine the ability of Fc to mediate electron transfer with the molecular recognition potentials of peptides. Is it possible to devise a strategy that uses Fc-peptide conjugates as biosensors? Labeling the peptide recognition site in a biosensor is potentially problematic. It is always interfering with the protein recognition process and may even prevent it. Thus, it was decided to explore this possibility and test the capability of Fca-peptide conjugates linked to surfaces to act as an effective electroactive probe for the detection of biological materials. This will be addressed in Chapter 4.

Fourth, the synthesis of metallopolymers is one major application of ferrocenes. Significant efforts have focused on the synthesis of poly(ferrocenylenes) in which the

Fc groups form part of the backbone or located in the side chain. To the best of my knowledge there are no examples of oligomers and polymers that have peptide-like characteristics and possess a Fc in their backbone. This raises a fundamental question if the individual Fc units will be able to interact with each others electronically in such oligomers and polymers? This will be addressed in Chapter 5.

Next I expand on these ideas and try to answer another question, what would be the effect of incorporating different linkers having different electronic environments, such as phenylene, cyclohexylene and lysyl groups on the electronic properties of Fc-containing oligomers or polymers? The phenylene group is expected to enhance the electronic communication between the Fc groups because of its strong conjugation effect however it should also give rise to a stiffer on the polymer. On the other hand, the cyclohexylene group is more flexible however it may not allow any communication because of the lack of conjugation system. The answers to this question will be addressed in Chapters 6.

By pointing out these important scientific questions, three challenges will be addressed in this growing field. The first is to investigate the biocompatibility of the organometallic moieties with the conjugated amino acids and peptides. New Fc building blocks such as Fca and 1,1'-bis(tert-butoxycarbonylamino)ferrocene are synthesized and employed for that purpose. In particular, the tendency of disubstituted Fc systems to impose secondary structural elements on the conjugated peptides was investigated in detail. The second is to design and synthesize specific Fca-peptide conjugates to develop a surface based electrochemical biosensor for proteins, in which the Fc label is part of the recognition site but will not interfere with the peptide-protein interactions.

Such systems were not available prior to my studies and, if successful, represent a significant step forward. The third is to build new electroactive peptide-like Fc oligo- and polyamides and to investigate their electronic properties, which could then be engaged in the bioelectronics applications.

1.5. References

[1] G. Jaouen, *J. Organomet. Chem.* **1999**, *589*, 1-1.
[2] G. Jaouen, A. Vessieres, I. S. Butler, *Acc. Chem. Res.* **1993**, *26*, 361-369.
[3] D. R. van Staveren, N. Metzler-Nolte, *Chem. Rev.* **2004**, *104*, 5931-5985
[4] R. H. Fish, G. Jaouen, *Organometallics* **2003**, *22*, 2166-2177.
[5] C. Biot, L. Delhaes, H. Abessolo, O. Domarle, L. A. Maciejewski, M. Mortuaire, P. Delcourt, P. Deloron, D. Camus, D. Dive, J. S. Brocard, *J. Organomet. Chem.* **1999**, *589*, 59-65.
[6] C. Biot, G. Glorian, L. A. Maciejewski, J. S. Brocard, *J. Med. Chem.* **1997**, *40*, 3715-3718.
[7] T. Moriuchi, T. Nagai, T. Hirao, *Org. Lett.* **2006**, *8*, 31-34.
[8] T. Moriuchi, T. Nagai, T. Hirao, *Org. Lett.* **2005**, *7*, 5265-5268.
[9] S. Chowdhury, G. Schatte, H.-B. Kraatz, *Dalton Trans.* **2004**, 1726-1730.
[10] T. Moriuchi, K. Yoshida, T. Hirao, *Org. Lett.* **2003**, *5*, 4285-4288.
[11] T. Moriuchi, K. Yoshida, T. Hirao, *J. Organomet. Chem.* **2003**, *668*, 31-34.
[12] A. Nomoto, T. Moriuchi, S. Yamazaki, A. Ogawa, T. Hirao, *Chem. Commun.* **1998**, 1963-1964.
[13] S. Chowdhury, D. A. R. Sanders, G. Schatte, H. B. Kraatz, *Angew. Chem. Int. Ed.* **2006**, *45*, 751-754
[14] F. Noor, A. Wuestholz, R. Kinscherf, N. Metzler-Nolte, *Angew. Chem. Int. Ed.* **2005**, *44*, 2429-2432.
[15] J. T. Chantson, M. V. V. Falzacappa, S. Crovella, N. Metzler-Nolte, *J. Organomet. Chem.* **2005**, *690*, 4564-4572.
[16] W. A. Petka, J. L. Harden, K. P. McGrath, W. D., D. A. Tirrell, *Science* **1998**, *281*, 389-392
[17] A. Aggeli, I. A. Nyrkova, M. Bell, R. Harding, L. Carrick, T. C. B. McLeish, A. N. Semenov, N. Boden, *Proc. Natl. Acad. Sci. USA* **2001**, *98*, 11857-11862
[18] J. P. Schneider, J. W. Kelly, *Chem. Rev.* **1995**, *95*, 2169-2187
[19] J. S. Nowick, *Acc. Chem. Res.* **1999**, *32*, 287-296
[20] a) M. R. Ghadiri, J.R. Granja, R.A.Milligan, D.E. McRee, A. Khazanovich, *Nature* **1993**, 366, 324-327; b) J.D. Hartgerink, J.R. Granja, R.A. Milligan , M.R. Ghadiri, *J. Am. Chem. Soc.* **1996**, 118, 43-50; c) T.D. Clark , J.M. Buriak, K. Kobayashi, M.P. Isler, D.E. McRee, M.R.Ghadiri, *J. Am. Chem. Soc.* **1998**, 120, 8949-8962.
[21] a) D. Ranganathan, V. Haridas, C.S. Sundari, D. Balasubramanian, K.P. Madhusudana, R. Roy, I. L.Karle, *J. Org. Chem.* **1999**, 64, 9230-9240; b) D. Ranganathan, M.P. Samant, , I. L.Karle, *J. Am. Chem. Soc*. **2001**, 123, 5619-5624.
[22] a) D. P. Pantarotto, C. D.; Graff, R.; Hoebeke, J.; Briand, J.-P.; Prato, M.; Bianco, A. *J. Am. Chem. Soc.* **2003**, 125, 6160-6164; b) Djalali, R.; Samson, J.; Matsui, H. *J. Am. Chem. Soc.* **2004**, 126, 7935-7939.
[23] M. Amorin, L. Castedo, J. R. Granja, *J. Am. Chem. Soc.* **2003**, *125*, 2844-2845.
[24] a) R. C. Claussen, B. M. Rabatic, S. I. Stupp, *J. Am. Chem. Soc.* 2003, **125,** 12680-12681; b) N. W. Shi Kam, T. C. Jessop, P. A. Wender, H. Dai, *J. Am. Chem. Soc.* 2004, **126**, 6850-6851.

[25] R. P. Lyon, W. M. Atkins, *J. Am. Chem. Soc.* **2001**, *123*, 4408-4413
[26] T. C. Holmes, S. deLasalle, X. Su, G. Liu, A. Rich, A. Zhang, *Proc. Natl. Acad. Sci. USA* **2000**, *97*, 6728-6733
[27] J. H. Collier, B.-H. Hu, J. W. Ruberti, J. Zhang, P. Shum, D. H. Thompson, P. B. Messersmith, *J. Am. Chem. Soc.* **2001**, *123*, 9463-9464
[28] C. U. Pittman, Jr., *J. Inorg. Organomet. Polym.* **2005**, *15*, 33-55.
[29] M. Haeussler, Q. Sun, K. Xu, J. W. Y. Lam, H. Dong, B. Z. Tang, *J. Inorg. Organomet. Polym.* **2005**, *15*, 67-81.
[30] A. S. Abd-El-Aziz, C. E. C. Jr., C. U. P. Jr., J. E. Sheats, M. Zeldin, *Macromolecules Containing Metal and Metal-Like Elements, Vol. 1*, Wiley& Sons Inc. , New Jersey, **2003**.
[31] E. W. Neuse, *J. Inorg. Organomet. Polym.* **2005**, *15*, 3-32.
[32] C. E. Carraher, Jr., *J. Inorg. Organomet. Polym.* **2005**, *15*, 121-145.
[33] H.-B. Kraatz, *J. Inorg. Organomet. Polym.* **2005**, *15*, 83-106.
[34] L. Barišić, V. Rapić, N. Metzler-Nolte, *Eur. J. Inorg. Chem.* **2006**, 4019-4021.
[35] L. Barišić, M. Dropucic, V. Rapić, H. Pritzkow, I. Kirin Srecko, N. Metzler-Nolte, *Chem. Commun.* **2004**, 2004-2005.
[36] L. Barišić, M. Čakić, K. A. Mahmoud, Y. N. Liu, H. B. Kraatz, H. Pritzkow, S. I. Kirin, N. Metzler-Nolte, V. Rapić, *Chem. Eur. J.* **2006**, 4965-4980.
[37] a) J. A.Cannizzaro, K. D.Janda, K. N. Houk, *J. Am. Chem. Soc.* **2003**, 125, 2489-2506; b) J. T. Yli-Kauhaluma, J. A. Ashley, C. -H. Lo, L. Tucker, Wolfe, M. M.; Janda, K. D., *J. Am. Chem. Soc.*, **1995**, 117, 7041-7047; c) A. Heine, E. A.Stura, J. T.Yli-Kauhaluma, C. Gao, Q. Deng, B. R.Beno, K. N. Houk, K. D. Janda, I. A.Wilson, *Science* **1998**, 279, 1934-1940.
[38] K. Plumb, H. B. Kraatz, *Bioconjugate Chem.* **2003**, *14*, 601.
[39] K. Severin, R. Bergs, W. Beck, *Angew. Chem. Int. Ed.* **1998**, *37*, 1635-1654
[40] K. A. Mahmoud, Y. T. Long, G. Schatte, H. B. Kraatz, *Eu. J. Inorg. Chem.* **2005**, 173-180.
[41] D. R. van Staveren, N. Metzler-Nolte, *Chem. Rev.* **2004**, *104*, 5931-5985.
[42] Y. Degani, A. Heller, *J. Am. Chem. Soc.* **1988**, *110*, 2615-2620
[43] Y. Degani, A. Heller, *J. Phys.Chem.* **1987**, *91*, 1285-1589.
[44] Y. Xu, P. Saweczko, H. B. Kraatz, *J. Organomet. Chem.* **2001**, *637-639*, 335-342
[45] Y. Xu, H. B. Kraatz, *Tetrahedron Lett.* **2001**, *42*, 2601-2603
[46] R. S. Herrick, R. M. Jarret, T. P. Curran, D. R. Dragoli, M. B. Flaherty, S. E. Lindyberg, R. A. Slate, L. C. Thornton, *Tetrahedron Lett.* **1996**, *37*, 5289-5292.
[47] M. Oberhoff, L. Duda, J. Karl, R. Mohr, G. Erker, R. Fröhlich, M. Grehl, *Organometallics* **1996**, *15*, 4005-4011
[48] H. Huang, L. Mu, J. He, C. J.-P., *J. Org. Chem.* **2003**, *68*, 7605-7611.
[49] M. M. Galka, H.-B. Kraatz, *ChemPhysChem* **2002**, *3*, 356-359.
[50] C. K. Smith, L. Regan, *Acc. Chem. Res.* **1997**, *30*, 153-161
[51] L.-L. Lai, T.-Y. Dong, *J. Chem. Soc. Chem. Commun.* **1994**, 2347-2348
[52] I. R. Butler, R. L. Davies, *Synthesis* **1996**, 1350-1362.
[53] I. R. Butler, S. C. Quayle, *J. Organomet. Chem.* **1998**, *552*, 63-68.
[54] L. Barisic, V. Kovac, V. Rapic, *Croat Chem. Acta* **2002**, *75*, 199-210.
[55] K. A. Mahmoud, H.-B. Kraatz, *J. Organomet. Chem.* **2004**, *689*, 2250-2255

[56] K. Heinze, M. Schlenker, *Eur. J. Inorg. Chem.* **2004**, 2974-2988.
[57] D. C. D. Butler, C. J. Richards, *Organometallics* **2002**, *21*, 5433-5436.
[58] T.-a. Okamura, K. Sakauye, N. Ueyama, A. Nakamura, *Inorg. Chem.* **1998**, *37*, 6731-6736.
[59] A. N. Nesmeyanov, V. A. Sazonova, V. N. Drosd, *Chemische Berichte* **1960**, *93*, 2717-2729.
[60] M. A. K. Khan, D. S. Thomas, H.-B. Kraatz, *Inorg. Chim. Acta.* **2006**, *359*, 3339-3344.
[61] M. A. K. Khan, Y.-T. Long, G. Schatte, H.-B. Kraatz, *Anal. Chem.* **2007**, *79*, 2877-2884.
[62] E. M. Acton, R. M. Silverstein, *J. Org. Chem.* **1959**, *24*, 1487-1490.
[63] F. S. Arimoto, A. C. Haven, *J. Am. Chem. Soc.* **1955**, *77*, 6295.
[64] W. E. Parham, V. J. Trynelis, *J. Am. Chem. Soc.* **1955**, *77*, 68.
[65] G. R. Knox, P. L. Pauson, *J. Chem. Soc.* **1961**, 4615.
[66] A. Shafir, M. P. Power, G. D. Whitener, J. Arnold, *Organometallics* **2000**, *19*, 3978 -3982.
[67] S. Chowdhury, K. A. Mahmoud, G. Schatte, H.-B. Kraatz, *Org. Biomol. Chem.* **2005**, *3*, 3018-3023.
[68] L. Lin, A. Berces, H.-B. Kraatz, *J. Organomet. Chem.* **1998**, *556*, 11-20.
[69] F. E. Appoh, T. C. Sutherland, H.-B. Kraatz, *J. Organomet. Chem.* **2004**, *689*, 4669-4677.
[70] A. S. Georgopoulou, D. M. P. Mingos, A. J. P. White, D. J. Williams, B. R. Horrocks, A. Houlton, *J. Chem. Soc., Dalton Trans.* **2000**, 2969-2974
[71] A. Nomoto, T. Moriuchi, S. Yamazaki, A. Ogawa, T. Hirao, *Chem. Commun.* **1998**, 1963-1964.
[72] T. Moriuchi, A. Nomoto, K. Yoshida, A. Ogawa, T. Hirao, *J. Am. Chem. Soc.* **2001**, *123* 68 -75.
[73] T. Moriuchi, A. Nomoto, K. Yoshida, T. Hirao, *J. Organomet. Chem.* **1999**, *589*, 50-58.
[74] D. R. van Staveren, T. Weyhermüller, N. Metzler-Nolte, *Dalton Trans.* **2003**, 210-220
[75] J. F. Gallagher, P. T. M. Kenny, M. J. Sheehy, *Acta Crystallogr.* **1999**, *C55*, 1257-1260.
[76] J. F. Gallagher, P. T. M. Kenny, M. Sheehy, *J. Inorg. Chem. Commun.* **1999**, *2*, 200-202.
[77] T. Moriuchi, A. Nomoto, K. Yoshida, T. Hirao, *Organometallics* **2001**, *20*, 1008-1013.
[78] A. S. Abd-El-Aziz, I. Manners, *J. Inorg. Organomet. Polym.* **2005**, *15*, 157-195.
[79] K. E. Gonsalves, X. Chen*, Vol. 10* (Eds.: A. Togni, T. Hayashi), VCH, Weinheim, Germany, **1995**, p. 496.
[80] I. Manners, *Angew. Chem. Int. Ed.* **1996**, *35*, 1603-1621
[81] I. Manners, *Can. J. Chem.* **1998**, *76*, 371-381.
[82] E. W. Neuse, *J. Inorg. Organomet. Polym.* **2005**, *15*, 3-32.
[83] E. W. Neuse, L. Bednarik, *Macromolecules* **1979**, *12*, 187-195.
[84] P. Nguyen, P. Elipe-Gomez, I. Manners, *Chem. Rev.* **1999**, *99*, 1515-1548.

[85] T. J. Peckham, P. Gomez-Elipe, I. Manners, (Eds.: A. Togni, R. L. Haltermann), Wiley-VCH, Weinheim, **1998**, p. 723.
[86] H. Nishihara, M. Murata, *J. Inorg. Organomet. Polym.* **2005**, *15*, 147-156.
[87] C. E. Carraher, Jr., *Journal of Inorganic and Organometallic Polymers and Materials* **2005**, *15*, 121-145.
[88] H. R. Allcock, *J. Inorg. Organomet. Polym.* **2005**, *15*, 57-65.
[89] E. W. Neuse, *Journal of Inorganic and Organometallic Polymers and Materials* **2005**, *15*, 3-32.
[90] E. W. Neuse, H. Rosenberg, *J. Macromol. Sci. Rev. Macromol. Chem.* **1970**, *C4*, 1-64.
[91] M. G. Meirim, E. W. Neuse, G. Cadwell, *J. Inorg. Organomet. Polym.* **1998**, *8*, 225-236.
[92] M. A. Buretea, T. D. Tilley, *Organometallics* **1997**, *16*, 1507-1510.
[93] C. E. Stanton, T. R. Lee, R. H. Grubbs, N. S. Lewis, J. K. C. Pudelski, M. R., M. S. Erickson, M. L. McLaughlin, *Macromolecules* **1995**, *28*, 8713-8721.
[94] A. S. Gamble, J. T. Patton, J. M. Boncella, *Makromol. Chem., Rapid Commun.* **1993**, *13*, 109-115.
[95] R. W. Heo, J.-S. Park, T. R. Lee, *Macromolecules* **2004**, *38*, 2546-2573.
[96] K. A. Mahmoud, Y.-T. Long, G. Schatte, H.-B. Kraatz, *Eur. J. Inorg. Chem.* **2005**, 173-180.
[97] F. Knobloch, W. Rauscher, *J. Polym. Sci.* **1961**, *54*, 651-658.
[98] C. M. Casado, M. Moran, J. Losada, I. Cuadrado, *Inorg. Chem.* **1995**, *34*, 1668-1680.
[99] Q.-W. Han, X.-Q. Zhu, X.-B. Hu, J.-P. Cheng, *Chem. J. Chin. Univ.* **2002**, *23*, 2076.
[100] Z. Akhter, A. Bashir, M. S. Khan, *Appl. Organometal. Chem.* **2005**, *19*, 848.
[101] N. Iqbal, Z. Akhter, M. A. Saeed, M. S. Khan, *Appl. Organometal. Chem.* **2006**, *20*, 344-350.
[102] S. Mehdipour-Ataei, A. Tadjarodi, S. Babanzadeh, *Eur. Polym. J.* **2007**, *43*, 498-506.
[103] K. Heinze, M. Schlenker, *Eur. J. Inorg. Chem.* **2005**, 66-71.
[104] S. Chowdhury, G. Schatte, H.-B. Kraatz, *Angew. Chem. Int. Ed.* **2006**, *45*, 6882-6884.
[105] S. Maricic, A. Ritzen, U. Berg, T. Frejd, *Tetrahedron* **2001**, *57*, 6523-6529
[106] S. Maricic, U. Berg, T. Frejd, *Tetrahedron* **2002**, *58*, 3085-3093
[107] S. Kaluz, S. Toma, *Collect. Czech. Chem. Commun.* **1988**, *53*, 638-642
[108] R. F. W. Jackson, D. Turner, M. H. Block, *Synlett* **1996**, 862-870.
[109] A.-S. Carlström, T. Frejd, *J. Org. Chem.* **1990**, *55*, 4175-4180
[110] B. Basu, S. K. Chattopadhyay, A. Ritzen, T. Frejd, *Tetrahedron: Asymmetry* **1997**, *8*, 1841-1846.
[111] S. Maricic, T. Frejd, *J. Org. Chem.* **2002**, *67*, 7600-7606.

CHAPTER 2

REARRANGEMENT OF THE ACTIVE ESTER INTERMEDIATE DURING HOBT/EDC AMIDE COUPLING

2.0. Connecting Text

The carbodiimide coupling protocol is often used in the peptide coupling for the activation of the carboxylic termini, which is then couples to the N terminal of the second amino acid. In order to begin this investigation, it was necessary to evaluate if the standard coupling protocol is applicable to the synthesis of ferrocene-peptides conjugates. This chapter describes the synthesis and full characterization of the new active ester benzotriazol-1-yl 1-(*tert*-butyloxycarbonylamino) ferrocene-1-carboxylate, which is a key intermediate in the coupling of Fca to the amino acids and peptides. This chapter also addresses the transformation of this active ester into inactive N-oxide derivative, 3-{[1-(*tert*-Butyloxycarbonylamino)ferrocen-1-yl]carbonyl}-benzotriazole 1-oxide, which represents a "non-productive" side products resulting in the loss of the organometallic label.

2.1. Introduction

1-Hydroxybenzotriazole (HOBt) is widely used in peptide synthesis as an activating agent for the acid component and for its ability to suppress racemization. The intermediate benzotriazole active ester **A** then reacts with an amino group to form urethane bond.[1] The conversion of **A** into the *N*-oxide isomer **B** was reported.[2, 3]

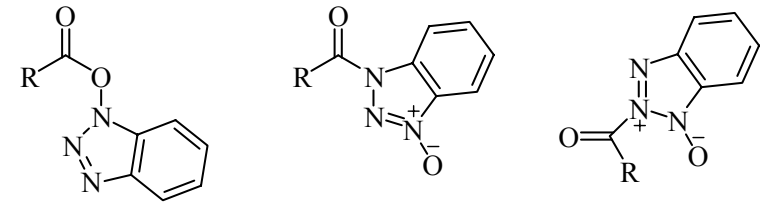

A **B** **C**

The *N*-oxide is favored in polar solvents, while the desired active ester **A** predominates in less-polar solvents.[4] It appears that the active ester **A** is the kinetic product, which is reactive towards rearrangement to the corresponding urethane form **B**.[5] In addition, Davies et al proposed the intermediacy of isomer **C** to explain enhanced racemization rates for certain amino acid esters.[6] Formation of the *N*-oxide under mild conditions was reported by Lu and coworkers by reacting Os_3 cluster with HOBt.[7] Carbon-13 NMR spectroscopy, used to identify the different isomers, confirmed the predominance of the active ester form **A** in DMSO,[8] while acetone will stabilize the more polar zwitterionic *N*-oxide.[9] More recently, Carpino reported a detailed investigation into the reactivity of the guanidinium salts HBTU and HATU. It was shown that the *O*-substituted uronium salt is significantly more reactive in peptide coupling reactions than the *N*-substituted guanidinium salt.[10]

In the context of organometallic peptide conjugates, OBt-active esters provide convenient route to label peptides under very mild conditions, which are also readily automated for solid-phase peptide synthesis (SPPS). That was shown by the use of ferrocenoyl hydroxybenzotriazole (Fc-CO-OBt) as a stoichiometric delivery reagent for the redox active ferrocene (Fc) group, or more recently by the use of one-pot reactions involving cobaltocenium carboxylic acid and TBTU and HATU.[11] Whether the active ester is used stoichiometrically or used as an intermediate in a one-pot reaction or during SPPS, there is the potential for lowered incorporation of the organometallic label due to different reaction kinetics. During the preparation and column separation of Fc-peptide conjugates, we and other groups noticed the appearance of a red Fc-containing material, which appears to possess also an OBt substituent. However, it was not possible to properly identify this material. Given the central role of OBt active ester intermediates for the preparation of organometallic peptide conjugates, we decided to investigate this in more detail. Here we describe our results of the study into the preparation of the OBt active ester of 1'-^{t}butylcarbamato-1-ferrocenecarboxylic acid (**2**) and its isomer 1-(3-benzotriazole-1-*N*-oxide)-1'-^{t}butylcarbamato ferrocene (**3**).

2.2. Results and Discussion

2.2.1 Synthesis and Characterization

During the synthesis of the active ester 1-(1-benzotriazolato)-1'-^{t}butylcarbamato ferrocene (**2**), from 1'-^{t}butylcarbamato-1-ferrocenecarboxylic acid (**1**) in the presence of HOBt, and EDC, we prepared and isolated in addition to the desired product **2**, the zwitterionic *N*-oxide 1-(3-benzotriazole-1-*N*-oxide)-1'-^{t}butylcarbamato ferrocene (**3**)

(Scheme 2.1). We have no indication for the formation of the 2-*N*-ferrocenylated product. The two forms are readily separated from each other by chromatography, giving **2** as an orange-red compound and compound **3** as a dark red crystalline compound. The experimental results show that the active ester **2** is kinetic product, which is reactive towards rearrangement to the corresponding urethane form.[5] The rearrangement process is a phase dependant; in dry dichloromethane give a product 4% of **3** while in aqueous acetone the rearrangement is faster producing 11% yield of **3**. . Although, we expected a higher reactivity according to earlier reports[10], the electron withdrawing effect of N-Oxide group most likely deactivates **3** with respect to its reactivity with the amino acids. Thus, we do not observe any reactivity with glycine.

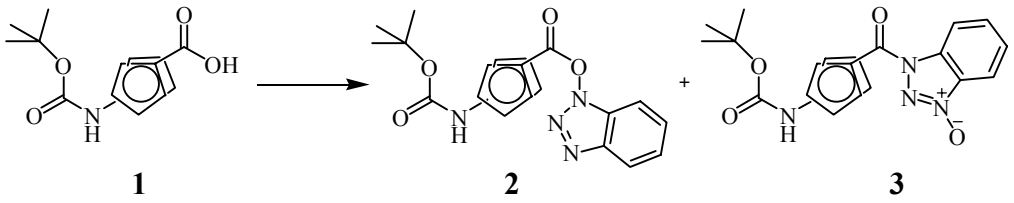

1 **2** **3**

Scheme 2.1. Two isolated products 1-(1-benzotriazolato)-1'-^{t}butylcarbamato ferrocene **2** and *N*-oxide 1-(3-benzotriazole-1-*N*-oxide)-1'-^{t}butylcarbamato ferrocene **3** resulted form the activation of 1'-^{t}butylcarbamato-1-ferrocenecarboxylic acid **1**

Compounds **2** and **3** were characterized by NMR spectroscopy ^{1}H, ^{13}C., DEPT-135 NMR, HMQC (Heteronuclear Multiple Quantum Correlation), and HMBC (Heteronuclear Multiple Bond Correlation). Table 2.1 summarizes the complete assignment of the NMR signals for compounds **2** and **3**. It is interesting to note that the signals due to H2, H5 and H2', H5' are observed at significantly different chemical shifts, indicating changes in local environment due to the change in the substituent, which undoubtedly affects both C rings. Changes are also significant in the ^{13}C

chemical shifts of the *ipso*-Cs indicating that electronic differences due to the substitutents are "seen" by the Fc system. C1 is affected more by the change from ester to amide N-oxide than C1', the ipso-C to which the different substituent is attached. Comparing the chemical shifts for the proton H11 in **2** and **3**, then this proton is particularly deshielded on due to the proximity to the N-oxide group in **3**. The NH proton showed broad singlet at δ 6.42 and 5.75 for **2** and **3**, respectively.

Table 2.1. Spectroscopic characterization of compounds **2** and **3.**

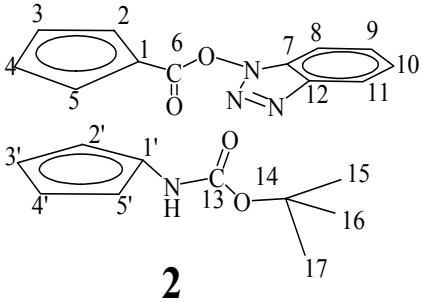

2

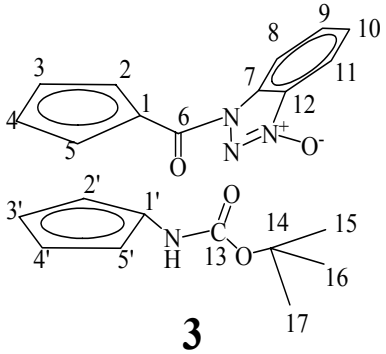

3

Site	^{1}H	^{13}C	HMQC	HMBC	^{1}H	^{13}C	HMQC	HMBC
1'				100.2				98.9
1				65.2				71.6
2' , 5'	4.71		62.9		4.52		62.7	
2 , 5	5.00		72.3		5.36		74.1	
3' , 4'	4.08		55.9		3.94		67.0	
3 , 4	4.62		74.7		4.63		74.8	
6		167.5				168.0		
7				129.5				132.4
8	8.02		120.8		7.97		115.7	
9	7.38		125.2		7.49		127.0	
10	7.49		129.1		7.72		133.2	
11	7.45		109.1		8.46		117.3	
12				143.9				133.82
13		153.5				153.5		
14				80.6				80.5
15-17	1.27		28.5				28.5	

Table 2.2. Relevant bond distances (Å) and angles (º) for **2** and **3**

	2	**3**
av Fe(1)-C(Cp1)	2.038(14)	2.039(13)
av Fe(1)-C(Cp2)	2.043(16)	2.047(12)
C(10)-C(15A)/ C(10)-C(15A)	1.489(9)	1.459(2)
C(15A)-O(11A)/ C(15)-O(11)	1.172(9)	1.210(2)
C(15A)-O(12A)/C(15)-N(11)	1.429(8)	1.426(2)
O(12A)-N(11)	1.358(3)	
N(11)-N(12)	1.342(2)	1.364(2)
N(12)-N(13)	1.302(4)	1.308(2)
N(13)-O(12)		1.2699(19)
C(20)-N(21)	1.411(4)	1.401(2)
N(21)-C(25)	1.349(4)	1.366(2)
C(25)-O(22)	1.350(3)	1.348(2)
C(25)-O(21)	1.207(3)	1.206(2)
C(10)-C(15A)-O(12A)/C(10)-C(15)-	106.6(6)	119.2(1)
C(10)-C(15)-O(11A)/C(10)-C(15)-O(11)	131.7(6)	125.4(2)
C(20)-N(21)-C(25)	123.7(2)	124.9(1)
N(11)-N(12)-N(13)	106.4(3)	105.5(1)
N(21)-C(25)-O(22)	109.6(2)	107.3(1)
N(21)-C(25)-O(21)	124.8(3)	126,0(1)

Both compounds exhibit a single broad absorbance in the visible region. For compound **2**, λ_{max} = 453 nm, while for **3** the band is observed at λ_{max} = 484 nm. This bathochromic shift clearly shows electronic coupling of the *N*-oxide OBt with the Fc group. Shifts were also observed for pyridine *N*-oxides (305-333 nm) and quinoline *N*-oxides (>320 nm) with substituents that are in direct conjugation with the *N*-oxide

group, and rationalized in terms of tautomer and resonance contributions. In quinoxaline-*N*,*N*-dioxide shifts are due to intramolecular charge transfer.[12] The IR spectra of both compounds show two carbonyl bands. For compound **2** a band due to the active ester is observed at 1788 cm^{-1}. This band is absent in compound **3** and is replaced by an amide band at 1688 cm^{-1}. Both compounds exhibit a strong absorption around 1722 cm^{-1}, due to the carbamate carbonyl group on the other Cp ring.

2.2.2. Crystal Structures of Compounds 2 and 3

Selected bond distances and angles for **2** and **3** are given in Table 2.2. ORTEP views are of these complexes are presented in Figures 2.1 and 2.2, respectively. Compound **2** crystallizes in the polar orthorhombic space group $Pna2_1$ as a twinned racemic crystal, whereas compound **3** crystallizes in the monoclinic space group $P2_1/c$. In both complexes, the Cp rings are virtually parallel to each other (Cp-Fe-Cp angles: **2**: 2.1(3)º; **3:** 2.98(14)º). The distances of the Fe atoms to the carbon atoms of the Cp rings are in the expected range in comparison to other ferrocene structures.[13]

For compound **2**, the bond distances and angles of the Cp-ester-benzotriazole moiety are almost identical to those reported for Fc-CO-OBt.[14, 15] The ester bond to the benzotriazole moiety in **2** is expectedly long (1.429(8) Å). The benzotriazole (Bt) substituent is rotated out of the ester plane only by 80.8(2)º, compared to 96.56(6)º in Fc-CO-OBt.[15] In case of Fc-CO-OBt, this does not permit the efficient interaction between the two π-systems,[15] but increases reactivity of the carbonyl C towards external nucleophiles to the carbonyl C and therefore allows a faster reaction of the ester. A similar observation was made for (S)-3-(O^{γ}-methyl.N^{α}-

triphenylmethylglutamyl) benzotriazole 1-oxide[16], which bears the acyl and OBt groups on the same plane, resulting in a slower reactivity towards amines compared to the OBt active ester.[17] 3-(N$^{\alpha}$-Tritylmethionyl)benzotriazole 1-oxide also exhibits the same structural features with co-planar OBt and acyl groups.[18]

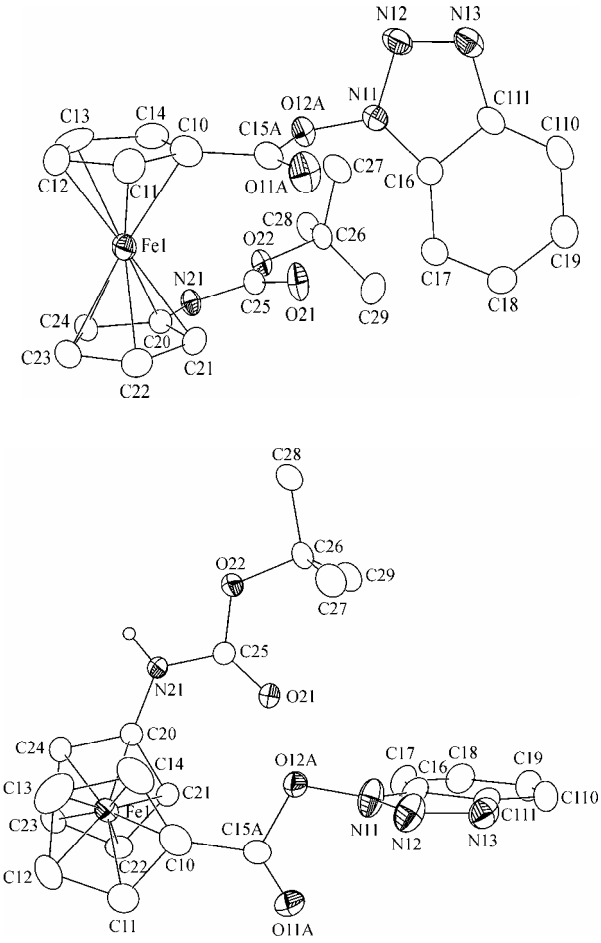

Figure 2.1. Ortep drawing of compound **2** (30% probability). H atoms omitted for clarity. Side-on view and view down the Cp-Fe-Cp axis to visualize the 1,2'-conformation of the Fc group.

The geometry and conformation for a variety of esters and amides derivatives of HOBt, HOAt and HOOBt have been reported.[19, 20] A more recent investigation into the reactivity of HATU showed that the O-substituted uronium salt is significantly more

reactive in peptide coupling reactions than the *N*-substituted guanidinium salt[10], in line with earlier investigations on OBt derivatives. In compound **3**, the planar OBt-N-oxide, the urethane and the Cp ring to which it is attached are not coplanar (OBt-N-oxide/Cp, 16.5(1)º; amide/Cp, 18.9(1)º). Just like the parent benzotriazole-1-oxide and hydroxybenzotriazole, the heterocycle in compound **3** is essentially flat. In the N-oxide, the N-N bond distances are shortened compared to hydroxybenzotriazole.

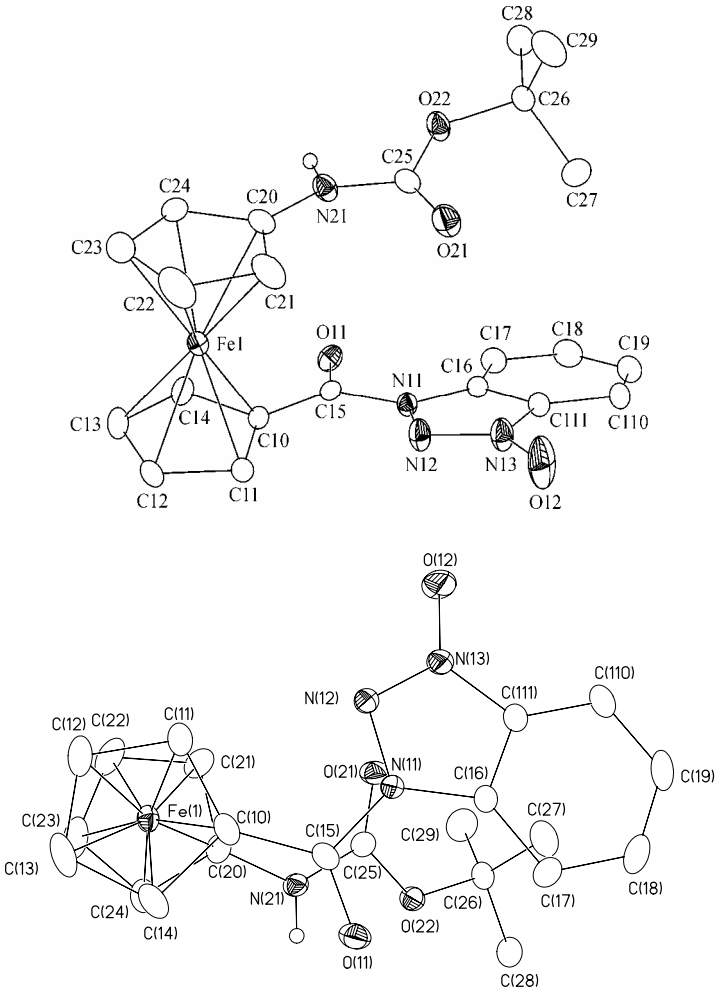

Figure 2.2. Ortep drawing of compound **3** (30% probability). H atoms omitted for clarity. Side-view and view down the Cp-Fe-Cp axis to show the 1,1'-conformation of the Fc system.

For compound **3**, the N-N bond distances in the heterocycle are non-equidistant. The distance between the N(O)-N are shorter and the distance N(12)-N(13) of 1.3084(19) Å indicates significant double bond character between the two nitrogen atoms. Similar observations were made before for (S)-3-(O^{γ}-methyl.N^{α}-triphenylmethylglutamyl) benzotriazole 1-oxide and 3-(N^{α}-tritylmethionyl)-benzotriazole 1-oxide. As you see from Table 2.3**,** the urethane moieties in **2** and **3** are not coplanar with the Cp rings. The observed ω angle for **2** is close to the ideal value for a 1,2' conformation (-72º), while **3** crystallizes in the 1,1'-conformation with ω = 13.3(8)°.

Table 2.3. Torsions angles (º) for **2** and **3**

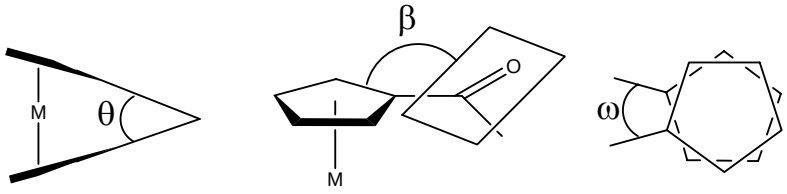

Angle	**2**	**3**
θ[a]	2.1(3)	2.98(14)
β[b]	5.0(7) [C(*ipso*)-C=O] / 12.3(2) [N-C=O]	18.8(2) [C(*ipso*)-C=O] / 18.9(1) [N-C=O]
ω[c]	-70.8(8)	13.3(8)

[a] The dihedral angle between two Cp rings. [b] The dihedral angle between the plane of the Cp ring and the C(*ipso*)C=O bond or between the plane of the Cp ring and the N-C=O bond. [c] The torsion angle is defined as C(*ipso*)-Cp(centroid)-Cp(centroid)-C(*ipso*). of the Cp ring and the C(*ipso*)C=O bond or between the plane of the Cp ring and the N-C=O bond. [c] The torsion angle is defined as C(*ipso*)-Cp(centroid)-Cp(centroid)-C(*ipso*).

There is no H-bonding present between adjacent molecules of **2**. The amide proton is does not point towards the Bt substituent. In contrast, H-bonding is observed

in the structure of compound **3** between oxygen atom attached to one of the nitrogen atoms of the Bt substituent, carrying a partial negative charge, and the amide proton in an adjacent molecule. The O(12)…N(21)* bond distances of 2.859(2) Å indicates the presence of strong H-bonding in the solid state.

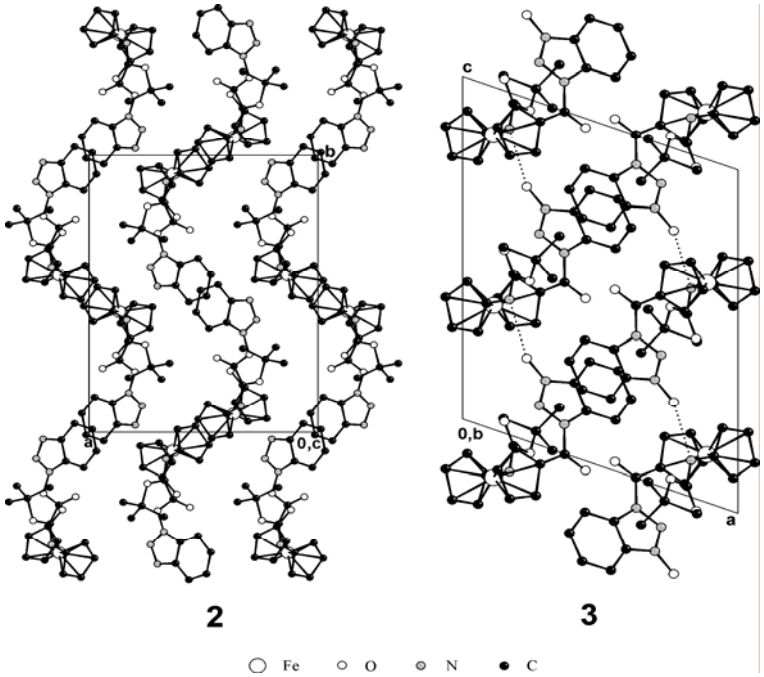

Figure 2.3. Packing diagrams for compounds **2** and **3**.

The packing arrangements in **2** and **3** are very different (Figure 2.3). In compound **3**, the Fc groups are lined up with the NO groups of the Bt group in the adjacent the molecules forming strands along the *c*-axis. In **2,** the molecules form a strand-like arrangement along the 2_1-axis with the Fc groups adjacent to each other.

Heinze recently[14] reported the structural properties of the acetylamino-analogue of compound **2**. In the solid state, the molecule displayed significant intramolecular H-

bonding. The Boc-derivative **2** on the other hand, does not display any intramolecular H-bonding involving the urethane NH. Compound **3** on the other hand displays intermolecular H-bonding in the solid state. This raises the question if the presence of the Boc-protecting group can account for the differences in H-bonding behavior in the solid-state structures. Is the lack of intramolecular H-bonding in compound **2** due to the spatial requirement of the bulky Boc carbamate group? In order to answer these questions, we decided to investigate the H-bonding behavior of compounds **2** and **3** in solution. Variable-temperature ^{1}H-NMR studies of compounds **2** and **3**, recorded at 1 and 50 mM in $CDCl_3$ in a temperature range between 215 and 308 K, showed a significant difference in the NH chemical shift between the two compounds with the temperature variation. A plot of the $\Delta\delta$ versus T is shown in Figure 2.4. For compound **2**, the chemical shift of the amide NH was affected by temperature but the temperature dependence was independent of concentration (1 mM: -5.1 ppb K^{-1}; 50 mM: -6.4 ppb K^{-1}). In contrast, compound **3** displayed a concentration dependent temperature behavior (1 mM: -2.8 ppb K^{-1}; 50 mM: -7.1 ppb K^{-1}), indicating the presence of intermolecular H-bonding in compound **3** in solution. The temperature behavior of the NH chemical shift indicates the presence of intramolecular H-bonding in compound **2** in solution.[11, 21] However, the crystal structure does not show any H-bonding, presumably as a result of crystal packing.

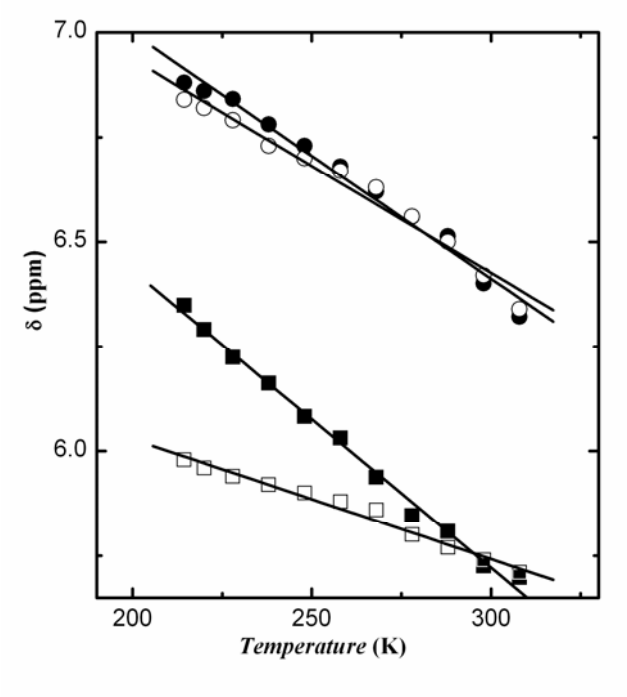

Figure 2.4. Temperature dependence of the chemical shifts for NH signals of compounds **2** (●,○) , **3**. (■,□) in $CDCl_3$. (○,□)-open shapes indicate 1 mM; (●,■)-solid shapes indicate 50 mM.

Interestingly, the Cp protons in compound **2** undergo some temperature dependent changes, as is shown in Figure 2.5. The signals due to H2 and H5 in compound **2** are very broad at low temperatures (215 - 220K) temperatures but appear at 228 K, and gradually sharpen. Heinze's Ac-derivative displays a similar temperature behavior and which was interpreted as a possible interconversion between two ferrocenyl rotamers of the molecule. Our results suggest that a similar equilibrium may exist also for compound **2**. The Cp region of compound **3** does not change with temperature (Figure 2.6).

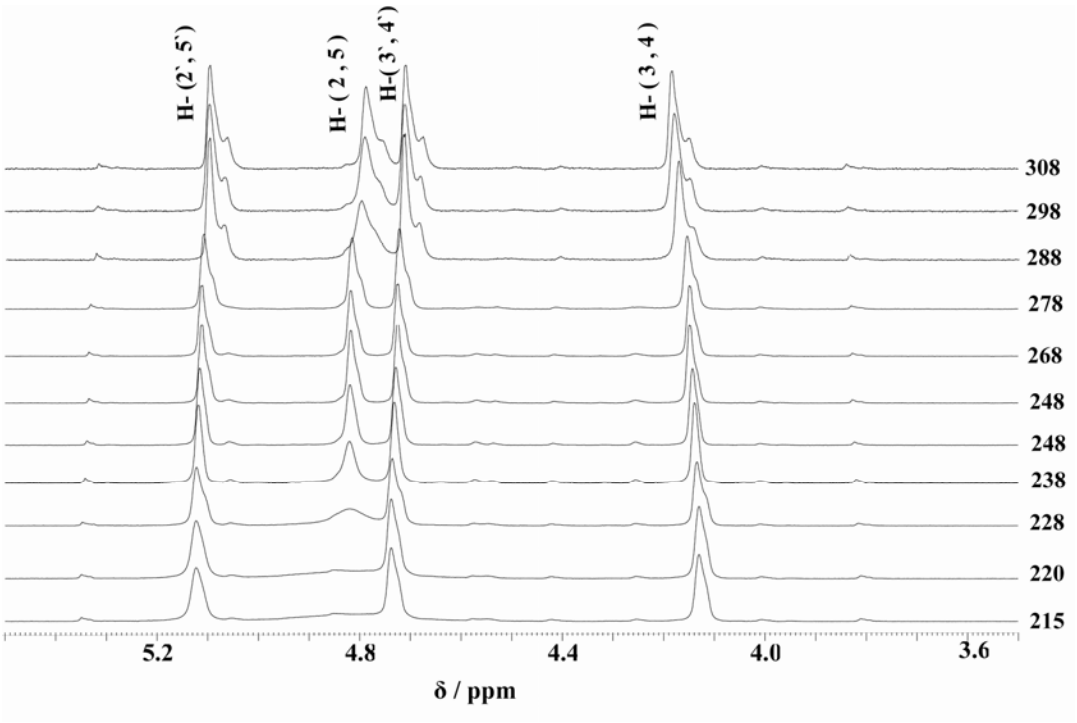

Figure 2.5. Variable temperature ^{1}H-NMR spectra of **2** (50 mM, $CHCl_3$) in a region of 215 – 308 K.

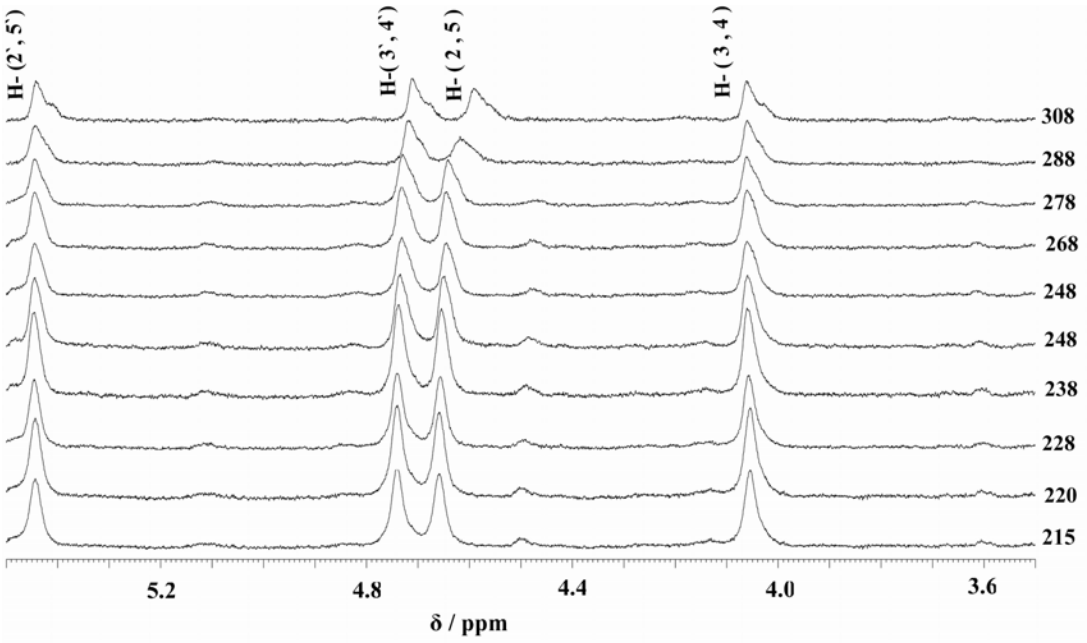

Figure 2.6. Variable temperature ^{1}H-NMR spectra of **3** (50 mM, $CDCl_3$).

2.2.3. Electrochemistry

Figure 2.7 shows the electrochemical behavior of compounds **2** and **3**. Both compounds show a quasi-reversible single one-electron oxidation. The separation between oxidative and reductive peak potentials ΔE_p is about 96±5 mV for **2** (87±5 mV for **3**). The ratio of peak currents is close to unity for both compounds (**2**: $i_c/i_a = 1$; **3**: $i_c/i_a = 1.05$). As expected for *N* and *O*-ferrocenylated systems, the halfwave potentials $E_{1/2}$ for **2** and **3** are significantly different. While $E_{1/2} = 672 \pm 5$ mV for the active ester **2**, the $E_{1/2} = 591 \pm 5$ mV for the *N*-oxide **3**.

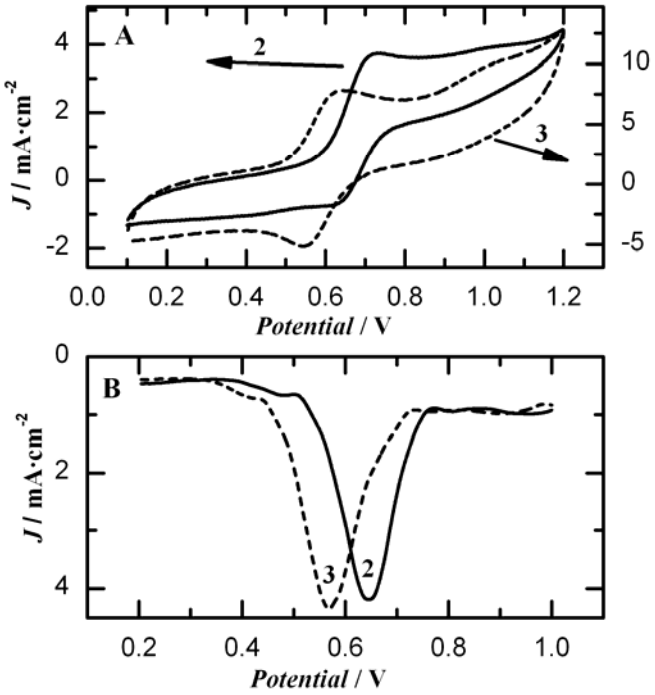

Figure 2.7. Electrochemical study of compounds **2** and **3** in CH_3CN/ 0.1 M TBAP: **A** shows the cyclic voltammetry at a scan rate of 100 mV/s (ΔE_p for the Fc/Fc^+ couple under identical conditions was 68 ±5 mV); **B** shows the differential pulse voltammetry at a scan rate 10 mV/s. for **2:** DPV, $E_p = 643 \pm 5$ mV; for **3**, $E_p = 566 \pm 5$ mV.

2.3. Conclusion

In summary, we have prepared the two ferrocene-amino acid derivatives (benzotriazol-1-yl)-1'-^{t}butylcarbamato ferrocene-1-carboxylate (**2**) and (benzotriazole-1-*N*-oxide-3-yl)-1'-^{t}butylcarbamato ferrocene-1- carboxylate (**3**) and report their full characterization. Initially, compound **3** was obtained as a by-product in the preparation of the desired active ester. Reports on HATU active esters show this to be a common reaction in peptide synthesis. Importantly, this by-product was not reported in ferrocene chemistry. Given the importance of Fc-OBt active ester intermediates in the preparation of Fc-bioconjugates and as potential intermediate for the stepwise synthesis of ferrocenamide-based polymers, our finding is significant. Importantly, the reactivity towards peptide coupling is different. Whereas, the active ester derivative **2** undergoes amide bond formation with glycine ethylester and other amino acids and peptides,[22] the *N*-oxide **3** does not react. This is in contrast with earlier reports on the reactivity of HATU *N*-oxide-derivatives, which were shown to undergo a slow conversion to the desired amide.

2.4. Experimental Section

2.4.1. General Procedure

The syntheses of 1'-^{t}butylcarbamato-1-ferrocenecarboxylic acid (**1**) was carried out using the published procedure.[23] All syntheses were carried out in air unless otherwise indicated. CH_2Cl_2 (BDH; ACS grade) used for synthesis was dried (CaH_2) and distilled prior to use. $CDCl_3$ (Aldrich) was dried (CaH_2) , and stored over molecular sieves (8-12 mesh; 4Å effective pore size; Fisher) before use. EDC·HCl, HOBt (Quantum), $MgSO_4$, and $NaHCO_3$ (VWR) were used as received. For column

chromatography, a column with a width of 2.7 cm (ID) and a length of 45 cm was packed 18-22 cm high with 230-400 mesh silica gel (VWR). For TLC, aluminum plates coated with silica gel 60 F_{254} (EM Science) were used. NMR spectra were recorded on a Bruker Avance-500 spectrometer using a 5-mm broadband probe operating at 500.134 MHz (^1H) and 125.766 MHz ($^{13}C\{^1H\}$). Peak positions in both ^1H and ^{13}C spectra are reported in ppm relative to TMS. The ^1H NMR spectra are referenced to the residual $CHCl_3$ signal at δ 7.27. All $^{13}C\{^1H\}$ spectra are referenced to the $CDCl_3$ signal at δ 77.23. Mass spectrometry was carried out on a VG Analytical 70/20 VSE instrument. Infrared spectra were obtained with a Perkin-Elmer model 1605 FT-IR.

2.4.2. Preparation of (Benzotriazol-1-yl)-1'-^{t}Butylcarbamato Ferrocene-1-Carboxylate (2) and (Benzotriazole-1-*N*-oxide-3-yl)-1'-^{t}Butylcarbamato Ferrocene-1-Carboxylate (3)

***Procedure A*:** To a solution of 1'-^{t}butylcarbamato-1-ferrocenecarboxylic acid (**1**) (3.68 mmol, 1.27 g) in CH_2Cl_2 (40 mL), solid HOBt (4.05 mmol, 0.62 g) and EDC·HCl (4.05 mmol, 0.78 g) were added. The reaction mixture was stirred for 2 hrs at room temperature (20°C) and then treated with an aqueous solution of saturated $NaHCO_3$, citric acid (10%), and water. The organic phase was separated and dried over Na_2SO_4, and the evaporated to dryness under reduced pressure. The crude product was purified by flash column chromatography (SiO_2, EthOAc:hexanes 1:2) to give dark orange crystals of compound **2** (1.32 g, 78%) (R_f = 0.74), followed by red crystals of compound **3** (68 mg, 4%) (R_f = 0.42).

***Procedure B*:** The same mixture as described under **A** was stirred for two hours at room temperature in aqueous acetone (30 ml). The reaction mixture was dried under

reduced pressure and re-dissolved in CH_2Cl_2. After the purification (vide supra), compounds **2** and **3** were obtained yields of (1.15 g, 64%) and (180 mg, 11%), respectively.

2.4.2.1 Characterization of Compound 2

FAB-MS (m/z): calc for $C_{22}H_{22}N_4O_4Fe$ $[M+1]^+$: 463.2; found: 463.1. FT-IR (KBr, cm^{-1}): 3322 (m, N-H), 1788, 1723 (s, C=O). UV-vis (MeCN; λ in nm (ε in $Lmol^{-1}cm^{-1}$)): 453 (706). ^{1}H-NMR $CDCl_3$, δ/ppm): 8.02 (1H, d, J_{HH} = 8.5 Hz, *Bt*-ArH), 7.49 (1H, t, J_{HH} = 15.0 Hz, *Bt*-ArH), 7.45 (1H, d, J_{HH} = 8.2 Hz, *Bt*-ArH), 7.38 (1H, t, J_{HH} = 15.2 Hz, *Bt*-ArH), 6.42 (1H, bs, NH), 5.00 (2H, s, H-2 and H-5, Fc), 4.71 (2H, s, H-2` and H-5`, Fc), 4.62 (2H, s, H-3 and H-4, Fc), 4.08 (2 H, s, H-3` and H-4`, Fc), 1.27 (9H, s, $C(CH_3)_3$). $^{13}C\{^1H\}$-NMR ($CDCl_3$, δ/ppm): 167.5 (s, *C*OON-Bt), 153.5 (s, $COOC(CH_3)_3$), 143.9, 129.5 (quaternary C of Ar Bt), 129.1, 125.2, 120.8, 109.1 (s, Ar Bt), 100.2 (C-1`, Fc), 80.58 ($C(CH_3)_3$), 74.7 (C-3 and C-4, Fc), 72.3 (C-2 and C-5, Fc), 66.9 (C-3` and C-4`, Fc), 65.2 (C-1, Fc), 62.3 (C-2` and C-5`, Fc), 28.5 ($C(CH_3)_3$).

2.4.2.2. Characterization of Compound 3

FAB-MS (m/z): calc for $C_{22}H_{22}N_4O_4Fe$ $[M+1]^+$: 463.2; found: 463.1. FT-IR (KBr, cm^{-1}): 3310 (m, N-H), 1721, 1688 (s, C=O). UV-vis (MeCN; λ in nm (ε in $Lmol^{-1}cm^{-1}$)): 484 (1200). ^{1}H-NMR $CDCl_3$, δ/ppm): 8.46 (1H, d, J_{HH} = 8.5 Hz, *Bt*-ArH), 7.97 (1H, d, J_{HH} = 8.4 Hz, *Bt*-ArH), 7.72 (1H, t, J_{HH} = 15.5 Hz, *Bt*-ArH), 7.49 (1H, t, J_{HH} = 17.3 Hz, *Bt*-ArH), 5.75 (1H, bs, NH), 5.36 (2H, s, H-2 and H-5, Fc), 4.63 (2H, s, H-3and H-4, Fc), 4.52 (2H, s, H-2` and H-5`, Fc), 3.94(2 H, s, H-3` and H-4`, Fc), 1.26

(9H, s, $C(CH_3)_3$). $^{13}C\{^1H\}$-NMR ($CDCl_3$, δ/ppm): 168.0 (s, *C*ON-Bt), 153.5 (s, $COO(CH_3)_3$), 133.8, 132.4 (quaternary C of Ar Bt), 133.2, 127.0, 117.3, 115.7 (Ar Bt), 98.9 (C-1`, Fc), 80.5 ($C(CH_3)_3$), 74.8 (C-3 and C-4, Fc), 74.1 (C-2 and C-5, Fc), 71.6 (C-1, Fc), 67.0 (C-3` and C-4`, Fc), 62.7 (C-2` and C-5`, Fc), 28.5 ($C(CH_3)_3$).

2.4.3. Attempted Coupling of (Benzotriazole-1-*N*-oxide-3-yl)-1'-^{t}Butylcarbamato Ferrocene-1-Carboxylate

A solution of H-Gly-OEt·HCl (0.24 mmol, 0.03 g) and Et_3N (0.4 ml) in dry CH_2Cl_2 (5 ml) was added to a stirring solution of **3** (0.22 mmol, 0.10 g) in dry CH_2Cl_2 (10 ml). Progress of the reaction was followed by TLC (EtOAc:hexanes:MeOH 4:5:1). No product was observed after 24 hrs.

2.4.4. Electrochemical Measurements

The electrochemical experiments were carried out at room temperature using CV-50W voltammetric analyzer. A gold electrode (diameter 50 μm) was used as working electrode. 1 mM solutions of compounds **2** and **3** were prepared in 0.1 M tetrabutylammonium perchlorate (TBAP) solution in a CH_3CN. The measurements carried out in a low scan rate of 100, 10 mV/s for cyclic voltammetry (CV) and Differential Pulse Voltammetry (DPV), respectively. A platinum wire (1 mm) was used as the counter electrode and a Ag/AgCl (BAS) was used a the reference electrode. The $E_{1/2}$ of the Fc/Fc^+ couple under the experimental conditions is 448(+/-5) mV (vs. Ag/AgCl).

2.4.5. X-ray Crystallography

Suitable crystals of compounds **2** (orange plate-like crystal; 0.15 × 0.15 × 0.10 mm) was obtained from a ether-layered solution of the compounds in chloroform, while **3** (dark red plate-like crystal; 0.25 × 0.20 × 0.13 mm) was obtained by a slow evaporation from Ethyl acetate- hexane (3:1) solvent mixture.

All measurements were made on a Nonius KappaCCD 4-Circle Kappa FR540C diffractometer using monochromated Mo K radiation (λ = 0.71073 Å) at -100 °C. An initial orientation matrix and cell was determined from 10 frames using φ scans.[24] Data were measured using φ- and ω-scans.[24] The data were processed using the standard Nonius software.[25] The structures were solved using direct methods (**2**: SIR-97; **3**: SHELXS-97)[26, 27] and refined by full-matrix least-squares method on F^2 with SHELXL97-2.[28] The non-hydrogen atoms were refined anisotropically. Hydrogen atoms were included at geometrically idealized positions (C-H bond distances 0.95/0.99 Å; N-H bond distances 0.88 Å) and were not refined. The isotropic thermal parameters of the hydrogen atoms were fixed at 1.2 times that of the preceding carbon or nitrogen atom. The carbon and oxygen atoms of one –C(O)O unit (labeled as C(15A), O(11A), O(12A), C(15B), O(11B), O(12B)) in **2** were disordered over two positions with site occupancy factors of 0.825(5) and 0.175(5). The refined absolute structure parameter [0.552(18)] for **2** was neither unity nor nil and was used as the scale parameter in the racemic twin refinement.

The hydrogen atom at nitrogen atom N(21) in **3** was located in Fourier difference map. Its coordinates were allowed to refine, whereas its isotropic thermal parameter was fixed at 1.2 times that of the preceding nitrogen atom. Data relating to

the structure determination are presented in Table 4. contains the supplementary crystallographic data for this paper. These data can be obtained free of charge at www.ccdc.cam.ac.uk/conts/retrieving.html [or from the Cambridge Crystallographic Data Centre, 12, Union Road, Cambridge CB2 1EZ, UK; fax: (internat.) +44-1223/336-033; E-mail: deposit@ccdc.cam.ac.uk].

Table 2.4. X-ray crystallographic data of complexes **2** and **3**.

	2	**3**
Formula	$C_{22}H_{22}FeN_4O_4$	$C_{22}H_{22}FeN_4O_4$
Molecular mass	462.29	462.29
Crystal dimensions /mm	0.15 × 0.15 × 0.10	0.25 × 0.20 × 0.13
Crystal system	Orthorhombic	monoclinic
Space group (no.)	$Pna2_1$	$P2_1/c$ (14)
a /Å	12.6580(2)	11.8140(2)
b /Å	17.2760(3)	12.0982(2)
c /Å	9.7170(5)	15.4850(3)
β /Å	90	110.9844(8)
Cell volume /Å^3	2124.91(2)	2066.45(6)
Molecular units per cell	4	4
μ /mm^{-1}	0.746	0.768
Density (calcd.) /g cm^{-3}	1.445	1.486
T /K	173	173
Scan range (2θ)	1.99 – 24.70	3.28 – 30.06
Scan speed /sec frame^{-1}	135	40
Measured reflections	3462	11239
Unique reflections	3462	6005
Obs. Reflections (I ≥ 2)	3187	4632
Parameters refined	312	286
Max. residual electron Density /Å^{-3}	0.297 / -0.211	0.357/-0.374
Agreement factors (F^2 refinement)	R_1 = 3.27%	R_1 = 3.90%
	R_w = 6.87%	R_w = 9.05%

[a] $R_1 = [\Sigma||F_o|-|F_c||]/[\Sigma|F_o|]$ for $[I > 2\sigma(I)]$

[b] $wR_2 = \{[\Sigma w(F_o^2-F_c^2)^2]/[\Sigma w(F_o^2)^2]\}^{1/2}$ [all data CCDC-241248 (**2**), 236850 (**3**)

2.5. References

[1] W. Konig, R. Geiger, *Chem. Ber.* **1970**, *103*, 788-794.
[2] S. I. Murahashi, H. Mitsui, T. Watanabe, S. I. Zenki, *Tetrahedron Lett.* **1983**, *24*, 1049-1052.
[3] R. Bosch, G. Jung, W. Winter, *Acta Chyst.* **1983**, *C39*, 1089-1092.
[4] F. T. Boyle, R. A. Y. Jones, *J. Chem. Soc. Perkin Trans* **1973**, *2*, 160-164.
[5] J. Singh, R. Fox, M. Wong, T. P. Kissick, J. l. Moniot, *J. Org. Chem.* **1988**, *53*, 205-208.
[6] J. S. Davies, A. K. Mohammed, *J. Chem. Soc. Perkin Trans* **1981**, *1*, 2982-2990.
[7] K. Lu, S. Kumaresan, Y. Wen, J. R. Hwu, *Organometallics* **1994**, *13*, 3170-3176.
[8] F. Alain, J. Elguero, A. F. Hegarty, D. G. McCarthy, *Organic Magnetic Resonance* **1980**, *13*, 339-345.
[9] E. Anders, A. R. Katritzky, N. Malhotra, J. Stevens, *J. Org. Chem.* **1992**, *57*, 3698-3705.
[10] L. A. Carpino, H. Imazumi, A. El-Faham, *Angew. Chem. Int. Ed. Engl* **2002**, *41*, 441-445.
[11] D. R. v. Staveren, T. Weyhermuller, N. Metzler-Nolte, *Dalton Trans* **2003**, 210-220.
[12] V. P. Andreev, A. V. Ryzhakov, *Khimiya Geterotsiklicheskikh Soedinenii* **1993**, *12*, 1662-1969.
[13] T. Okamura, K. Sakauye, N. Ueyama, A. Nakamura, *Inorg. Chem.* **1998**, *37*, 6731-6736.
[14] Heinze, M. Schlenker, *Eur. J. Inorg. Chem.* **2004**, *14,* 2974-2988.
[15] H.-B. Kraatz, J. Lusztyk, G. D. Enright, *Inorg. Chem.* **1997**, *36*, 2400-2405.
[16] p. Mamos, D. Papaioannou, C. Kavounis, V. Nastopoulos, *Acta Cryst.* **1997**, *C53*, 1973-1975.
[17] K. Barlos, D. Papaioannou, D. Theodoropoulos, *Int. J. Peptide Protein Res.* **1984**, *23*, 300-305.
[18] k. Barlos, D. Papaioannou, S. Voliotis, R. Prewo, J. Bieri, *J. Org. Chem.* **1985**, *50*, 696-697.
[19] M. Crisma, G. valle, V. Moretto, F. Formaggio, C. Toniolo, *Lett. Pept. Sci.* **1998**, *5*, 247-258.
[20] C. Toniolo, M. Crisma, F. Formaggio, *Biopolymers(Pept. Sci.)* **1996**, *40*, 627-651.
[21] E. S. Stevens, N. Sugawara, G. M. Bonora, C. Toniolo, *j. Am. Chem. Soc.* **1980**, *102*, 7048-7050.
[22] N. Metzler-Nolte, *private communication*.
[23] L. Barisic, V. Kovac, *Croat. Chem. Acta* **2002**, *75*, 199-206.
[24] COLLECT data collection software, N. B.V., **1998**.
[25] H. D. SCALEPACK, W. M. v1.96: Z. Otwinowski, *Processing of X-ray Diffraction Data Collected in Oscillation Mode, Methods in Enzymology, Vol. 276*, Macromolecular Crystallography, Part A, Carter, C. W., Jr., Sweet, R. M., Eds.; Academic Press, San Diego, CA, **1997**.
[26] A. Altomare, G. Cascarano, A. Giacovazzo, A. G. G. Guagliardi, M. C. Moliterni, G. Burla, M. Polidori, R. Camalli, S.-. Spagna, *J. Appl. Crystallogr.* **1999**, *32*, 115-119.
[27] G. M. Sheldrick, SHELXS-97., University of Gottingen, Gottingen, Germany, **1997**.
[28] G. M. S.-. Sheldrick, Program for the Solution of Crystal Structures; University of Gottingen, Gottingen, Germany, 1997.

CHAPTER 3

HELICALLY CHIRAL ALANINE PEPTIDES CONTAINING 1'-AMINOFERROCENE-1-CARBOXYLIC ACID SUBUNIT AS TURN INDUCER

3.0. Connecting Text

In Chapter 2 it was demonstrated that the synthesis of the Fca-active esters derivative of Fca allows effective coupling of Fca to the amino acids and peptides. This Chapter presents the next step in the investigation, which is a detailed structural study of Fca-peptide conjugates. Fca was attached to D- and L- amino acids and peptides from the carboxy and/or amino terminals. The structural properties of the conjugates in solid state as well as in solution were assessed by a variety of techniques including x-ray crystallography, IR, NMR, and circular dicroism. This study was aimed at investigating the ability of Fca to impose secondary structural elements on the peptide structure. By doing so, it was possible to develop a general strategy of using Fca to induce a turn-like structure in Fca-peptide conjugates, which are stable in solution and in the solid state.

This Chapter was extracted from the original international collaboration paper (Reference: Barišić, L.; Čakić, M.; Mahmoud, K. A.; Liu, Y. N.; Kraatz, H.-B.; Pritzkow, H.; Kirin, S. I.; Metzler-Nolte, N.; Rapić, V., *Chem. Eur. J.* **2006**, 12, 4965-4980 Copyright © 2006, Wiley VCH). Therefore, the Chapter is reformatted and only work carried out by me is described in terms of experimental and discussion.

3.1. Introduction

Architectural control of the supramolecular structure of peptides is of importance for the development of functional materials with potential applications in bioelectronics or biophotonics.[1] In addition, the design of structurally well-defined peptides is essential for understanding biochemical process of naturally occurring proteins and enzymes.[2]

Molecular scaffolds are commonly used to impart a specific secondary structure onto a peptide backbone. In addition to the known organic molecular scaffolds, ferrocenes (Fc) are widely recognized as organometallic redox active scaffold.[3] The structure of Fc has a central reverse-turn unit with inter-ring spacing of about 3.3 Å, which is suitable for intra-strand H-bonding interactions as was observed in β-sheets.[4] One advantage of utilizing Fc as scaffold is the ability to influence the formation H-bonded assemblies. Figure 3.1 describes three different types of disubstituted Fc peptide systems: derived from Fc-dicarboxylic acid ($Fc[COOH]_2$, **I**), Fc-amino acid (Fca, **II**), and Fc-diamine ($Fc[NH_2]_2$, **III**). Conjugates of type-**I** can give raise to H-bonded β-sheet like structure or even engage in chiral helical arrangements (Figure 3.1).[5-10] Only recently some peptide derivatives of Fca and Fc-diamine became available, from type-**II** and type-**III**, respectively.[11] It was proposed that more rigid macrocyclic peptides, based on Fc-diacid or Fc-diamine building blocks have allowed for systems able to engage in well defined inter-molecular H-bonding.[11] Derivatives of Fc-diacid was used as a transition state analogue in an antibody-catalyzed Diels-Alder reaction.[12] The same group reported an early synthesis of 1'-aminoferrocene-1-carboxylic acid ("ferrocene amino acid"; Fca).[12a, 13]

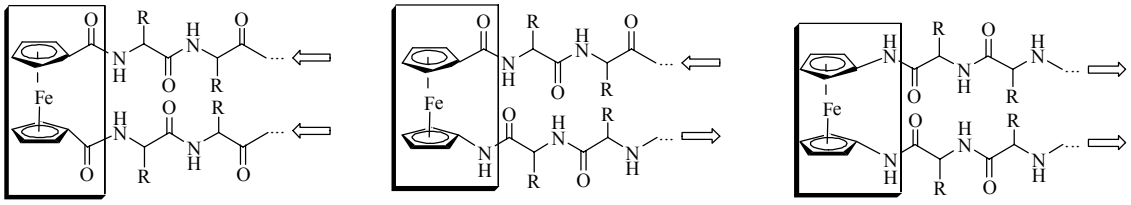

Fc-diacid **I**
parallel strands

Fca **II**
antiparallel strands

Fc-diamine **III**
parallel strands

Figure 3.1. The ferrocene-derived peptide conjugates. Arrows point from the C to the N terminals.

Rapić and coworkers reported on the efficient synthesis of Fca and described the synthesis of some related Fca-conjugates.[14] Recently, Rapić and Metzler-Nolte described the first Fca-peptides conjugate, initial studies proposed Fca can induce the formation of a peptide turn.[15] Herein, we wish to expand on the initial investigations and demonstrate the ability of Fca to impose specific secondary structural elements onto the peptide. Varity of systematic spectroscopic techniques such as CD NMR and IR as well as crystallographic conformational analysis will be utilized in the investigation.

3.2. Results and Discussion

3.2.1. Synthesis and Characterization

The preparation of the Fca-peptide conjugates **2-9** starting from Boc-Fca-OH **1** is summarized in Scheme 3. First, the acid terminus of Fca was activated by 1-hydroxybenzotriazole (HOBt) and *N*-(3-dimethylaminopropyl)-*N′*-ethylcarbodiimide hydrochloride (EDC) and coupled with L- and D-Ala of H-Ala-OMe resulting in the formation of the C-terminal peptide conjugates **2** (74%), **3** (75%), respectively.

Peptides **2** can be N-modified after Boc-deprotection of the organometallic core, followed by coupling with Boc-D-Ala-OH giving the tripeptide **4** (72%). In a similar

manner, dipeptide **3** was coupled with Boc-Ala-OH to yield tripeptide **5** (78%), The peptide can be elongated from the C- or the N-terminal side, followed by coupling with the desired amino acid derivative. For example, tetrapeptide **7** was prepared from **4** also tetrapeptide **6** was prepared following the same procedure. *N*-deprotection of compound **6**, followed by coupling with Boc-D-Ala-OH using O-(1H-benzotriazole-1-yl)-*N*,*N*,*N*′,*N*′-tetramethyluronium hexafluorophosphate HBTU/HOBt results cleanly in formation of the pentapeptide **8**. Analogously, N-terminal coupling of Boc-D-Ala-OH with compound **7** results in formation of the pentapeptide **9**.

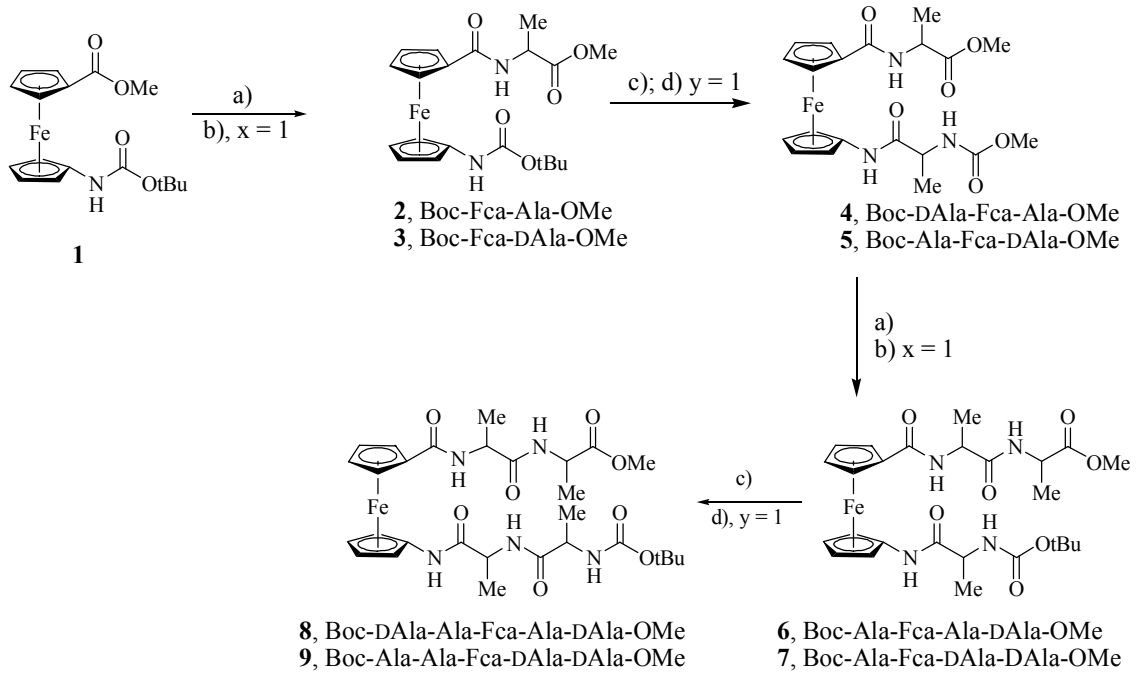

Scheme 3.1. Syntheses of Fca peptides. (a) 1 M NaOH; (b) 1. EDC/HOBt or HBTU/HOBt, CH_2Cl_2, 2. H-$(Aaa)_x$-OMe·HCl/NEt_3, CH_2Cl_2; (c) HCl (gas)/EtOAc or TFA; (d) 1. EDC/HOBt or HBTU/HOBt, CH_2Cl_2, 2. Boc-$(Aaa)_y$-OH/NEt_3, CH_2Cl_2.

Table 3.1. Chemical shifts of the amino-protons of Fca-peptides. and standard numbering scheme.

Compd.	Formula	δ (CD_3Cl)[a]	δ (DMSO)[a]	Δδ
2, 3	Boc-Fca-Ala-OMe	6.40 (s), 6.77(bs)	8.43(bs), 8.04(d)	2.03, 1.27
4	Boc- D-Ala1'-Fca-Ala1-OMe	7.35(d), 5.40(bs), 4.88(s)	9.31(bs), 8.06(d), 7.04(d)	1.96, 2.60, 2.16
5	Boc- Ala1'-Fca-D-Ala1-OMe	7.18(d), 5.29(bs), 4.92(m)	9.31(bs), 8.05(d), 7.04(d)	2.13, 2.66, 2.12
6	Boc-Ala-1'-Fca-Ala1-D-Ala2-OMe	9.41(bs), 7.84(d), 7.29(d), 5.10(d)	9.32(s), 8.28(d), 7.77(d), 7.01(d)	-0.09, 0.44, 0.48, 1.91
7	Boc-Ala-1'-Fca-D-Ala1-D-Ala2-OMe	8.61(bs), 7.41(d), 7.18(d), 5.14(d)	9.30(bs), 8.27(d), 7.74(d), 7.00(d)	0.69, 0.86, 0.56, 1.86
8	Boc-D-Ala2'-Ala1'-Fca-Ala1-D-Ala2-OMe	9.08(bs), 7.83(bs), 7.28b(s), 7.20(s), 5.20(d)	9.19(bs), 8.30(d), 8.02(d), 7.73(d), 7.01(d)	0.11, 0.47, 0.74, 0.53, 1.81

[a] 5×10^{-3} – 2×10^{-4} M; Fca ≡1'-aminoferrocene-1-carboxylic acid.

NMR measurements were carried out on all compounds in two solvents: DMSO-*d6* and $CDCl_3$. In general, it can be expected a presence of an equilibrium between intra-molecular H-bonded and non-H-bonded states in solution. In addition, it was expected that non-polar solvents, such as $CDCl_3$, favor intra-molecular H-bonded structures, while polar solvents such as DMSO disrupt H-bonding by competing with the H-bonding sites. Ideally, higher chemical shift of the amide protons should be observed for H-bonded structures when compared with the non-H-bonded structures. However, NMR timescale is not fast enough to determine the equilibrium between these states, which is a reason for not observing resolved signals for these states. Rather, an average value for δ is observed at shifts higher than expected for the putative non-H-bonded species. The position of this equilibrium is strongly solvent dependent. The resulting chemical shift differences (Δδ) from measurements in the two solvents will be used to determine the populations in the H-bonded and non-H-bonded states (see Table 3.1).[17]

Dipeptide **3** was used as an example to demonstrate this study. In $CDCl_3$ solution, compound **3** exhibits two amide resonances: at δ 6.77 for the NH_{Ala} and at 6.40 for the NH_{Fca} group. In DMSO-d_6, the resonances at δ 8.04 (NH_{Ala}) and 8.43 (NH_{Fca}) are observed. The chemical shift differences for the two amide protons in the two solvents are Δδ = 1.27 for the NH_{Ala} and Δδ = 2.03 for the Fca-NH group. That may indicate the presence of medium-strength hydrogen bonds.

Similarly, tetrapeptide **6** was used as another representative example. In $CDCl_3$, **6** displays four amide resonances at δ 5.10 ($NH_{Ala1'}$), 9.41 (NH_{Fca}), 7.87 (NH_{Ala1}), and 7.29 (NH_{Ala2}). In DMSO-d_6, the resonances shift to δ 7.01 for $NH_{Ala1'}$, 9.32 for NH_{Fca}, 7.77 for NH_{Ala1}, and 8.28 for NH_{Ala2}. The chemical shift of both proximal NH protons

(NH_{Fca} and NH_{Ala1}) moves strongly downfield in $CDCl_3$ solutions if both Cp rings a substituted by amino acids because of the formation of intra-molecular H-bonds which involve these two protons. This H-bonding is disrupted in DMSO and consequently the order of the Ala1 and Ala2 amide protons is reversed. The chemical shift differences $\Delta\delta$ for the four amide resonances in **6** are 0.44, 0.48, -0.09, 1.91

The length of the peptide chain dominates the ability to maintain a conformation. Thus, only a single H-bond was adopted by short Fca peptides such as **2** and **3** in solution. As a result, they exist as a mixture of conformers in solution. The longer Fca-peptides **4 - 9** can form two intra-molecular H-bonds between the podant peptide chains, resulting in a single conformer in the solid state as well as in solution.

Solution IR studies, recorded in dichloromethane ($c = 10^{-2}$ M L^{-1}), were used to discriminate between the specific hydrogen bonded and non-H-bonded isomers for the compounds under investigation. As examples for our discussion sample compounds will be discussed and compared with the results from NMR studies. IR spectra of the dipeptides **2** and **3** showed two Amide A bands of approximately equal intensities typical of non-H-bonded NH at the first one resonated at around 3433 cm^{-1} that is typical region for non-H-bonded NH and the second was around 3327 cm^{-1} representing the H-bonded NH. These results compared well with the NMR studies. Both NMR and IR analyses indicate that intra-molecular H-bonding in the tetrapeptide **6** is stronger compared to the related dipeptide **2**, since the IR band is slightly shifted to lower wavenumbers and compared to that found in compound **2**.

From the NMR results, we observe higher peptides **4** and **5** belong to another structural type having very strong H-bonds forming 9- and 11-membered ring.

Expectedly the IR spectra of these oligopeptides were very similar. They contained one relatively narrow band in the range 3426-3438 cm^{-1}, assigned to non-H-bonded NH and three broad signals at 3355-3373, 3283-3322, and 3251 cm^{-1} corresponding to intra-molecular H-bonding. The first absorption may be attributed to the weak or medium intra-molecular H-bonded NH subunits of Ala1', Ala2' and Ala2. We assign the other absorptions to the strongly H-bonded NH_{Fca} group.

3.2.2. X-Ray Crystallography

Single crystals suitable for an X-ray analysis were obtained for two compounds in this study. Peptides **2** and **3** were crystallized by slow diffusion of ether in a chloroform solution (γ = 10 mg ml^{-1}). Crystal structures of these compounds are shown in Figures 2 - 4. Three potential intra-molecular H-bonded conformers and one open conformer can be described for compound **2** (Figure 3.2).

For example, in conformer **2A** CO and NH groups directly attached to the Fc moiety are engaged in H-bonding resulting in a 6-membered ring. Conformer **2B** has an H-bond between the amide Fca-CO-NH and the CO-NH-Fca forming an 8-membered H-bonded ring. Conformer **2C** has the distal C=O group engaging in H-bonding with the NH-Fc group giving a 9-membered ring. While intra-molecular hydrogen bonding pattern differs significantly, the structures show a similar inter-molecular hydrogen bonding pattern. The two compounds **2** and **3** crystallize in the $P2_12_12_1$ space group and build chains along the crystallographic c axis, connected via one hydrogen bond, as exemplified for dipeptide **2** in Figure 3.3.

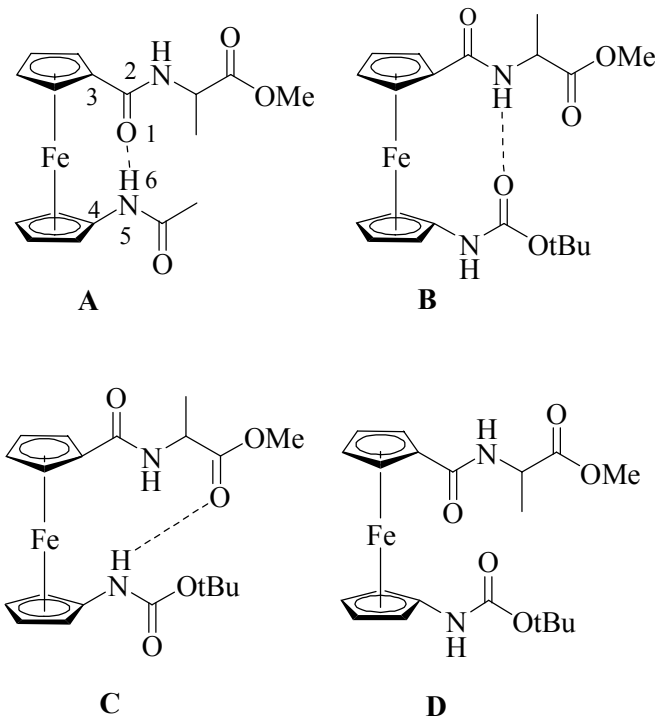

Figure 3.2. Possible H-bonding pattern in **2**. The numbering scheme is presented for conformer **A**, for the specification of ring size in the H-boded species. The pattern **D** has no intra-molecular H-bonds and could exist in equilibrium with an "open isomer.

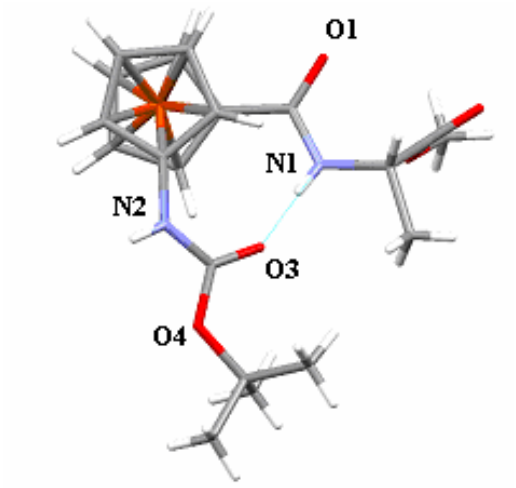

Figure 3.3. Crystal structure of **2** showing a L,*M*-configuration with one hydrogen bond.

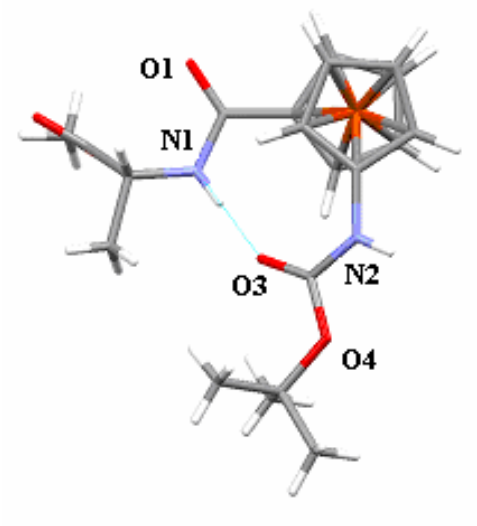

Figure 3.4. Crystal structure of **3** showing a D,*P*-configuration with one hydrogen bond.

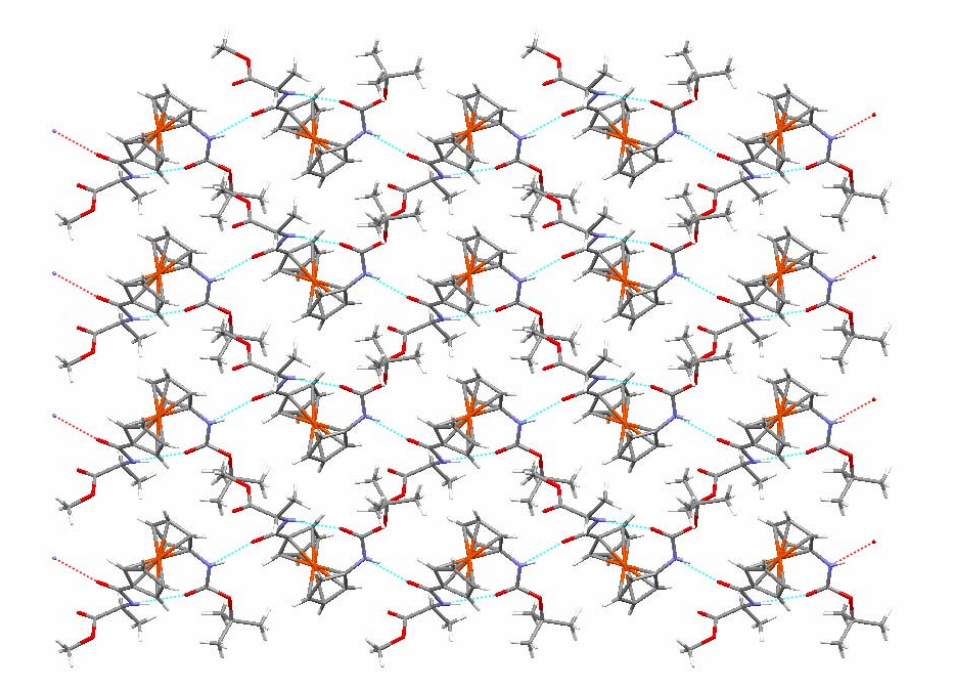

Figure 3.5. Crystal packing of **2**, view down the b axis.

The enantiomeric dipeptides **2** and **3** were crystallized from the same solvent system, and the same conformation was obtained. They represent the first examples where the "β-sheet like" conformer **B** was found in the solid state (Figures 3.3, 3.4 and

3.5). The stereochemistry is L,M for **2** and D,P for **3**, with one 8-membered intra-molecular hydrogen bond.

Bond lengths and angles found in the X-ray structures of **2** and **3** are in the expected range. A number of more significant structural parameters is collected in Table 3.2 and explained in Figure 3.6. In all three compounds, the two Cp rings are almost parallel to each other and consequently, the tilt angles are very small, $\theta < 4°$. The ω angles are close to the ideal value in a 1,2'-conformation (360° / 5 = 72°) in all cases. A more interesting example is provided by the dihedral angle β and the pyramidalization of the amide nitrogen atoms. Dipeptides **2** , **3** have some strain. In L-Ala conjugate **2** and D-Ala compound **3** the β_{CO} is about 10°, but the sum of angles around the amide nitrogen atom N51 is only about 353°. It can be concluded that dipeptides **2** and **3** have to accommodate some sterical hindrance in order to gain stabilization energy from the formation of one "β-sheet like" hydrogen bond.

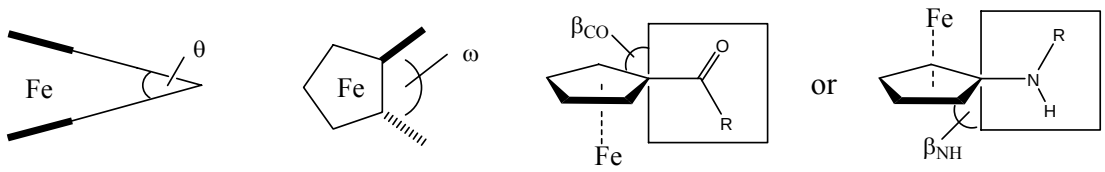

Figure 3.6. Tilt angle θ is the dihedral angle between the two Cp rings; ω is the dihedral angle between the two ring-bound substituents: C(*ipso*) - Cp(centroid) - Cp(centroid) - C(*ipso*); β is the dihedral angle between the Cp ring and the –NHR (β_{NH}) or –COR´ (β_{CO}) substituent.

Table 3.2. Selected parameters in the crystal structures of **2** and **3**.

Parameter	**2**	**3**
N1 – O3 / Å[a]	2.90	2.90
N2 – O1 / Å[b]	2.86	2.86
θ / °	2.0	1.9
β_{NH} / °	29.6	29.7
β_{CO} / °	9.3	9.3
ω / °	85.1	85.0
Angle sum around N2 / [°]	359.7	359.8
Angle sum around N1 / [°]	352.1	353.9

[a] intra-molecular hydrogen bond,[b] inter-molecular hydrogen bond.

3.2.3. CD-Spectroscopy

As we have learned from the crystallographic analyses of dipeptides **2** and **3,** intra-molecular H-bonds are present in the solid state. This raises the question if the H-bonded structure persists in solution. CD spectroscopy was used for conformational analysis of the ferrocene peptides **2** - **9** in CH_3CN solution. CD signals between 300 - 600 nm are characteristic for metal-centered transitions. In particular, the band at 480 nm was described as a strong indication for a helically chiral ferrocene moiety.[5b] Molar ellipticities, M_θ, were used in order to facilitate a comparison between different compounds. The CD spectra of ferrocene dipeptides **2** and **3**, both substituted at the C-terminus only, are displayed in Figure 3.7. As expected, the CD spectra of enantiomers **2** and **3** are a mirror image of each other. The L,M-derivative **2** displays a negative CD signal for the lowest energy band at about 500 nm, while this signal is positive for D,P-**3**.

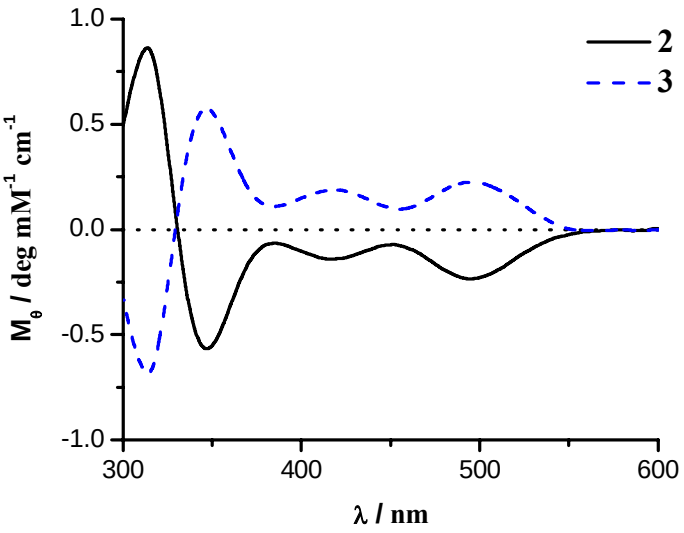

Figure 3.7. CD spectra (CH_3CN) of the dipeptides **2** and **3**

The CD spectra of higher Fca peptides are shown in Figure 3.8 with the examples of compounds **4**, **5** and **9**. All spectra of the ferrocene peptides **4** - **9** are qualitatively alike in the region above 400 nm with one signal centered at 480 nm, and differ significantly from the dipeptide **2** in Figure 3.7. This indicates that the solution conformation of ferrocene peptides **4** - **9** is similar, but different from that of **2**. However, an important finding is that the helical chirality of Fca peptides is dominated only by the chirality of the N-terminal amino acid on Fca: Boc-Ala-Fca-D-Ala-OMe **5** displays a positive CD signal at about 480 nm that is changed to negative in Boc-DAla-Fca-Ala-OMe **4**, Fig. 3.8. On the other hand, the same change on the C-terminus of Fca has no effect on the helicity of the central ferrocene core (**4** → **5**). The chirality of the outer Ala has no influence on the helical chiraliy of the ferrocene. In addition, a non-monotonous correlation between the magnitude of the CD signal and the number of Ala

subunits was observed, but roughly the intensity of the CD signal rise form shorter to longer oligopeptides (**4** → **9**).

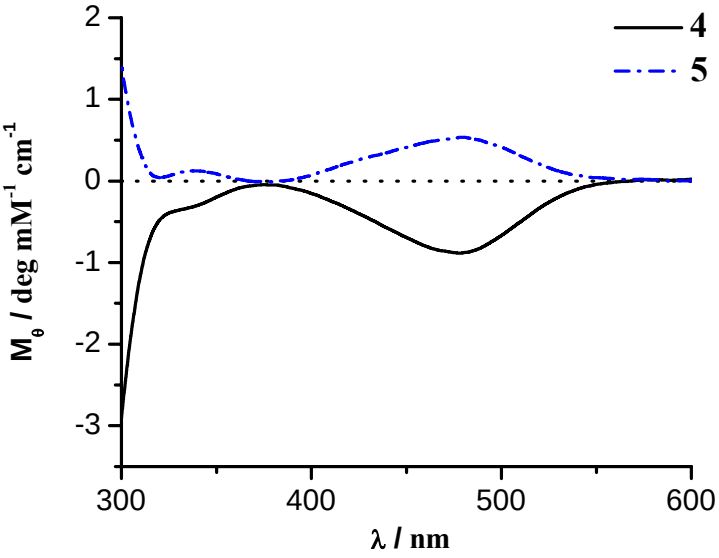

Figure 3.8. CD spectra (CH_3CN) of the tripeptides **4** and **5**

It should be noted that CD spectra give rise to relatively broad signals. Thus signals arising from structurally related but slightly different compounds such as the ones studied herein will not be resolved. In addition, dynamic equilibrium is impossible to detect by CD spectroscopy alone.

3.2.4. Electrochemistry

The electrochemical behavior of compounds **2-9** was studied by cyclic voltammetry (CV). All ferrocene-containing amino acid and peptide conjugates discussed in this study exhibit a reversible electrochemical one-electron oxidation. For Fca peptide derivatives, the half-wave potentials $E_{1/2}$ are observed in a range of 476 - 533 mV vs. Ag/AgCl, with peak-to-peak separation ΔE_p of 63 to 98 mV and with a

Faradic current ratio of close to unity. Importantly, we do not observe any amino acid or peptide specific trends. All experimental values are listed in Table 3.3.

Table 3.3. Solution electrochemical results for compounds **2-9.** Conditions: 1 mM in MeCN; glassy carbon working electrode (BAS), Pt counter, Ag/AgCl reference, 0.1 M TBAP; E in mV and I_p in μA; errors in the measured potentials are ± 5 mV from five independent measurements.

Compound	$E_{1/2}$	ΔE_p	I_a/I_c
2	481	73	1.1
3	488	75	1.0
4	502	78	1.1
5	533	62	1.0
6	471	81	1.0
7	488	73	1.1
8	476	98	1.1
9	483	74	1.1

3.3. Conclusions

Fca is one of the simplest organometallic amino acids based on the ferrocene sceleton. We provide a synthetic approach to amino acid and peptide conjugates of Fca, giving the desired compounds in good to excellent yields. We used standard peptide coupling techniques and two different synthesis strategies: The first strategy uses attachment of amino acids or dipeptides directly to the C- or the N-terminus of Fca. The second strategy includes coupling of one amino acid to Fca, its deprotection and subsequent coupling of the second amino acid. This second strategy can also be applied to both Fca termini.

Using this synthetic approach, di- to pentapeptides containing Fca as an organometallic amino acid was obtained by solution peptide chemistry. Depending on the substitution pattern, these compounds exhibit turn-like peptide structures, which are stable in solution and the solid state. Characterization of the H-bonding patterns in solution is particularly challenging and we have used a combination of various spectroscopic techniques to get detailed information about solution conformations. In order to distinguish between possible conformers we used a nomenclature that indicates the relative orientation of the amide groups directly bound to the ferrocene core, Fig. 3.2. More detailed description of a general nomenclature for metal-based peptides has been proposed recently.[5b]

From the X-ray structures of dipeptides **2** and **3** it was clear that the dipeptides show a conformer **B** in the solid state, with one intra-molecular inter-strand hydrogen bond. Helical chirality of the metallocene core, a very important property of the Fca peptides, was studied by X-ray crystallography and CD spectroscopy. The representative examples **2** and **3** differ not only in their H-bonding pattern, but also in helical chirality. Dipeptide **2** was found to be in the L, M stereochemistry in the solid state. The CD spectrum of **2** shows a negative band at about 500 nm. For **3** on the other hand, the crystal structure reveals and D, P stereochemistry and the CD spectrum shows a positive signal at about 480 nm. CD spectroscopy has been previously used to elucidate. In an attempt to determine the metal-centred chirality in peptide derivatives of ferrocene-1,1'-dicarboxylic acid, Hirao and coworkers showed that peptides made from H-bonding L-amino acids on both Cp rings induce P-chirality of the metallocene core.[5b, 7b] Also, Metzler-Nolte reported that equilibrium mixtures of M and P helicity

can coexist when amino acids of different chirality are attached to either ring in such systems.[9c] our result showed different behavior for Fca peptides as was observed from this study. Fc chirality is completely dependent on the chirality of the first amino acid attached to the Fca amino group.

The energetic barrier for rotation of the two Cp rings is small. This provides a degree of flexibility to such systems that is not achievable with the more common organic peptide mimetics. Janda and co-workers made use of this low rotational barrier in disubstituted ferrocenes to generate catalytic antibodies for endo- and exo-stereoselective Diels-Alder reactions from one single ferrocene hapten.[12] Oligopeptides derived from Fca therefore possess special properties and may form unique secondary and tertiary structures. The systematic work described herein lays a solid foundation for the rational design of such unique Fc peptides. Further studies are going to investigation the obtained results in more details.

3.4. Experimental Section

3.4.1. General Procedure

Most of synthesis were carried out under argon. CH_2Cl_2 used for synthesis and FT-IR was dried (P_2O_5), distilled over CaH_2 and stored over molecular sieves (4 Å). EDC, HOBt, HBTU (Aldrich), Ala (Merck), were used as received. Products were purified by preparative thin layer chromatography on silica gel (Merck, Kieselgel 60 HF_{254}) using the mixtures CH_2Cl_2/ EtOAc and CH_2Cl_2/ MeOH. Melting points were determined with a Buechi apparatus. The infrared spectra were recorded as CH_2Cl_2 solutions between NaCl windows or as KBr disks with a Bomem MB 100 mid, a Bruker

Equinox55 FT-IR or a Perkin-Elmer model 1605 FT-IR spectrometer. Wavenumbers, ν, are given in cm^{-1}. The ^{1}H- and ^{13}C-NMR spectra were recorded on a Varian EM 360, Varian Gemini 300 spectrometer in $CDCl_3$ and DMSO-d_6 solutions with Me_4Si as internal standard. NMR spectra were determined on a Bruker AM 360 spectrometer, ^{1}H at 360.14 MHz and ^{13}C at 90.56 MHz. High field 1D and 2D NMR spectra were recorded on Bruker DRX 500 or Bruker Avance-500 spectrometers, ^{1}H at 500.13 MHz. Spectral assignment for peptide oligomers was carried out with the help of standard 2D NMR spectroscopy. Peak positions are reported in ppm relative to TMS and are referenced with the help of the residual undeuterated solvent signal. UV/VIS spectra were measured on a Varian CARY 100 instrument in 1 cm quarz Suprasil cells thermostated at 20 °C. Absorption maxima, λ_{max}, and molar absorption coefficients, ε_{max}, are given in nm and M^{-1} cm^{-1}, respectively. Mass spectra (MS) were run on MAT 8200 (EI, FAB) or Hewelett-Packard HP 5989 (ESI). Only characteristic fragments with possible composition are given in brackets. For fragments containing metals, only the isotopomer with highest intensity was described. Crystallographic analyses were performed using Bruker SMART-CCD difractometer. CD-spectra were recorded as CH_3CN solutions (c = 1 M) with CD-spectropolarimeter Jasco-810 in 1 cm quarz Suprasil cells under inert atmosphere thermostated at 20 °C. Ellipticity maxima, θ_{max}, are given in nm. Molar ellipticity coefficients, M_θ, were calculated as $M_\theta = 100\ [\theta]/\ c \times l$, where ellipticity $[\theta]$ is in deg, concentration c in $mol.1^{-1}$ and pathlength l in cm, thus giving deg mM^{-1} cm^{-1}.[19] Elemental analyses were determined in-house. The numbering of Ala subunits is presented in Table 2.

3.4.2. General Synthesis of the Ferrocene Dipeptides 2 and 3

1′-(*tert*-Butoxycarbonyl-amino)ferrocene-1-carboxylate (**1**, Boc-Fca-OH) (200 mg, 0.58 mmol) was activated using EDC (167 mg, 0.87 mmol) and HOBt (117 mg, 0.87 mmol) and H-Aaa-OMe (1.16 mmol, obtained from H-Aaa-OMe·HCl by treatment with Et_3N in CH_2Cl_2, pH ~ 8) was added. The mixture was stirred for 30 minutes. After the standard aqueous work-up, the crude products were purified by TLC (CH_2Cl_2/EtOAc (10:1) to give orange crystalline materials upon standing in the refrigerator.

3.4.2.1. Boc-Fca-Ala-OMe (2)

Orange powder, m.p.: 61-64 ºC. Silica gel column (hexane:ethyl acetate=1:1 R_f = 0.37) got yellowish crystal 337mg (yield: 78%). Re-crystallization from ethyl acetate gave yellow X-ray quality crystals (vide infra). EI-MS for $C_{20}H_{26}N_2O_5Fe$: Calc. for $[M]^+$:430.1191, found: 430.1204. FT-IR(KBr,cm^{-1}): 3300(m, N-H), 1724, 1698 (m, C=O), 1638 (s, Amid I), 1546 (s, Amid II). UV-vis(λ_{max} in nm, [ε in M^{-1},cm^{-1}]): 442[253]. ^{1}H-NMR (δ, $CDCl_3$): 6.70 (s, 1H, Cp*H*CO), 6.88 (s, 1H, N*H*, LAla), 6.50 (s, 1H, NH, LAla), 4.71 (s, 1H, *H*-2,Cp), 4.68 (2 overlapping, m, 2H, H^{α} +*H*-5,Cp), 4.57 (s, 1H, *H*-2'), 4.51 ((s, 1H, *H*-5',Cp), 4.36 (s, 1H, *H*-3, Cp), 4.33 (s, 1H, *H*-4, Cp), 4.05 (s, 1H, *H*-3',Cp), 3.98 (s, 1H, *H*-4',Cp), 3.78 (s, 3H, COOC*H*$_3$), 1.52 (s, 3H, C*H*$_3$, Ala), 1.51 (s, 9H, C(C*H*$_3$)$_3$, Boc). ^{13}C{^{1}H}-NMR ($CDCl_3$, δ in ppm): 174.9 (*C*$OOCH_3$), 170.5(*C*ONH), 153.9 (*C*O, Boc), 97.2 (*C*-1', Cp), 80.7 (C(*C*H_3)$_3$), 77.7 (*C*-1,Cp), 72.1 (*C*-2,Cp), 71.0 (*C*-5,Cp), 70.1 (*C*-2',Cp), 66.5 (*C*-5',Cp), 65.8 (*C*-3,Cp), 65.5 (*C*-4,Cp), 63.4 (*C*-3',Cp), 62.3 (*C*-4',Cp), 53.0 (COO*C*H_3), 28.7 (C(*C*H_3)$_3$), 18.2 (*C*H_3, LAla).^{1}H-

NMR (DMSO-d_6, δ in ppm): 8.43 (bs, 1H, NH_{Fca}), 8.04 (d, 1H, NH_{Ala}, J = 5.6 Hz), 4.75 (s, 1H, H-2, Fn), 4.70 (s, 1H, H-5, Fn), 4.49 (m, 1H, CH_{Ala}), 4.40 (m, 2H, H-2' H-5', Fn), 4.25 (s, 2H, H-3 H-4, Fn), 3.92 (m, 2H, H-3' H-4', Fn), 3.64 (s, 3H, OCH_3), 1.45 (s, 9H, $C(CH_3)_3$), 1.38 (d, 3H, CH_{3Ala}, J = 7.2 Hz). ^{13}C-NMR (DMSO-d_6, δ in ppm): 173.4 (COOCH$_3$), 168.9 (CO_{Fca}), 153.1 (COO*t*Bu), 98.0 (C-1', Fn), 78.7 ($C(CH_3)_3$), 75.6 (C-1, Fn), 71.3 (C-2 C-5, Fn), 68.9 (C-3' C-4', Fn), 65.4 (C-3 C-4, Fn), 61.1 (C-2′ C-5′, Fn), 51.7 (OCH_3), 47.7 (CH_{Ala}), 28.04 (C(CH$_3$)$_3$), 16.8 (CH_{3Ala}).

3.4.2.2. Boc-Fca-D-Ala-OMe (3)

Orange powder, Silica gel column (hexane: ethyl acetate=1:1 R_f=0.37) got yellowish power (326mg, 75.8%). Re-crystallization from ethyl acetate gave yellow X-ray quality crystals (vide infra). EI-MS(+vs) for $C_{20}H_{26}N_2O_5Fe$: Calc. $[M]^+$: 430.1191, found: 430.1190. FT-IR (KBr, cm^{-1}): 3298 (m,N-H), 1724, 1698 (m, C=O), 1637 (s, Amid I), 1546(s, Amid II). UV-vis(λ_{max} in nm,[ε in M^{-1},cm^{-1}]): 441[248]. ^{1}H NMR ($CDCl_3$, δ in ppm): 6.78 (s, 1H, Cp*H*CO), 6.42 (s, 1H, N*H*, DAla), 4.71 (s, 1H, *H*-2,Cp), 4.68 (s, 1H, *H*-5,Cp), 4.50 (s, 1H, *H*-2',Cp), 4.48 (m, 1H, *H*-5',Cp), 4.38 (s,1H,*H*-3,Cp), 4.34 (s,1H, *H*-4,Cp), 4.07 (s,1H, *H*-3',Cp), 4.00 (s, 1H, *H*-4,Cp), 3.80 (s, 3H, COOC*H*$_3$), 1.52 (s, 3H,C*H*$_3$, DAla), 1.50 (s, 9H, C(C*H*$_3$)$_3$, Boc). ^{13}C NMR ($CDCl_3$, δ in ppm): 174.9 (COOCH$_3$), 170.5 (CONH), 153.9 CO, Boc), 97.2 (*C*-1',Cp), 80.7 (C(CH$_3$)$_3$), 77.7 (*C*-1,Cp), 72.1 (*C*-2,Cp), 71.4 (*C*-5,Cp), 70.0 (*C*-2',Cp), 66.5 (*C*-5',Cp), 65.8 (*C*-3,Cp), 65.6 (*C*-4,Cp), 63.4 (*C*-3',Cp), 62.8 (*C*-4',Cp), 53.0 (COOCH$_3$), 29.0 (C(CH$_3$)$_3$), 18.3 (CH$_3$, DAla).

3.4.3. Synthesis of Boc-D-Ala-Fca-Ala-OMe (4)

This compound was prepared as described above using HBTU as a coupling reagent. Boc-Fca-Ala-OMe (430 mg, 1 mmol), Boc-Ala-OH (190 mg, 1 mmol), HBTU (418 mg, 1.1 mmol). Silica gel column (hexane:EtOAc, 2:3, R_f = 0.33) to give yellow crystal (360 mg, 72 %). EI-MS(+vs) for $C_{23}H_{31}N_3O_6Fe$: Calc. for $[M]^+$: 501.1562, found: 501.1565. FT-IR (KBr, cm^{-1}): 3301(m, N-H), 1745, 1683 (m, C=O), 1637 (s, Amid I), 1531 (s, Amid II). IR (CH_2Cl_2, ν_{max}/cm^{-1}): 3429 m (N–H free), 3307 b, m (N–H, H-bonded), 1734 s (C=O), 1697 s, 1653 s, 1540 s, 1521, 1507 s. UV-vis (λ_{max} in nm, [ε in M^{-1} cm^{-1}]): 440 [247]. ^{1}H-NMR ($CDCl_3$, δ in ppm): 9.10 (s, 1H, CpN*H*), 7.35 (d, J = 7.8 Hz, 1H, NH_{DAla}), 5.40(s, 1H, NH_{LAla}), 4.88 (m, 1H, NH_{LAla}), 4.63 (s,1H, *H-2*,Cp), 4.57 (s, 1H, *H*-5Cp4.52. m, 1H, H^{α}_{DAla}), 4.47 (s,1H, *H*-2',Cp), 4.40 (s,1H,*H*-5', Cp), 4.34 (s,1H, *H-3*,Cp), 4.29 (s, 1H, *H-4*,Cp), 4.02 (s, 1H, *H*-3',Cp), 4.00 (s,1H, *H*-4',Cp), 3.78 (s,3H,COOCH_3), 1.47 (s, 3H,CH_{3LAla}), 1.45 (s, 9H, C(CH_3)$_3$, Boc), 1.39 (s,3H,CH_{3DAla}). ^{1}H-NMR (DMSO, assignments based on COSY spectra, δ in ppm): 9.31 (s, 1H, FcN*H*CO), 8.06 (d, *J* = 6.5 Hz, 1H, NH_{DAla}), 7.04(d, *J* = 5.6 Hz, 1H, NH_{LAla}), 4.77 (s, 1H, H_{Cp}), 4.74 (s, 1H, H_{Cp}), 4.69 (s, 1H, H_{Cp}), 4.53 (s, 1H, H_{Cp}), 4.40 (m, 1H, C$H_{\square LAla}$), 4.28 (s, 2H, H_{Cp}), 3.98 (s, 2H, H_{Cp}), 3.93 (m, 1H, C$H_{\square DAla2}$), 3.65 (s, 3H, COOCH_3), 1.40 (s, 9H, C(CH_3)$_3$), 1.38 (s, 3H, CH_{3LAla1}), 1.20 (d, *J* = 7.7 Hz, 3H, CH_{3DAla2}). ^{13}C{^{1}H}-NMR ($CDCl_3$, δ in ppm): 174.6 (*C*OOCH$_3$), 171.4 (*C*ONH$_{DAla}$), 170.1 (Cp*C*ONH$_{LAla}$), 155.9 (*C*O, Boc), 95.0 (*C*-1',Cp), 80.4 (C(*C*H$_3$)$_3$), 78.5 (*C*-1,Cp), 76.8 (*C*-2,Cp), 76.2 (*C*-5,Cp), 71.7 (*C*-2',Cp), 71.2 (*C*-5',Cp), 69.6 (*C*-3,Cp), 66.0 (*C*-

4,Cp), 64.0 (*C*-3',Cp), 63.5 (*C*-4',Cp), 52.6 (COO*C*H_3), 51.2 (C^{α}_{DAla}), 50.9 (C^{α}_{LAla}), 28.3 (C(*C*H_3)$_3$), 18.2 (*C*H_{3DAla}), 16.9 (*C*H_{3LAla}).

3.4.4. Synthesis of Boc-Ala-Fca-D-Ala-OMe (5)

The synthesis procedure is similar to that of compound **4**. Silica gel column (hexane:ethyl acetate = 2:3 R_f = 0.32) to give yellow crystals (390 mg, 78%). EI-MS(+vs) for $C_{23}H_{31}N_3O_6Fe$ Calc. $[M]^+$: 501.1562, found: 501.1579. FT-IR (KBr, cm^{-1}): 3299 (m, N-H), 1741, 1684 (s, C=O), 1637 (s, Amid I), 1532 (s, Amid II). IR (CH_2Cl_2) ν_{max}/cm^{-1}: 3430 m (N–H free), 3359, 3317 (N–H, H-bonded), 1741 s (C=O), 1696 s, 1636 s, 1650 s, 1563, 1503 s. UV-vis (λ_{max} in nm, [ε in M^{-1} cm^{-1}]): 438 [241]. ^{1}H-NMR ($CDCl_3$, δ in ppm): 8.55 (s, 1H, CpN*H*), 7.18 (d, J = 7.6 Hz, 1H, NH_{DAla}), 5.29 (s, 1H, NH_{LAla}), 4.92 (m, 1H, NH_{DAla}), 4.63 (s, 1H, *H-2*,Cp), 4.59 (s, 1H, *H*-'Cp4.52 overlapping, m, 2H, H^{α}_{DAla} +*H*-2', Cp), 4.43 (s, 1H, *H*-5', Cp), 4.39 (s, 1H, *H-3*, Cp), 4.34 (s, 1H, *H-4*, Cp), 4.07 (s, 1H, *H*-3',Cp), 4.04 (s, 1H, *H*-4', Cp), 3.82 (s, 3H, COOC*H*$_3$), 1.56 (s, 3H, C*H*$_{3DAla}$), 1.47 (s, 9H, C(C*H*$_3$)$_3$, Boc), 1.41 (s, 3H, C*H*$_{3LAla}$). ^{1}H-NMR (DMSO, assignments based on COSY spectra, δ in ppm): 9.31 (s, 1H, FcN*H*CO), 8.05 (d, *J* = 6.5 Hz, 1H, NH_{LAla}), 7.04(d, *J* = 5.6 Hz, 1H, NH_{DAla}), 4.77 (s, 1H, H_{Cp}), 4.73 (s, 1H, H_{Cp}), 4.69 (s, 1H, H_{Cp}), 4.53 (s, 1H, H_{Cp}), 4.40 (m, 1H, C$H_{\square DAla}$), 4.30 (s, 2H, H_{Cp}), 4.00 (s, 2H, H_{Cp}), 3.95 (m, 1H, C$H_{\square LAla}$), 3.56 (s, 3H, COOC*H*$_3$), 1.38 (s, 9H, C(C*H*$_3$)$_3$), 1.37 (s, 3H, C*H*$_{3DAla}$), 1.20 (s, 3H, C*H*$_{3Ala}$). ^{13}C{^{1}H}-NMR ($CDCl_3$, δ in ppm): 174.6 (*C*OOCH$_3$), 171.6 (*C*ONH$_{LAla}$), 170.4 (Cp*C*ONH$_{DAla}$), 160.1 (*C*O, Boc), 94.3 (*C*-1', Cp), 79.6 (C(*C*H$_3$)$_3$), 78.5 (*C*-1, Cp), 76.8 (*C*-2, Cp), 75.4 (*C*-5, Cp), 72.0 (*C*-2', Cp), 71.2 (*C*-5', Cp), 70.5 (*C*-3, Cp), 65.4 (*C*-4, Cp), 64.0 (*C*-3', Cp), 63.4 (*C*-4',

Cp), 52.6 (COO*C*H_3), 51.4 (C^{α}_{LAla}), 50.9 (C^{α}_{DAla}), 28.3 (C(*C*H_3)$_3$), 18.1 (*C*H_{3LAla}), 16.8 (*C*H_{3DAla}).

3.4.5. Synthesis of Boc-Ala-Fca-Ala-D-Ala-OMe (6)

To the solution of Boc-Ala-Fca-Ala-OMe (**4**) (500 mg, 1 mmol) in THF (12 ml), NaOH aqueous solution (0.1 M, 12 ml) was added dropwise at 0°C for 30 mins, then reacted at room temperature overnight. THF was evaporated and 50ml water was added to the aqueous solution. Then the solution was washed with EtOAc (3 × 20 ml). The aqueous solution and 100 ml EtOAC were put in a flask and cooled to 0°C, 0.1 M HCl was added slowly to the solution to pH 1-2. The aqueous phase was washed with EtOAc (3 × 100 ml) and dried over $NaSO_4$, then filtered and evaporated under reduced pressure in a rotorvap to give the free acid as an orange solid 448 mg (92%). Boc-Ala-Fca-Ala-OH (245 mg, 0.5 mmol) was dissolved in dry DCM (100ml), and reacted with H-D-Ala-OMe. The procedure is similar to that of compound **4**. Silica gel column (hexane:EtOAc = 1:3, R_f = 0.21) giving yellow crystals of compound **6** (214 mg, yield = 75 %). EI-MS(+vs) for $C_{26}H_{36}N_4O_7Fe$ Calc. $[M]^+$: 572.1933, found: 572.1938. FT-IR (KBr, cm^{-1}): 3277 (m, N-H), 1724, 1683 (m, C=O), 1637 (s, Amid I), 1531 (s, Amid II). IR (CH_2Cl_2) ν_{max}/cm^{-1}: 3433 m (N–H free), 3328 b, m (N–H, H-bonded), 1716 s (C=O), 1654 s, 1538 s, 1509 s. UV-vis (λ_{max} in nm, [ε in M^{-1} cm^{-1}]): 445[384]. ^{1}H-NMR ($CDCl_3$, δ in ppm): 9.41 (s, 1H, CpN*H*), 7.84 (d, J = 7.0 Hz, 1H, NH_{DAla}), 7.29 (d, *J* = 7.2 Hz, 1H, NH_{LAla1}), 5.31 (s, 1H, *H*-2, Cp), 5.10 (d, J = 7.0 Hz, 1H, NH_{LAla}), 4.80 (s, 1H, *H*-5, Cp), 4.70 (m, 1H, H^{α}_{DAla}), 4.58 (s, 1H, *H-2*', Cp), 4.56 (overlapping, m, 2H, H^{α}_{DAla}+*H*'Cp), 4.27 (s, 1H, *H*-3, Cp4.11. s, 1H, *H*-4, Cp), 4.06 (s, 1H, *H*-3', Cp), 4.00 (s,

1H, *H*-4', Cp), 3.75 (s, 3H, COOCH_{3LAla2}), 1.52 (s, 3H, CH_{3DAla}), 1.45 (s, 9H, C(CH_3)$_3$, Boc), 1.42 (s, 3H, CH_{3LAla1}), 1.36 (s, 3H, CH_{3DAla}). ^{1}H-NMR (DMSO, assignments based on COSY spectra, δ in ppm): 9.32 (s, 1H, FcN*H*CO), 8.28 (d, *J* = 6.7 Hz, 1H, NH_{DAla2}), 7.77 (d, *J* = 7.1 Hz, 1H, NH_{LAla1}), 7.01 (d, *J* = 6.1 Hz, 1H, NH_{LAla3}), 4.77 (s, 1H, H_{Cp}), 4.68 (s, 1H, H_{Cp}), 4.67 (s, 1H, H_{Cp}), 4.56 (s, 1H, H_{Cp}), 4.45 (m, 1H, C$H_{\alpha LAla1}$), 4.31 (m, 1H, C$H_{\alpha DAla2}$), 4.28 (s, 2H, H_{Cp}), 3.98 (s, 2H, H_{Cp}), 3.91 (m, 1H, C$H_{\alpha LAla3}$), 3.65 (s, 3H, COOCH_3), 1.39 (s, 9H, C(CH_3)$_3$), 1.34 (m, 6H, CH_{3LAla1} + CH_{3DAla2}), 1.21 (d, *J* = 6.6 Hz, 3H, CH_{3LAla3}). ^{13}C{^{1}H}-NMR ($CDCl_3$, δ in ppm): 173.4 (*C*OOCH$_3$), 171.5 (*C*ONH$_{DAla}$), 170.5 (Cp*C*ONH$_{LAla1}$), 156.4 (*C*ONH$_{LAla2}$), 95.3 (*C-1'*, Cp), 78.0 (*C*(CH$_3$)$_3$, Boc), 77.4 (*C*-1, Cp), 71.7 (*C*-2, Cp), 70.2 (*C*-5, Cp), 69.3 (*C*-2', Cp), 69.0 (*C*-5', Cp), 66.3 (*C*-3, Cp), 66.1 (*C*-4, Cp), 64.0 (*C*-3', Cp), 62.9 (*C*-4', Cp), 52.8 (COO*C*H$_3$), 50.2 (C^{α}_{LAla1}), 48.8 (C^{α}_{LAla1}), 47.2 (C^{α}_{DAla1}), 28.2 (C(*C*H$_3$)$_3$), 17.8 (*C*H$_{3LAla1}$), 17.5 (*C*H$_{3LAla2}$), 16.5 (*C*H$_{3DAla}$).

3.4.6. Synthesis of Boc-Ala-Fca-D-Ala-D-Ala-OMe (7)

The synthetic procedure is identical to that described for **6**. Silica gel column (hexane:EtOAc = 1:3 R_f = 0.20) to get yellow crystals (205 mg yield = 73 %). EI-MS(+vs) for $C_{26}H_{36}N_4O_7Fe$ Calc. $[M]^+$: 572.1933, found: 501.1579. FT-IR (KBr, cm^{-1}): 3289 (m, N-H), 1745, 1666 (m, C=O), 1635 (s, Amid I), 1531 (s, Amid II). IR (CH_2Cl_2, ν_{max}/cm^{-1}): 3426 m (N–H free), 3307 b, m (N–H, H-bonded), 1741 s (C=O), 1685 s, 1654 s, 1558 s, 1507 s. UV/vis (in MeCN, UV-vis (λ_{max} in nm,[ε in M^{-1},cm^{-1}]): 445[384]. ^{1}H-NMR ($CDCl_3$, δ in ppm): 8.61 (s, 1H, CpN*H*), 7.41 (d, J = 7.0 Hz, 1H, NH_{DAla2}), 7.18 (d, J = 7.2 Hz, 1H, NH_{LAla}), 5.38 (s, 1H, *H*-2, Cp), 5.14 (d, J = 7.0 Hz,

1H, NH_{LAla}), 4.80 (s, 1H, *H*-5, Cp), 4.73 (m, 1H, H^{α}_{DAla}), 4.65 (s, 1H, *H*-2', Cp), 4.60 (overlapping, m, 2H, $H^{\alpha}_{DAla1 + LAla}$), 4.47 (s, 2H, H-2'+*H*-5', Cp4.39. s, 1H, *H*-3, Cp), 4.36 (s, 1H, *H*-4, Cp), 4.20 (m, 1H, C^{α}_{DAla2}), 4.05 (s, 2H, *H*-3'+*H*-4', Cp), 3.77 (s, 3H, COOCH_3), 1.54 (s, 3H, CH_{3LAla}), 1.50 (s, 3H, CH_{3DAla1}), 1.48 (s, 9H, C(CH_3)$_3$, Boc), 1.42 (s, 3H, CH_{3DAla2}). ^{1}H-NMR (DMSO, assignments based on COSY spectra, δ in ppm): 9.30 (s, 1H, FcN*H*CO), 8.27 (d, *J* = 6.6 Hz, 1H, NH_{DAla2}), 7.74 (d, *J* = 7.6 Hz, 1H, NH_{DAla1}), 7.00 (d, *J* = 5.4 Hz, 1H, NH_{LAla3}), 4.77 (s, 1H, H_{Cp}), 4.69 (s, 1H, H_{Cp}), 4.66 (s, 1H, H_{Cp}), 4.56 (s, 1H, H_{Cp}), 4.43 (m, 1H, CH^{α}_{DAla1}), 4.30 (m, 1H, CH_{DAla2}), 4.26 (s, 2H, H_{Cp}), 3.97 (s, 2H, H_{Cp}), 3.94 (m, 1H, CH^{α}_{LAla3}), 3.62 (s, 3H, COOCH_3), 1.39 (s, 9H, C(CH_3)$_3$), 1.33 (m, 6H, CH_{3DAla1} + CH_{3DAla2}), 1.21 (d, *J* = 6.6 Hz, 3H, CH_{3LAla3}). ^{13}C{^{1}H}-NMR ($CDCl_3$, δ in ppm): 173.3 (*C*OOCH$_3$), 171.6 (*C*ONH$_{DAla1}$), 170.5 (Cp*C*ONH$_{LAla}$), 155.9 (*C*ONH$_{DAla2}$), 94.9 (*C*-1', Cp), 80.4 (*C*(CH$_3$)$_3$, Boc), 77.0 (*C*-1, Cp), 76.8 (*C*-2, Cp), 76.4 (*C*-5, Cp), 71.6 (*C*-2', Cp), 70.0 (*C*-5', Cp), 66.9 (*C*-3, Cp), 65.4 (*C*-4, Cp), 64.0 (*C*-3', Cp), 63.3 (*C*-4', Cp), 52.3 (COO*C*H$_3$), 50.8 (C^{α}_{DAla2}), 50.0 (C^{α}_{LAla}), 48.0 (C^{α}_{DAla1}), 28.4 (C(*C*H$_3$)$_3$), 18.4 (*C*H$_{3LAla}$), 17.9 (*C*H$_{3DAla2}$), 17.7 (*C*H$_{3DAla1}$).

3.4.7. Synthesis of Boc-D-Ala-Ala-Fca-Ala-D-Ala-OMe (8)

Boc-Ala-Fca-Ala-D-Ala-OMe (285 mg, 0.5 mmol) Boc-D-Ala-OH (85 mg, 0.5 mmol), HBTU (210 mg, 0.55 mmol). Silica gel column (hexane:EtOAc:MeOH = 10:85:5, R_f = 0.12) to give a yellow solid 103 mg (yield = 31%). EI-MS (+vs) for $C_{29}H_{41}N_5O_8Fe$: Calc. for $[M+1]^+$: 643.2304, found: 644.2370. FT-IR (KBr, cm^{-1}): 3287 (m, N-H), 1740, 1659 (m, C=O), 1634 (s, Amid I), 1530 (s, Amid II). IR (CH_2Cl_2,

ν_{max}/cm^{-1}): 3424 m (N–H free), 3325 b, m (N–H, H-bonded), 1742 s (C=O), 1684 s, 1670 s, 1517 b, s. UV-vis (λ_{max} in nm,[ε in M^{-1},cm^{-1}]): 439[416]. ^{1}H-NMR ($CDCl_3$, δ in ppm): 9.08 (s, 1H, CpN*H*), 7.83 (s, 1H, N*H*,), 7.28 (s, 1H, N*H*), 7.20 (s, 1H, N*H*), 5.37 (s, 1H, *H*-2, Cp), 5.20 (d, J = 7.0 Hz, 1H, N*H*), 4.86 (overlapping, 2*H*), 4.46 (s, 1H, Cp), 4.47 (s, 1H, Cp), 4.26 (overlapping, 2H), 4.17 (m, 1H), 4.11 s, 2H), 3.91 (s, 1H), 3.82 (s, 3H, COOC*H*$_3$), 1.46 (overlapping, 12H, C*H*$_{3Ala}$+C(C*H*$_3$)$_3$, Boc), 1.43-1.42 (overlapping, 9H, C*H*$_{3Ala}$). ^{1}H-NMR (DMSO, assignments based on COSY spectra, δ in ppm): 9.19 (s, 1H, FcN*H*CO), 8.30 (d, *J* = 5.8 Hz, 1H, N*H*$_{DAla2}$), 8.02 (d, *J* = 6.2 Hz, 1H, N*H*$_{LAla4}$), 7.73 (d, *J* = 6.8 Hz, 1H, N*H*$_{LAla1}$), 7.01 (d, *J* = 5.5 Hz, 1H, N*H*$_{LAla3}$), 4.78 (s, 1H, *H*$_{Cp}$), 4.71 (s, 1H, *H*$_{Cp}$), 4.66 (s, 1H, *H*$_{Cp}$), 4.57 (s, 1H, *H*$_{Cp}$), 4.43 (m, 1H, C*H*$_{LAla1}$), 4.30 (m, 2H, C*H*$_{DAla2}$ & C*H*$_{DAla3}$), 4.25 (s, 2H, *H*$_{Cp}$), 3.99 (s, 2H, *H*$_{Cp}$), 3.98 (m, 1H, C*H*$_{LAla4}$), 3.62 (s, 3H, COOC*H*$_3$), 1.37 (s, 9H, C(C*H*$_3$)$_3$), 1.32 (m, 6H, C*H*$_{3LAla1}$ + C*H*$_{3DAla2}$), 1.27 (d, *J* = 7.0 Hz, 3H, C*H*$_{3LAla4}$), 1.18 (d, *J* = 7.0 Hz, 3H, C*H*$_{3LAla3}$). ^{13}C{^{1}H}-NMR ($CDCl_3$, δ in ppm): 176.8 (*C*OOCH$_3$), 173.4, 170.9, 165.7, 155.6 (*C*ONH), 95.3 (Cp), 80.3 (*C*(CH$_3$)$_3$, Boc), 72.4, 71.5, 70.7, 70.5, 70.0, 66.0, 65.8, 65.3, 64.4, 62.8 (Cp), 52.7(COO*C*H$_3$), 50.4, 50.0, 48.5, 48.0 (*C*$^{\alpha}_{Ala}$), 28.3 (C (*C*H$_3$)$_3$), 19.6, 18.2, 17.5, 17.3 (*C*H$_{3Ala}$).

3.4.8. Synthesis of Boc-Ala-Ala-Fca-D-Ala-D-Ala-OMe (9)

Identical procedure to **6**. Silica gel column (hexane:EtOAc:MeOH = 10:85:5, R_f = 0.12) to give a yellow solid (137 mg, 43%). EI-MS (+vs) for $C_{29}H_{41}N_5O_8Fe$: Calc. for [M+1]$^{+}$: 644.2304, found: 644.2379. FT-IR (KBr, cm^{-1}): 3293 (m, N-H), 1742, 1668 (s, C=O), 1629 (s, Amid I), 1527 (s, Amid II). UV/vis (in MeCN, (λ_{max} in nm,[ε in M^{-1},cm^{-}

[1]): 448[323]. ^{1}H-NMR ($CDCl_3$, δ in ppm): 9.27 (s, 1H, CpN*H*), 7.88 (s, 1H, N*H*), 7.28 (s, 1H, N*H*), 6.68 (s, 1H, N*H*), 5.18 (s, 1H, *H*-2, Cp), 4.95 (d, *J* = 7.0 Hz, 1H, N*H*), 4.87 (s, 1H), 4.68 (s, 1H), 4.53-4.50 (overlapping, 3*H*), 4.27 (overlapping, 3H), 4.10 (s, 2H), 3.90 (s, 1H), 3.76 (s, 3H, COOCH_3), 1.47 (overlapping, 12H, C$H_{3\text{Ala}}$ + C(CH_3)$_3$, Boc), 1.43-1.38 (overlapping, 9H, C$H_{3\text{Ala}}$). ^{13}C{^{1}H}-NMR ($CDCl_3$, δ in ppm): 174.6 (*C*OOCH$_3$), 173.5, 170.9, 166.1, 156.4 (*C*ONH), 95.3 (Cp), 80.3 (*C*(CH$_3$)$_3$, Boc), 72.0, 71.5, 71.6, 70.4, 70.1, 66.5, 66.4, 66.1, 64.4, 63.8 (Cp), 52.9 (COO*C*H$_3$), 51.3, 50.3, 48.9, 48.6 (C^{α}_{Ala}), 28.7 (C(*C*H$_3$)$_3$), 18.3, 18.2, 17.9, 17.8 (*C*H$_{3\text{Ala}}$).

3.5. References

[1] a) S. G. Zhang, Nature Biotech. **2003**, 21, 1171-1178; b) V. Balzani, A. Credi, F. M. Raymo, J. F. Stoddart, Angew. Chem. Int. Ed. **2000**, 39, 3348-3391.

[2] M. A. Shogren-Knaak, P. J. Alaimo, K. M. Shokat, Annual Rev. Cell Dev. Biol. **2001**, 17, 405-433.

[3] T. Moriuchi, T. Hirao, Chem. Soc. Rev. **2004**, 33, 294-301.

[4] R. S. Herrick, R. M. Jarret, T. P. Curran, D. R. Dragoli, M. B. Flaherty, S. E. Lindyberg, R. A. Slate, L. C. Thornton, Tetrahedron Lett. **1996**, 37, 5289-5292.

[5] For recent reviews see: a) D. R. van Staveren, N. Metzler-Nolte, Chem. Rev. **2004**, 104, 5931-5985; b) S. I. Kirin, H.-B. Kraatz, N. Metzler-Nolte, Chem. Soc. Rev. **2006**, 35, 348-354.

[6] a) M. J. Sheehy, J. F. Gallagher, M. Yamashita, Y. Ida, J. White-Colangelo, J. Johnson, R. Orlando, P. T. M. Kenny, J. Organomet. Chem. **2004**, 689, 1511-1520; b) D. Savage, G. Malone, J. F. Gallagher, Y. Ida, P. T. M. Kenny, J. Organomet. Chem. **2005**, 690, 383-393.

[7] a) A. Nomoto, T. Moriuchi, S. Yamazaki, A. Ogawa, T. Hirao, Chem. Commun. **1998**, 1963-1964; b) T. Moriuchi, A. Nomoto, K. Yoshida, A. Ogawa, T. Hirao, J. Am. Chem. Soc. **2001**, 123, 68-75; c) T. Moriuchi, A. Nomoto, K. Yoshida, T. Hirao, Organometallics **2001**, 20, 1008-1013; d) T. Moriuchi, K. Yoshida, T. Hirao, Org. Lett. **2003**, 5, 4285-4288; e) T. Moriuchi, K. Yoshida, T. Hirao, J. Organomet. Chem. **2003**, 668, 31-34; f) T. Moriuchi, T. Nagai, T. Hirao, Org. Lett. **2005**, 7, 5265-5268; g) T. Moriuchi, T. Nagai, T. Hirao, Org. Lett. **2006**, 8, 31-34.

[8] a) Y. Xu, P. Saweczko, H.-B. Kraatz, J. Organomet. Chem. **2001**, 637-639, 335-342; b) Y. Xu, H.-B. Kraatz, Tetrahedron Lett. **2001**, 42, 2601-2603; c) F. E. Appoh, T. C. Sutherland, H.-B. Kraatz, J. Organomet. Chem. **2004**, 689, 4669-4677; d) F. E. Appoh, T. C. Sutherland, H.-B. Kraatz, J. Organomet. Chem. **2005**, 690, 1209-1217.

[9] a) D. R. van Staveren, T. Weyhermüller, N. Metzler-Nolte, Dalton Trans. **2003**, 210-220; b) X. de Hatten, T. Weyhermüller, N. Metzler-Nolte, J. Organomet. Chem. **2004**, 689, 4856-4867; c) S. I. Kirin, D. Wissenbach, N. Metzler-Nolte, New J. Chem. **2005**, 29, 1168-1173.

[10] a) K. Heinze, M. Schlenker, Eur. J. Inorg. Chem. **2004**, 2974-2988; a) K. Heinze, M. Schlenker, Eur. J. Inorg. Chem. **2005**, 66-71; c) K. Heinze, M. Beckmann, Eur. J. Inorg. Chem. **2005**, 3450-3457.

[11] a) S. Chowdhury, G. Schatte, H.-B. Kraatz, Dalton Trans. **2004**, 1726-1730; b) S. Chowdhury, K. A. Mahmoud, G. Schatte, H.-B. Kraatz, Org. Biomol. Chem. **2005**, 3, 3018-3023; c) S. Chowdhury, D. A. R. Sanders, G. Schatte, H.-B. Kraatz, Angew. Chem. Int. Ed. Engl. **2006**, 45, 751-754.

[12] a) J. T. Yli-Kauhaluoma, J. A. Ashley, C.-H. Lo, L. Tucker, M. M. Wolfe, K. D. Janda, J. Am. Chem. Soc., **1995**, 117, 7041-7047; b) A. Heine, E. A. Stura, J. T. Yli-Kauhaluoma, C. Gao, Q. Deng, B. R. Beno, K. N. Houk, K. D. Janda, I. A. Wilson, Science, **1998**, 279, 1934-1940; c) C. E. Cannizzaro, J. A. Ashley, K. D. Janda, K. N. Houk, J. Am. Chem. Soc., **2003**, 125, 2489-2506.

[13] Other synthetic pathways to Fca: a) I. R. Butler, S. C. Quayle, J. Organomet. Chem. **2004**, 689, 4856-4867; b) T. Okamura, K. Sakauye, N. Ueyama, A. Nakamura, Inorg. Chem. **1998**, 37, 6731-6736; and references 10a and 14a.
[14] a) L. Barišić, V. Rapić, V. Kovač, Croat Chem. Acta **2002**, 75, 199-210; b) G. Pavlović, L. Barišić, V. Rapić, I. Leban, Acta Cryst., Sect. E **2002**, 58, m13-m15; c) G. Pavlović, L. Barišić, V. Rapić, V. Kovač, Acta Cryst., Sect. C **2003**, 59, m55-m57; d) L. Barišić, V. Rapić, H. Pritzkow, G. Pavlović, I. Nemet, J. Organomet. Chem. **2003**, 682, 131-142.
[15] L. Barišić, M. Dropučić, V. Rapić, H. Pritzkow, S. I. Kirin, N. Metzler-Nolte, Chem. Commun. **2004**, 2004-2005.
[16] D. W. Hall, J. H. Richards, J. Org. Chem. **1963**, 28, 1549-1554.
[17] a) B. Ishimoto, K. Tonan, S. Ikawa, Spectrochim. Acta Part A **1999**, 56, 201-209; b) Y. Jin, K. Tonan, S. Ikawa, Spectrochim. Acta Part A **2002**, 58, 2795-2802; c) K. Tonan, S. Ikawa, Spectrochim. Acta Part A **2003**, 59, 111-120.
[18] N. Metzler-Nolte, in: Bioorganometallics (Ed.: G. Jaouen), Wiley-VCH, Weinheim, **2005**; p 125-192.
[19] a) A. Rodger, B. Norden, Circular Dichroism & Linear Dichroism, Oxford University Press, Oxford, UK, **1997**; b) S. M. Kelly, T. J. Jess, N. C. Price, Biochem. Biophys. Acta **2005**, 1751, 119-139.
[20] W. Bauer, K. Polborn, W. Beck, J. Organomet. Chem. **1999**, 579, 269-279.

CHAPTER 4

A BIOORGANOMETALLIC APPROACH FOR THE ELECTROCHEMICAL DETECTION OF PROTEINS: A STUDY ON THE INTERACTION OF FERROCENE-PEPTIDE CONJUGATES WITH PAPAIN IN SOLUTION AND ON AU SURFACES

4.0. Connecting Text

This chapter describes the first application of ferrocene-peptide bioconjugates. It was demonstrated in Chapters 2 and 3 that 1'-amino-ferrocene-1-carboxylic acid (ferrocene amino acid, Fca) effectively conjugates to amino acids and peptides. In addition, it was shown that this artificial amino acid has the ability to impose secondary structural elements on the supramolecular structure of Fca-peptide conjugates; therefore, it may be possible to exploit the redox properties of the Fc group for the recognition of bimolecular interactions. This has led to a successful study on the interaction between selected series of surface modified Fca-peptide conjugates and papain. This novel approach may overcome some of the drawbacks of known electrochemical biosensors where the presence of a terminal redox probes significantly interferes with the molecular recognition processes.

4.1. Introduction

Enzymatic transformations of substrates are often exploited for the development of amperometric sensors. The electrochemical sensors have received a major attention in the biosensing technology, in particular the use of glucose oxidase for the development of an electrochemical glucose sensitive detector.[1-7] The resulting devices exploiting this technology are simple to use, inexpensive and accurate. More importantly, they are amenable to miniaturization and hence the design of high-density arrays.[8]

The detection of biomolecular interactions by electrochemical methods requires in general the presence of a redox-active probe as part of the detection system (Scheme 4.1). The redox probe can be in solution or can be covalently attached to the molecule capturing the biomolecule from solution. In both cases, the interaction of the surface with the biomolecule will alter the electron transfer properties of the systems. For solution-based redox probes, significant differences exist in the electron transfer properties or ability of the redox probe and/or counter ions to diffuse into the film (Scheme 4.1.A). These differences can be exploited for the detection of protein binding to a range of capture probes. In essence, this approach is "label-free", since no chemical modifications of the capture probe or of the target protein are necessary.[9, 10] An interesting variation on the theme of a solution-based electroactive probe is the use of a redox-active polymer. Using a ferrocene (Fc)-labeled polythiophene which electrostatically binds to duplex DNA or duplex DNA-PNA), it was possible to detect thrombin.[10-13] More recently, electrochemical immunoassays (EIA) were developed in which an analyte binds to an immobilized antibody, followed by binding of a redox

mediator bound to an antibody which binds to the electrode-bound analyte (Scheme 4.1.B).[14, 15] In cases where the redox-probe is covalently attached to a terminal position of a molecule such as single stranded DNA, the interaction with the appropriate target will result in large structural changes of the capture probe causing changes in the electron transfer kinetics of the system. Heeger's DNA-hairpin loop is an example for this approach (Scheme 4.1.C).[16] In the absence of a suitable target, a Fc probe attached to the 5'-position in a single stranded DNA is in close proximity to the electrode surface and gives rise to a significant redox response. Upon hybridization of a target strand to the Fc-labeled capture strand, significant structural changes occur which change the distance between the Fc group and the surface, resulting in a decrease of the electrochemical response. Although this approach is useful in cases of DNA-DNA or DNA-protein detection where the interaction does not involve the site of the redox probe,[17] it will have limited utility for monitoring peptide-protein interactions. In this case, the presence of a terminal redox probe may significantly interfere with the interaction and may even prevent it.

We are proposing a new approach making use of our expertise in bioorganometallic chemistry to join a peptide recognition sequence to a redox probe. The idea is that a surface-bound redox probe is in close proximity to the electrode surface and thus unaffected by diffusive processes. Interaction between the recognition sequence and electrode surface will not be hindered by the interaction with the target analyte. This in turn may enhance the sensitivity and may render a potential device less susceptible to environmental influences.

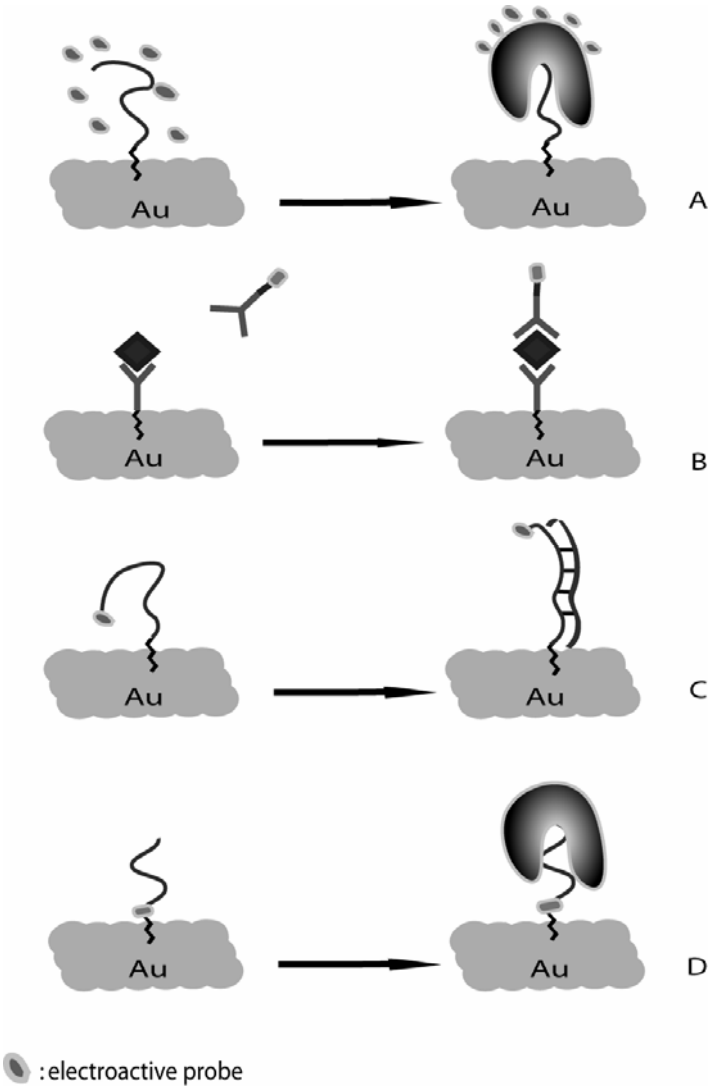

Scheme 4.1. Schematic representation of some of the common electrochemical biosensor systems (A-C) and the new proposed system making use of an ferrocene-peptide conjugate (D): (A) The redox active probe in solution and the target protein blocks its interaction with the surface. (B) In the electrochemical immunoassay (EIA) a protein binds to a surface-bound capture probe followed by binding labeled antibody. (C) Conformational changes take place upon binding of a target DNA to a single stranded capture DNA. Changes in the distance between the redox label and the surface alter the electrochemical behavior of the system. (D) Bioorganometallic capture probe: protein binding is detected by monitoring the electrochemical properties before and after protein binding.

Fc-peptide conjugates are an attractive class of organometallic peptide conjugates that are conveniently obtained by solution or solid-phase synthetic strategies,[18] that have the potential to be tailored to target DNA and specific proteins.[19-22] In a recent

study, it was demonstrated that 1'-aminoferrocene-1-carboxylic acid (ferrocene amino acid, Fca) induces a turn into a peptide sequence and thereby allows control over the peptide secondary structure.[23] Recently, Rapić et al and Heinze et al independently used solid phase peptide synthesis (SPPS) to produce Fca-oligopeptides by combining Fmoc- and Boc- procedures.[24, 25]

In this contribution, we outline how Fca-peptide conjugates can be used in protein detection and demonstrate our approach for the detection of papain a cysteine-protease commonly found in the papaya fruit and used commercially as a meat tenderizer. In our approach (see Scheme 4.1.D), a thin film on gold prepared from a conjugate of Fca with an inhibitory peptide sequence to papain is used for the detection of papain. We are reporting the results of a combined synthetic, spectroscopic and electrochemical study into the properties of these films and their behavior in the presence of papain.

4.2. Results and Discussion

4.2.1. Synthesis

In an early report, it was shown that the organometallic peptide conjugate Fc-Gly-Gly-Tyr-Arg interacts with papain and acts as a competitive inhibitor.[22] Based on this result, it was decided to work with two peptide systems, making use of conjugation Fca, exploiting the papain-binding sequence Gly-Gly-Tyr-Arg and Gly-Gly-Arg-Tyr. Conjugation of the tetrapeptide to the C-terminal side of Fca will allow the interaction with the protein, while the N-terminal side will be exploited to surface binding of the Fca-conjugate. The synthesis of Fca-peptide conjugate **4** was achieved by carbodiimide coupling in solution and is summarized in Scheme 4.2. Compound **4** displayed a broad band in the IR assigned to the OH stretch and the expected carbonyl stretch for the acid

group at 1741 cm^{-1}. Unfortunately, it was not possible to deprotect the guanidine group of peptide conjugate **4** by hydrogenation, presumably due to Pd catalyst poisoning due to the thiostic acid (Thc) disulfide group. In order to overcome this problem, we decided to implement a small positional change in the sequence involving the Tyr and Arg, which facilitated the synthesis and did not require protection of the Tyr. The Arg guanidine group was protected by Mtr, which could be deprotected in the presence of TFA and thioanisol. The synthesis of Fca-peptide conjugates **9** and **10** is summarized in Scheme 4.3.

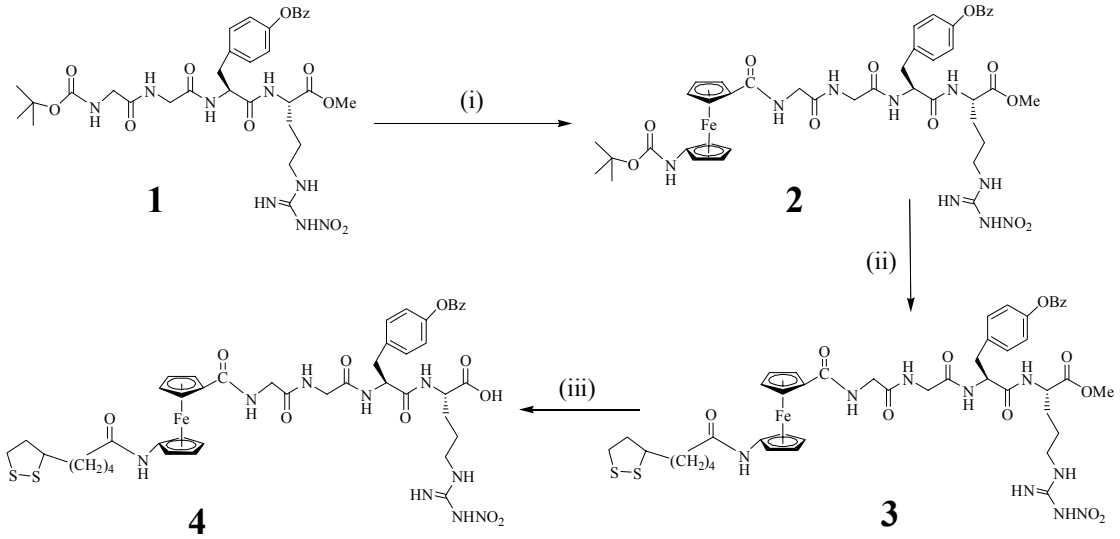

Scheme 4.2 Synthesis of Fca-peptide conjugate **4**. (i) TFA/CH_2Cl_2; Boc-Fca-OBt; Et_3N, CH_2Cl_2 (ii) TFA/CH_2Cl_2; ThcOH, EDC/HOBt; Et_3N, CH_2Cl_2 (iii) NaOH/CH_3OH/H_2O.

The peptide building block **6** was synthesized from Boc-Gly_2-OH and the corresponding dipeptide H-Arg(Mtr)-Tyr-OMe **5**. Boc-deprotection and conjugation to the carboxylic acid group of Fca resulted in the desired conjugate **7**. After Boc-deprotection of the amino group of Fca under anaerobic conditions, the thiostic acid (Thc) conjugate **8** was formed. Stepwise deprotection of the methyl ester by hydrolysis

and of the Mtr group by TFA/anisol resulted in the formation of compound **9** and **10**, respectively. Final purification of compound **10** was carried out by HPLC. The identity of compounds **9** and **10** was confirmed by full spectroscopic analysis including ToF-MS, IR and ^{1}H-NMR spectroscopy. In the IR, compounds **9** and **10** showed Amide-A bands at 3306 and 3447 cm^{-1} respectively and carbonyl stretch at 1748 and 1725 cm^{-1} respectively. Figure 4.1 shows the ^{1}H-NMR spectra in DMSO-d_6 for the main three peptides **4**, **9**, and **10** under investigation. In all three peptides, the amide as well as guanidine protons were observed in the region δ 8.6-7.3. The peaks assigned for Mtr protecting group in peptide **9** disappeared in peptide **10** indicating the successful deprotection.

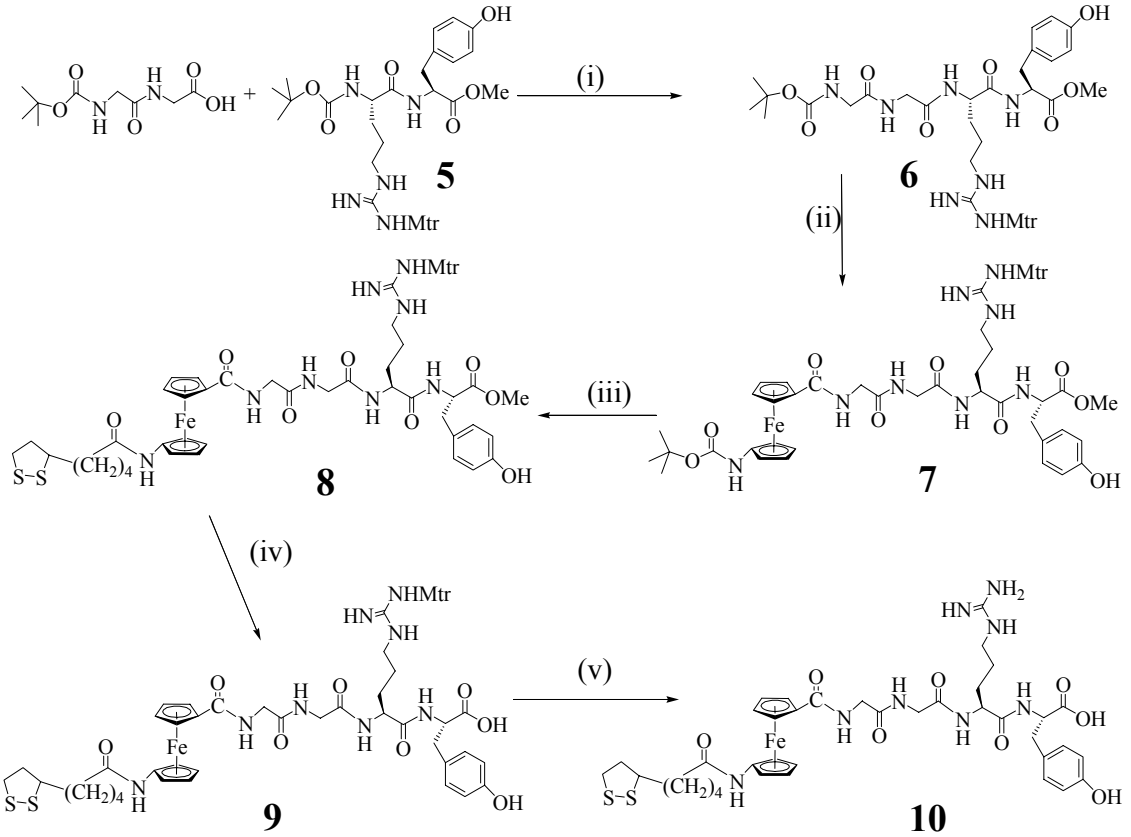

Scheme 4.3. Synthesis of Fca-peptide conjugates **7**-**10**. (i) TFA/CH_2Cl_2; EDC/HOBt; Et_3N,/CH_2Cl_2 (ii) TFA/CH_2Cl_2; Boc-Fca-OBt; Et_3N,/CH_2Cl_2 (iii)TFA/CH_2Cl_2; ThcOH/EDC/HOBt; Et_3N,/CH_2Cl_2 (iv) NaOH/CH_3OH, (v) TFA/ thioanisol/CH_2Cl_2.

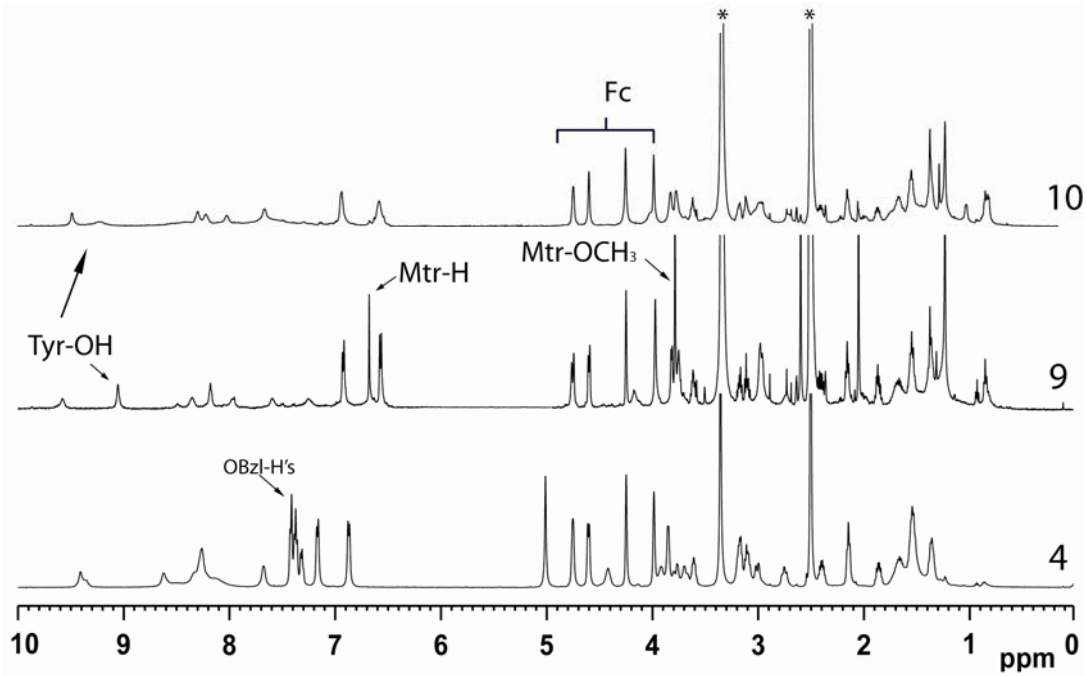

Figure 4.1. ^{1}H-NMR of peptides **4**, **9**, and **10**. * (D_5)DMSO trace at δ2.50, water trace at δ3.33.

4.2.2. Inhibition Studies

Before linking the Fca-peptide conjugates to a gold surface, it was important to evaluate the Fca-conjugates for their ability to inhibit papain in solution. For this purpose, papain was assayed with the chromogenic substrate Z-Phe-Arg-NHNp in the absence and presence of the Fca-peptide conjugates **4**, **9** and **10**. The Michaelis-Menten constant (K_m) for papain as well as the inhibition constant K_i for the peptides were determined. A K_m value of 980 ± 26 μM was determined at pH 6.2 by non-linear regression fit of the concentration velocity curve using Michaelis-Menten equation ($\upsilon = \upsilon_{max}[S]/(K_m+[S])$, where υ is the velocity and υ_{max} is the maximum velocity, and [S] is the substrate concentration (Figure 4.S2). The value compared well with the previously reported one, 965±244 μM.[26] Figure 4.S3 shows a representative kinetic analysis of

papain inhibition by the two Fca-peptide conjugates **9** and **10**. The Dixon-Webb plots indicate a time-independent inhibition. The slopes of the progress curves were directly used to determine K_i' value, from which K_i value was calculated to be 210 ± 1.4 μM for compound **9** and 6.9 ± 0.2 μM for compound **10**. Our results suggest that these Fca-peptide conjugates exhibit competitive inhibition behavior.[26] The inhibition constants for **10** indicates very good competitive inhibition of papain, comparable to that of the Fc-conjugate Fc-Gly-Gly-Try-Arg-OH, which has a K_i = 9 μM at pH 6.2 (Table 4.1).[22]

Table 4.1. Inhibition constant K_i of the Fc-peptide conjugates **4**, **9**, and **10** and some literature compounds.

Compound	pH	K_i' (μM)	K_i (μM)	Ref
4	6.2	2510.6± 8.8	820.9 ± 2.5	This work
9	6.2	639.1±1.1	210 ± 1.4	This work
10	6.2	21.1±0.3	6.9 ± 0.2	This work
Gly_2TyrArg	6.0		150	[27]
Gly_2Tyr(Bz)Arg	6.0		123	[28]
Fc- Gly_2TyrArg	6.2		9	[22]

On the other hand, lower affinities were observed for the Fca-peptide conjugates **4** (K_i = 820.9 ± 2.5 μM) and **9** (K_i = 210 ± 1.4 μM), which is rationalized by the presence of protecting groups which may not allow a proper interaction with Cys-25 and His-159 in the active site of papain.[29-31] It is interesting to note that switching the peptide sequence from the original sequence employed by Kaiser for purification of papain by affinity chromatography Gly-Gly-Tyr-Arg[28] to Gly-Gly-Arg-Tyr, the

peptide became a more potent inhibitor. Blumberg[27] and Kaiser[28] used Gly-Gly-Tyr(Bzl)-Arg for the purification of papain by affinity chromatography. It was shown that papain inhibition can be achieved by peptides that have Arg and an aromatic amino acid in the P_1 and P_2 subsites (nomenclature according to Schechter and Berger,[32] see supplemental material Figure 4.S4). It was found that the peptide sequence Z-Arg-Leu-Val-Gly-DAM gave the most potent inhibitor of papain with apparent second order rate constants of the same order of magnitude as those determined for {1-[N-[(L-3-trans-carboxyoxirane-2-carbonyl)-L-leucyl]amino]-4-guanidinobutane} E-64, the most common inhibitor of cysteine proteases.[33] Moreover, a strong electron-withdrawing phenyl groups at the C-terminus constructs a good irreversible inhibitor for papain.[34] Crystal structures of related papain-inhibitor complexes showed that the inhibitor extends along the S_n (n= 1~2) subsites of the enzyme and is stabilized in the active-site groove by a series of hydrogen bonds and hydrophopic interactions which may have higher priority than the P–S interactions.[34-36] Based on X-ray structures showing the interaction of inhibitor molecules with papain, it is proposed that our inhibitor interacts with His 158, Gly-66, Asp-158 and Gln-19(Figure 4.2).[34, 36, 37] Despite the recent results obtained by Gütschow[26] that papain prefers aromatic residues over aliphatic ones in the P_2 position, the structural basis of this argument was not clearly addressed. It appears that the binding pocket is more flexible with regards to molecular recognition. Peptide **10** possesses Arg in P_2 and Tyr in P_1 and exhibits good molecular recognition properties. The new sequence Thc-Fca-Gly-Gly-Arg-Tyr exhibits the strongest inhibition of papain, K_i = 6.9 ± 0.2 μM. Presumably, N-conjugation of the inhibitory sequence with Thc-Fca residues enhances the affinity for papain binding site.[22] As was

demonstrated earlier in solution studies on the Fc derivative,[22] the organometallic Fca group is most likely encapsulated, which appears to enhance the interaction with the protein.

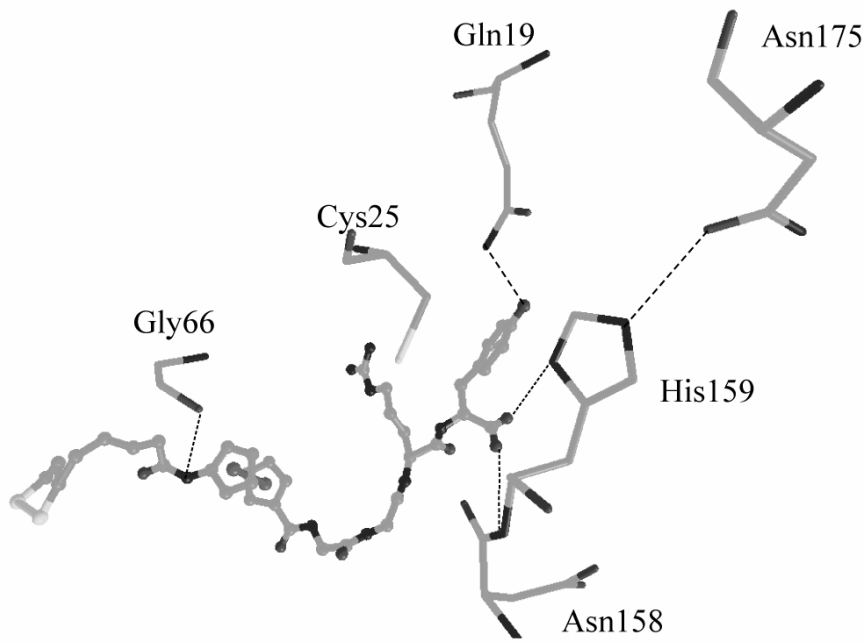

Figure 4.2. Proposed structure of peptide **10** interacting with the binding site of papain. The initial enzyme-inhibitor structure was modeled in the VEGA ZZ 2.0.5 program[38] based on the papain structure **1PE6** studied by Yamamoto et al.[36] The papain-peptide complex model was constructed by replacing the inhibitor in structure **1PE6** with peptide **10** as the chosen inhibitor in our case. The initial geometry of peptide **10** and papain-peptide complex were modeled by energy minimization using molecular mechanics calculation method (MM) in Spartan. The enzyme-inhibitor complex distances were in good agreement with x-ray crystallographic studies.[36]

4.2.3. SPR Imaging

The next step in this investigation was to determine the potential of the Fca-peptide conjugates to be active towards papain binding when linked on a surface. This will allow us to evaluate the formation of the peptide-protein complex on the surface and is a useful step towards the evaluation of the interaction by electrochemical methods. The idea was to exploit the Thc disulfide of conjugates **4**, **9**, and **10** for

binding to a gold surface. The resulting Fca-peptide film will have the Fca groups firmly embedded in the film and the inhibitory peptide exposed allowing papain to bind. SPR imaging was selected as a method of choice because of its powerful ability to study the bio-affinity interactions of thin films on gold.[39-42] The quantitative measurements of papain interactions with the Fca-peptide modified surface by SPR imaging allowed to measure the change in the percentage reflectivity (Δ%R) which was directly proportional to the fractional surface coverage θ of the peptide-modified surface by papain, providing Δ%R is below 10%.[43] Using this method, the adsorption and desorption kinetics of papain were determined. Peptides **4**, **9** and **10** were immobilized on spot ready SPR microchips by spotting ethanolic solutions of the conjugates onto the four gold pads each per chip and then monitored the selective binding to papain by real-time SPR imaging, as described in the Experimental Section (Figure 4.3). This was achieved by monitoring changes in percentage reflectivity (Δ%R) as a function of papain concentration (up to 200 nM) under continuous flow. Conjugate **10** exhibited a significantly higher change in Δ%R compared to the other two conjugates **4** and **9**. This was in agreement with the solution studies (*vide supra*). Figure 4.4 shows the increase in Δ%R due to papain-surface interaction.

The binding curve reaches a steady state when papain adsorption and desorption rates were equal. At this point, papain-free buffer was injected and flowed over the peptide array. In order to extract values for the association (k_a) and dissociation (k_d) rate constants, sequential fitting of the response curves over a series of different protein concentrations was required. Assuming a 1:1 interaction model between papain and the surface-bound Fca-peptide, Equation 4.1 was used to determine the rate of desorption.

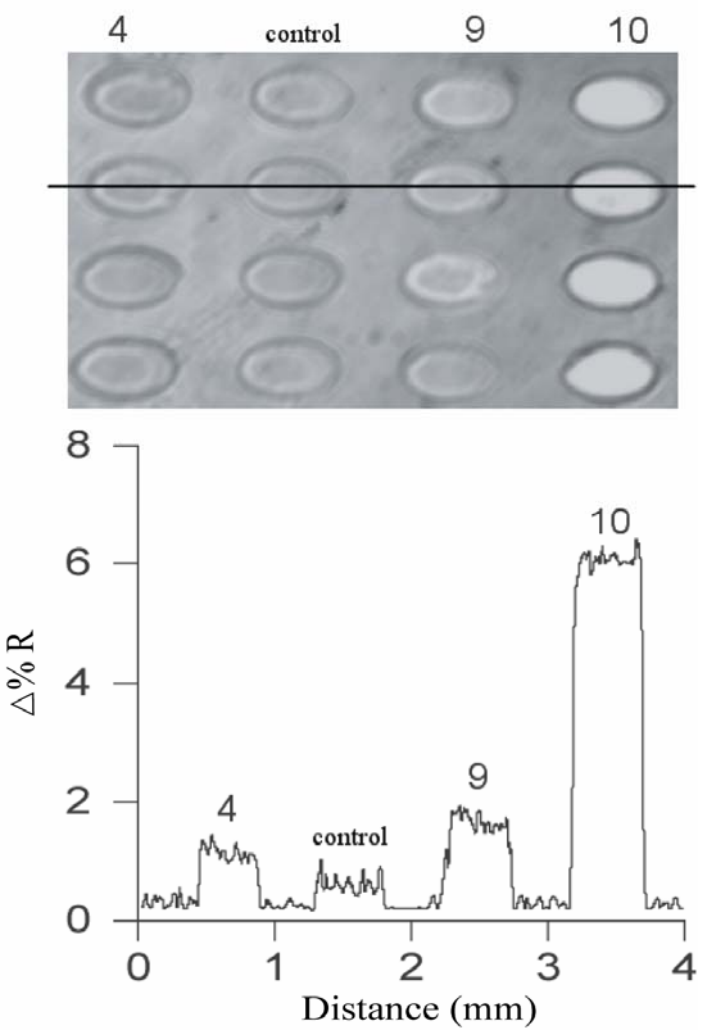

Figure 4.3. SPR imaging measurements showing the interaction of papain (150 nM) with surface-bound Fca-peptide conjugates **4**, **9**, and **10** and a decanethiol control. Papain was dissolved in a buffer solution (0.1 M sodium phosphate pH 6.2, 2.5 mM EDTA, 300 μM DTT, and 30% DMSO, 23 °C. (A) SPR difference image resulting from subtraction of the buffer image from the ones obtained after interaction with papain; (B) The line profile, taken across the difference images, shows significant differences in the Δ%R for measurements taken in the absence and presence of papain.

$$\Delta\ \%R(t) = \Delta R \exp(-k_d t) \qquad (4.1)$$

The adsorption curves are determined using a simplified Langmuir isotherm by:

$$\Delta\ \%R(t) = \Delta R\ (1 - e^{\gamma t}) \qquad (4.2)$$

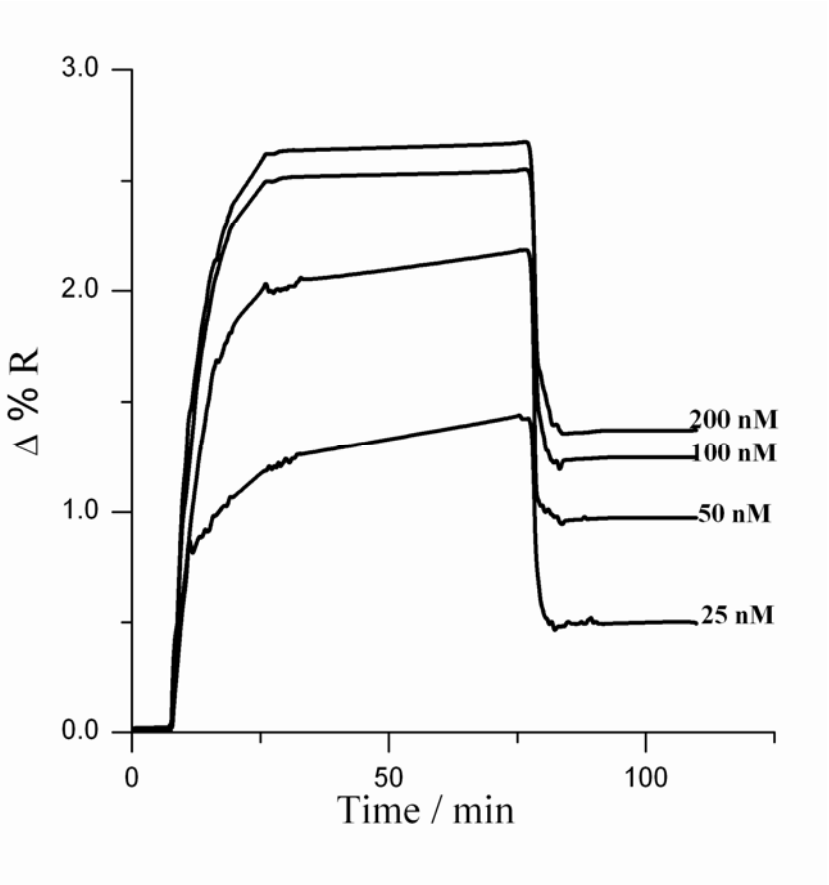

Figure 4.4. Plot of Δ%R versus time for the interaction of papain with thin films of Fca-peptide conjugate **10** on gold. The concentration of papain was increased from 25 – 200 nM.

Where $\gamma = k_a C + k_d$ with C being the protein concentration. ΔR can also be defined as equal to the product $\Delta R_{max}\theta$, where ΔR_{max} is the maximum SPR signal obtained when all surface binding sites are occupied and θ is the fraction of the total surface coverage. Figure 4.5 shows a plot of γ versus papain concentration by fitting the adsorption curves shown in Fig (4.S5) to Equation 4.2. $k_a = 1.75 \pm 0.05 \times 10^5\ M^{-1}\ s^1$ and $k_d = 2.90 \pm 0.05 \times 10^{-2}\ s^{-1}$ were obtained from the slope and intercept, respectively. Moreover, the equilibrium adsorption constant $K_{ads} = 6.03 \times 10^6\ M^{-1}$ was obtained from the ratio of k_a

and k_d. The K_{ads} value was falling within the reported range of binding constants for the interaction between proteins with immobilized peptides from 1.7 x 10^6 M^{-1} to 1.5 x 10^8 .[42, 44-47]

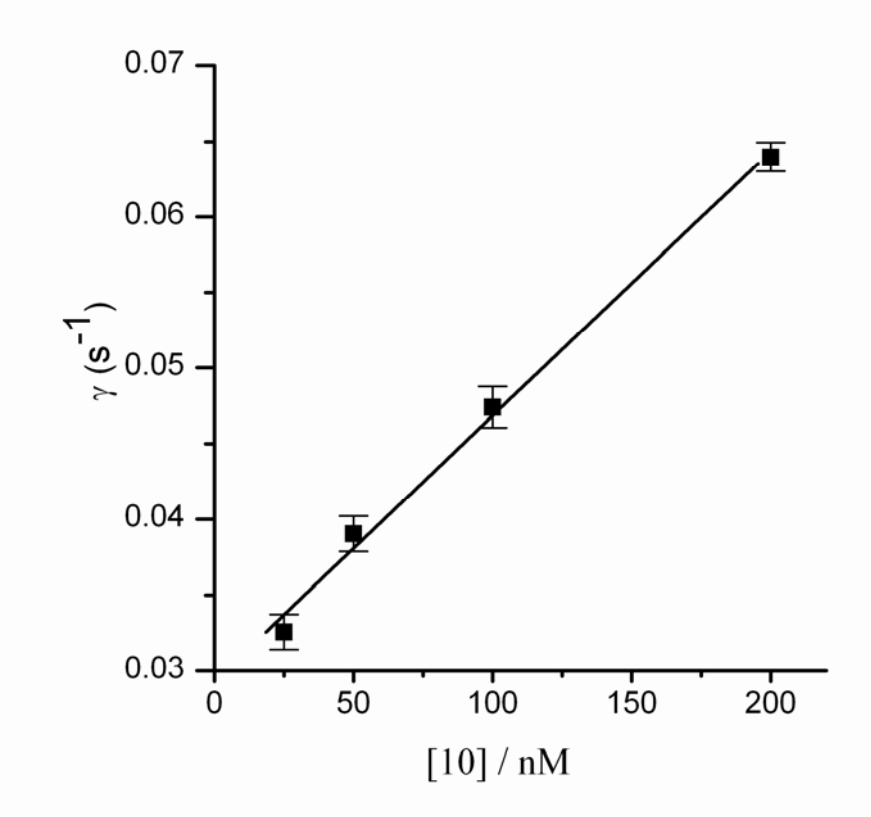

Figure 4.5. Plot of γ versus papain concentration for conjugate **10** obtained from fitting the adsorption curves to Eq 4.2. The linear slope corresponds to the adsorption rate constant k_a = 1.75 ± 0.05 x 10^5 M^{-1} s^1 and the y-intercept corresponds to the desorption rate constant k_d = 2.90 ± 0.05 x 10^{-2} s^{-1}

4.2.4. Electrochemistry

Fca-peptide conjugates **10** displayed the lowest inhibition constant in solution and also performed well when present as a thin film. Next, we decided to test our major hypothesis of the new label-based electrochemical detection and exploit the redox activity of the Fca group to detect the binding of papain to the inhibitory peptide sequence in conjugate **10**. The electrochemical studies were carried out using Fca-peptide films prepared on 25-μm gold microelectrodes. The peptide films were prepared

by immersing the microelectrodes in Thc-terminated peptides prepared in 5% (by volume) acetic acid in ethanol at concentration of approximately 1 mM for 36 hours. As described in Scheme 4.1.D Fca label is located at the base of the peptide capturing-layer allowing direct connection and close proximity to the gold surface. Under these conditions, the disulfide-containing Thc group adsorbed to the gold surface involving a stable Au-S linkage.[48, 49]

The next step involved the dilution of the Fca-peptide in order to close available pinholes present in the film and cover any solution accessible gold. The dilution was carried out by immersing the Fca-peptide-modified gold microelectrodes in an ethanolic solution of decanethiol (0.5 mM) for about two minutes. The electrochemical response of the films was evaluated by cyclic voltammetry (CV) measurements in papain activation buffer at pH 6.2 containing $NaClO_4$ (2 M) as supporting electrolyte. Measurements were repeated for ten separate microelectrodes in order to obtain statistically meaningful results. The films exhibited a single fully reversible one-electron redox peak with a formal potential E° of 0.459± 0.005 V at a scan rate of 10 V/s *versus* Ag/AgCl. Figure 4.6 shows the change of the CVs as a function of increasing papain concentration.

As the enzyme concentration increased, the formal potential of the Fca probe was shifting to higher potentials, indicating that oxidation of the Fca group became increasingly more difficult as papain was binding to the inhibitory peptide. In case of the Fc derivative Fc-Gly-Gly-Tyr-Arg, these changes were caused by slight changes in the chemical environment around the Fc group.[22] This change is illustrated in Figure 4.6, which shows a plot of E^o as a function of papain concentration.

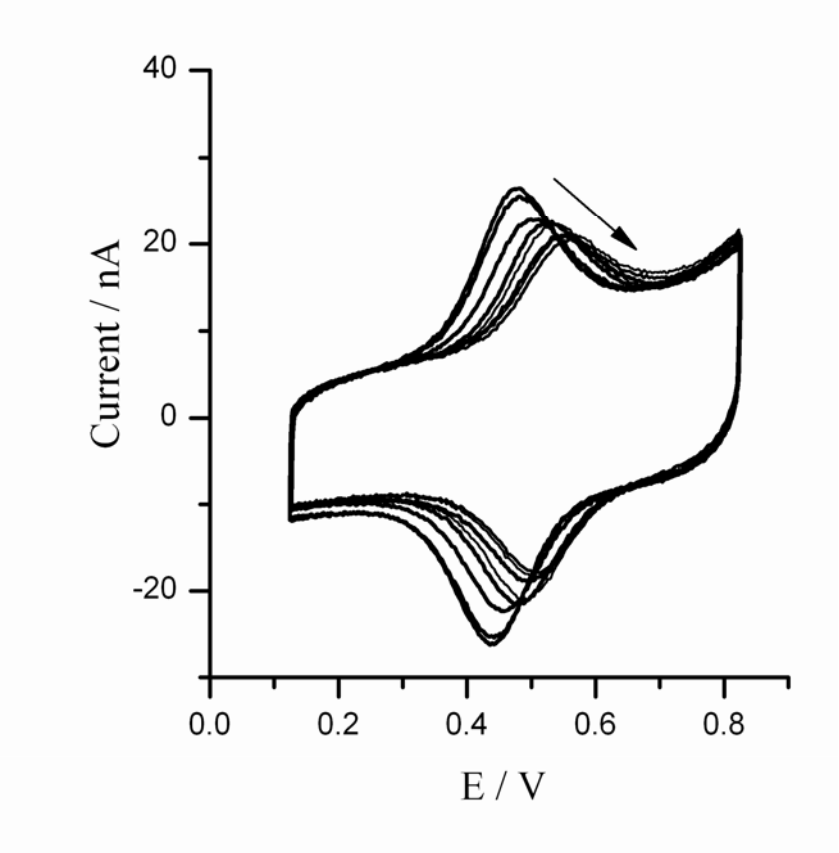

Figure 4.6. Cyclic voltammogram of 25 μm diameter gold microelectrodes modified with a mixed film of Fca-peptide **10** and decanethiol in the presence of increasing concentrations of papain (The arrow direction indicates a signal decrease and shift to higher potential with increasing the concentration from 0 to 200 nM). Enzyme activation buffer (0.1 M sodium phosphate pH 6.2, 2.5 mM EDTA, 300 μM DTT, and 30% DMSO, 23°C) with 2M $NaClO_4$. Scan rate of 10 Vs^{-1}, Pt counter, Ag/AgCl reference.

A linear relationship was observed for papain concentration of up to 80 nM, after this concentration the potential reaches a steady state indicating potentially the saturation of the surface with papain. The detection limit was 4 x 10^{-9} M, estimated from $3(S_b/m)$, where S_b is the standard deviation of the measurement signal for the blank and m the slope of the analytical curve in the linear region.[50]

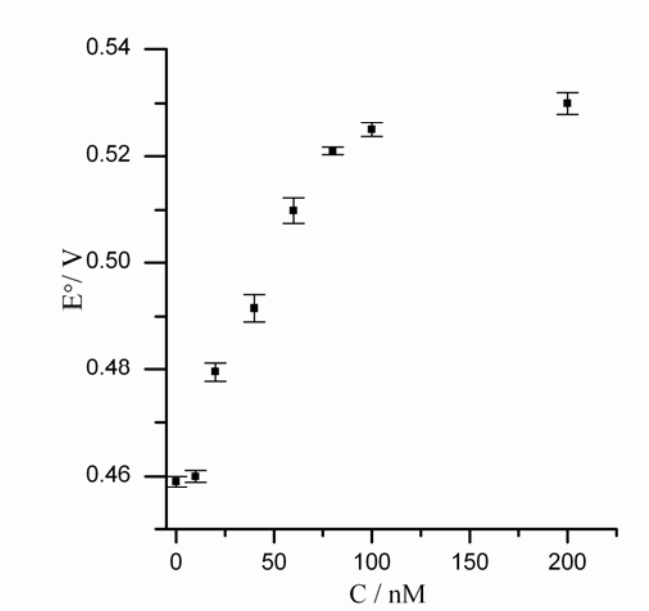

Figure 4.7. A plot of the formal potential ($E°$) *vs* papain concentration.

In addition, a small decrease in the overall signal intensity was observed, most likely as a result of less efficient penetration of the film by the supporting electrolyte, thereby decreasing the ability of the Fca to be oxidized. However, we do not lose the ability to detect the interaction between the peptide and the protein. In contrast to our observations, in some cases severe problems can occur that will result in the loss of signal. In Katayama's sensor system,[9] a significant reduction in current was observed as a function of c-AMP addition to the system, ultimately leading to loss of signal at high c-AMP concentrations. It is likely that these changes are caused by decreased access of the $[Fe(CN)_6]^{3-/4-}$ redox probe to the surface. In aptamer-based systems, the aptamer is highly dynamic in the absence of the target analyte allowing efficient electron transfer between the redox tag and the surface. The electron transfer is affected by analyte binding and in some cases even inhibited.[51-54]

In order to gain further support for the interaction of papain with films of conjugate **10**, measurements were carried out involving a quartz crystal microbalance.

For this purpose, peptide films were immobilized on the gold pad on the quartz crystals following the identical procedure used for gold microelectrodes. In the QCM measurements, changes in the frequency are monitored as a function of time, Figure 4.3.8. In the presence of the blank activation buffer solution, only continuous decay of Δf was observed, most likely caused by buffer migration. In the presence of papain, the protein adsorbes to the film of conjugates **10** and after some time reaches steady state. The change in frequency Δf before and after papain addition is 34.1± 3 Hz, which is converted into a mass change using the Sauerbrey equation (Eq. 4.3.5). The average mass of papain adsorbed to the surface was 245± 3 ng cm^{-2} or 1.62 x 10^{-12} mol cm^{-2}, which compared very well with the theoretical value (1.35 x 10^{-12} mol cm^{-2}) assuming 100% surface coverage.

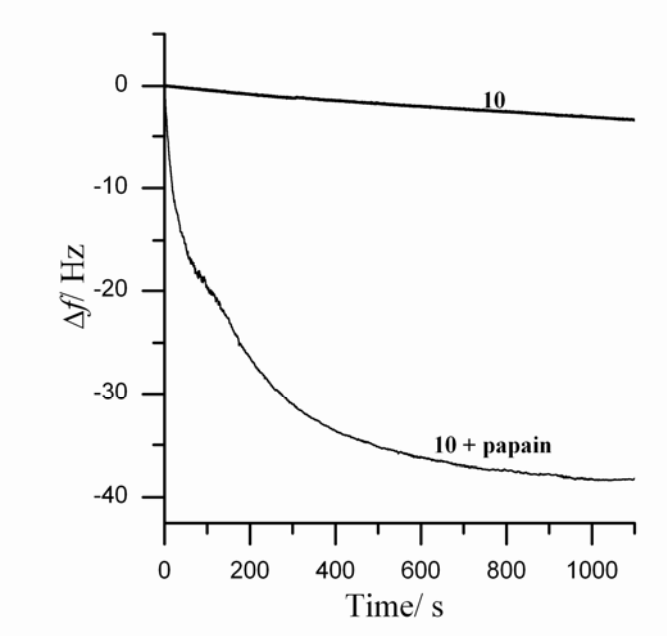

Figure 4.8. QCM measurement of papain adsorption on films of Fca-peptide conjugate **10** on gold covered AT-cut type crystals. Papain activation buffer: 0.1 M sodium phosphate pH 6.2, 2.5 mM EDTA, 300 μM DTT, and 30% DMSO, 23°C with 2.0 M $NaClO_4$.

4.3. Conclusion

In summary, we have synthesized a bioorganometallic conjugate of Fca equipped with an inhibitory peptide sequence that targets papain. Competitive inhibitions from solution assays and adsorption-desorption kinetics from real-time SPR imaging studies allowed the selection of peptide **10** as the most efficient capture probe for papain detection. The electrochemical measurements of surface-bound Fca-peptide **10** showed a significant electrochemical response of the sensor upon binding to papain. The signal is shifting anodically as well as decreasing in intensity, presumably due to the partial shielding of the Fca group by the papain. This represents proof of concept that our approach using bioorganometallic sensor systems provides an attractive alternative for the electrochemical detection of non-labeled non-redox active proteins, which under current detection schemes remains a significant challenge. Thus, the next step in our investigation is to optimize the sensor platform and expand our studies to include multiplexed measurements of several analytes by varying the recognition sequence on the Fca redox probe.

4.4. Experimental Section

Materials and General Procedure: All syntheses were carried out under dry nitrogen gas unless otherwise indicated. CH_2Cl_2 (ACS grade) used for synthesis was dried (CaH_2) and distilled prior to use. $CDCl_3$ (Aldrich) was dried (CaH_2), and stored over molecular sieves (8-12 mesh; 4Å effective pore size; Fisher) before use. THF was dried by benzophenone/sodium still, and stored over molecular sieves (8-12 mesh; 4Å effective pore size; Fisher) before use. 2-(1-H-Benzotriazol-1-yl-)-1,1,3,3-tetramethyluronium (HBTU), hydroxybenzotrizole (HOBt) (Nova), $MgSO_4$, and

$NaHCO_3$ (VWR) were used as received. For column chromatography, a column with a width of 2.7 cm (ID) and a length of 45 cm was packed 18-22 cm high with 230-400 mesh silica gel (VWR). For TLC, aluminum plates coated with silica gel 60 F_{254} (EM Science) were used. NMR spectra were recorded on a Bruker Avance-500 spectrometer using a 5-mm broadband probe operating at 500.134 MHz (^{1}H) or 125.766 MHz (^{13}Cc). Peak positions in the ^{1}H-NMR spectra are reported in ppm relative to TMS. All otherwise it is described $^{13}C\{^1H\}$ spectra are referenced to the DMSO-*d6* signal at δ 39.85. Mass spectrometry was carried out on a VG Analytical 70/20 VSE instrument. Infrared spectra were recorded on a Perkin-Elmer model 1605 FT-IR spectrometer. Analytical RP-HPLC for peptide 10 was performed on a Dionex HPLC system equipped with a Dionex Acclaim 3 lm C-18 (150 · 4.6 mm) column with a flow rate of 1 mL/min. Semi-preparative RP-HPLC was performed on a Dionex HPLC system equipped with a Phenomenex Gemini 5 lm C-18 (250 · 10 mm) column with a flow rate of 2.0 mL/ min. Mobile phase A was 0.1% TFA in water, mobile phase B was 0.1% TFA in acetonitrile. The gradiant was T= 0 min, B = 5%; T= 20 min, B = 65%; T= 25 min, B = 90%; T= 27 min, B = 95%; T= 27.1 min, B = 8%; T= 35 min, B = 5%.

Papain, lyophilized powder, ≥10 units/mg protein (E1%/280) and thiostic acid (Thc-OH) were purchased from Sigma. DTT (±-threo-2,3-dihydroxy-1,4-butanedithiol) was obtained from Fluka. Z-Phe-Arg-NHNP was purchased from Bachem, Bubendorf, Switzerland. The amino acid derivatives were purchased from Advanced ChemTech. Spot-ready SPR chips having sixteen 1 mm gold spots and plane gold SPR chips were purchased from GWC technologies. The syntheses of Boc-Gly-Gly-Tyr(Bzl)-Arg(NO_2)-

OMe,[22] benzotriazol-1-yl-1′-(*tert*-butyloxycarbonylamino)ferrocene-1-carboxylate (Boc-Fca-OBt)[55] were described elsewhere.

4.4.1. Synthesis of Boc-Fca-Gly-Gly-Tyr(Bz)-Arg(NO_2)-OMe (2)

Boc-Gly-Gly-Tyr(Bz)-Arg(NO_2)-OMe **1** (2.2 mmol, 1.54 g) was dissolved in CH_2Cl_2 and treated with TFA (3 mL) in CH_2Cl_2 (3 mL) for 30 min. The TFA and CH_2Cl_2 were subsequently removed in vacuo. The resulting residue was redissolved in CH_2Cl_2 and cooled in ice bath prior to the dropwise addition of Et_3N (0.45 mL). To this was added a solution of Boc-Fca-OBt (2 mmol, 0.92 g). The reaction mixture was then warmed to room temperature and left to stir overnight. Purification of the crude product was carried out by column chromatography on silica ($CDCl_3$, MeOH 90:10) to give yellow crystals of compound **2** (1.41 g, 76%). ^{1}H-NMR [D_6]DMSO, (δ in ppm): 7.43 (2H, d, *J* = 8 Hz, Bz), 7.38 (2H, t, *J* = 9 Hz, Bz), 7.32 (1H, t, *J* = 9 Hz, Bzl), 7.15 (2H, d, *J* = 8 Hz, Tyr-Bz), 6.89 (2H, d, *J* = 9 Hz, Tyr-Bz), 5.05 (2H, s, Tyr(O-CH_2)), 4.78 (s, 2 H, H-2 and H-5, Fc), 4.59 (s, 2 H, H-2′ and H-5′, Fc), 4.47 (1H, m, Tyr(αCH)), 4.42 (s, 2 H, H-3 and H-4, Fc), 4.28 (1H, m, Arg(αCH)), 4.06 (s, 2 H, H-3′ and H-4′, Fc), 3.71(2H, s, Gly1(αCH)), 3.67 (2H, s, Gly2(αCH)), 3.61 (3H, s, $COOCH_3$), 3.03 (2H, m, CH_2 of C*H*$_2$$CH_2CH_2NH$), 2.89 (1H, m, one H of the two diastereotopic CH_2 of Tyr), 2.70 (1H, m, one H of the two diastereotopic CH_2 of Tyr), 1.69 (1H, m, one H of the two diastereotopic CH_2 of CH_2CH_2C*H*$_2$NH), 1.54 (1H, m, one H of the two diastereotopic CH_2 of CH_2CH_2C*H*$_2$NH), 1.45 (2H, m, 2H of CH_2 of $CH_2CH_2CH_2NH$), 1.43 (9H, s, Boc C(C*H*$_3$)$_3$). ^{13}C{^{1}H}-NMR [D_6]DMSO, (δ in ppm): 172.6 ,171.8, 170.4, 169.9, 168.9, 157.4, 153.5, 137.7, 130.7, 130.3, 128.9, 128.2, 128.1, 114.8, 89.6, 76.9,

70.7 ,69.5, 69.4, 65.9, 61.4, 45.3, 52.4, 52.2, 42.3, 37.2, 31.4, 28.6, 28.5, 22.5, 14.4. FT-IR (KBr, υ_{max}/cm^{-1}): 3301 (m, N-H), 1741 (s, C=O). TOF-MS (m/z): calc for $C_{43}H_{53}N_9O_{11}Fe$ $[M]^+$: 927.3214; found: 927.3217.

4.4.2. Synthesis of Thc-Fca-Gly-Gly-Tyr(Bz)-Arg(NO_2)-OMe (3)

After the removal of the Boc group from **2** (1.1 mmol, 1.01 g) using TFA (1.5 mL), the excess acid was removed in vacuo and Et_3N (1.0 mL) in CH_2Cl_2 (10 mL) was added. To this was added a solution of Thc-OBt, prepared in situ from thiostic acid (1.0 mmol, 0.206 g), HOBt (1.1 mmol, 0.153 g), and EDAC•HCl (1.1 mmol, 0.191 g) in dry CH_2Cl_2 (15 mL, 0 °C). The reaction mixture was then warmed to room temperature and left to stir overnight. The reaction mixture was then treated consecutively with aqueous solutions of $NaHCO_3$ (sat.), citric acid (10%), and water, dried over Na_2SO_4, and evaporated to dryness under reduced pressure. The crude product was purified by flash column chromatography (SiO_2, 95:5 EtOAc:MeOH) to give pale yellow crystals of compound **3** (0.69 g, 68%). ^{1}H-NMR [D_6]DMSO, (δ in ppm): 8.38 (1H, s, NH), 8.36 (1H, s, NH), 8.10 (2H, b s, NH), 8.04 (2H, b s, NH), 7.43 (2H, d, *J* = 7 Hz, Bz), 7.38 (2H, t, *J* = 9 Hz, Bz), 7.32 (1H, t, *J* = 9 Hz, Bz), 7.15 (2H, d, *J* = 8 Hz, Tyr-Bz), 6.90 (2H, d, *J* = 8 Hz, Tyr-Bz), 5.06 (2H, s, Tyr(O-CH_2)), 4.78 (s, 2 H, H-2 and H-5, Fc), 4.58 (s, 2 H, H-2′ and H-5′, Fc), 4.44 (1H, m, Tyr αH), 4.42 (s, 2 H, H-3 and H-4, Fc), 4.26 (1H, m, Arg αH), 4.05 (s, 2 H, H-3′ and H-4′, Fc), 3.96 (2H, s, Gly1αH), 3.66 (2H, s, Gly2 αH), 3.64 (3H, s, $COOCH_3$), 3.61 (1H, m, one H of the two diastereotopic CH_2 of Thc), 3.20 (1H, m, one H of the two diastereotopic CH_2 of Thc), 3.14 (1H, m, one H of the two diastereotopic CH_2 of Thc) 3.03 (2H, m, CH_2 of C*H*$_2$$CH_2CH_2NH$), 2.89 (1H,

m, one H of the two diastereotopic CH_2 of Tyr), 2.70 (1H, m, one H of the two diastereotopic CH_2 of Tyr), 2.49 (1H, m, 1H of the two diastereotopic CH_2 of Thc), 2.30 (2H, m, Thc (CH_2)), 1.90 (1H, m, Thc (CH)), 1.75 (4H, m, two CH_2 of Thc), 1.69 (1H, m, one H of the two diastereotopic CH_2 of $CH_2CH_2C\mathit{H}_2NH$), 1.54 (1H, m, one H of the two diastereotopic CH_2 of $CH_2CH_2C\mathit{H}_2NH$), 1.53 (2H, m, Thc (CH_2)), 1.45 (2H, m, 2H of CH_2 of $CH_2CH_2CH_2NH$). $^{13}C\{^1H\}$-NMR [D_6]DMSO, (δ in ppm): 172.6, 171.8, 171.4, 170.6, 169.7, 168.9, 157.4, 137.7, 130.6, 130.2, 128.8, 128.2, 128.1, 114.8, 97.1, 77.0, 71.7, 69.6, 69.6, 69.4, 66.0, 62.2, 65.6, 54.4, 52.4, 52.2, 42.7, 42.3, 38.6, 37.2, 36.2, 34.7, 34.6, 28.8, 28.7, 28.4, 25.3, 24.7. FT-IR (KBr, υ_{max}/cm^{-1}): 3297 (b m, N-H), 1741, 1653, 1538 (s, C=O). TOF-MS (m/z): calc for $C_{46}H_{57}O_{10}N_9S_2Fe$ $[M]^+$: 1015.3019; found: 1015.3025.

4.4.3. Synthesis of Thc-Fca-Gly-Gly-Tyr(Bz)-Arg(NO_2)-OH (4)

To a solution of compound **3** (0.50 g, 0.49 mmol) in MeOH (2.0 mL) a solution of 1 N NaOH in water (2.6 mL) was added while stirring. The reaction was stored at room temperature for 6 h after which 1 N HCl (1.5 mL) was added. The MeOH was then removed in vacuo followed by cooling of the solution in a ice bath prior to the dropwise addition of 1 N HCl (3.0 mL). The solution was then stored in the fridge for 3 h after which the precipitate was filtered off and washed three times with cold, distilled water (50 mL) and dried under reduced pressure overnight to give compound **4** as a yellow solid (0.69 g, 68%). m. p. 152-159 °C. ^{1}H-NMR [D_6]DMSO, (δ in ppm): 9.44 (1H, s, COOH), 8.63 (1H, s, NH), 8.29 (1H, s, NH), 8.22 (1H, s, NH), 8.12 (2H, b s, NH), 7.36 (1H, b s, NH), 7.42 (2H, d, J = 8 Hz, Bz), 7.38 (2H, t, J = 9 Hz, Bz), 7.32

(1H, t, *J* = 8 Hz, Bz), 7.15 (2H, d, *J* = 9 Hz, Tyr-Bz), 6.90 (2H, d, *J* = 9 Hz, Tyr-Bz), 5.06 (2H, s, Tyr(O-CH_2)), 4.78 (s, 2 H, H-2 and H-5, Fc), 4.58 (s, 2 H, H-2′ and H-5′, Fc), 4.44 (1H, m, Tyr αH), 4.42 (s, 2 H, H-3 and H-4, Fc), 4.26 (1H, m, Arg αH), 4.05 (s, 2 H, H-3′ and H-4′, Fc), 3.96(2H, s, Gly1αH), 3.66 (2H, s, Gly2 αH), 3.61 (1H, m, one H of the two diastereotopic CH_2 of Thc), 3.20 (1H, m, one H of the two diastereotopic CH_2 of Thc), 3.14 (1H, m, one H of the two diastereotopic CH_2 of Thc) 3.03 (2H, m, CH_2 of C*H*$_2$$CH_2CH_2NH$), 2.89 (1H, m, one H of the two diastereotopic CH_2 of Tyr), 2.70 (1H, m, one H of the two diastereotopic CH_2 of Tyr), 2.49 (1H, m, one H of the two diastereotopic CH_2 of Thc), 2.30 (2H, m, Thc CH_2), 1.90 (1H, m, Thc CH), 1.75 (4H, m, two CH_2 of Thc), 1.69 (1H, m, one H of the two diastereotopic CH_2 of CH_2CH_2C*H*$_2$NH), 1.54 (1H, m, one H of the two diastereotopic CH_2 of CH_2CH_2C*H*$_2$NH), 1.53 (2H, m, Thc CH_2), 1.45 (2H, m, two H of CH_2 of $CH_2CH_2CH_2NH$). $^{13}C\{^1H\}$-NMR [D_6]DMSO, (δ in ppm): 188.5, 171.4, 169.6, 159.8, 157.4, 137.7, 130.7, 128.9, 128.2, 114.8, 97.2, 77.1, 71.6, 69.6, 69.5, 65.9, 62.3, 56.6, 42.6, 38.6, 36.2, 43.7, 28.8, 25.4. FT-IR (KBr, υ_{max}/cm^{-1}): 3297 (b m, N-H), 1741, 1654, 1546 (s, C=O). TOF-MS (m/z): calc for $C_{45}H_{55}O_{10}N_9S_2Fe$ $[M]^+$: 1001.2863; found: 1001.2865.

4.4.4. Synthesis of Boc-Arg(Mtr)-Tyr-OMe (5)

Boc-Arg(Mtr)-OH (4.11 mmol, 2.00 g), HOBt (4.52 mmol, 0.75 g), and EDAC·HCl (4.52 mmol, 0.95 g) were mixed in dry CH_2Cl_2 (30 mL, 0 °C) and allowed to stirred for 30 minutes. To this, a solution of H-Tyr-OMe, obtained by treatment of H-Tyr OMe·HCl (4.52 mmol, 1.14 g) with Et_3N (1.5 mL) in dry CH_2Cl_2 (20 mL) was

added and the stirring continued at room temperature. The reaction mixture was then treated consecutively with aqueous solutions of saturated $NaHCO_3$, citric acid (10%), again saturated $NaHCO_3$ and water, dried over Na_2SO_4, filtered and evaporated to dryness under reduced pressure. The crude product was purified by flash column chromatography (SiO_2, 1:2 EtOAc-hexane) to give compound **5** as a white crystalline solid (yield: 2.32 g, 85%). ^{1}H-NMR $CDCl_3$, (δ in ppm): 7.48 (1H, s, Bz-OH), 6.97 (2H, d, *J* = 8 Hz, Tyr-Bz), 6.91 (1H, b s, α NH Arg), 6.78 (2H, d, *J* = 8 Hz, Tyr-Bz), 6.55 (1H, s, Ar-H (Mtr)), 6.20 ((2H, b, NH of guanidine group) 5.98 (1H, b, NH of guanidine group), 5.41 (1H, b, NH of guanidine group), 4.79 (1H, m, Arg αH), 4.00 (1H, m, Tyr αH), 3.89 (3H, s, $COOCH_3$), 3.75 (3H, s, OCH_3 of Mtr), 3.15 (2H, m, CH_2 of $CH_2CH_2CH_2NH$), 3.09 (1H, m, one H of the two diastereotopic CH_2 of Tyr), 2.88 (1H, m, one H of the two diastereotopic CH_2 of Tyr), 2.70 (3H, s, Ar-CH_3 of Mtr), 2.62 (3H, s, Ar-CH_3 of Mtr), 2.14 (3H, s, Ar-CH_3 of Mtr), 1.54 (2H, m, CH_2 of $CH_2CH_2CH_2NH$), 1.42 (9H, s, Boc C(CH_3)$_3$), 1.23 (1H, m, one H of the two diastereotopic CH_2 of $CH_2CH_2CH_2NH$). TOF-MS (m/z): calc for $C_{31}H_{45}O_9N_5S$ $[M]^+$: 663.2938; found: 663.2940.

4.4.5. Synthesis of Boc-Gly-Gly-Arg(Mtr)-Tyr-OMe (6)

Boc-Arg(Mtr)-Tyr-OMe (3.01 mmol, 2.00 g) was dissolved in CH_2Cl_2, (3 mL) and treated with TFA (3 mL) for 30 min. The CH_2Cl_2 and TFA were subsequently removed in vacuo. The resulting residue was redissolved in CH_2Cl_2 (10 mL) and cooled in an ice bath prior to the dropwise addition of Et_3N (1.2 mL). To this was added a solution of Boc-Gly-Gly-OBt, prepared in situ from Boc-Gly-Gly-OH (2.74 mmol, 0.64

g), HOBt (3.0 mmol, 0.46 g), and EDAC·HCl (3.0 mmol, 0.58 g) in dry CH_2Cl_2 (20 mL, 0 °C). The reaction mixture was then warmed to room temperature and left to stir overnight. The resulting solution was then treated as per **5**. The product was purified by flash column chromatography (SiO_2, 1:2 EtOAc-hexane) and recrystallized from $CHCl_3$ to yield white crystalline compound 6 (yield: 1.73 g, 74%): ^{1}H-NMR [D_6]DMSO, (δ in ppm): 9.22 (1H, s, Bz-OH), 8.42 (1H, s, NH-C(NH)-NH(Mtr), 8.30 (1H, d, *J* = 6 Hz, αNH(Arg), 8.09 (1H, s, NH of guanidine group), 8.05 (1H, s, NH of guanidine group), 7.96 (1H, d, *J* = 6 Hz, αNH(Tyr), 6.97 (2H, d, *J* = 8 Hz, Tyr-Bz), 6.68 (1H, s, Ar-H of Mtr), 6.64 (2H, d, *J* = 8 Hz, Tyr-Bz), 6.38 ((2H, b, NH of guanidine group) 4.60 (1H, m, Tyr αH), 4.30 (1H, m, Arg αH), 3.82 (2H, d, Gly αH), 3.78 (3H, s, $COOCH_3$), 3.70 (2H, d, Gly αH), 3.53 (3H, s, OCH_3 of Mtr), 3.01 (2H, m, CH_2 of C*H*$_2$CH$_2$CH$_2$NH), 2.88 (1H, m, one H of the two diastereotopic CH_2 of Tyr), 2.82 (1H, m, one H of the two diastereotopic CH_2 of Tyr), 2.59 (3H, s, Ar-CH_3 of Mtr), 2.49 (3H, s, Ar-CH_3 of Mtr), 2.04 (3H, s, Ar-CH_3 of Mtr), 1.62 (1H, m, one H of the two diastereotopic CH_2 of $CH_2CH_2CH_2NH$), 1.43 (9H, s, Boc C(C*H*$_3$)$_3$), 1.36 (2H, m, CH_2 of $CH_2CH_2CH_2NH$), 1.23 (1H, m, one H of the two diastereotopic CH_2 of $CH_2CH_2CH_2NH$). ^{13}C{^{1}H}-NMR [D_6]DMSO, (δ in ppm): 172.3, 171.9, 170.2, 168.9, 1579, 156.6, 156.5, 156.3, 138.1, 136.1, 130.6, 130.5, 127.5, 115.5, 112.2, 78.6, 56.0, 54.5, 52.3, 52.2, 52.1, 43.7, 42.3, 63.4, 28.7, 24.1, 22.5, 18.5, 12.2. TOF-MS (m/z): calc for $C_{35}H_{51}O_{11}N_7S$ $[M]^+$: 777.3367; found: 777.3370.

4.4.6. Synthesis of Boc-Fca-Gly-Gly-Arg(Mtr)-Tyr-OMe (7)

Boc-Gly-Gly-Arg(Mtr)-Tyr-OMe (1.9 mmol, 1.50 g) was dissolved in CH_2Cl_2 and treated with TFA (2 mL) in CH_2Cl_2 (2 mL) for 30 min. The TFA and CH_2Cl_2 were subsequently removed in vacuo. The resulting residue was re-dissolved in CH_2Cl_2 and cooled in ice bath prior to the dropwise addition of Et_3N (0.50 mL). To this was added a solution of Boc-Fca-OBt (1.73 mmol, 0.80 g). The reaction mixture was then warmed to room temperature and left to stir overnight. The residue was chromatographed ($CDCl_3$, MeOH 90:10) to give compound **7** as a yellow solid (1.47 g, 85%): ^{1}H-NMR [D_6]DMSO, (δ in ppm): 9.22 (1H, s, Bz-OH), 8.42 (1H, s, NH of guanidine group), 8.30 (1H, d, *J* = 6.3 Hz, αNH Arg), 8.09 (1H, s, NH of guanidine group), 8.05 (1H, s, NH of guanidine group), 7.96 (1H, d, *J* = 6 Hz, αNH Tyr), 6.97 (2H, d, *J* = 8 Hz, Tyr-Bz), 6.68 (1H, s, Ar-H of Mtr) 6.64 (2H, d, *J* = 8 Hz, Tyr-Bz), 6.38 ((2H, b, NH of guanidine group) 4.72 (s, 2 H, H-2 and H-5, Fc), 4.60 (1H, m, Tyr αCH), 4.47 (s, 2 H, H-2′ and H-5′, Fc), 4.30 (1H, m, Arg αCH), 4.24 (s, 2 H, H-3 and H-4, Fc), 3.95 (s, 2 H, H-3′ and H-4′, Fc), 3.82 (2H, d, αCH$_2$ Gly αCH$_2$), 3.78 (3H, s, COOCH$_3$), 3.70 (2H, d, Gly αCH$_2$), 3.53 (3H, s, OCH$_3$(Mtr)), 3.01 (2H, m, CH$_2$ of C*H*$_2$CH$_2$CH$_2$NH), 2.88 (1H, m, one H of the two diastereotopic CH$_2$ of Tyr), 2.82 (1H, m, one H of the two diastereotopic CH$_2$ of Tyr), 2.59 (3H, s, Ar-CH$_3$ of Mtr), 2.49 (3H, s, Ar-CH$_3$ of Mtr), 2.04 (3H, s, Ar-CH$_3$ of Mtr), 1.62 (1H, m, one H of the two diastereotopic CH$_2$ of CH$_2$CH$_2$CH$_2$NH), 1.43 (9H, s, Boc C(C*H*$_3$)$_3$), 1.36 (2H, m, CH$_2$ of CH$_2$CH$_2$CH$_2$NH), 1.23 (1H, m, one H of the two diastereotopic CH$_2$ of CH$_2$CH$_2$CH$_2$NH). ^{13}C{^{1}H}-NMR [D_6]DMSO, (δ in ppm): 172.7, 172.4, 170.3, 170.0, 169.4, 157.9, 156.6, 153.5, 138.1, 138.1, 136.1, 130.5, 127.3, 124.0, 115.6, 112.2, 100.0, 79.7, 76.8, 71.7, 69.3, 65.8, 56.0,

5.3, 52.2, 42.9, 42.1, 36.5, 28.6, 24.1, 18.5, 12.2. TOF-MS (m/z): calc for $C_{46}H_{60}O_{12}N_8SFe$ $[M]^+$: 1004.3401; found: 1004.3402.

4.4.7. Synthesis of Thc-Fca-Gly-Gly-Arg(Mtr)-Tyr-OMe (8)

The Boc group was removed from compound **7** (1.2 mmol, 1.20 g) by addition of TFA (1.5 mL). After 30 minutes, the excess acid was removed in vacuo and Et_3N (0.7 mL) in CH_2Cl_2 (10 mL) was added. To this was added a solution of Thc-OH (1.1 mmol, 0.224 g), HOBt (1.2 mmol, 0.184 g), and EDAC·HCl (1.2 mmol, 0.230 g) in dry CH_2Cl_2 (15 mL, 0 °C). The reaction mixture was left to stir overnight at room temperature and then treated to an aqueous work up as described above. The crude product was purified by flash column chromatography (SiO_2, 90:10 EtOAc:MeOH) to give a pale yellow solid of compound **8** (0.89 g, 68%). ^{1}H-NMR [D_6]DMSO, (δ in ppm): 9.22 (1H, s, Bz-OH), 8.42 (1H, s, NH of guanidine group), 8.30 (1H, d, J = 6 Hz, αNH Arg), 8.09 (1H, s, NH of guanidine group), 8.0 (1H, s, NH of guanidine group), 7.96 (1H, d, J = 6 Hz, αNH Tyr), 6.97 (2H, d, J = 8 Hz, Tyr-Bz), 6.68 (1H, s, Ar-H of Mtr) 6.64 (2H, d, J = 8 Hz, Tyr-Bz), 6.38 ((2H, b, NH of guanidine group) 4.72 (s, 2 H, H-2 and H-5, Fc), 4.60 (1H, m, Tyr αH), 4.47 (s, 2 H, H-2′ and H-5′, Fc), 4.30 (1H, m, Arg αH), 4.24 (s, 2 H, H-3 and H-4, Fc), 3.95 (s, 2 H, H-3′ and H-4′, Fc), 3.82 (2H, d, Gly αH_2), 3.78 (3H, s, $COOCH_3$), 3.70 (2H, d, Gly αH_2), 3.61 (1H, m, one H of the two diastereotopic CH_2 of Thc), 3.53 (3H, s, OCH_3 of Mtr), 3.20 (1H, m, one H of the two diastereotopic CH_2 of Thc), 3.14 (1H, m, one H of the two diastereotopic CH_2 of Thc), 3.01 (2H, m, CH_2 of C$H_2$$CH_2CH_2NH$), 2.88 (1H, m, one H of the two diastereotopic CH_2 of Tyr), 2.82 (1H, m, one H of the two diastereotopic CH_2 of Tyr), 2.59 (3H, s, Ar-

$CH_3$of Mtr), 2.49 (1H, m, one H of the two diastereotopic CH_2 of Thc), 2.49 (3H, s, Ar-CH_3 of Mtr), 2.30 (2H, m, Thc CH_2), 1.90 (1H, m, Thc (CH)), 2.04 (3H, s, Ar-CH_3 of Mtr), 1.75 (4H, m, two CH_2 of Thc), 1.62 (1H, m, one H of the two diastereotopic CH_2 of $CH_2CH_2CH_2NH$), 1.53 (2H, m, Thc (CH_2)), 1.36 (2H, m, CH_2 of $CH_2CH_2CH_2NH$), 1.23 (1H, m, one H of the two diastereotopic CH_2 of $CH_2CH_2CH_2NH$). $^{13}C\{^1H\}$-NMR [D_6]DMSO, (δ in ppm): 188.5, 172.2, 172.1, 171.9, 171.4, 170.6, 169.8, 169.0, 157.9, 156.6, 149.6, 138.1, 136.1, 135.0, 124.0, 122.0, 112.2, 97.1, 79.7, 77.0, 71.7, 69.4, 66.0, 62.2, 56.5, 56.5,. 56.0, 52.3, 38.6, 34.7, 34.5, 25.3, 24.6, 24.1, 12.2. FT-IR (KBr, υ_{max}/cm^{-1}): 3315, 3090 (b m, N-H), 1722, 1655, 1548 (s, C=O). TOF-MS (m/z): calc for $C_{49}H_{64}O_{11}N_8S_3Fe$ $[M]^+$: 1092.3206; found: 1092.3208.

4.4.8. Synthesis of Thc-Fca-Gly-Gly-Arg(Mtr)-Tyr-OH (9)

The methylester **8** (0.20 g, 0.18 mmol) was deprotected as described for compound **4** to give the free acid **9** as a yellow solid (0.16 g, 82%). m. p. 125-133 °C. ^1H-NMR [D_6]DMSO, (δ in ppm): 9.58 (1H, s, COOH), 9.05 (1H, s, Tyr-OH), 8.49 (1H, s, NH of guanidine group), 8.35 (1H, d, *J* = 6 Hz, αNH Arg), 8.18 (1H, s, NH of guanidine group), 8.05 (1H, s, NH of guanidine group), 7.95 (1H, d, *J* = 6 Hz, αNH(Tyr)), 7.59 (1H, m, αNH(Gly)), 7.25 (1H, m, αNH(Gly)), 6.94 (2H, d, *J* = 8 Hz, Tyr-Bz), 6.67 (1H, s, Ar-H of Mtr), 6.57 (2H, d, *J* = 8 Hz, Tyr-Bz), 4.75 (d, 2 H, *J* = 9 Hz, H-2 and H-5, Fc), 4.60 (1H, m, Arg αH), 4.59 (d, 2 H, *J* = 9 Hz, H-2′ and H-5′, Fc), 4.24 (s, 2 H, H-3 and H-4, Fc), 4.17 (1H, m, Tyr αH), 3.97 (s, 2 H, H-3′ and H-4′, Fc), 3.84 (2H, d, Gly αCH_2), 3.84 (3H, s, Ar-O-CH_3 of Mtr), 3.75 (2H, d, Gly αCH_2), 3.61 (1H, m, 1H of the two diastereotopic CH_2 of Thc), 3.53 (3H, s, OCH_3 of Mtr), 3.17

(1H, m, 1H of the two diastereotopic CH_2 of Thc), 3.11 (1H, m, 1H of the two diastereotopic CH_2 of Thc), 2.97 (2H, m, CH_2 of C*H*$_2$CH$_2$CH$_2$NH), 2.88 (1H, m, one H of the two diastereotopic CH_2 of Tyr), 2.82 (1H, m, one H of the two diastereotopic CH_2 of Tyr), 2.60 (3H, s, Ar-CH_3 of Mtr), 2.49 (1H, m, one H of the two diastereotopic CH_2 of Thc), 2.49 (3H, s, Ar-CH_3 of Mtr), 2.30 (2H, m, Thc CH_2), 1.91 (1H, m, Thc CH), 2.04 (3H, s, Ar-CH_3 of Mtr), 1.74 (4H, m, two CH_2 of Thc), 1.60 (1H, m, one H of the two diastereotopic CH_2 of $CH_2CH_2CH_2NH$), 1.53 (2H, m, Thc CH_2), 1.36 (2H, m, CH_2 of $CH_2CH_2CH_2NH$), 1.22 (1H, m, one H of the two diastereotopic CH_2 of $CH_2CH_2CH_2NH$), 0.85 (1H, m, one H of the two diastereotopic CH_2 of $CH_2CH_2CH_2NH$). $^{13}C\{^1H\}$-NMR [D_6]DMSO, (δ in ppm): 188.5, 172.2, 172.1, 171.9, 171.4, 170.6, 169.8, 169.0, 157.9, 156.6, 149.6, 138.1, 136.1, 135.0, 124.0, 122.0, 112.2, 97.1, 79.7, 77.0, 71.7, 69.4, 66.0, 62.2, 56.5, 56.5,. 56.0, 52.3, 38.6, 34.7, 34.5, 25.3, 24.6, 24.1, 12.2. FT-IR (KBr, υ_{max}/cm^{-1}): 3306, 3086 (m, N-H), 1748 (s, C=O), 1656 Amide I, 1550 Amide II. TOF-MS (m/z): calc for $C_{48}H_{62}O_{11}N_8S_3Fe$ $[M]^+$: 1078.3049; found: 1078.3049.

4.4.9. Synthesis of Thc-Fca-Gly-Gly-Arg-Tyr-OH (10)

Thc-Fca-Gly-Gly-Arg(Mtr)-Tyr-OH (**9**) (60 mg, 0.07 mmol) was suspended in CH_2Cl_2 (2 mL) and a mixture (TFA/thioanisol/H_2O 96:3:1, 3 mL) was added and the mixture left to stir for 4 hours at room temperature. The reaction mixture was concentrated in vacuo, the resulting residue was dissolved in TFA and precipitated by a dropwise addition to ice-cold Et_2O. The precipitate was collected by centrifugation, and purified by semi-preparative HPLC (tR = 22.4 min, λ = 220 nm) to yield a faint yellow

solid of compound **10** (22 mg, 0.03 mmol, 37%). RP-HPLC (analytical, tR = 9.8 min). m. p. 118-122 °C. ^{1}H-NMR [D_6]DMSO, (δ in ppm): 9.48 (1H, s, COOH), 9.23 (1H, s, Tyr-OH), 8.30 (1H, m, αNH Arg), 8.22 (1H, s, NH of guanidine group), 8.02 (1H, s, NH of guanidine group), 7.66 (1H, m, αNH(Tyr), 7.56 (2H, m, αNH(Gly)), 6.93 (2H, d, *J* =8 Hz, Tyr-Bz), 6.57 (2H, d, *J* = 8 Hz, Tyr-Bz), 4.75 (s, 2 H, H-2 and H-5, Fc), 4.60 (s, 2 H, H-2' and H-5', Fc), 4.26 (1H, m, Arg αH), 4.25 (s, 2 H, H-3 and H-4, Fc), 4.01 (1H, m, Tyr αH),3.98 (s, 2 H, H-3' and H-4', Fc), 3.80 (2H, d, Gly αH_2), 3.77 (2H, d, Gly αH_2), 3.61 (1H, m, 1H of the two diastereotopic CH_2 of Thc), 3.20 (1H, m, 1H of the two diastereotopic CH_2 of Thc), 3.18 (1H, m, one H of the two diastereotopic CH_2 of Thc),), 3.11 (1H, m, one H of the two diastereotopic CH_2 of Tyr), 2.98 (2H, m, CH_2 of C*H*$_2$CH$_2$CH$_2$NH), 2.83 (1H, m, 1H of the two diastereotopic CH_2 of Tyr), 2.71 (2H, s, NH_2 of guanidine group), 2.41 (2H, m, Thc CH_2), 2.36 (1H, m, 1H of the two diastereotopic CH_2 of Thc), 2.15 (1H, m, 1H of the two diastereotopic CH_2 of Thc), 1.66 (2H, m, CH_2 of $CH_2CH_2CH_2NH$), 1.55 (2H, m, Thc CH_2), 1.35 (2H, m, CH_2 of $CH_2CH_2CH_2NH$), 1.23 (1H, m, 1H of the two diastereotopic CH_2 of $CH_2CH_2CH_2NH$), 0.85 (1H, m, 1H of the two diastereotopic CH_2 of $CH_2CH_2CH_2NH$). ^{13}C{^{1}H}-NMR [D_6]DMSO, (δ in ppm): 172.1, 172.0, 171.8, 171.4, 170.5, 169.8, 157.8, 156.6, 138.1, 136.1, 135.0, 123.9, 121.9, 112.2, 97.1, 79.7, 76.9, 71.7, 69.4, 65.9, 62.2, 56.5, 56.4, 52.3, 38.5, 34.7, 34.5, 25.3, 24.6, 24.2. FT-IR (KBr, υ_{max}/cm^{-1}): 3447 (m, N-H), 1725 (s, C=O), 1658 Amide I, 1547 Amide II. TOF-MS (m/z): calc for $C_{38}H_{50}O_8N_8S_2Fe$ $[M]^+$: 866.2542; found: 866.2541.

4.4.10. Papain Inhibition Studies

For the inhibition studies, the following stock solutions were prepared:

A 5 mM stock solution of the chromogenic substrate Z-Phe-Arg-NHNp was prepared in DMSO. Stock solutions of the Fca-peptide inhibitors were prepared in DMSO.

A papain stock solution was prepared in 1 mM HCl. For daily activation, the papain stock solution was diluted 1:100 in 0.1 M sodium phosphate pH 6.5, containing 2.5 mM EDTA and 15 mM DTT and was incubated at 23 °C for 1 h. The activated enzyme was kept on ice.

Inhibition of papain enzyme was assayed at 23 °C with the chromogenic substrate Z-Phe-Arg-NHNp (200 μM) in the presence of increasing concentrations of the inhibitory peptides **4**, **9** and **10**. The buffer solution used for the assay was 0.1 M sodium phosphate pH 6.2, 2.5 mM EDTA, 300 μM DTT, and 30% DMSO. Rates were determined by duplicate measurements of seven different concentrations of each single inhibitor. The concentration of the liberated p-nitroaniline (*p*NA) was monitored spectrophotometrically by measuring the absorbance at λ = 405 nm against a blank sample containing no enzyme and an extinction coefficient of ε = 9.96 $cm^2/\mu mol$. The final volume made up to 1 mL. The reaction was initiated by addition of the enzyme (20 μL); its final concentration catalyze the conversation of the substrate with a rate of 1-2 μM/min. Progress curves were monitored over 10 min. A control assay to determine the total hydrolysis of Z-Phe-Arg-NHNp (480 μM) was carried out in the absence of the inhibitors (70 μL DMSO was added to the cuvette). The papain concentration was 20 fold higher than the inhibition assays. The resulting activity was considered as 100%. A

Lineweaver-Burk plot was constructed and the value of the Michaelis-Menten constant (K_m) was determined. The apparent inhibition constants K_i' were determined by fitting equation 3[26] to the experimental data.

$$\upsilon = \upsilon_o / (1 + [I] / K_i') \quad (4.3)$$

Where υ is the rate, υ_o is the rate in the absence of the inhibitor, [I] is the inhibitor concentration and K_i' is the apparent inhibition constant. The true inhibition constants K_i were calculated by correction of K_i' according to equation 4.4[26]

$$K_i = K_i' / (1 + [S] / K_m) \quad (4.4)$$

Where [S] is the substrate concentration and K_m is the Michaelis-Menten constant.

4.4.11. Preparation of Peptide Arrays

Peptide arrays on spot ready SPR chips were prepared by spotting three different peptides **4**, **9** and **10** on three arrays. The gold chip was placed on a piece of clean parafilm in a humidity chamber and the freshly prepared peptide solutions were spotted immediately 5 mM in DMSO (100 mM TEA pH 8) for 20 hours. As a control experiment, a 5 mM solution of decanethiol was used to immobilize the decanethiol onto the control array. The excess probe solutions were then removed with a pipet prior to rinsing with the few mL of buffer solution (0.1 M sodium phosphate, pH 6.2, 2.5 mM EDTA, 300 μM DTT, and 30% DMSO, T = 23±3°C).

Preparation of films on flat substrates: Each peptide was immobilized on the gold surface of a plane SPR chip by soaking the chips overnight in a 1 mM solution of disulfide-terminated peptides **4**, **9** and **10** in absolute ethanol.

4.4.12. Real-Time SPR Imaging Studies

An SPR imaging system (GWC Technologies) was used for the real-time monitoring of the interaction between immobilized peptides and papain enzyme. Briefly, a collimated p-polarized light at a fixed angle reflected from the sample/gold/prism assembly was sent through a narrow band-pass filter and then detected with a CCD camera. The data were collected using the software package V++ (Digital Optics, NZ). Custom macros were used so that data could be collected with simultaneous processing of several specific user designated regions of interest (ROIs) on the array surface.[42] Kinetic data for each ROI were obtained by collecting one data point approximately every 1 second, which was the average of five camera frames. The difference in percent reflectivity for each probe area was normalized with respect to the average change in percent reflectivity measured for the buffer background. Kinetic data from multiple identical array elements were averaged to obtain the final SPR response curves. Microsoft Excel and Origin 7.5 were used for all data processing and kinetic model fitting in these experiments.

4.4.13. Surface Electrochemistry

Peptide films were immobilized on home made 25 μm diameter microelectrodes by soaking the gold electrodes in 1 mM solution of disulfide terminated peptides for 36 h. Then, the concentrated film was diluted by immersing the modified electrodes in 1 mM ethanolic solution of decanethiol for 2 min. The CVs were recorded in aqueous solutions of $NaClO_4$ (2.0 M). Ag/AgCl was used as a pseudo-reference electrode, and Pt wire as a counter electrode. Ten gold microelectrodes with peptide films were measured

for each compound and all experiments were carried out at room temperature (23±3°C). Blocking studies were carried out in a solution containing 0.1 mM $Ru(NH_3)_6Cl_3$ and 0.1 N $HClO_4$, See Figure 4.S6.

Studies using the electrochemical quartz crystal microbalance: An EQCM system interfaced to a PC (CH instruments 440) was used for recording the frequency change during the process of protein adsorption onto the peptide film. The EQCM electrodes with a fundamental resonant frequency of 8 MHz and 13.7 mm diameter were of the AT-cut type, with optically polished surfaces coated on both sides with 200 nm thick gold layer, 5 mm diameter, over a thin chromium adhesion mediator film. Since the EQCM operated in time-resolved mode, the frequency difference of the working crystal and the reference crystal was measured. The relationship between the changes in mass per unit area (m) and frequency (f) are given by Sauerbrey equation (Eq. 4.5)[56]

$$\Delta f = \frac{-2\Delta m n f_o^2}{A\sqrt{\mu_q \rho_q}} \qquad (4.5)$$

Where A is the surface area of the electrode, μ_q is shear modulus of quartz and ρ_q is the density of quartz.

4.5. References

[1] A. P. Turner, I. Karube, G. Wilson, in *Bionsensors: Fundamentals and Applications.*, Oxford Science Publications, Oxford, **1986**, p. 770.
[2] J. Wang, *Analytical Electrochemistry*, 2ed ed., Wiley, New York, **2000**.
[3] L. Murphy, *Curr. Opin. Chem. Biol.* **2006**, *10*, 177-184.
[4] J. Wang, *Analyst* **2005**, *130*, 421-426.
[5] E. Bakker, Y. Qin, *Anal. Chem.* **2006**, *78*, 3965-3983.
[6] M. Mehrvar, M. Abdi, *Anal. Sci.* **2004**, *20*, 1113-1126.
[7] J. Wang, *Biosen. Bioelectron.* **2006**, *21*, 1887-1892.
[8] J. Wang, *J. Pharm. Biomed. Anal.* **1999**, *19*, 53–74.
[9] Y. Katayama, Y. Ohuchi, H. Higashi, Y. Kudo, M. Maeda, *Anal. Chem.* **2000**, *72*, 4671-4674.
[10] F. Le Floch, H. A. Ho, M. Leclerc, *Anal. Chem.* **2006**, *78*, 4727-4731.
[11] J. N. Barisci, D. Hughes, A. Minett, G. G. Wallace, *Anal. Chim. Acta* **1998**, *371*, 39-48.
[12] W. Lu, T. A. Nguyen, G. G. Wallace, *Electroanalysis* **1998**, *10*, 1101-1107.
[13] W. Lu, G. G. Wallace, A. A. Karayakin, *Electroanalysis* **1998**, *10*, 472-476.
[14] M. S. Wilson, W. Y. Nie, *Anal. Chem.* **2006**, *78*, 2507-2513.
[15] J. Liu, S. Tian, L. Tiefenauer, P. E. Nielson, W. Knoll, *anal. Chem.* **2005**, *77*, 2756-2761.
[16] C. Fan, K. W. Plaxco, A. J. Heeger, *Proc. Natl. Acad. Sci. USA* **2003**, *100*, 9134-9137.
[17] C. Fan, K. W. Plaxco, A. J. Heeger, *J. Am. Chem. Soc.* **2002**, *124*, 5642-5643.
[18] D. R. van Staveren, N. Metzler-Nolte, *Chem. Rev.* **2004**, *104*, 5931-5985.
[19] C. H. Devillers, D. Boturyn, C. Bucher, P. Dumy, P. Labbe, J.-C. Moutet, G. Royal, E. Saint-Aman, *Langmuir* **2006**, *22*, 8134-8143.
[20] C. Baldoli, C. Rigamonti, S. Maiorana, E. Licandro, L. Falciola, P. R. Mussini, *Chem. Eur. J.* **2006**, *12*, 4091-4100.
[21] H.-B. Kraatz, *J. Inorg. Organomet. Polym.* **2005**, *15*, 83-106.
[22] K. Plumb, H. B. Kraatz, *Bioconj. Chem.* **2003**, *14*, 601-606.
[23] L. Barišić, M. Čakić, K. A. Mahmoud, Y. N. Liu, H. B. Kraatz, H. Pritzkow, S. I. Kirin, N. Metzler-Nolte, V. Rapić, *Chem. Eur. J.* **2006**, 4965-4980.
[24] L. Barisic, V. Rapic, N. Metzler-Nolte, *Eur. J. Inorg. Chem.* **2006**, 4019-4021.
[25] K. Heinze, U. Wild, M. Beckmann, *Eur. J. Inorg. Chem.* **2007**, 617-623.
[26] R. Loser, K. Schilling, E. Dimmig, M. Gutschow, *J. Med. Chem.* **2005**, *48*, 7688-7707.
[27] S. Blumberg, I. Schechte, A. Berger, *Eur. J. Biochem.* **1970**, *15*, 97-102.
[28] M. O. Funk, Y. Nakagawa, J. Skochdopole, E. T. Kaiser, *Int. J. Pept. Protein Res.* **1979**, *13*, 296-303.
[29] A. Albeck, S. Kliper, *Biochem. J.* **1997**, *322*, 879-884.
[30] M. J. Harrison, N. A. Burton, I. H. Hillier, *J. Am. Chem. Soc.* **1997**, *119*, 12285-12291.
[31] A. E. Howard, P. A. Kollman, *J. Med. Chem.* **1988**, *31*, 1669-1675.
[32] I. Schechter, A. Berger, *Papain. Biochem. Biophys. Res. Commun.* **1967**, *27*, 157-162.

[33] A. Hall, M. Abrahamson, A. Grubb, J. Trojnar, P. Kania, R. Kasprzykowska, F. Kasprzykowski, *J. Enzyme. Inhib.* **1992**, *6*, 113- 123.
[34] Z. Grzonka, E. Jankowska, F. Kasprzykowski, R. Kasprzykowska, L. Lankiewicz, W. Wiczk, E. Wieczerzak, J. Ciarkowski, P. Drabik, R. Janowski, M. Kozak, M. Jaskolski, A. Grubb, *Acta Biochim. Pol.* **2001**, *48*, 1-20.
[35] R. Janowski, M. Kozak, E. Jankowska, Z. Grzonka, M. Jasko´ lski, *J. Peptide Res.* **2004**, *64*, 141-150.
[36] D. Yamamoto, K. Matsumoto, H. Ohishi, T. Ishida, M. Inoue, K. Kitamura, H. Mizuno, *J. Biol. Chem.* **1991**, *266*, 14771-14777.
[37] K. Matsumoto, M. Murata, S. Sumiya, K. Mizoue, K. Kitamura, T. Ishida, *Biochim. Biophys. Acta* **1998**, *1383*, 93-100.
[38] A. Pedretti, L. Villa, G. Vistoli, *J. Mol. Graphics Modell.* **2002**, *21*, 47-49.
[39] T. T. Goodrich, A. W. Wark, R. M. Corn, H. J. Lee, *Methods Mol. Biol.* **2006**, *328*, 113-130.
[40] S. O. Jung, H.-S. Ro, B. H. Kho, Y.-B. Shin, M. G. Kim, B. H. Chung, *Proteomics* **2005**, *5*, 4427-4431.
[41] G. J. Wegner, H. J. Lee, R. M. Corn, *Anal. Chem.* **2002**, *74*, 5161-5168.
[42] G. J. Wegner, A. W. Wark, H. J. Lee, E. Codner, T. Saeki, S. Fang, R. M. Corn, *Anal. Chem.* **2004**, *76*, 5677-5684.
[43] B. P. Nelson, T. E. Grimsrud, M. R. Liles, R. M. Goodman, R. M. Corn, *Anal. Chem.* **2001**, *73*, 1-7.
[44] P. R. Connelly, R. Varadarajan, J. M. Sturtevant, F. M. Richards, *Biochemistry* **1990**, *29*, 6108-6114.
[45] J. M. Goldberg, R. L. Baldwin, *Proc. Nat. Acad. Sci. USA,* **1999**, *96*, 2019-2024.
[46] R. P. Hearn, F. M. Richards, J. Sturtevant, G. D. Watt, *Biochemistry* **1971**, *10*, 806-817.
[47] S. H. Park, R. T. Raines, *Protein Sci.* **1997**, *6*, 2344-2349.
[48] H. A. Biebuyck, C. D. Bian, G. M. Whitesides, *Langmuir* **1994**, *10*, 1825-1831.
[49] T. M. Willey, A. L. Vance, C. Bostedt, T. van Buuren, R. W. Meulenberg, L. J. Terminello, C. S. Fadley, *Langmuir* **2004**, *20*, 4939-4944.
[50] J. C. Miller, J. N. Miller, in *Ellis Horwood Series in Analytical Chemistry* (Eds.: R. A. Chalmers, M. Masson), Chichester, **1993**, p. 119.
[51] W. U. Dittmer, A. Reuter, F. C. Simmel, *Angew. Chem. Int. Ed.* **2004**, *43*, 3550-3553.
[52] J. W. Li, X. H. Fang, W. H. Tan, *Biochem. Biophys. Res. Commun.* **2002**, *292*, 31-40.
[53] R. F. Macaya, P. Schultze, F. W. Smith, J. A. Roe, J. Feigon, *Proc. Natl. Acad. Sci. USA* **1993**, *90*, 3745-3749.
[54] Y. Xiao, A. A. Lubin, A. J. Heeger, K. W. Plaxco, *Angew. Chem., Int. Ed.* **2005**, *44*, 5456-5459.
[55] K. A. Mahmoud, Y. T. Long, G. Schatte, H. B. Kraatz, *Eur. J. Inorg. Chem.* **2005**, 173-180.
[56] G. Sauerbrey, *Z. Phys.* **1959**, *155*, 206-222.

4.6. Supplemental Material

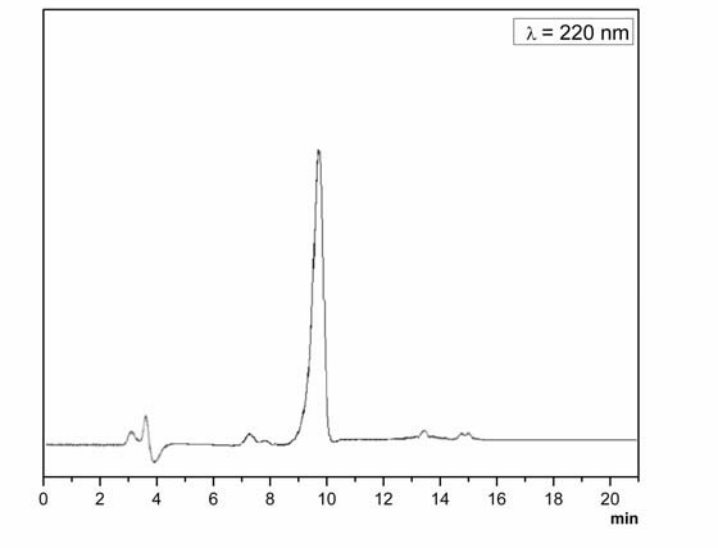

Figure 4.S1. HPLC trace of peptide **10**.

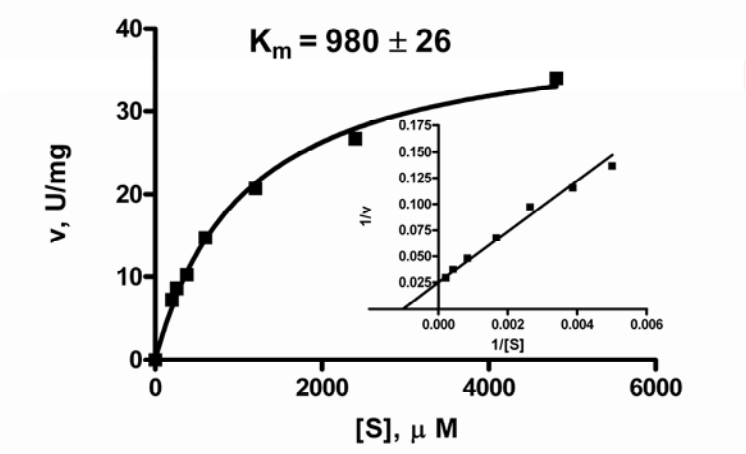

Figure 4.S2. Michaelis-Menten plot, with an inset Lineweaver-Burk plot. Michaelis-Menten constant (K_m) was determined by non linier regression fit of the concentration velocity curve using Michaelis-Menten equation {$V= V_{max}$ [S]/(K_m+[S]). The K_m value was determined by monitoring the total papain-catalyzed hydrolysis of Z-Phe-Arg-NHNp in the absence of the inhibitors and at high initial concentration of the substrate. The fitting was performed using GraphPad Prism version 4.03 for Windows, GraphPad Software, San Diego California USA.

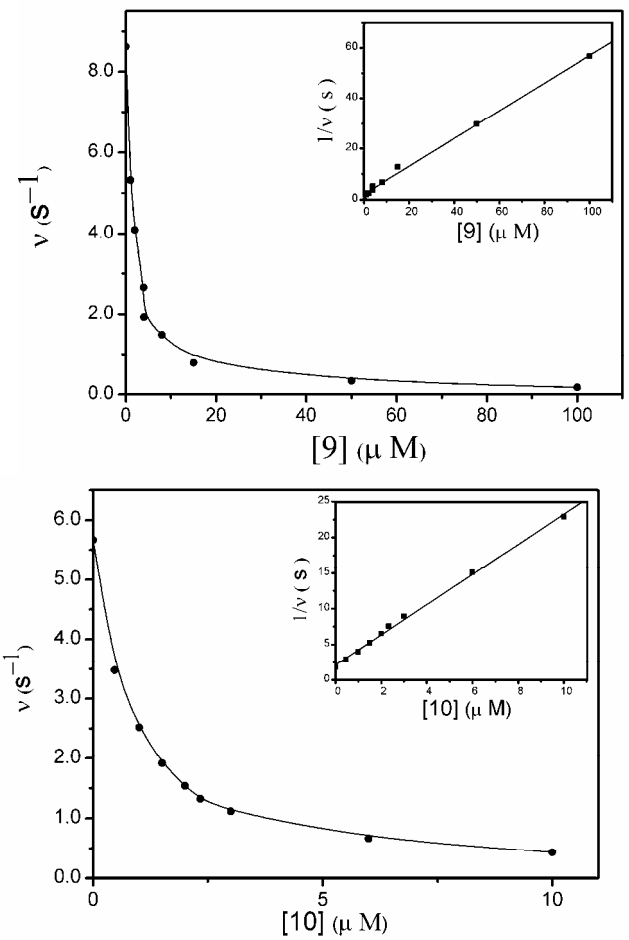

Figure 4.S3. Plot of the rates of hydrolysis of Z-Phe-Arg-NHNp versus concentrations of Fca-peptide **9** (upper) and Fca-peptide **10** (lower) monitoring of the papain-catalyzed hydrolysis of Z-Phe-Arg-NHNp (90 μM) in the presence of increasing concentrations of the Fca-peptide conjugate (0.1 M sodium phosphate pH 6.2, 2.5 mM EDTA, 300 μM DTT, and 30% DMSO, 23°C). The reaction was initiated by addition of the enzyme. Data were obtained by measuring the absorption at λ = 405 nm. The linear dependence shown in the Dixon plot (inset) indicates competitive inhibition. Nonlinear regression gave an apparent inhibition constant $K_i' = (1 + [S]/K_m)K_i = 639.1 \pm 1.1$μM for conjugate **9** and 21.1 ± 0.3 μM for conjugate **10**. A Michaelis constant K_m = 980 ± 26 μM was determined separately according to the Michaelis-Menten equation.

Papain enzyme is considered as the archetype of cysteine proteases. It consist of 212 amino acid residues folded to form two domains with a deep cleft between them, Cys-25, His-159, and Asn-175 residues represent the catalytic site of the enzyme.[1, 2] While the first two of which are responsible for a permanent thiolate-imadozelium Ione

pair, the last residue acts as hydrogen bond acceptor during the catalytic process of the enzyme. According to Schechter and Berger[3] nomenclature, S_2, S_1 binding sites are mainly responsible for the recognition of substrate residues (P_2, P_1) N- to C- terminus. S_2 and S_3 pockets consist of Val-133, Val-157 and Asp 158 and of Tyr61, Gly-66 and Tyr-67 residues of papain, respectively.

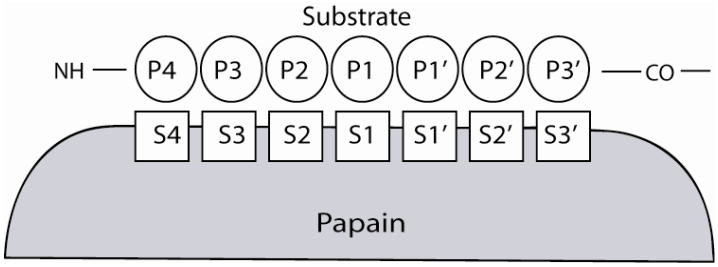

Figure 4.S4. Substrate-papain subsites according to Schechter and Berger,[3] S_2 and S_3 pockets consist of Val-133, Val-157 and Asp 158 and of Tyr61, Gly-66 and Tyr-67 residues of papain, respectively.

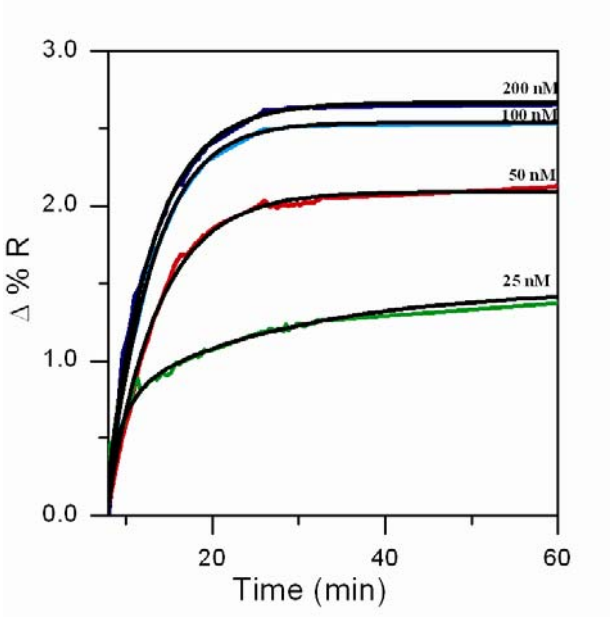

Figure 4.S5: Curve fitting for the adsorption curves obtained for various concentrations of peptide **10,** fitted using Equation (4.2).

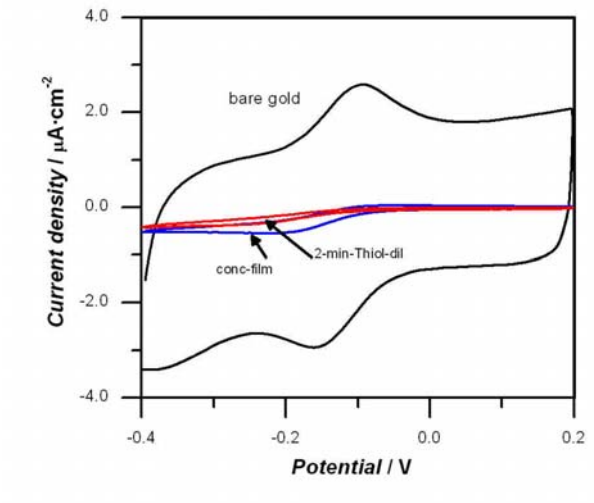

Figure 4.S6. Representative figure describing the dilution studies of the peptide **10** films. The diluted films were characterized by observing their blocking effect on the electrochemical response of the $Ru(NH_3)_6^{3+/2+}$ redox probe. The reversible redox behavior was observed on bare gold electrode with $E_{1/2}$ = -0.16 V vs Ag/AgCl has almost disappeared that may implies a fully covered surface.

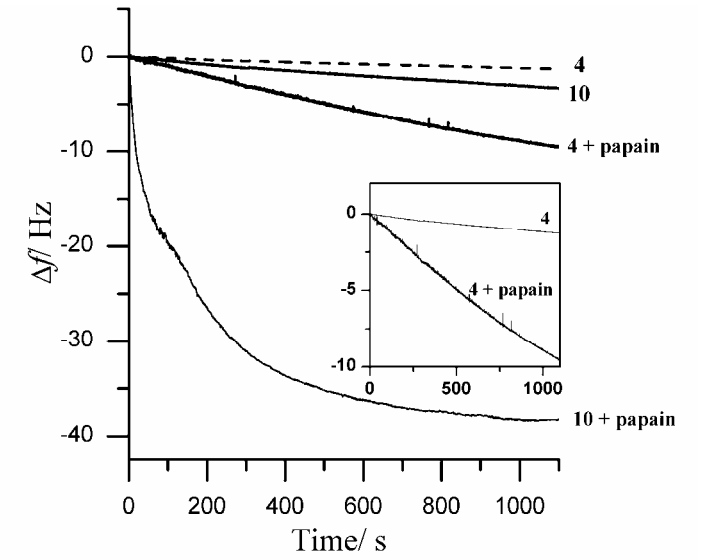

Figure 4.S7. Control QCM measurement demonstrating a comparison between the binding efficiency of peptides **10** and **4** to papain. The inset shows only peptide **4**, which was used as a control. The peptide films were formed on gold covered AT-cut type crystals. Papain activation buffer: 0.1 M sodium phosphate pH 6.2, 2.5 mM EDTA, 300 μM DTT, and 30% DMSO, 23°C with 2.0 M $NaClO_4$.

[1] J. Drenth, K. H. Kalk, H. M. Swen, *Biochemistry* **1976**, *15*, 3731-3738.
[2] I. G. Kamphuis, K. H. Kalk, M. B. A. Swarte, J. Drenth, *J. Mol. Biol.* **1984**, *17*, 233-256.
[3] I. Schechter, A. Berger, *Papain. Biochem. Biophys. Res. Commun.* **1967**, *27*, 157-162.

CHAPTER 5

SYNTHESIS AND ELECTROCHEMICAL INVESTIGATION OF OLIGOMERIC FERROCENE AMIDES: TOWARDS FERROCENE POLYAMIDES

5.0. Connecting Text

One major potential application of ferrocene compounds in material science is as standing motive for the synthesis of metallopolymers. These polymers may have novel and interesting properties. This chapter builds on the application of our novel achievement described in Chapter 1 where we were able to demonstrate a very convenient synthon for a protected 1,1'-diaminoferrocene. By utilizing this very stable diamine, it was possible to describe the synthesis and investigation of oligomeric and polymeric ferrocene peptides as a novel class of ferrocene-containing metallopolymers. To the best of our knowledge, there were no examples of peptide-like Fc-containing long chains oligomers or polymers. This chapter describes the condensation reaction of 1,1'-diaminoferrocene and 1,1'-ferrocene dicarboxylic acid to give rise to a series of novel oligo- and poly-ferrocene peptides. These materials are fully soluble in a variety of solvents and are fully characterized spectroscopically. Finally, electrochemical investigation of the electronic interaction between the individual ferrocene units is described.

 This paper is co-authored by H.-B. Kraatz. All work described in this paper, in terms of the experimental study, hypothesis, and initial writing of the manuscript were carried out by me. The text below is a *verbatim* copy of the published paper.

5.1. Introduction

Metallopolymers have received considerable attention in recent years.[1, 2] Significant efforts focused on the synthesis of poly(ferrocenylenes), in which the ferrocene (Fc) groups form part of the backbone and are either linked directly to each other[3] or are linked by π-conjugated organic bridges (**1**) and on polymers in which the Fc is located in the side chain (**2**).[4-9] However, in many cases, these polymers are sparingly soluble which limits their characterization.[10] Significant progress has been made by Manners whose research group was able to exploit the ring strain in silaferrocenophanes to develop high molecular weight Fc-backbone polymers (**3**) by ring-opening metathesis.[10-12]

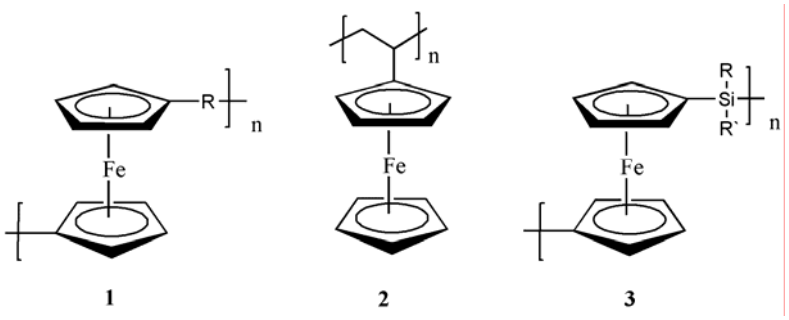

1 **2** **3**

In some cases, electronic interactions between neighboring Fc centers were observed.[7-13] Intermolecular electronic interactions in conjugated Fc oligomers and polymers have been subjected to considerable studies due to their potential applications in the construction of electronic devices and electron storage media.[14-17] In some cases, the extent of communication between the redox centers was controlled and modulated in several ways; including protonation or alkylation of the compounds and changing the solvent polarities.[18]

Polyferroceneamides (**4**) based on 1'-aminoferrocene-1-carboxylic acid, linking the Fc subunits via an amide linkage, were proposed in the literature and there have

been several reports of Fc- amide dimers, obtained via stepwise amide coupling.[19-22] Work by Nakamura shows the presence of intra- as well as intermolecular H-bonding between Fc-amide dimers in solution as well as in the solid state. Moreover, he proposes that H-bonding would play an important role in determining the secondary structure of the polymeric Fc-pseudopeptide.[21]

In contrast, the alternative poly- and oligoamides (**5**) derived from 1,1'-ferrocenedicarboxylic acid and 1,1'-ferrocenediamine subunits are not known to date. The lack of a facile method to generate a suitable Fc-diamine precursor is most likely responsible for this. We recently reported the synthesis of the stable precursor 1,1'-bis(Boc-amino)ferrocene (**6**),[23] which serves as a convenient precursor for 1,1'-diaminoferrocene.

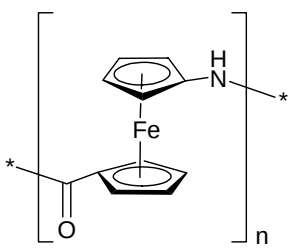

4

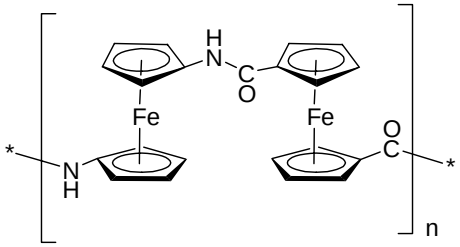

5

Here we report the reaction of 1,1'-bisaminoferrocene with ferrocenecarboxylic acid chlorides, with the aim to study the use of the diamine for the synthesis of ferrocene amide polymers. We report the synthesis and spectroscopic characterization of a series of well-defined Fc-amide oligomers, having the repeat unit as shown in **5**, as well as of a high molecular weight Fc-amide polymer. Their electrochemical and optical properties are reported and compared to other oligoferrocenes in order to assess the magnitude of the electronic interaction between the Fc centres.

5.2. Results and Discussion

5.2.1. Synthesis

In order to assess the use of 1,1'-bis(Boc-amino)ferrocene **6** as a useful precursor the synthesis of Fc-amide polymers, we initially studied the reaction of **6** with the Fc-acid chloride **7** or the active ester **10**. An overview of these reactions is shown in Scheme 5.1. In both cases, deprotection of the bis-Boc-Fc derivative **6** followed by coupling with the acid chloride **7** or the active ester **10** resulted in the formation of triferrocenes **8** and **10**, in which the Fc-diamine was flanked on either side by the Fc-acid component. Triferrocene **8** is a diester, while the triferrocene **10** is a Boc-protected diamine. Both compounds were characterized spectroscopically.

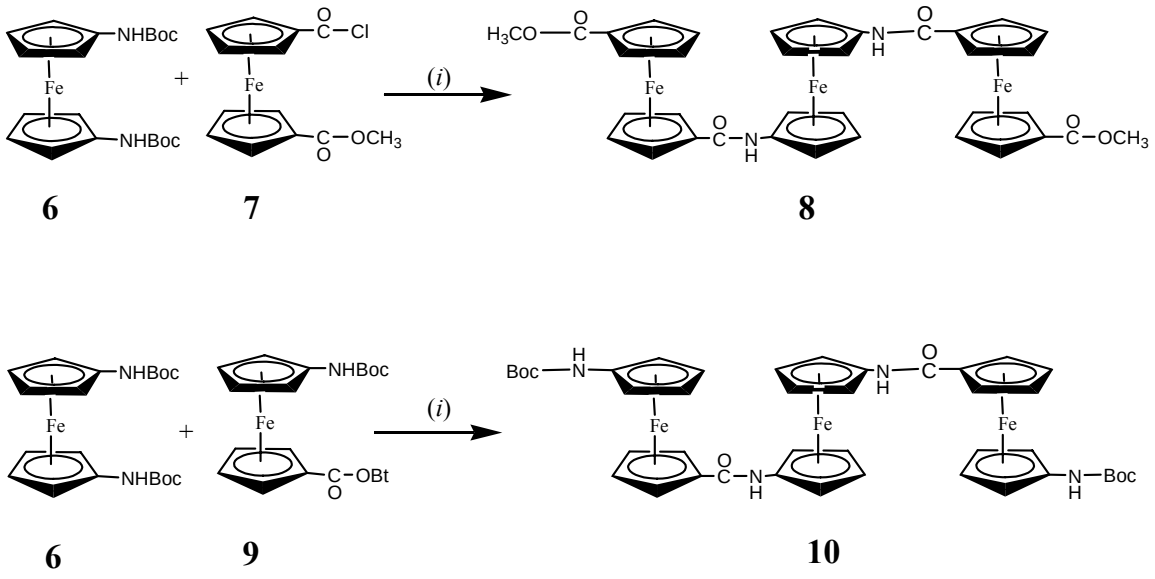

Scheme 5.1. Synthesis of compounds **8** and **10** (*i*) a) TFA, CH_2Cl_2; b) Et_3N/THF.

The Amide A absorption bands of the triferrocene amides **8** and **10** indicate at least in the case of **11** the presence of H-bonding in the solid state. While for **10**, the Amide A band was observed at 3340 cm^{-1}, in a region typically associated with H-

bonding, this band was shifted to higher energies for **8**, indicating a lack of strong H-bonding. However, we cannot conclude the complete absence of H-bonding. Differences in behavior were observed also in the ^{1}H-NMR spectra of the two triferrocenes in $CDCl_3$. The two equivalent Fc-amide NH groups in **8** gave rise to a single resonance at δ 8.19. In compound **10**, two sets of NH signals are observed, one due to the Fc-amide NH at δ 9.07, indicating potentially less involvement of H-bonding, and a second signal downfield at δ 6.49 due to the Boc-carbamide (Figure 5.1).

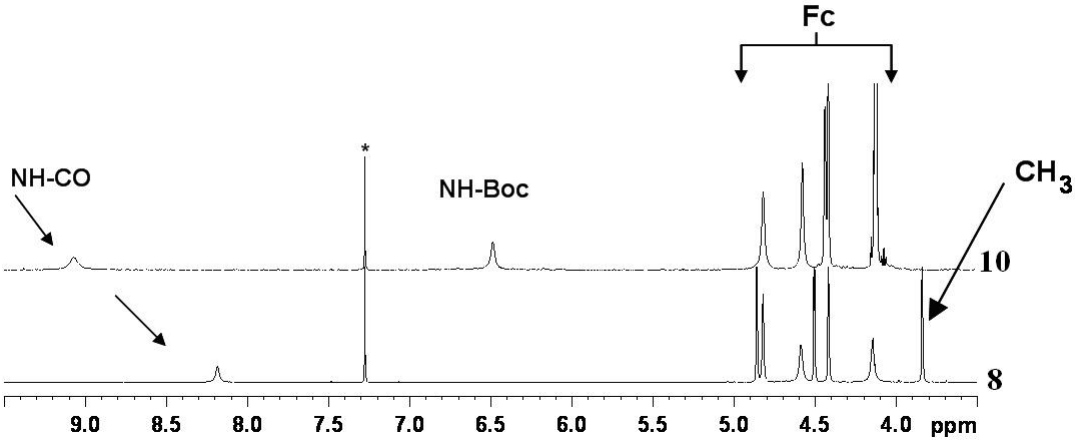

Figure 5.1. The ^{1}H-NMR patterns of compounds **8** and **10** in $CDCl_3$: * residual peak of $CHCl_3$

Next, we attempted the polymerization of the Fc-diamine with Fc-bis-acid chloride **8**. Polymer **15** was obtained from the Boc-protected Fc-diamine **6** after Boc-deprotection followed by coupling to ferrocene-1,1'-dicarbonyl chloride **8** in THF. The yellow polymer **15** was filtered off and washed with methanol. The remaining solution was dried *in vacuo* and subjected to chromatography, allowing us to isolate the four bis-ester oligomers **8**, **12**-**14** (Scheme 5.2). These ranged from the dimer **12**, to the trimer **8**, which was also prepared independently (vide supra), to the pentaferroceneamide **13** and

the heptaferroceneamide **14**. The isolation of the dimer **12** was surprising since it suggested partially incomplete Boc-deprotection of **6**. All compounds were obtained as methyl esters. Esterification most likely was the result of the presence of methanol during the work up. In nonpolar solvents, such as chloroform, the Fc-oligomers engage in H-bonding as detected in the analyses of the IR and ^{1}H NMR spectra and comparison to related oligoferrocenes.

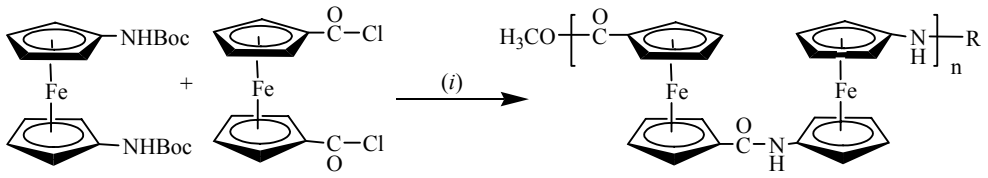

6 **11**

12: n = 1, R = Boc
13: n = 2, R = [CO-Fc-COOCH$_3$]
14: n = 3, R = [CO-Fc-COOCH$_3$]
15: poly Fc-peptide

Scheme 5.2. Synthesis of compounds **8, 12-14** and of polymer **15**. (*i*) a) TFA, CH_2Cl_2; b) Et_3N/THF.

Figure 5.2 shows the IR absorption patterns of compounds **8** and **10** in chloroform solution and allows a comparison of their H-bonding interactions. The positions of the Amide A band in both compounds indicate the presence of H-bonding in both compounds. Both systems display a strongly H-bonded Amide A band at 3305 cm^{-1} for **10** and at 3264 cm^{-1} for **8**. In addition, the weak band at 3519 and 3505 cm^{-1} indicates the presence of amides that are not involved in H-bonding. This may be rationalized by invoking an equilibrium between H-bonding and non-H-bonding states in solution. The position of the Amide A band shifts to approximately lower wavenumbers with increasing number of Fc units and oligomer length. This is intuitive since elongation of the Fc-oligomer generates more H-bonding sites.

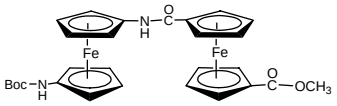

12

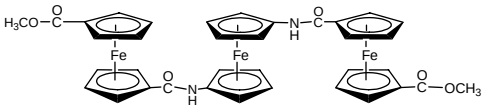

9

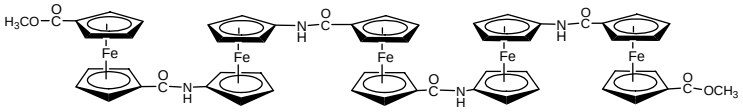

13

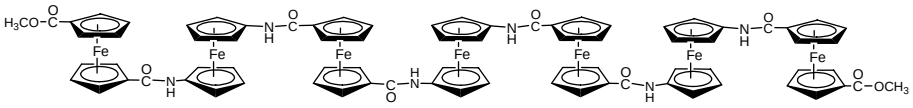

14

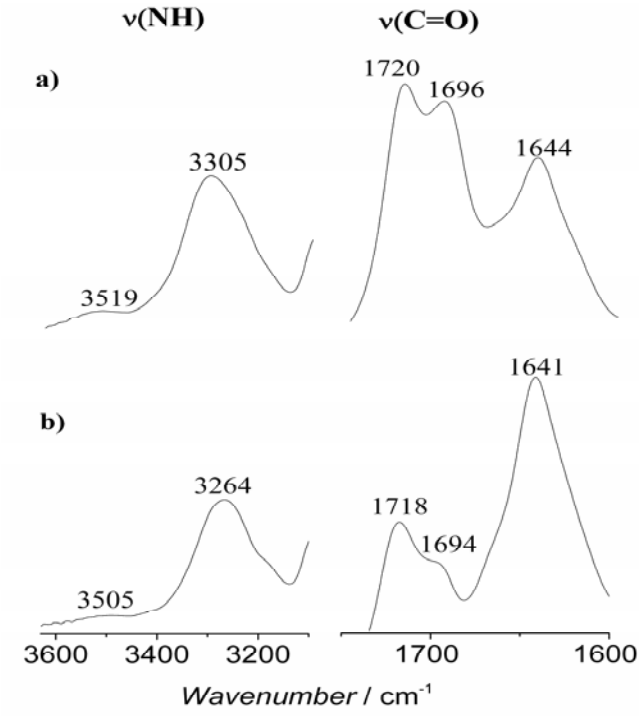

Figure 5.2. IR spectra of (a) BocNH-Fc-NHCO-Fc-COOMe (**12)** and (b) MeOOC-Fc-CONH-Fc-NHCO-Fc-COOMe (**8)** in $CHCl_3$ solution.

In this regard, the position of the Amide A band in compound **12**, Boc-NH-Fc-NHCO-Fc-COMe, was very low. However, this dimer is closely related to Nakamura's Ac-NH-Fc-CONH-Fc-CONHMe, which was proposed to engage in strong intramolecular H-bonding in solution and the solid state, enabled by its structure which aligns the amide NH and amide CO resulting in effective interactions.[14]

Interestingly, ^{1}H-NMR spectrum of compounds **8**, **12**, **13**, and **14** showed a downfield shift of the amide signal as the number of Fc units increased (Figure 5.3). The amide signal shifts downfield from δ 8.19 for **8**, to δ 8.33 for **13,** and to δ 8.41 for compound **14**. This spectroscopic evidence lends additional support to the presence of NH····OC hydrogen bonds, which shift to lower field with increasing the number of Fc units.

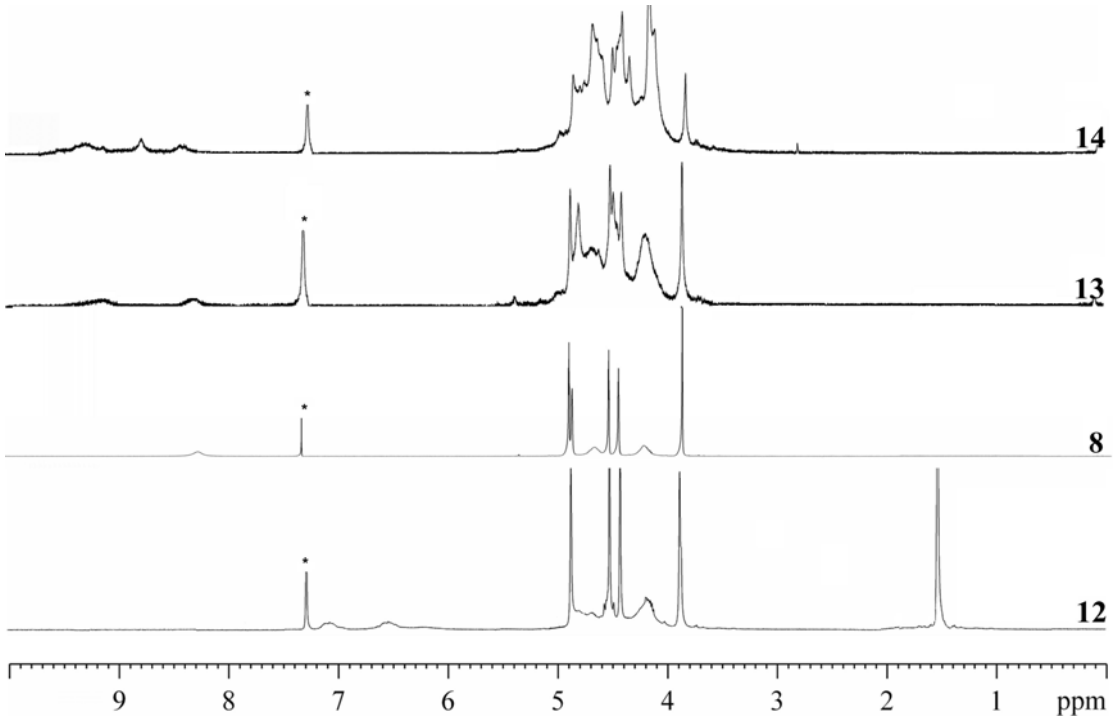

Figure 5.3. ^{1}H-NMR spectra in $CDCl_3$ of ferroceneamide oligomers, **12-14** in $CDCl_3$. * residual peak of $CHCl_3$.

MALDI-TOF analysis of polymer **15** showed a broad envelope centred around $2.8x10^4$ Da. Interestingly, the poly-Fc "peptide" **15** is soluble in water. This maybe rationalized by the "protein-like" nature of this polymer. Its average molecular weight, as determined by dynamic light scattering experiments of the polymer in water, was $2.7x10^4$ Da with an average molecular diameter of 4.2 nm, which in line with the MS results.

5.2.2. Electrochemistry

The electrochemical properties of the oligo-Fc compounds **8, 10** and **12-14** were investigated by cyclic voltammetry (CV) and differential pulse voltammetry (DPV) in dichloromethane containing 0.1 M tetrabutylammonium perchlorate (TBAP) as a supporting electrolyte. The CVs of compounds **8** and **10** are shown in Figure 5.4. Both compounds displayed two well-separated redox waves. While the more cathodic oxidation was a one-electron oxidation, and was ascribed to oxidation of the central diamino-Fc unit, the more anodic wave was a two-electron wave and was ascribed to the simultaneous oxidation of the two terminal Fc groups. The experimental results are summarized in Table 5.1.

Since the terminal Fc groups for compounds **8** and **10** have different substituents, the redox potential was expected to vary. Compound **8** possesses electron withdrawing ester groups and thus the second more anodic redox wave for **8** was observed at $E_{1/2}$ = 973 mV (vs Ag/AgCl). The terminal Fc group in compound **10** possesses more electron-rich Boc-NH substituents making the terminal Fc group easier

to oxidize compared to compound **8**. Thus, for compound **10**, the oxidation of the terminal Fc groups was cathodically shifted to $E_{1/2}$ = 584 mV (vs Ag/AgCl).

Our results are in sharp contrast to results obtained in other triferrocenyl systems in which three separate oxidation waves were observed, indicating significant electronic communication in the triferrocenes. Oxidation of the two outer Fc groups to the dication proceeded stepwise giving rise to two poorly resolved one-electron waves, which were separated from the oxidation of the central Fc unit by 0.31 V.[24-26] In the system under study here, electronic communication was significantly diminished. The electrochemical oxidation of compounds **8** and **10** can be described as two separated electron transfer processes as shown in Scheme 5.3.

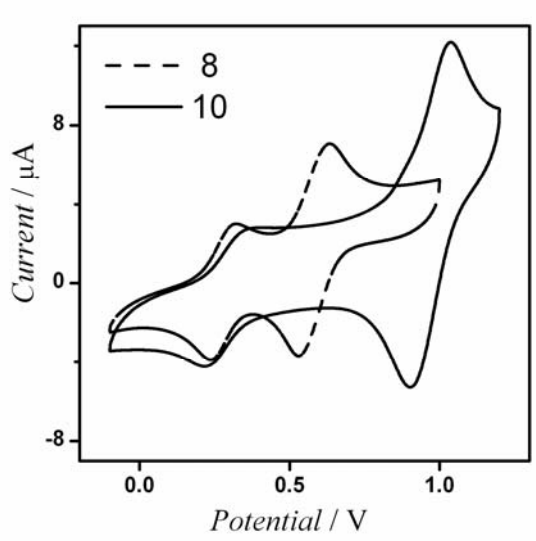

Figure 5.4: Cyclic voltammetry of compounds **8** and **10** in CH_2Cl_2. All solutions contain 0.1 mM of the compounds and 0.1 M TBAP. GCE vs. Ag/AgCl. Scan rate = 100 mV/s. The $E_{1/2}$ of the Fc/Fc^+ couple under the experimental conditions was 448(±5) mV (*vs*. Ag/AgCl).

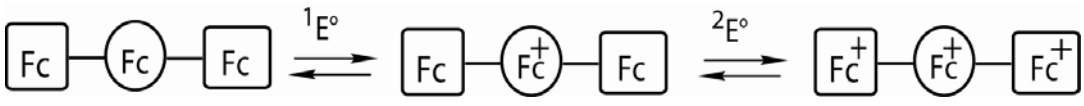

Scheme 5.3. Representation of the two oxidation steps of compounds **8** and **10**.

The CVs and DPVs of compounds **12-14** are shown in Figure 5.5. Interestingly, all compounds displayed only two redox waves and not multiple redox waves as maybe expected for systems in which a strong electronic interaction between the redox centers is present.

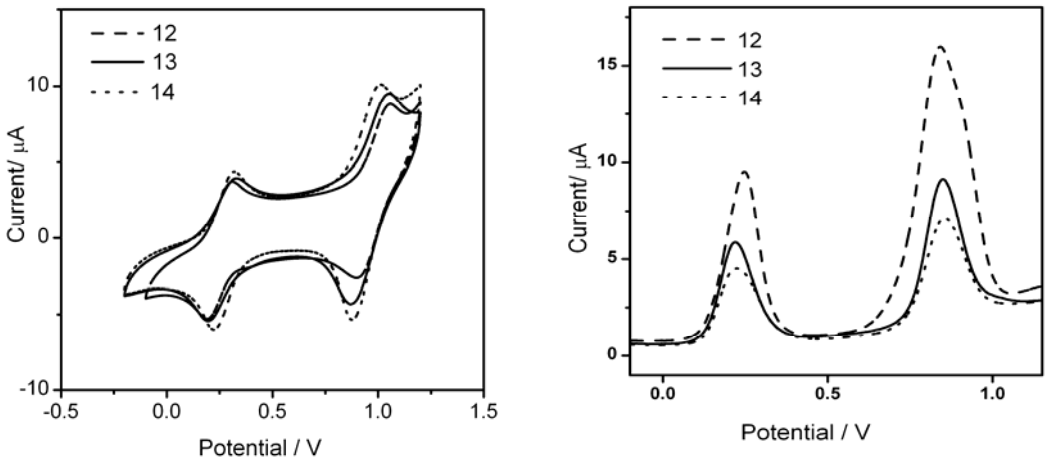

Figure 5.5. Cyclic voltammetry (CV) (left) and differential pulse voltammetry (DPV) (right) of compounds **12-14** in CH_2CL_2. All solutions contain 0.1 mM of the compounds and 0.1 M TBAP. GCE vs. Ag/AgCl. Scan rate = 0.1 v/s.

The first more cathodic wave was due to oxidation of the Fc groups that are derived from Fc-diamine, while the more anodic oxidation was ascribed to the Fc-dicarbonyl groups. Our studies indicated that either no or very small amount of electronic interaction existed between the Fc centers in our systems. This may be attributed to ineffective redox-matching between the Fc units, as suggested by Swager and coworkers.[27] A similar lack of electronic communication between redox centers was observed in other Fc-containing oligomers.[28-31] The approximate ratio of the signals due to the Fc-diamine and Fc-dicarboxyl groups was 2:3 for **13** and 3:4 for **14** (within experimental error). The appearance of a stripping cathodic peak in compounds

13 and **14** compared to the redox behavior was most likely due to solubility changes of the compounds after oxidation.[31]

Table 5.1. Half-wave potential of tri-ferrocene analogues **8** and **10** and oligo-ferrocene peptides **12-14** in CH_2Cl_2 (0.1 M TBAP. GCE vs. Ag/AgCl. Scan rate = 0.1 V/s).

	$^1E_{1/2}$(mV)	$^2E_{1/2}$(mV)	$^1\Delta E_p$	$^2\Delta E_p$	$^1(i_a/i_c)$	$^2(i_a/i_c)$
8	292 ± 5	973 ± 5	131	137	0.99	1.04
10	277 ± 5	584 ± 5	73	103	1.04	1.01
12	241 ± 5	1032 ± 5	106	156	1.01	1.03
13	268 ± 5	943 ± 5	127	121	1.02	0.97
14	274 ± 5	936 ± 5	94	125	0.99	0.94

5.2.3. Ultraviolet/Visible Spectroscopy

UV-Vis spectra of compounds **8**, **10**, **12-14** were recorded in dichloromethane over the range of 190-600 nm to examine the degree of electronic delocalization and are shown in Figure 5.6. Analysis of the UV-vis spectra for the oligomers **12-14** revealed a slight blue shift of the Fc-based transition upon elongation of the oligomer. For example, while the Fc-based transition for **8** was observed at λ_{max} = 454 nm, the transition shifts to λ_{max} = 446 nm for **13** (see Table 5.2). A comparison of compounds **8** and **10**, which differ only in the substituent on the terminal Fc groups (COOMe for **8** and NH-Boc for **10**) showed a significant increase in the signal intensity and thus an increase in the extinction coefficient ε, indicating an effect of the substituent on orbital overlap.

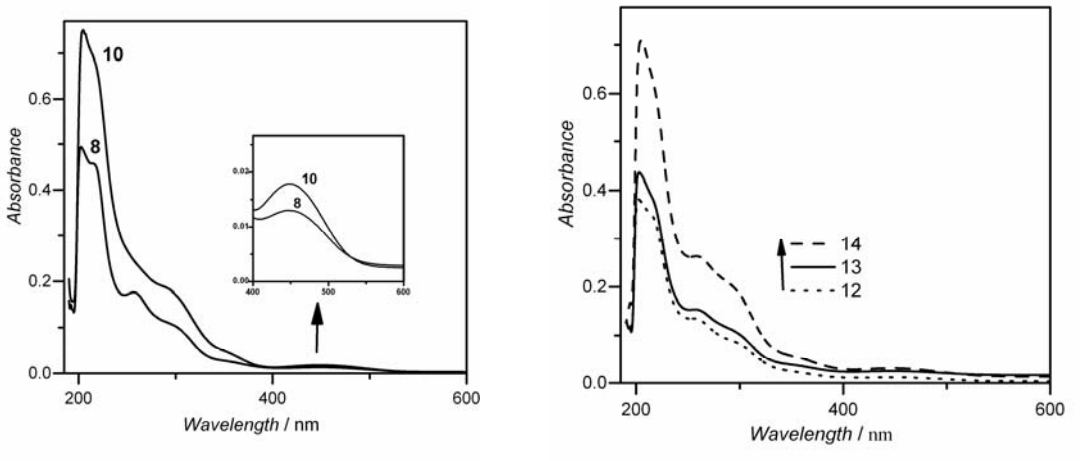

Figure 5.6. Electronic spectra of the triferrocenes **8** and **10** (left) and the ferrocene amide oligomers **12-14.** All concentrations were 0.1 mM in CH_2Cl_2.

Table 5.2: UV-vis data for compounds **8**, **10** and **12-14** in CH_2Cl_2.

Compound	Wave length (nm) (ε in $Lmol^{-1}cm^{-1}$)				
8	202(9910)	215(9140)	259(3520)	296(2019)	454(280)
10	205(15019)			296(36874)	449(401)
12	203(7588)	213(7020)	260(2720)	296(1642)	446(252)
13	203(8762)	214(7663)	259(3102)	296(2021)	447(504)
14	204(14140)		259(5305)	296(3960)	447(644)

5.3. Conclusion

We successfully achieved the synthesis of a series of novel Fc-amide oligomers based on ferrocenediamine. We were able to isolate and characterize oligomers ranging from two to seven Fc units in their backbone. Spectroscopic evidence suggests the presence of H-bonding in these oligomers, which is in line with oligo-Fc-amides derived from 1'-aminoferrocene-1-carboxylic acid. Interestingly, no evidence for electronic interaction was observed for our systems, which is somewhat surprising and

requires further investigation. As part of this study, we also succeeded in the preparation of the first Fc-amide polymer by polycondensation of Fc-diamine with Fc-dicarboxylic acid derivatives. The polymer was water soluble, which maybe rationalized by assuming a globular "protein-like" nature of this polymer. Hydrophilic groups may be exposed to the exterior of the polymer. At the present time, we are continuing to explore condensation reactions involving Fc-diamine and are exploring the electronic properties of this polymer in more detail.

5.4. Experimental

5.4.1. General Procedure

All syntheses were carried out under dry nitrogen gas unless otherwise indicated. CH_2Cl_2 (BDH; ACS grade) used for synthesis was dried (CaH_2) and distilled prior to use. $CDCl_3$ (Aldrich) was dried (CaH_2), and stored over molecular sieves (8-12 mesh; 4Å effective pore size; Fisher) before use. THF was dried over benzophenone/sodium, and stored over molecular sieves (8-12 mesh; 4Å effective pore size; Fisher) before use. 1'-methoxycarbonyl ferrocene-1-carboxylic acid and 1'-Boc-aminoferrocene-1-OBt were prepared according to literature procedures, hydroxybenzotriazole (HOBt) (Nova), $NaSO_4$, and $NaHCO_3$ (VWR) were used as received. For column chromatography, a column with a width of 2.7 cm (ID) and a length of 45 cm was packed 18-22 cm high with 230-400 mesh silica gel (VWR). For TLC, aluminum plates coated with silica gel 60 F_{254} (EM Science) were used. NMR spectra were recorded on a Bruker Avance-500 spectrometer using a 5-mm broadband probe operating at 500.134 MHz (^1H) and 125.766 MHz ($^{13}C\{^1H\}$). Peak positions in

^{1}H spectra are reported in ppm relative to TMS. All, unless otherwise described $^{13}C\{^{1}H\}$ spectra are referenced to the $CDCl_3$ signal at δ 77.23. Mass spectrometry was carried out on a VG Analytical 70/20 VSE instrument. Infrared spectra were obtained with a Perkin-Elmer model 1605 FT-IR. Dynamic light scattering experiments were carried out on a Dynampro-MS800 instrument using a 20 μL sample in a quartz cuvette.

5.4.2. Preparation of 1'-methoxycarbonyl ferrocene-1-carbonyl chloride (7)

A mixture of 1'-methoxycarbonyl ferrocene-1-carboxylic acid (0.86 g 3.0 mmol), freshly distilled 2 M oxalyl chloride in dichloromethane (3.5 mL), 0.5 mL pyridine and dry dichloromethane (20 mL) was stirred in dark at r. t. for 20 hours and then at reflux for 4 hours. The mixture was evaporated to dryness. The crude product was extracted by hot dry ether several times. Purification was accomplished by flash column chromatography (SiO_2, EtOAc: hexane 1:3) to give pale red crystals of compound **7** (0.85 g, 92%). TOF-MS (m/z): calc for $C_{13}H_{11}Cl\ FeO_3\ [M]^+$: 306.5270; found: 306.1746. IR (CH_2Cl_2, υ_{max}/cm^{-1}): 1760 (s, C=O, COCl), 1710 (s, C=O, COOMe). UV-vis (CH_2Cl_2; λ in nm (ε in $Lmol^{-1}cm^{-1}$)): 453 (706). ^{1}H-NMR ($CDCl_3$, δ in ppm): 5.00 (2H, t, *J* = 4 Hz, H-2' and H-5', Fc), 4.95 (2H, t, *J* = 4 Hz, H-2 and H-5, Fc), 4.64 (2H, t, *J* = 4 Hz, H-3' and H-4', Fc), 4.61 (2 H, m, *J* = 3 Hz, H-3 and H-4, Fc), 3.84 (3H, s, $COOCH_3$).

5.4.3. Preparation of MeOOC-[Fc-NHCO]$_2$-Fc-COOMe (8)

1,1'-bis(Boc-amino)ferrocene[23] **1** (0.42 g, 1.0 mmol) was dissolved with stirring in CH_2Cl_2 (2.0 mL) and after cooling to 0 ºC with an ice bath, TFA (2.0 mL)

was added dropwise under a nitrogen atmosphere. Then the ice bath was removed and stirring was continued. After 30 min, CH_2Cl_2 (10 mL) was added and the solution was cooled to 0 ºC before an excess Et_3N was added dropwise. To this, a solution of 1'-methoxycarbonyl ferrocene-1-carbonyl chloride **7** (0.67 g, 2.2 mmol) in dry CH_2Cl_2 was added. The reaction mixture was stirred for 2 h at room temperature and then washed consecutively with saturated aqueous sodium bicarbonate, 10% aqueous citric acid, saturated sodium bicarbonate, and water. The organic phase was separated and dried over Na_2SO_4, filtered and then evaporated to dryness. After purification by flash column chromatography (EtOAc: hexane 2:1), orange crystals of compound **8** were obtained (0.66 g, 88%). TOF-MS (m/z): calc for $C_{36}H_{32}N_2O_6Fe_3$ $[M]^+$: 756.0308; found: 756.0305. Anal. Calc. C 57.18, H 4.27, N 3.70%; Found C 57.39, H 4.11, N 3.62%. FT-IR (KBr, υ_{max}/cm^{-1}): 3406 (m, N-H), 1709 (s, C=O). UV-vis (MeCN; λ in nm (ε in $Lmol^{-1}cm^{-1}$)): 454 (800). m. p 172-178 ºC. ^{1}H-NMR $CDCl_3$, (δ in ppm): 8.19 (2H, s, NH), 4.87 (4H, t, *J* = 4 Hz, Fc), 4.82 (4H, s, Fc), 4.59 (4H, b s, Fc), 4.51 (4 H, t, *J* = 4 Hz, Fc), 4.42 (4H, m, Fc), 4.15 (4 H, m, Fc), 3.84 (6H, s, $COOCH_3$). $^{13}C\{^1H\}$ NMR ($CDCl_3$, δ in ppm) 172.3 *C*ONH, 162.7 *C*$OOCH_3$, 96.3, 78.8, 73.2, 72.6, 72.3, 72.2, 70.2, 65.7, 63.1 Fc, 52.4 OCH_3

5.4.4. Preparation of BocNH-[Fc-NHCO]$_2$-Fc-NHBoc (10)

1,1'-bis(Boc-amino)ferrocene[23] **6** (0.42 g, 1.0 mmol) was treated as described above for compound **8** prior the reaction with 1'-Boc-aminoferrocene-1-OBt[8] **9** (1.01 g, 2.2 mmol) in 5.0 mL dry CH_2Cl_2. The resulting solution was stirred at r. t. overnight, worked up as described above, and the solvent was removed under reduced pressure.

The residue was chromatographed (SiO_2, hexane: EeOAc 60:40) to give a dark yellow powder of compound **10** (0.49 g, 56%). TOF-MS (m/z): calc for $C_{42}H_{46}N_4O_6Fe_3$ $[M]^+$: 870.3900; found: 870.1450. Anal. Calc. C 57.96, H 5.33, N 6.44%; Found C 58.13, H 5.16, N 6.33%. FT-IR (KBr, υ_{max}/cm^{-1}): 3340, 3286 (m, N-H), 1697 (s, C=O). UV-vis (CH_2Cl_2; λ in nm (ε in $Lmol^{-1}cm^{-1}$)): 449 (600). m. p 173-177 ºC. ^{1}H-NMR $CDCl_3$, (δ in ppm): 9.07 (2H, s, NH, NHCO), 6.49 (2H, s, NH, NHBoc), 4.82 (4H, s, Fc), 4.58 (4H, s, Fc), 4.44 (4H, s, Fc), 4.42 (4 H, t, *J* = 4 Hz, Fc), 4.13 (8H, m, Fc), 1.52 (18H, s, $C(CH_3)_3$). $^{13}C\{^1H\}$ NMR ($CDCl_3$, δ in ppm) 172.8 CONH, 153.5 $COOC(CH_3)_3$, 80.4 $C(CH_3)_3$, 99.8, 78.9, 74.7, 73.3, 72.5, 70.9, 66.9, 66.0, 65.2, 62.3 Fc , 28.7 $C(CH_3)_3$.

5.4.5. Preparation of Ferrocene-1,1'-dicarbonylchloride (11)

A mixture of 1,1'- ferrocenedicarboxylic acid (2.00 g 7.3 mmol), freshly distilled 2 M oxalyl chloride in dichloromethane (7.5 mL), 1.0 mL pyridine and dry dichloromethane (30 mL) was allowed to stirred in dark at r. t. for 20 hours and then at reflux for 4 hours. The mixture was evaporated to dryness. The crude product was purified by flash column chromatography (SiO_2, EtOAc:hexane 1:3) to give red crystals of compound **8** (1.32 g, 97%). TOF-MS (m/z): calc for $C_{12}H_8Cl_2FeO_2$ $[M]^+$: 310.9454; found: 310.7321. IR (CH_2Cl_2, υ_{max}/cm^{-1}): 1761 (s, C=O, COCl). UV-vis (CH_2Cl_2; λ in nm (ε in $Lmol^{-1}cm^{-1}$)): 453 (706). ^{1}H-NMR $CDCl_3$, (δ in ppm): 4.85 (2H, t, *J* = 4 Hz, H-2 and H-5, Fc), 4.43 (2 H, t, *J* = 4 Hz, H-3 and H-4, Fc).

5.4.6. Synthesis and Characterization of Oligo- and Poly-Ferrocene Peptides

1,1'-bis(Boc-amino)ferrocene[23] **6** (1.00 g, 2.4 mmol) was dissolved in CH_2Cl_2 (2.0 mL) and after cooling to 0ºC, 30:70 (v/v) CH_2Cl_2: TFA (3.0 mL) was added dropwise, then the solvent was evaporated under dry nitrogen stream. To the residue, 20 mL of dry THF was added followed by dropwise addition of Et_3N (3.0 mmol) at 0° C. To this, ferrocene-1,1'-dicarbonyl chloride **11** (1.49 g, 2.8 mmol) in THF (10 ml) was added, the solution was allowed to stir for 1 hour at 0° C, then 2 hours at room temperature. The reaction product was filtered; the solid residue was washed successively with chloroform, Methanol, and then recrystallized from methanol/water to produces faint yellow powder of polymer **15** (0.36 g, 34.2%). The remaining solutions from filtration and successive washings of polymer **15** were combined and evaporated to dryness, and then the crude residue was purified by flash column chromatography (SiO_2, EtOAc:hexane 1:1) to give compounds **12** (0.04 g, 2.6%, R_f = 0.78), **9** (0.08 g, 6.2%, R_f = 0.54), **13** (0.05 g, 7.3%, R_f = 0.31) and **14** (0.10 g, 12.2%, R_f = 0.24).

5.4.6.1. Characterization of Compound 12

TOF-MS (m/z): calc for $C_{28}H_{30}N_2O_5Fe_2$ $[M]^+$: 586.2485; found: 586.0862. FT-IR (KBr, υ_{max}/cm^{-1}): 3302 (m, N-H), 1720, 1697 (s, C=O). UV-vis (CH_2Cl_2; λ in nm (ε in $Lmol^{-1}cm^{-1}$)): 445 (766). m. p 158-163 ºC. ^{1}H-NMR $CDCl_3$, (δ in ppm): 7.06 (1H, s, NH, NHCO), 6.57 (1H, s, NH, NHBoc), 4.86 (2H, s, Fc), 4.81 (2H, s, Fc), 4.51 (4H, s, Fc), 4.41 (4 H, s, Fc), 4.14 (4 H, m, Fc), 3.37 (3H, s, $COOCH_3$), 1.39 (9H, s, $C(CH_3)_3$). $^{13}C\{^1H\}$ NMR ($CDCl_3$, δ in ppm) 172.4 CONH, 153.7 $COOC(CH_3)_3$, , 81.0 $C(CH_3)_3$, 98.7, 73.3, 72.2, 71.4, 70.2, 65.7, 63.2 Fc, 52.0 OCH_3, 28.6 $C(CH_3)_3$.

5.4.6.2. Characterization of Compound 13

TOF-MS (m/z): calc for $C_{58}H_{50}N_4O_8Fe_5$ $[M]^+$: 1210.2860; found: 1210.0376. FT-IR (KBr, υ_{max}/cm^{-1}): 3278 (m, N-H), 1771, 1717 (s, C=O). UV-vis (CH_2Cl_2; λ in nm (ε in $Lmol^{-1}cm^{-1}$)): 446 (784). m. p 168-174 ºC. ^{1}H-NMR $CDCl_3$, (δ in ppm): 9.17 (2H, b, s, NH), 8.33 (2H, b, s, NH), 4.85 (m, 16H, Fc-CO), 4.64 (m, 8H, Fc-N) 4.46 (m, 16H, Fc-CO), 4.01(m, 8H, Fc-N), 3.84 (6H, s, $COOCH_3$). $^{13}C\{^1H\}$ NMR ($CDCl_3$, δ in ppm) 172.8, 172.3 *C*ONH, 162.7 *C*$OOCH_3$, 96.2, 78.8, 73.2, 72.6, 72.4, 72.2, 70.2, 69.8, 65.7, 65.2, 63.8, 63.2 Fc, 52.4 OCH_3.

5.4.6.3. Characterization of Compound 14

TOF-MS (m/z): calc for $C_{80}H_{68}N_6O_{10}Fe_7$ $[M]^+$: 1664.3747; found: 1664.0452. FT-IR (KBr, υ_{max}/cm^{-1}): 3267 (m, N-H), 1717, (s, C=O). UV-vis (CH_2Cl_2; λ in nm (ε in $Lmol^{-1}cm^{-1}$)): 446 (781). m. p 183-187 ºC. ^{1}H-NMR $CDCl_3$, (δ in ppm): 9.33 (2H, b s, NH), 8.86 (2H, br s, NH), 8.41 (2H, b s, NH), 4.93-4.01 range (m, 68H, Fc), 3.83 (6H, s, $COOCH_3$). $^{13}C\{^1H\}$ NMR ($CDCl_3$, δ in ppm) 173.6, 173.1, 172.4 *C*ONH, 162.8 *C*$OOCH_3$, 93.7, 78.8, 73.2, 73.5, 72.6, 72.3, 71.9, 69.8, 65.7, 65.3, 64.3Fc, 52.4 OCH_3.

5.4.6.4. Characterization of the Polyferrocene Peptide 15

TOF-MS (m/z): found: 2.8 x 10^4, FT-IR (KBr, υ_{max}/cm^{-1}): 3307 (m, N-H), 3000 (v b, υ(OH)). UV-vis (CH_2Cl_2; λ in nm (ε in $Lmol^{-1}cm^{-1}$)): 448 (512). m. p >200 ºC. ^{1}H-NMR DMSO-D_6, (δ/ppm): 9.11 (124 H, m, NH, b, NHCO), 4.76 (m, Fc), 4.68 (m, Fc), 4.41 (m, Fc), 4.03 (m, Fc).

5.5. References

[1] a) T. J. Peckham, P. Gomez-Elipe, I. Manners, (Eds.: A. Togni, R. L. Haltermann), Wiley-VCH, Weinheim, **1998**, p. 723-754.
b) C. U. Pittman, Jr., *J. Inorg. Organometal. Polym.* **2005**, *15*, 33-56.
c) H. R. Allcock, *J. Inorg. Organometal. Polym.* **2005**, *15*, 57-66.
d) C.E. Carraher, Jr., *J. Inorg. Organometal. Polym.* **2005**, *15*, 121-146.
e) H. Nishihara and M. Murata, *J. Inorg. Organometal. Polym.* **2005**, *15*, 147-156.

[2] A. S. Abd-El-Aziz, C. E. Carraher, Jr., C. U. Pittman, Jr., J. E. Sheats, M. Zeldin, *Macromolecules Containing Metal and Metal-Like Elements, Vol. 1*, Wiley& Sons Inc., New Jersey, **2003**.

[3] E. W. Neuse, L. Bednarik, *Macromolecules* **1979**, *12*, 187-195

[4] M. A. Buretea, T. D. Tilley, *Organometallics* **1997**, *16*, 1507-1510

[5] C. E. Stanton, T. R. Lee, R. H. Grubbs, N. S. Lewis, J. K. C. Pudelski, M. R., M. S. Erickson, M. L. McLaughlin, *Macromolecules* **1995**, *28*, 8713-8721.

[6] A. S. Gamble, J. T. Patton, J. M. Boncella, *Makromol. Chem., Rapid Commun.* **1992**, *13*, 109-115.

[7] R. W. Heo, J.-S. Park, T. R. Lee, *Macromolecules* **2005**, *38*, 2546-2573.

[8] K. A. Mahmoud, Y.-T. Long, G. Schatte, H.-B. Kraatz, *Eur. J. Inorg. Chem.* **2005**, 173-180.

[9] A. S. Abd-El-Aziz, I. Manners, *J. Inorg. Organomet. Polym.* **2005**, *15*, 157-195.

[10] I. Manners, *Angew. Chem. Int. Ed. Engl.* **1996**, *35*, 1603-1621.

[11] P. Nguyen, P. Elipe-Gomez, I. Manners, *Chem. Rev.* **1999**, *99*, 1515-1548.

[12] I. Manners, *Can. J. Chem.* **1998**, *76*, 371-381.

[13] R. W. Heo, J.-S. Park, J. T. Goodson, G. C. Claudio, M. Takenaga, T. A. Albright, T. R. Lee, *Tetrahedron* **2004**, *60*, 7225-7235.

[14] J. Alvarez, Y. Ni, T. Ren, A. Kaifer, *J. Supramol. Chem.* **2001**, *1*, 7-16.

[15] L. Ding, K. M, M. Bolt, P. Zanello, M. Wagner, *Organometallics* **2001**, *20*, 1041-1043.

[16] H. Nishihara, *Bull. Chem. Soc. Jpn.* **2001**, *74*, 19-29.

[17] X. J. Wang, L. Wang, J. J. Wang, *J. Funct. Polym.* **2002**, *15*, 1709-1711.

[18] M. Heitzmann, J.-C. Moutet, J. Pecaut, O. Reynes, G. Royal, G. Serratrice, *Eur. J. Inorg. Chem.* **2003**, 3767-3773.

[19] K. Heinze, M. Schlenker, *Eur. J. Inorg. Chem.* **2004**, 2974-2988.

[20] K. Heinze, M. Schlenker, *Eur. J. Inorg. Chem.* **2005**, 66-71.

[21] T.-a. Okamura, K. Sakauye, N. Ueyama, A. Nakamura, *Inorg. Chem.* **1998**, *37*, 6731-6736.

[22] I. R. Butler, S. C. Quayle, *J. Organomet. Chem.* **1998**, *552*, 63-68.

[23] S. Chowdhury, K. A. Mahmoud, G. Schatte, H.-B. Kraatz, *Org. Biomol. Chem.* **2005**, *3*, 3018-3023.

[24] R. Rulkens, A. J. Lough, I. Manners, *Journal of the American Chemical Society* **1994**, *116*, 797-798.

[25] K. H. Pannell, V. V. Dementiev, H. Li, F. Cervantes-Lee, M. T. Nguyen, A. F. Diaz, *Organometallics* **1994**, *13*, 3644-3650.

[26] H. Atzkern, J. Hiermeier, F. H. Kohler, A. Steck, *J. Organomet. Chem.* **1991**, *408*, 281-296.

[27] S. S. Zhu, P. J. Carroll, T. M. Swager, *J. Am. Chem. Soc.* **1996**, *118*, 8713.
[28] J. Alvarez, T. Ren, A. E. Kaifer, *Organometallics* **2001**, *20*, 3543-3549.
[29] A. Tarraga, P. Molina, D. Curiel, M. Desamparados Velasco, *Organometallics* **2001**, *20*, 2145-2152.
[30] S. Sengupta, S. K. Sadhukhan, *Organometallics* **2001**, *20*, 1889-1891.
[31] S. Maricic, T. Frejd, *J. Org. Chem* **2002**, *67*, 7600-7606.

5.6. Supplemental Material

Table 5.S1. Summary of selected ^{1}H-NMR spectroscopic data for compounds **9, 11-15,** chemical shifts in ppm.

Compd.	δ (NH)	Fc-H's	Substituents
8[a]	8.19 (2H, s, NH)	4.87 (4H, t, J_{H-H} = 4.0 Hz), 4.82 (4H, s), 4.59 (4H, b s), 4.51 (4 H, t, J_{H-H} = 4.0 Hz), 4.42 (4H, m,), 4.15 (4 H, m).	3.84 (6H, s)
10[a]	9.07 (2H, s, NH, NHCO), 6.49 (2H, s, NH, NHBoc)	4.82 (4H, s, Fc), 4.58 (4H, s, Fc), 4.44 (4H, s, Fc), 4.42 (4 H, t, J_{H-H} = 4.0 Hz, Fc), 4.13 (8H, m, Fc).	1.52 (18H, s, $C(CH_3)_3$).
12[a]	7.06 (1H, s, NH, NHCO), 6.57 (1H, s, NH, NHBoc),	4.86 (2H, s, Fc), 4.81 (2H, s, Fc), 4.51 (4H, s, Fc), 4.41 (4 H, s, Fc), 4.14 (4 H, m, Fc)	3.37 (3H, s, $COOCH_3$), 1.39 (9H, s, $C(CH_3)_3$).
13[a]	9.17 (2H, b, s, NH), 8.33 (2H, b, s, NH),	4.85 (overlapping, 16H, Fc-CO), 4.64 (overlapping, 8H, Fc-N) 4.46 (overlapping, 16H, Fc-CO), 4.01(overlapping, 8H, Fc-N)	3.84 (6H, s, $COOCH_3$).
14[a]	NH), 8.86 (2H, br s, NH), 8.41 (2H, br s, NH),	9.33 (2H, br, 4.93-4.01 range (overlapping, 68H, Fc).	3.83 (6H, s, $COOCH_3$).
15[b]	9.11 (overlapping, NH, b, NHCO),	4.76 (overlapping, Fc), 4.68 (overlapping, Fc), 4.41 (overlapping, Fc), 4.03 (overlapping, Fc).	

[a] In $CDCl_3$, [b] In DMSO-*d6*

Table 5.S2. Summary of selected IR (KBr, cm^{-1}) spectroscopic data for compounds **8, 10, 12-15**.

		υ(C=O)		
Compounds	υ(NH)	COOR	CONH	δ(NH)
8	3406 b	1709 s	1651	1542 s
10	3340, 3286 b	1697 s	1639	1554 s
12	3302 m	1720,1697 s	1645 s	1547 s
13	3278 m	1771, 1717 s	1642	1547 s
14	3267 m	1717 s	1641	1547 s
15	3307 m		1640	1548 s

Table 5.S3. Some characterization and Physical properties of compounds **8, 10, 12-15**.

Compounds	Color	Mol. Formula (M.Wt)	Yield%	MP (°C)
8	Orange	$C_{36}H_{32}N_2O_6Fe_3$(756.0305)	88	172-178
10	Yellow	$C_{42}H_{46}N_4O_6Fe_3$ (870.1450)	56	173-177
12	Orange	$C_{28}H_{30}N_2O_5Fe_2$ (586.0862)	3	158-163
13	Orange	$C_{58}H_{50}N_4O_8Fe_5$ (1210.0376)	5	168-174
14	yellow	$C_{80}H_{68}N_6O_{10}Fe_7$ (1664.0452)	7	183-187
15	Yellow	(Av. 2.8 x 10^4)	11	>200

CHAPTER 6

SYNTHESIS AND ELECTROCHEMICAL INVESTIGATION OF OLIGOMERIC AND POLYMERIC FERROCENYL-AMIDES HAVING CYCLOHEXYL, PHENYLENE AND LYSYL SPACERS

6.0. Connecting Text

This chapter expands on the hypothesis demonstrated in Chapter 5 and discusses the use of disubstituted Fc-derivatives as precursors for the synthesis of a series of novel Fc-polyamides. The synthesis and electrochemical analysis for a series of different polymeric and oligomeric ferrocenyl amides having different spacer groups is described. The solution voltammetric analysis performed on the oligomeric ferrocene amides (Chapter 5) revealed very little electronic communication between the iron centres. The main theme of this chapter is the electronic effect of different linker groups connecting the ferrocene units in these polymers and the effect on the electronic communication between the redox centres. This chapter will be showing that varying the distances between the iron centres and altering through-bond conjugation has an effect on the electronic properties of these polymers.

This manuscript is to be published material and will be co-authored by H.-B. Kraatz. All the work described in this manuscript, in terms of the experimental study, hypothesis, and writing of the manuscript was carried out by me.

6.1. Introduction

Ferrocene (Fc)-based polymers and copolymers are of great interest because of their potential electrical, optical, and catalytic applications.[1, 2] Fc-polyester and polyamides having the metallocene in the backbone and being derived from bifunctional Fc derivatives by condensation reactions are of particular interest due to their ease of preparation from convenient starting materials and the potential to vary the properties of the polymer by introducing linker groups that connect the Fc groups.[3, 4] In addition, such systems may allow the development of macromolecular conjugates systems which may have interesting electronic properties and may find applications in optoelectronic devices and chemical sensors.[5]

Controlling the extent of the electronic communication between the Fc sites through a spacer that separated the electroactive sites is particularly important and significant efforts have been made to control and modulate the extent of such electronic communication by varying the distances between the iron centers and altering through-bond conjugation. Several investigations of Fc-oligomers showed that the linkers between Fc units modulate the interaction between the iron centers by changing the Fc-Fc distances and by tuning through-bond orbital conjugation.[6-10] In an attempt to enhance the electronic communication between the Fc centers, Curtis and coworkers reported poly(ferrocenylenearylene)s (**I**).[11, 12] Electrochemical measurements on these systems showed significant interactions between the iron centers. Nishihara and others presented oligo- and poly-ferrocenylenes (**II**) as representative class of polymers that showed a promising electronic communications between the metal sites. The electrochemical studies showed redox waves that are corresponding to the ferrocene

units of the molecule due to the formation of mixed valence state.[13-15] Similar electronic properties were observed by Manners and coworkers in oligo- and poly-ferrocenylsilanes (**III**),[10, 16] in which the high molecular weight polymer displays two redox waves, rationalized by an initial oxidation at alternating iron sites as a result of interactions between the iron atoms.[16]

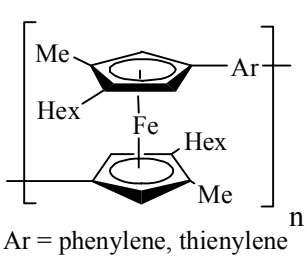

Ar = phenylene, thienylene

I

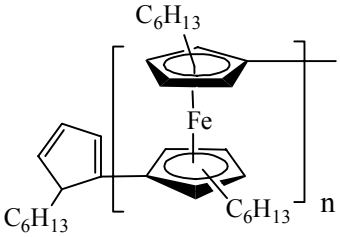

II

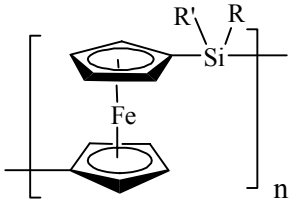

R, R` = alyphatic or aromatic

III

On the other hand, several linear Fc-containing polyesters and polyamides derived from organic diols and diamines (**IV**) do not display any electronic communication between the Fc groups. These systems display a single redox event in the differential pulse voltammetry (DPV), suggesting simultaneous oxidation of all ferrocenyl moieties.[17, 18] This suggests that such a spacer having large insulating organic groups will reduce the electronic interaction, effectively isolating the Fc groups.[17] Chao prepared Fc-polyamides having oligoaniline spacers (**V**).[19] The polymers were lacking the communication between the Fc units and showed week electrical conductivity compared to HCl-doped polyaniline. Similarly, the electrochemical investigation by Deck on perfluorinated biphenylene-linked Fc oligomers (**VI**) revealed a lack of the interaction between the adjacent iron centers.[20-22]

Recently, we have reported the polycondensation of 1,1'-diaminoferrocene with 1,1'-ferrocene acid chloride and on the isolation of a series of oligomeric and polymeric

Fc-polyamide systems.[23] The electrochemical investigations performed on these polyamides also show insignificant electronic communications between the Fc units. The cyclic voltammetry measurements revealed two distinct redox waves which are clearly assigned to the two Fc environments ($Fc(CO\text{-})_2$ and $Fc(NH\text{-})_2$).

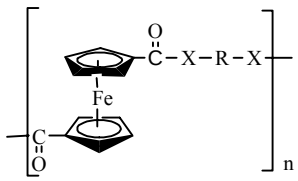

X = O or NH
R = linear oligosiloxanes

IV

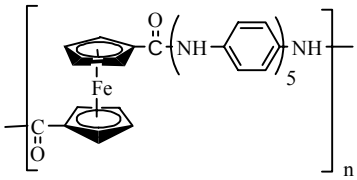

V

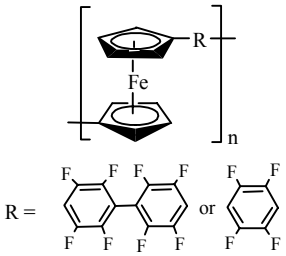

VI

In this paper, we focus our attention on the spacer material linking the Fc-diamine units and report the synthesis of a series of Fc-backbone oligomers and polymers by polycondensation. In addition, model oligomers are reported that help us in the assignment and characterization of the polymeric materials.

We are using three spacer materials for our study that vary in their electronic properties, ranging from a phenylene spacer, which should enhance the Fc to Fc communication, [24, 25] to a cyclohexylene spacer, which should give the polymer more flexibility but should reduce the interaction between the Fc groups, to a lysyl spacer, where we do not expect any interactions between the Fc groups. In all three systems, the presence of the amide group as an internal polar function within the polymeric structure should play a crucial role in influencing the properties of these systems.[18]

6.2. Results and Discussion

6.2.1. Synthesis and Characterization

For a more detailed investigation of the electronic communication between the Fc groups in Fc-containing polymers, various Fc-containing polymers and oligomers were prepared by polycondensation reactions between Fc-diamine and the acid chlorides, terephthaloyl chloride (**2**) and 1,4-cyclohexyldicarboxylic chloride (**4**).

At first, two model compounds were synthesized to help in the characterization of the polymers. These model compounds are derived from a ferrocene amino acid derivative, in which the amino group can be selectively coupled with a diacid chloride, resulting in the formation of well-defined symmetrical bis-Fc systems linked by the desired spacer. Model compounds **3** and **5** were prepared from Boc-protected Fc amino acid methylester (**1**) and terephthaloyl chloride and 1,4-cyclohexylenedicarboxylic chloride, respectively (Scheme 6.1).

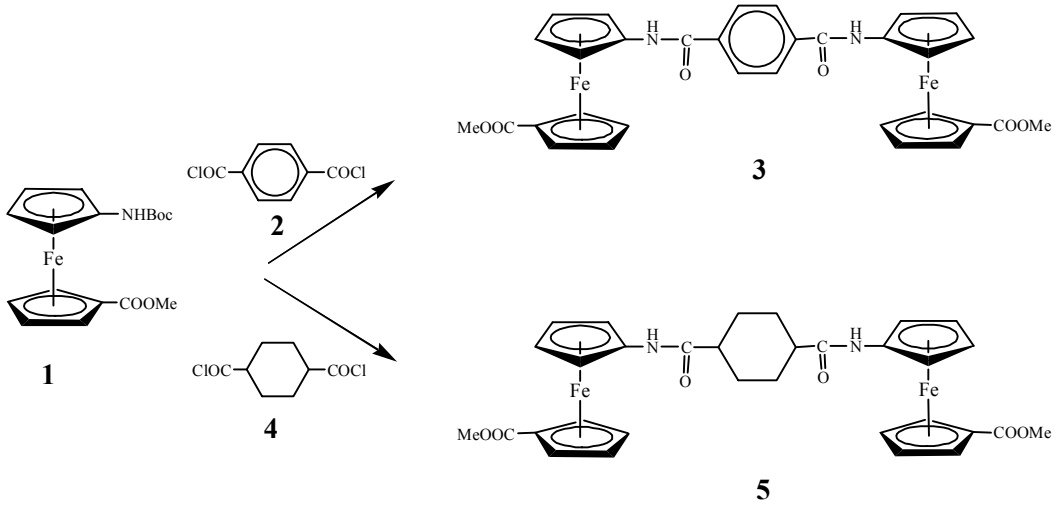

Scheme 6.1. Schematic overview of the synthesis of compounds **3** and **5** from ferrocene amino acid derivative **1** and terephthaloyl chloride (**2**) and 1,4-cyclohexyldicarboxylic chloride (**4**).

After purification by flash column chromatography, compounds **3** and **5** were obtained in good yields and characterized spectroscopically. In the IR, both compounds display a strong Amide A band around 3283, 3252 cm^{-1} indicative of hydrogen bonding in the solid state. In addition, a strong C=O stretching vibration is observed at 1694 cm^{-1}. The ^{1}H-NMR spectrum in DMSO-*d6* showed significant differences in the chemical shift of the amide NH of compound **3** (δ 7.82) and that of compound **5** (δ 9.16).

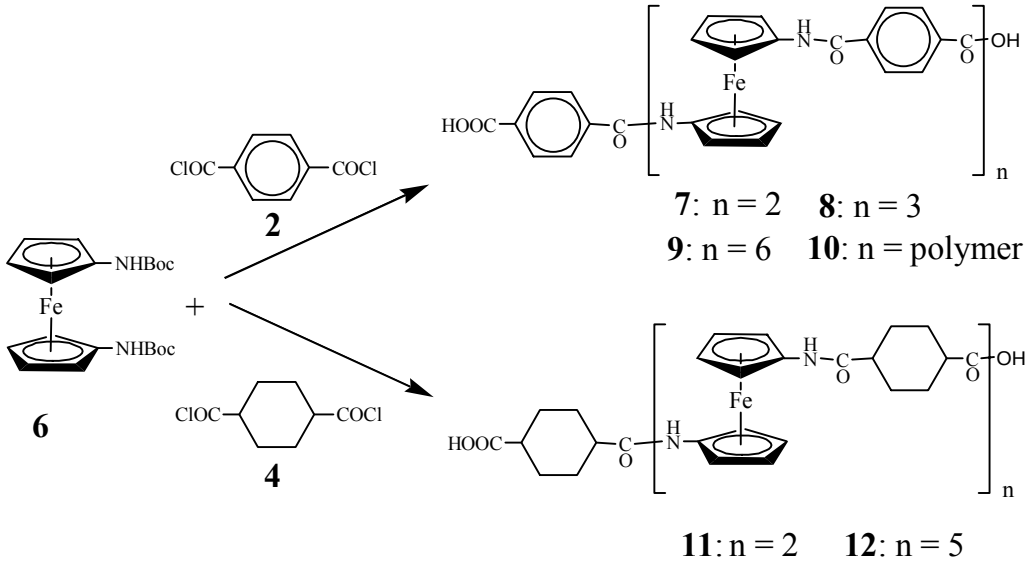

Scheme 6.2. Schematic overview of the synthesis of compounds **7** – **12** from the ferrocene diamine derivative **6** and terephthaloyl chloride (**2**) and 1,4-cyclohexyldicarboxylic chloride (**4**).

As a next step, we carried out reactions of the Fc-diamine, derived from the Boc-protected derivative **6** and the diacid chlorides **2** and **4** (Scheme 6.2). The Boc groups were removed from the starting material **6** by treatment with trifluoroacetic acid, followed by the addition of Et_3N prior to reaction with the diacid chlorides. This needs to be done under an inert atmosphere and at low temperatures.

In the case of the reaction with terephthaloyl chloride and immediately after mixing, polymer **10** starts to precipitate and is isolated by filtration, followed by washing and recrystallization from methanol. The remaining solutions from filtrations and successive washings were combined and purified by flash column chromatography (EtOAc:MeOH 9:1), allowing the isolation of oligomers **7-9** as shown in Scheme 6.2. The polymer **10** is soluble only in DMSO and DMF, and attempts to determine the molecular mass of the polymer by MALDI-TOF were unsuccessful. The estimated molecular mass was obtained from dynamic light scattering measurements. Assuming a globular protein model, the average molecular was 125 ± 4 kDa and the mean hydrodynamic diameters were in the range of 5.5 (±0.5) nm. The size distribution showed a narrow unimodal pattern (Figure 6.1).

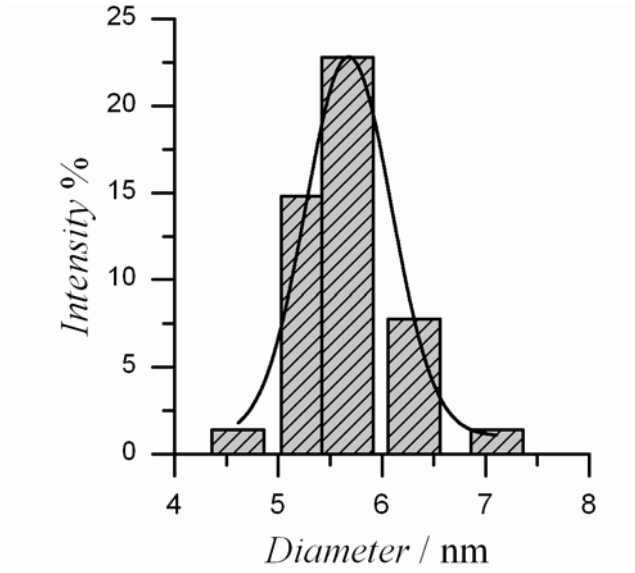

Figure 6.1. Intensity size distributions of 0.1 mM of polymer **10** in DMSO measured by dynamic light scattering at 23°C.

The IR spectrum of **10** shows a simple but expected pattern, with broad peak at 3229 cm^{-1} assigned to the Amide A, and two peaks at 1641 and 1555 cm^{-1} assigned to

amide I and II bands, respectively. A small peak for the residual hydroxyl group was observed around 3485 cm^{-1} (Table 6.1 and Figure 6.2).

The ^{1}H-NMR spectrum for the oligomers in DMSO-*d6* of the compounds showed a downfield shift of the amide signals with increasing degree of oligomerization from δ 7.87 for **7**, to δ 8.33, 8.28 for **8**, and δ 8.53-8.20 for **9**, which lending support to the assumption of increasing levels of intramolecular H-bonding in these systems.

Table 6.1. Selected IR spectral data (KBr, cm^{-1}) for compounds **7-10**.

	Amide-A	Amide-I	Amide-II	CH	OH	COOH
7	3372	1645	1550	3095-2850	3327	1717
8	3284	1648	1545	3086-2850	3386	1710
9	3279	1647	1547	3093-2853	3385	1714
10	3229	1641	1555	3098-2960	3435	
11	3267	1656	1542	3089-2950	3427	
12	3274	1667	1542	3089-2950	3436	

A representative ^{1}H-NMR spectrum of polymer **10** is shown in Figure 6.3 and is surprisingly simple, showing only two singlets appearing at δ 4.83 and 4.01 corresponding to the Fc protons. The phenylene protons merge together and appear in the region of δ 8.10 - 7.89. The amide protons are observed in the range of δ 8.91-8.30 indicating a strong engagement in H-bonding.

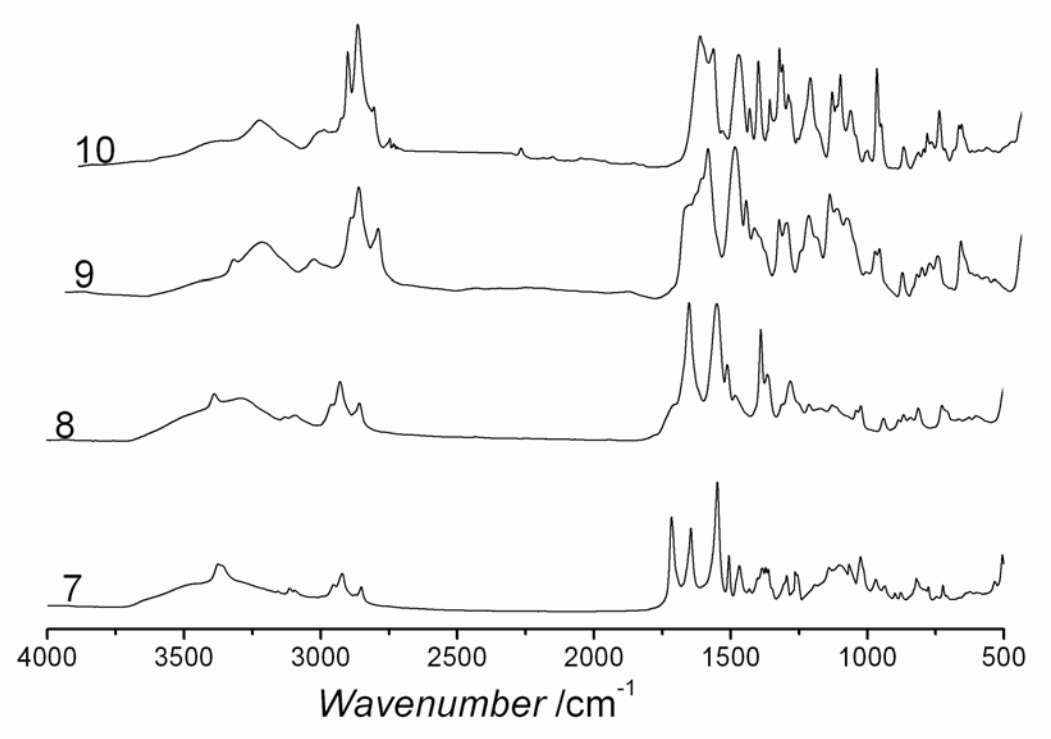

Figure 6.2. IR spectra (KBr) of the oligomers **7-9** and the polymer **10**.

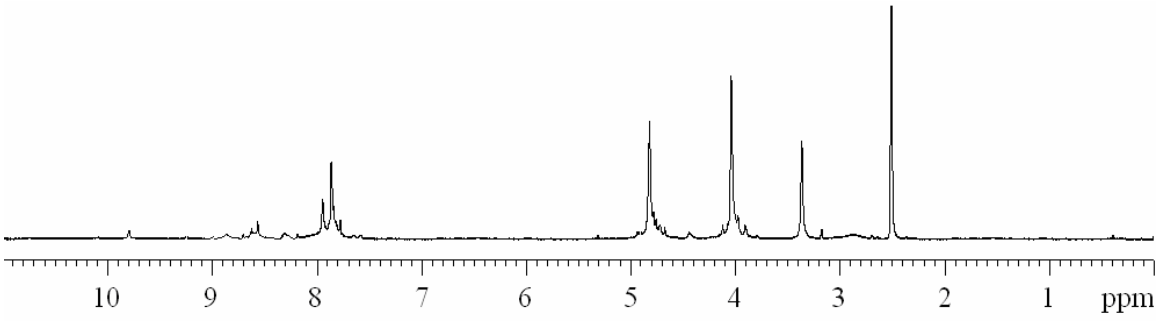

Figure 6.3. ^{1}H-NMR spectra in DMSO-*d6* of the polymer **10**.

In contrast to the successful polymerization of Fc diamine with terephthaloyl chloride, the reaction with 1,4-cyclohexyldicarboxylic chloride (**4**) did not lead to any polymeric product. Even upon increasing the reaction time or reaction temperature, we were able to isolate only two oligomeric products **11** and **12**, having two and five repeat

units, respectively (Scheme 6.2). The two oligiomers are soluble in common organic solvents such as CH_2Cl_2 and CH_3CN were fully characterized by MALDI-TOF, NMR, and IR spectroscopy. Figure 6.4 shows the IR spectra for both compounds. Amide I and II bands are observed at 1660 and 1542 cm^{-1}, respectively. In addition, broad CH stretching signals are observed in the range of 3089-2950 cm^{-1} (Table 6.1).

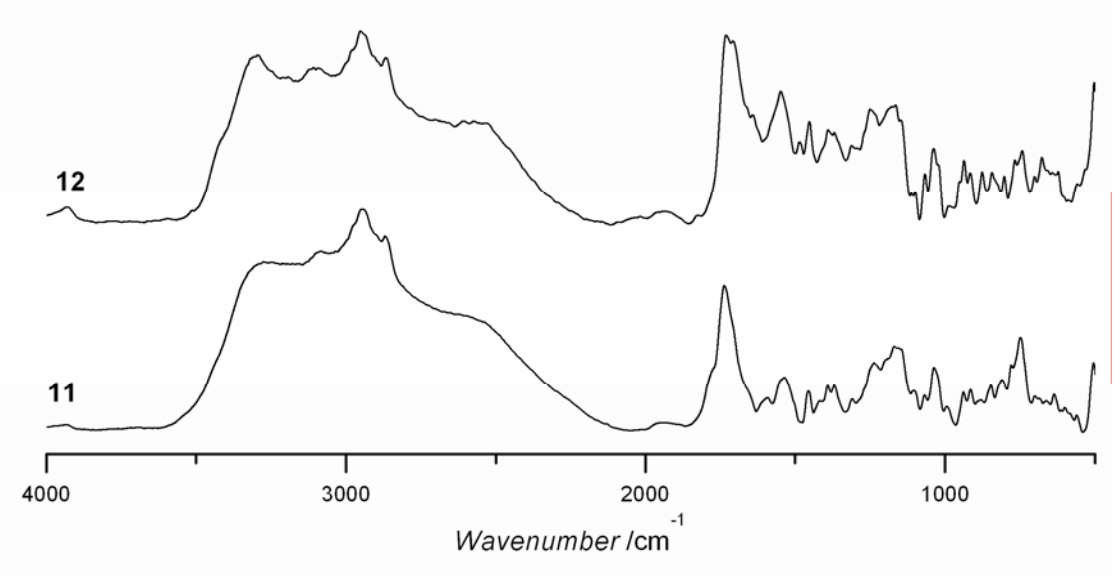

Figure 6.4. Selected regions from FT-IR spectra (KBr) of the oligomers **11** and **12**.

The ^{1}H-NMR spectra of these oligomers in DMSO-*d6* shows amide NH signals at δ 7.78 for compound **11** and at δ 7.97-7.75 for compound **12**. The NMR and IR spectra also provide evidence for the presence of carboxylic OH groups at around δ 9.8, and in the IR with an OH stretching vibration shoulder observed as a shoulder around 3437 cm^{-1} (Figure 6.4).

Next, a polymer based on the reaction of Fc diacid chloride with lysine methylester was synthesized. As a first step in the synthesis of the polymer, the conjugate 1,n'-bis(Lys(Boc)-OMe)ferrocene **14** was prepared by amide coupling of Fc-

acid chloride with the amino acid in the presence of Et_3N.' Next, the polymer Fc-Lys polymer **15** was prepared by solution polycondensation of equimolar ratios of Fc diacid chloride with Boc-deprotected 1,1´-bis(Lys-OMe)Fc in the presence of Et_3N (Scheme 6.4).

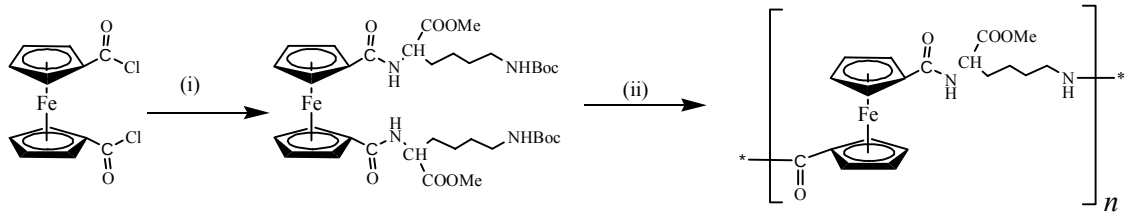

13 **14** **15** Polymer

Scheme 6.4. Schematic overview of the synthesis of compounds **14** and **15**. (i) Et_3N, CH_2Cl_2, 0 °C, H-Lys(Boc)-OMe; (ii) a) TFA, CH_2Cl_2 , b) Et_3N, CH_2Cl_2, c) $Fc[CO\text{-}Cl]_2$.

The IR spectra of compounds **14** and the polymer **15** are shown in Figure 6.5 and are very similar. The IR spectrum of compound **14** has Amide A absorption bands at 3378 and 3260 cm^{-1}. In the case of polymer **15,** this region is shifted to lower energy and registered at 3127-2864 cm^{-1} indicating more engagement in hydrogen bonding. Both compounds showed similar absorptions around 1710 cm^{-1} for the ester C=O and at 1634, 1545 cm^{-1} for Amide I and II bands, respectively. The ^{1}H-NMR spectrum of compound **14** has a single signal for the methoxy group at δ 3.66 and for the amide NH protons at δ 8.10 for the Fc-NH and at δ 6.79 for the Boc-NH. Polymer **15** was completely soluble in water and partially soluble in DMSO. Its ^{1}H-NMR spectra, recorded in D_2O, showed similar spectra to those of **14**. However, in this case the majority of the signals are unresolved multiples reflecting the presence of a polymeric species.

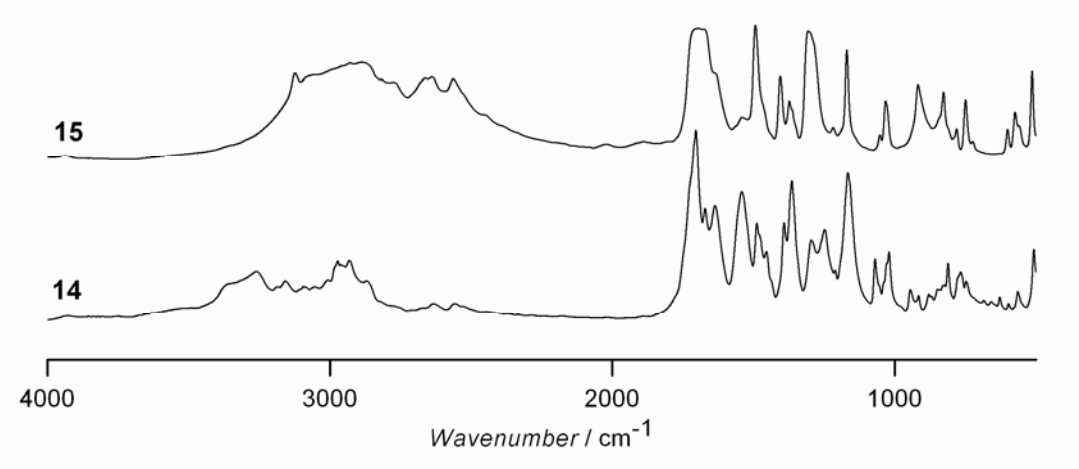

Figure 6.5. FT-IR spectra of compounds **14** and **15** recorded as KBr disk.

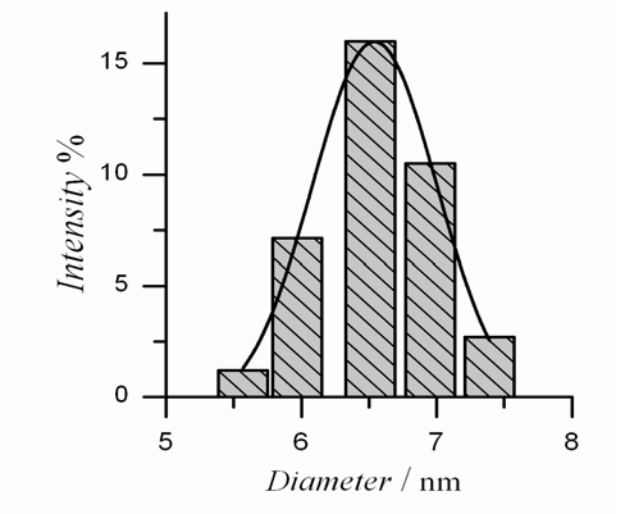

Figure 6.6. Intensity size distributions of 0.1 mM of polymer **15** in H_2O measured by dynamic light scattering at 23°C.

It was not possible to determine the molecular mass of the polymer **15** by MALDI-TOF. DLS measurements were used to estimate the molecular mass, assuming globular protein model, which gave an average of 79.4 ± 3 kDa and the mean hydrodynamic diameters was 6.5 (±0.5) nm. Similar to the polymer **10**, the size distribution is narrow (Figure 6.6).

Figure 6.7 shows the circular dichroic spectra of compounds **14** and **15**. The axial chirality about the Fc group can be evaluated by the band in the 440 nm region.[26] Both compounds displayed a CD signal with a positive Cotton effect at 495 nm, indicating P-helical chirality about the Fc group. Surprisingly, the intensity of the absorption decreases for the polymer, indicating that the polymer does not adopt a helical conformation but rather a random coil.

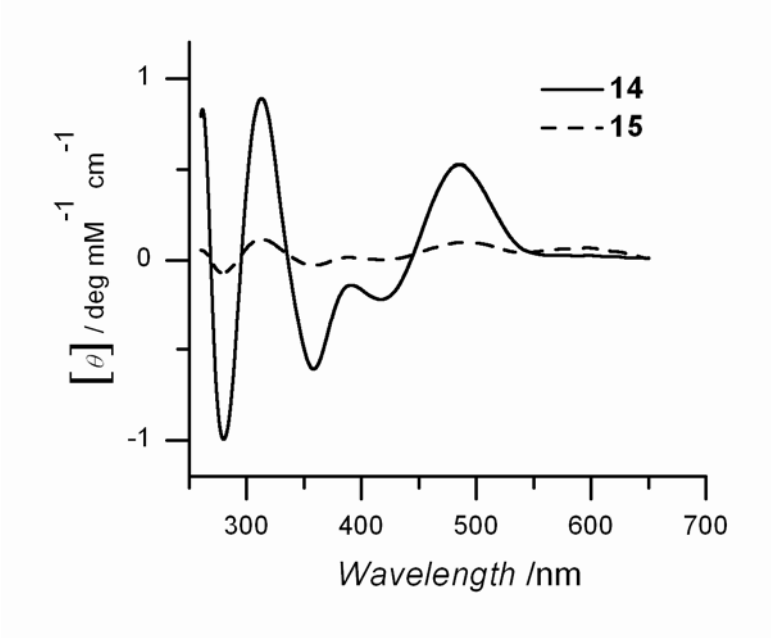

Figure 6.7. CD spectra of compounds **14** and **15** (1 mM in CH_3CN).

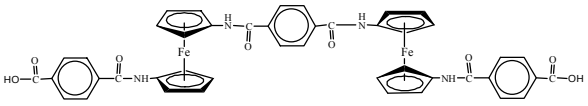

7

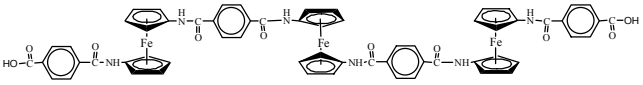

8

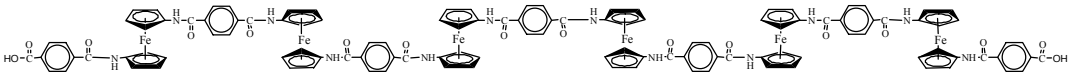

9

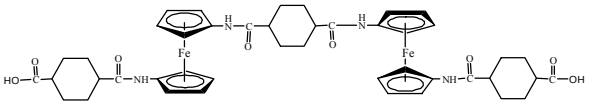

11

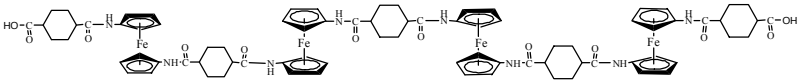

12

6.2.2. Electrochemistry

In order to assess the electronic interactions between the oligoferrocenyl amides prepared here, and evaluate the role of the linker group, we carried out a series of electrochemical studies in acetonitrile solution. The results of our study are summarized in Table 6.2.

The cyclic voltammograms (CVs) and differential pulse voltammograms (DPVs) of the precursor compounds **3**, **5** and of the oligomers **7**-**9** are shown in Figure 6.8. The two ferrocene amino acid derived model complexes **3** and **5** both exhibit a

single redox wave with peak separations indicating a reversible one-electron oxidation, indicating that both Fc groups are functioning as isolated units. The halfwave potential $E_{1/2}$ of phenylene-bridged compound **3** is shifted anodically by 75 mV compared to that of the cyclohexyl-bridged compound **5**. The phenylene spacer appears to enable delocatization of electrons into the aromatic ring, but does not appear to facilitate the electronic communication between the two Fc groups, in which case, we would have expected to see two distinct redox waves.

Table 6.2. Solution electrochemical results for compounds **3**, **5**, **7-12**, and **14** and **15**.

Compound	$E_{1/2}$(mV)	ΔE_p	(i_a/i_c)
3	573 ± 5	65	1
5	498 ± 5	75	1
7	327 ± 5	88	0.9
8	316 ± 5	76	0.8
9	300 ± 5	67	0.7
10	308 ± 4	57	1.1
11	200 ± 3	195	0.8
12	207 ± 5	412	0.9
14	782 ± 5	265	1.1
15	754 ± 3	456	1.4

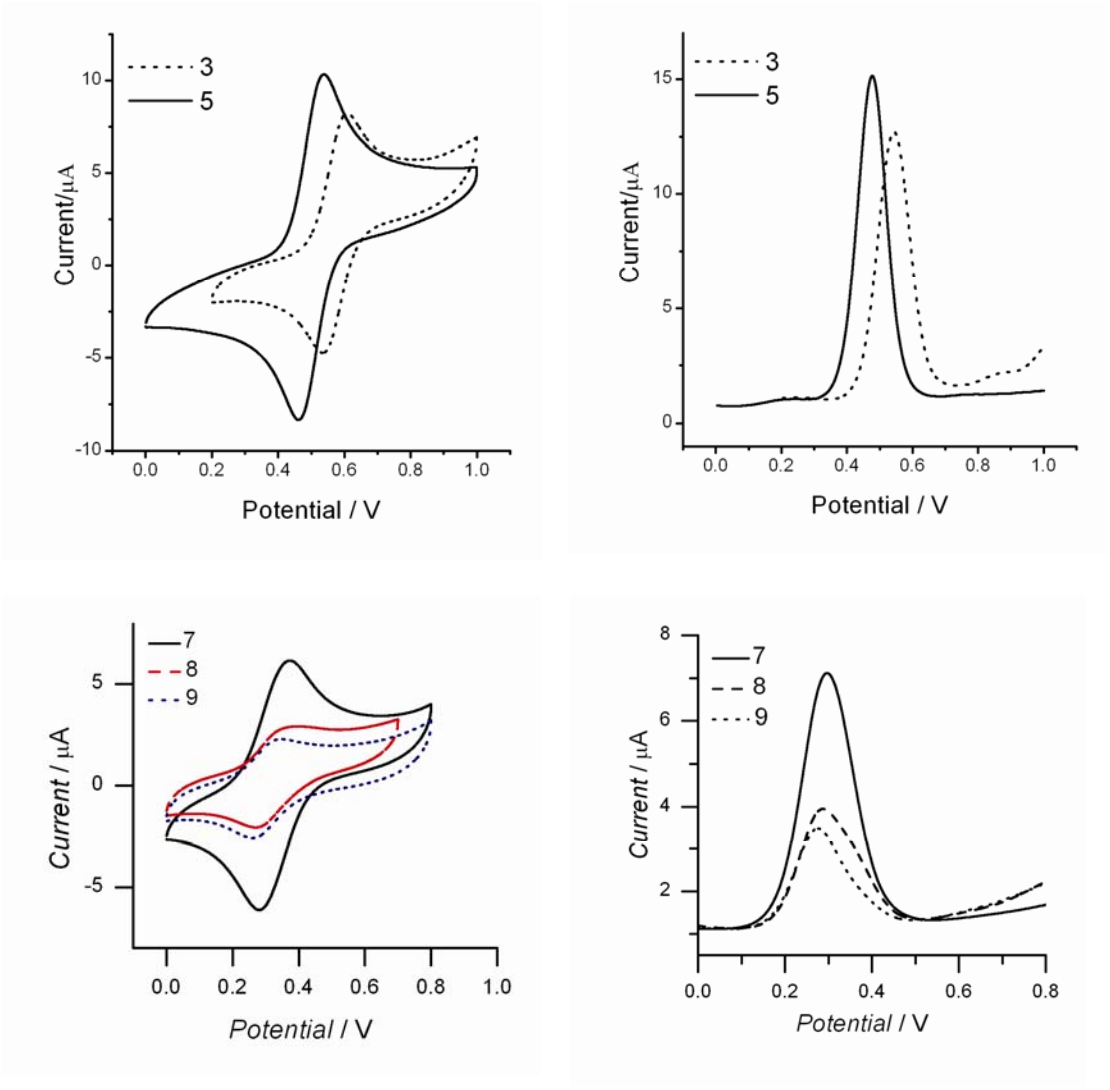

Figure 6.8. Cyclic voltammetry (left) and differential pulse voltammetry (right) of compounds **3**, **5, 7-9** in CH_3CN. All solutions contain 0.1 mM of the compounds and 0.1 M TBAP. GCE vs. Ag/AgCl. Scan rate = 100 mV/s. The $E_{1/2}$ of the ferrocene/ferrocenium redox couple under the experimental conditions was 449(±5) mV (*vs*. Ag/AgCl).

The CVs and DPVs of compounds **7-9** are shown in Figure 6.9 Similar to what was observed for the compound **3**, the oligomers exhibit a single reversible to quasireversible redox wave. These results suggest unresolved or no interaction between the ferrocene groups among the oligomers. One has to point out that upon increasing the length of the oligomers, the $E_{1/2}$ for the systems is shifting cathodically

and signals undergo significant peak broadening. This may indicate increasing but small electron delocalization between the ferrocene and the spacer group from **7** to **8** to **9**. Thus, the phenylene group allows only a week and unresolved electronic communication between the relevant ferrocenyl subunits,[27, 28] and may be due to a mismatch between the phenylene spacer group and the ferrocene units as was suggested by Swager for other compounds.[29] In addition, the peak current decreases, as would be expected for systems with increasing oligomeric chain length.[30]

Next, we investigated the electrochemical properties of the polymer **10** as a thin film on a glassy carbon electrode. The results are shown in Figure 6.9. Interestingly, two redox waves were observed.

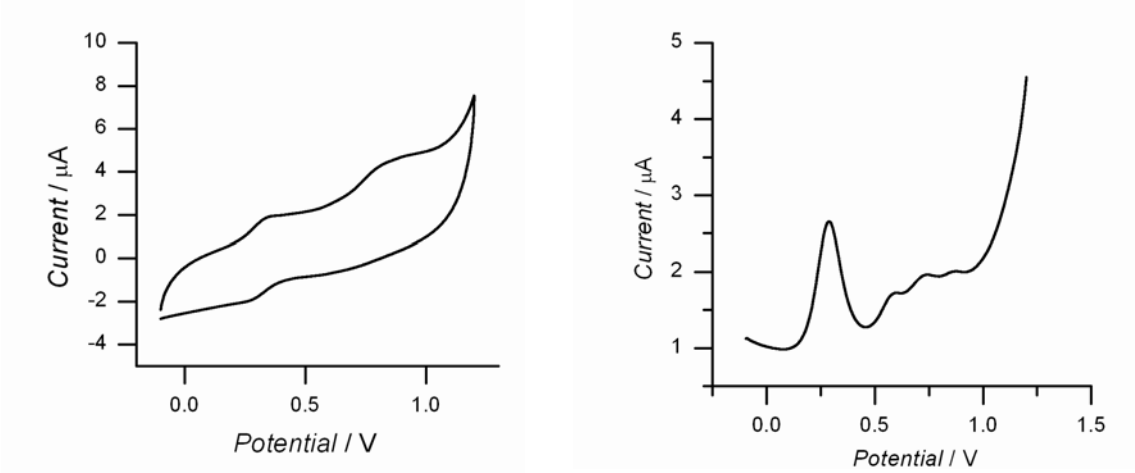

Figure 6.9. Cyclic voltammetry (left) and differential pulse voltammetry (right) of deposited film of the polymer **10** on glassy carbon electrode. All solutions contain 0.1 M TBAP in CH_3CN. GCE vs. Ag/AgCl. Scan rate = 100 mV/s. The $E_{1/2}$ of the ferrocene/ferrocenium$^+$ couple under the experimental conditions was 449(±5) mV (*vs*. Ag/AgCl).

The first one recorded at $E_{1/2}$ = 308 mV with peak separation 57 mV was stable and reproducible after many sweeps. Another irreversible oxidation wave was observed at 847 mV, which it decreased with repeat scans. Nguyen and co-workers reported for

polymer films that the reduction of in peak current may be attributed to loss of electroactivity rather than loss of material from the electrode surface.[31] The broad characteristic of this second peak was resolved to at least three waves in DPV. Different studies on polymer film electrodes suggested that the charge transfer between redox centers among the polymer matrix could happen via different mechanisms such as electron hoping, counter-ion diffusion, and diffusion of electroactive species.[32-35]

Like the phenylene-spaced systems, the cyclohexyl-spaced oligomers **11** and **12** exhibited a single redox wave, which compared to compounds **7-9**, are shifted to lower potential and located at 200 and 207 mV respectively (see Figure 6.10).

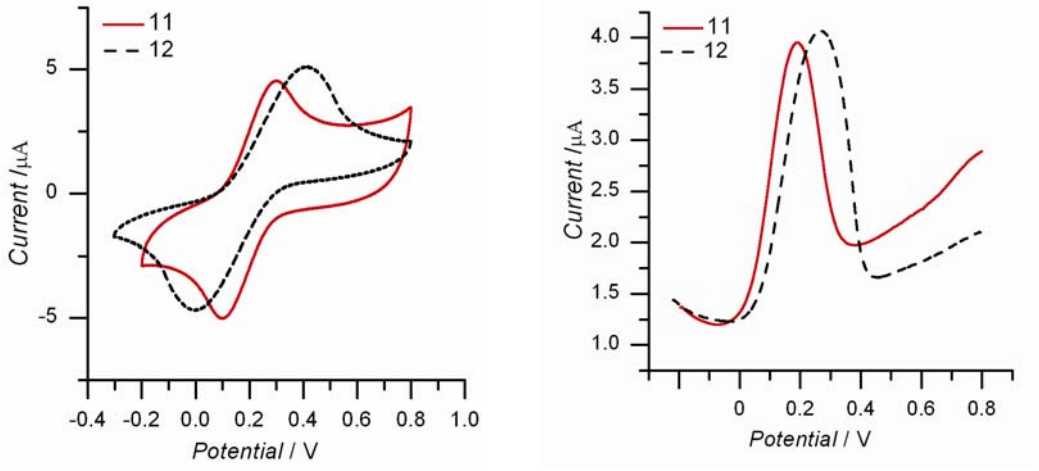

Figure 6.10. Cyclic voltammetry (left) and differential pulse voltammetry (right) of compounds **11** and **12** in CH_3CN. All solutions contain 0.1 mM of the compounds and 0.1 M TBAP. GCE vs. Ag/AgCl. Scan rate = 100 mV/s. The $E_{1/2}$ of the Ferrocene/Ferrocene$^+$ couple under the experimental conditions was 449(±5) mV (*vs*. Ag/AgCl).

This is in line with the observation of a cathodic shift for the cyclohexylene systems **5** compared to the phenylene system **3**. However, it is interesting to note that the reversibility of the redox events in compounds **11** and **12** is significantly reduced.

Both systems exhibit large peak separations and a ratio of the peak current that is significantly removed from unity.

Lastly, we investigated the electrochemical properties of the lysyl systems **14** and **15**. Figure 6.11 shows the CVs and DPVs of monomer **14** and the polymeric **15**. Both systems display a single quasi-reversible redox waves with large peak separations. However, the peaks shapes are significantly different. The polymer **15** has significantly broader peaks. In addition, the peak separation increases by 191 mV compared to the monomer **14**, which may indicate very week and unresolved electronic interaction between the Fc centers.

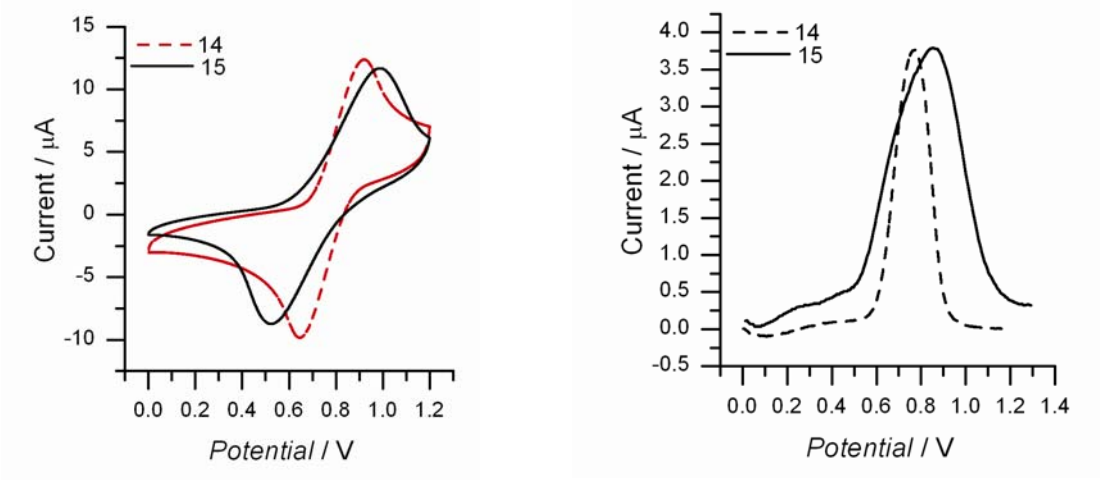

Figure 6.11. Cyclic voltammetry (left) and differential pulse voltammetry (right) of compounds **14** and **15** in CH_3CN. All solutions contain 0.1 mM of the compounds and 0.1 M TBAP. GCE vs. Ag/AgCl. Scan rate = 100 mV/s. The $E_{1/2}$ of the Ferrocene/Ferrocene$^+$ couple under the experimental conditions was 449(±5) mV (*vs*. Ag/AgCl).

6.3. Conclusion

We have successfully synthesized a series of oligomeric and polymeric Fc-amides with different spacer groups, aimed at changing the electronic coupling between

the Fc units. Lysyl, cyclohexylene, and phenylene groups were used as the spacer groups. In our study, we isolated two polymeric materials. In both materials, electronic interactions between the Fc groups are weak. For the phenylene polymer **15**, clear evidence for some weak electronic interactions is obtained from our electrochemical studies. However, since the redox peaks are unresolved, we are unable to evaluate the magnitude of the electronic interactions. The same is true for the Lys polymer **15**. In this system, electronic interactions are even weaker leading to a distortion of the redox signal only. The next step in our study is to evaluate systems with alkene and alkyne spacers in the hope to increase the coupling between the Fc groups.

6.4. Experimental

6.4.1. General Procedure

All syntheses were carried out under dry nitrogen gas unless otherwise indicated. CH_2Cl_2 (BDH; ACS grade) used for synthesis was dried (CaH_2) and distilled prior to use. $CDCl_3$ (Aldrich) was dried (CaH_2), and stored over molecular sieves (8-12 mesh; 4Å effective pore size; Fisher) before use. THF was dried over benzophenone/sodium, and stored over molecular sieves (8-12 mesh; 4Å effective pore size; Fisher) before use. 1'-methoxycarbonyl Ferrocene-1-carboxylic acid and 1`-Boc-aminoFerrocene-1-OBt were prepared according to literature procedures, hydroxybenzotriazole (HOBt) (Nova), $NaSO_4$, and $NaHCO_3$ (VWR) were used as received. For column chromatography, a column with a width of 2.7 cm (ID) and a length of 45 cm was packed 18-22 cm high with 230-400 mesh silica gel (VWR). For

TLC, aluminum plates coated with silica gel 60 F_{254} (EM Science) were used. NMR spectra were recorded on a Bruker Avance-500 spectrometer using a 5-mm broadband probe operating at 500.134 MHz (^{1}H) and 125.766 MHz (^{13}C{^{1}H}). Peak positions in ^{1}H spectra are reported in ppm relative to TMS. All, unless otherwise described ^{13}C{^{1}H} spectra are referenced to the $CDCl_3$ signal at δ 77.23. Mass spectrometry was carried out on a VG Analytical 70/20 VSE instrument. Infrared spectra were obtained with a Perkin-Elmer model 1605 FT-IR. Dynamic light scattering experiments were carried out on a Dynampro-MS800 instrument using a 20 μL sample in a quartz cuvette. Cells with a diameter of 10 mm were carefully flushed using distilled acetone and were dried before being filled with sample solutions. Samples were filtered into the cells using 0.45 μm PTFE filters.

6.4.2. Preparation of Bis-(1'-Methoxycarbonylferrocenyl-1'-Amide)-1,4-Terephthaloyl (3)

1'-Boc-aminoferrocene-1-OMe (Fca) **1** (2.1 mmol, 0.78 g) was dissolved in CH_2Cl_2 and treated with TFA (3 ml) in CH_2Cl_2 (3 ml) for 30 min. The TFA and CH_2Cl_2 were subsequently removed in vacuo. The resulting residue was redissolved in CH_2Cl_2 and cooled in ice bath prior to the dropwise addition of Et_3N (0.45 ml). To this was added a solution of terephthaloyl chloride **2** (0.99 mmol, 0.20 g) in CH_2Cl_2 with vigorous stirring for 1 hour. The residue was chromatographed by ($CHCl_3$: MeOH 9:1) to give yellow crystals of compound **3** (0.48 g, 74%)**:** m. p. 130-138 °C; UV-vis (CH_3CN; λ in nm (ε in $Lmol^{-1}cm^{-1}$)): 448 (610); FT-IR (KBr, υ_{max}/cm^{-1}): 3283 (m, N-H), 1694 (s, C=O). ^{1}H-NMR DMSO-*d*$_6$, (δ in ppm): 8.20 (4H, s. Ph's), 7.82 (2H, s, NH,

NHCO), 4.90 (4H, s, Fc), 4.71 (4H, s, Fc), 4.42 (4H, s, Fc), 4.08 (4 H, s, Fc), 3.52 (6H, s, $COOCH_3$); $^{13}C\{^1H\}$-NMR DMSO-d_6, (δ in ppm): 172.3 (CONH), 162.7 ($COOCH_3$), 138.7, 127.3 (Ph's), 99.9, 72.6, 71.0, 65.9, 62.45 (Fc), 52.3 (OCH_3); TOF-MS (m/z): calc for $C_{32}H_{28}N_2O_6Fe_2$ $[M]^+$: 648.0641; found: 648.0665.

6.4.3. Preparation of 1,4-Cyclohexyldicarboxylic Chloride (4)

1,4-cyclohexyldicarboxylic acid (8.61 g, 0.05 mol) was suspended in freshly distilled thionyl chloride (30 mL, 0.5 mol). Under stirring, one drop N, N-dimethylformamide (DMF) was added as a catalyst, and the solution was refluxed for 3 h. At this point dry toluene was added in excess and the mixture was fractionally distilled at 50 °C under vacuum to drive of thionyl chloride. Needle like white crystals of 1,4-Cyclohexyldicarboxylic acid chloride were obtained. The crystals were purified by recrystallization from n-hexane with a yield of 8.53 g (82%). m. p. 68-70 °C ^1H-NMR $CDCl_3$, (δ in ppm): 2.78 (2H, m, CH), 2.35 (4H, m, CH_2), 1.61 (4H, m, CH_2).

6.4.4. Preparation of Bis-(1'-Methoxycarbonylferrocenyl-1'-Amide)-1,4 Cyclohexyldicarbonyl (5)

Compound **1** was treated as per **3** to remove the Boc group prior the mixing with solution of cyclohexanedicarbonyl chloride in CH_2Cl_2. The reaction was vigorously stirred for 1 hour at room temperature. The crude product was purified by flash column chromatography (SiO_2, 95:5 EtOAc:MeOH) to give yellow crystals of compound **5** (78%). m. p. 80-84 °C; UV-vis (CH_3CN; λ in nm (ε in $Lmol^{-1}cm^{-1}$)): 448 (712); FT-IR (KBr, υ_{max}/cm^{-1}): 3252 (m, N-H), 1696 (s, C=O). ^1H-NMR DMSO-d_6, (δ

in ppm): 9.16 (2H, s, NH, NHCO), 4.67 (4H, s, Fc), 4.63 (4H, s, Fc), 4.38 (4H, s, Fc), 4.00 (4 H, s, Fc), 3.70 (6H, s, $COOCH_3$), 2.37 (2H, m, cyclohexane), 1.94 (4H, m, cyclohexane), 1.59 (4H, m, cyclohexane). $^{13}C\{^1H\}$-NMR DMSO-d_6, (δ in ppm): 174.1 (CONH), 163.4 ($COOCH_3$), 99.9, 72.8, 70.9, 65.8, 62.0 (Fc), 51.8 (OCH_3), 44.3, 28.8 (cyclohexane); TOF-MS (m/z): calc for $C_{32}H_{28}N_2O_6Fe_2$ $[M]^+$: 654.1110; found: 654.1108.

6.4.5. Polycondensation of 1,1'-bis(Boc-amino)Ferrocene and terephthaloyl chloride

1,1'-bis(Boc-amino)ferrocene[36] **6** (0.30 g, 0.75 mmol) was dissolved with stirring in CH_2Cl_2 (2.0 mL) and after cooling to 0 ºC with an ice bath, TFA (2.0 mL) was added dropwise under a nitrogen atmosphere. Then the ice bath was removed and stirring was continued. After 30 min, CH_2Cl_2 (10 mL) was added and the solution was cooled to 0 ºC before an excess Et_3N was added dropwise. To this, a solution of terephthaloyl chloride **2** (0.67 g, 2.2 mmol) in dry CH_2Cl_2 was added. And the reaction mixture was allowed to stir for 1 hour. The content of the flask was added to 200 mL cyclohexane and the precipitated polymer **10** (0.23 g) was filtered off and washed by a mixture of cyclohexane/dichloromethane. The remaining solutions from filtration and successive washings of polymer **10** were combined and evaporated to dryness, and then the crude residue was purified by flash column chromatography (EtOAc:MeOH 9:1). Oligomers **7** (0.09 g, R_f = 0.56), **8** (0.13 g, R_f = 0.41), **9** (0.06 g, R_f = 0.28) were successfully isolated for further characterizations.

6.4.5.1. Characterization of Compound 7

m. p. 171-184 °C; UV-vis (CH_3CN; λ in nm (ε in $Lmol^{-1}cm^{-1}$)): 447 (604); FT-IR (KBr, υ_{max}/cm^{-1}): 3360 (m, N-H), 17063, 1661 (s, C=O). ^{1}H-NMR DMSO-*d*$_6$, (δ in ppm): 9.76 (2H, COOH), 8.10 (12H, m, Ph's), 7.78 (2H, s, NH, NHCO), 4.93 (4H, overlapping, Fc), 4.72 (4H, overlapping, Fc), 4.43 (4H, overlapping, Fc), 4.07 (4 H, overlapping, Fc); ^{13}C{^{1}H}-NMR DMSO-*d*$_6$, (δ in ppm): 190.1 (COOH), 172.3 (CONH), 145.9, 138.7, 128.7, 127.4, 127.2 (Ph's), 100.0, 7.3.1, 72.6, 72.5, 71.0, 65.9, 62.1 (Fc); TOF-MS (m/z): calc for $C_{44}H_{34}N_4O_8Fe_2$ $[M]^+$: 858.1070; found: 858.1064.

6.4.5.2. Characterization of Compound 8

m. p. 198-201 °C; UV-vis (CH_3CN; λ in nm (ε in $Lmol^{-1}cm^{-1}$)): 447 (601); FT-IR (KBr, υ_{max}/cm^{-1}): 3425 (m, N-H), 3374, 3114 (s, N-H), 1717, 1644 (s, C=O). ^{1}H-NMR DMSO-*d*$_6$, (δ in ppm): 9.77 (1H, s, COOH), 8.33 (2H, s, NH, NHCO), 8.28 (4H, s, NH, NHCO), 8.02 (16H, m, Ph's), 4.94 (6H, overlapping, Fc), 4.73 (6H, overlapping, Fc), 4.45 (6H, overlapping, Fc), 4.09 (6 H, overlapping, Fc); ^{13}C{^{1}H}-NMR DMSO-*d*$_6$, (δ in ppm): 190.2 (COOH), 172.3 (CONH), 145.9, 138.7, 128.7, 127.4, 127.2 (Ph's), 100.0, 73.1, 72.6, 72.5, 71.0, 66.0, 62.9, 62.01 (Fc); TOF-MS (m/z): calc for $C_{62}H_{48}N_6O_{10}Fe_3$ $[M]^+$: 1204.1475; found: 1204.1508.

6.4.5.3. Characterization of Compound 9

m. p. > 300 °C; UV-vis (CH_3CN; λ in nm (ε in $Lmol^{-1}cm^{-1}$)): 447 (598); FT-IR (KBr, υ_{max}/cm^{-1}): 3495, 3295, 2978 (m, N-H), 1690 (s, C=O). ^{1}H-NMR DMSO-*d*$_6$, (δ in

ppm): 9.78 (2H, s, COOH), 8.53-8.29 (11H, range of NH, NHCO), 8.10 (28H, overlapping, range of Ph's protons), 4.94-4.01 (48H, overlapping, range of Fc protons); $^{13}C\{^{1}H\}$-NMR DMSO-d_6, (δ in ppm): 190.2 (COOH), 172.3, 172.1, (CONH), 145.9, 138.7, 138.5, 128.7, 128.2, 127.4, 127.2 (Ph's), 100.0, 73.1, 72.6, 72.5, 71.0, 69.9, 66.0, 62.9, 62.01 (Fc); TOF-MS (m/z): calc for $C_{116}H_{90}N_{12}O_{16}Fe_6$ $[M]^+$: 2242.2689; found: 2242.2694.

6.4.5.4. Characterization of Polymer 10

m.p. > 300 °C; FT-IR (KBr, υ_{max}/cm^{-1}): ^{1}H-NMR DMSO-d_6, (δ in ppm): 9.80 (2H, s, COOH), 8.91-8.30 (range of NH, NHCO), 8.10-7.69 (overlapping, range of Ph's protons), 4.83 (Fc protons), 4.01 Fc protons). $^{13}C\{^{1}H\}$-NMR DMSO-d_6, (δ in ppm): 190.2 (COOH), 172.3, 172.1, 171.8, 164.7 (CONH), 145.9, 138.7, 138.5, 137.17, 128.7, 128.2, 127.6, 127.4, 127.2 (Ph's), 100.0, 73.1, 72.6, 72.5, 71.0, 69.9, 66.0, 62.9, 62.01 (Fc); DLS: average Mw = 1.25 x 10^5.

6.4.6. Polycondensation of 1,1'-bis(Boc-amino)Ferrocene and 1,4-Cyclohexyldi-carboxylic Chloride.

After deprotection of Boc group from 1,n'-bis(Boc-amino)Ferrocene **6** (0.30 g, 0.75 mmol) as described above, it was mixed with equimolar amount of 1,4-cyclohexyldicarboxylic chloride (0.53 g, 2.2 mmol) in dry CH_2Cl_2. After stirring for 8 h the content of the flask was diluted with CH_2Cl_2 and washed consecutively with 10% aqueous citric acid and saturated $NaHCO_3$. The organic phase was separated and evaporated to dryness then chromatographed by ($CHCl_3$, MeOH 9:1) to extract the oligiomers **11** (0.19 g, 30%, R_f = 0.68) and **12** (0.21 g, 18%, R_f = 0.41).

6.4.6.1. Characterization of Compound 11

m.p. 146-151 °C; UV-vis (CH_3CN; λ in nm (ε in $Lmol^{-1}cm^{-1}$)): 448 (626); FT-IR (KBr, υ_{max}/cm^{-1}): 3267 (b, m, N-H), 3089, 2950, 1696, 1542. ^{1}H-NMR DMSO-*d*$_6$, (δ in ppm): 9.26 (2H, COOH), 7.78 (2H, s, NH, NHCO), 4.64 (4H, overlapping, Fc), 4.38 (4H, overlapping, Fc), 4.17 (4H, overlapping, Fc), 3.99 (4H, overlapping, Fc), 2.17 (2 H, m, cyclohexane), 1.80 (4H, m, cyclohexane), 1.34 (4H, m, cyclohexane); ^{13}C{^{1}H}-NMR DMSO-*d*$_6$, (δ in ppm): 203.7 COOH, 175.5 (CONH), 99.9, 73.8, 73.6, 71.2, 71.1, 70.9, 66.1, 65.9, 61.9 (Fc), 44.3, 34.3, 39.6, 28.8, 25.5, 21.1 (cyclohexane); TOF-MS (m/z): calc for $C_{44}H_{52}N_4O_8Fe_2$ $[M]^+$: 876.2478; found: 876.2516.

6.4.6.2. Characterization of Compound 12

m.p. 173-179 °C; UV-vis (CH_3CN; λ in nm (ε in $Lmol^{-1}cm^{-1}$)): 448 (626); FT-IR (KBr, υ_{max}/cm^{-1}): 3274 (b, m, N-H), 3089, 2950, 1667, 1542. ^{1}H-NMR DMSO-*d*$_6$, (δ in ppm): 9.85 (2H, COOH), 7.94-7.75 (8H, range of NH, NHCO), 5.03-4.00 (32H, overlapping, range of Fc protons), 2.23-1.28 (50H, overlapping, range of Cyclohexane protons). ^{13}C{^{1}H}-NMR DMSO-*d*$_6$, (δ in ppm): 203.6 COOH, 175.4, 175.1, 174.7 (CONH), 99.9, 73.8, 73.6, 72.6, 71.2, 71.2, 71.0, 69.3, 66.1, 65.9, 61.9 (Fc), 49.2, 44.3, 39.6, 34.3, 28.8, 25.6, 24.8, 21.1 (cyclohexane); TOF-MS (m/z): calc for $C_{98}H_{112}N_{10}O_{14}Fe_5$ $[M]^+$: 1700.4227; found: 1700.4231.

6.4.7. Preparation of 1, n'-bis(Lys(Boc)-OMe)Ferrocene (14)

H-Lys(Boc)-OMe·HCl (4.00 g, 13.5 mmol) was dissolved in CH_2Cl_2 (20 mL) and cooled in an ice path prior to the dropwise addition of Et_3N (15.0 mmol). The mixture was added to a stirred solution of Fc-1,1'-dicarbonyl chloride **13** (2.00 g, 6.43 mmol) in CH_2Cl_2 (30 mL) and left to stir for two hours. The reaction completion was checked by TLC. The crude product was purified by flash column chromatography (SiO_2, 1:2 EtOAc-hexane) and recrystallized from $CHCl_3$ to yield yellow crystalline compound (4.49 g, 92%). m. p. 112-117 °C; UV-vis (CH_3CN; λ in nm (ε in $Lmol^{-1}cm^{-1}$)): 449 (719); FT-IR (KBr, υ_{max}/cm^{-1}): 3378, 3260 (b, m, N-H), 2971, 2932, 2637, 2557, 1703, 1634, 1545; ^{1}H-NMR $CDCl_3$, (δ in ppm): 8.10 (1H, d, *J* = 7.3 Hz, Lys α NH), 6.79 (1H, m, Lys εNH), 4.87 (1H, s, Fc-H), 4.81 (1H, s, Fc-H), 4.41 (1H, s, Fc-H), 4.36 (1H, s, Fc-H), 4.32 (1H, m, Lys α CH), 3.66 (3H, s, $COOCH_3$, 2.92 (2H, m, Lys CH_2), 1.76 (2H, m, Lys CH_2), 1.40 (4H, m, Lys CH_2), 1.34 (9H, s, Lys NHBoc); $^{13}C\{^1H\}$-NMR $CDCl_3$, (δ in ppm): 175.5, 174.3, 156.4, 100.0, 72.0, 71.5, 70.8, 70.0, 69.9, 66.9, 66.2, 65.9, 63.3, 62.8, 52.9, 52.5, 33.4, 30.0, 29.7, 28.8, 25.7, 14.2; TOF-MS (m/z): calc for $C_{36}H_{54}N_4O_{10}Fe$ $[M]^+$: 758.3184; found: 758.3210.

6.4.8. Reaction of Compound 14 and Ferrocenediacid Chloride

After Boc deprotection of 1,1'-bis(Lys(Boc)-OMe)ferrocene by TFA/CH_2Cl_2 the product was reacted with ferrocene 1,1'-dicarboxilic acid chloride in equimolar quantities with stirring in dry CH_2Cl_2 for two hours. The polymeric product which precipitated was filtered off. Successive washings with methanol then acetone produced the polymeric compound **15** (0.26 g). m.p. 235-238 °C; UV-vis (CH_3CN; λ in nm (ε in $Lmol^{-1}cm^{-1}$)): 449 (629); FT-IR (KBr, υ_{max}/cm^{-1}): 3127-2864 (b, m, N-H), 2650, 2567,

1717, 1636, 1543; ^{1}H-NMR D_2O, (δ in ppm): 4.90-4.53 (overlapping, Fc), 4.52-4.37 (overlapping, Lys α CH), 4.3 (overlapping, Fc), 3.69 (s, $COOCH_3$ groups), 3.37, 3.23, 2.80, 1.86, 1.72, 1.60, 1.37 (Lys CH_2's); $^{13}C\{^{1}H\}$-NMR $CDCl_3$, (δ in ppm): 174.6, 173.1, 99.9, 74.6, 71.2, 70.2, 69.9, 53.0, 52.7, 47.1, 39.1, 29.6, 26.2, 22.4, 18.3; DLS: average Mw = 7.94 x 10^4.

6.4.9. Electrochemical Measurements

The electrochemical measurements were performed using a CHI 660B electrochemical analyzer (CH Instruments, Inc., Austin, Texas). A conventional three electrodes system consisting of glassy carbon disk working electrode (φ = 3 mm, geometrical area = 0.071 cm^2), a platinum wire counter electrode, and Ag/AgCl (3M KCl) reference electrode were used. The experiments were carried out with a 1 mM solution sample in dry CH_3CN containing 0.1 M tetrabutylammonium perchlorate (TBAP) as supporting electrolyte. All measurements were carried out at room temperature. The working electrode surface was hand-polished to a mirror finish with 0.05 μm Al_2O_3 before it was used and was cleaned after each run. Polymer **10** coated electrode was prepared by the pipetting of methanolic solution of the polymer onto glassy carbon disk electrode. The solvent was allowed to evaporate at room temperature to form the film electrodes.

6.4. References

[1] I. Manners, *Pure Appl. Chem.* **1999**, *71*, 1471-1476.

[2] B. Alonso, B. Gonzalez, B. Garcia, E. Ramirez-Oliva, M. Zamora, C. M. Casado, I. Cuadrado, *J. Organomet. Chem.* **2001**, *637-639*, 642-652.

[3] A. S. Abd-El-Aziz, P. O. Shipman, in *Frontiers in Transition Metal-Containing Polymers* (Eds.: A. S. Abd-El-Aziz, I. Manners), John Wiley & Sons, Inc., Hoboken, NJ., **2007**, pp. 45-133.

[4] K. A. Mahmoud, H.-B. Kraatz, in *Frontiers in Transition Metal-Containing Polymers* (Eds.: A. S. Abd-El-Aziz, I. Manners), John Wiley & Sons, Inc., Hoboken, NJ., **2007**, pp. 473-498.

[5] J. P. Launay, Editor, *Molecular Electronics*, Gauthier-Villars, Paris, **1991**.

[6] J. Alvarez, A. E. Kaifer, *Organometallics* **1999**, *18*, 5733-5734.

[7] T. Hirao, M. Kurashina, K. Aramaki, H. Nishihara, *J. Chem. Soc., Dalton Trans.* **1996**, 2929-2933.

[8] A.-C. Ribou, J.-P. Launay, M. L. Sachtleben, H. Li, C. W. Spangler, *Inorg. Chem.* **1996**, *35*, 3735-3740.

[9] T.-Y. Dong, C.-H. Huang, C.-K. Chang, H.-C. Hsieh, S.-M. Peng, G.-H. Lee, *Organometallics* **1995**, *14*, 1776-1785.

[10] R. Rulkens, A. J. Lough, I. Manners, *J. Am. Chem. Soc.* **1994**, *116*, 797-798.

[11] G. E. Southard, M. D. Curtis, *Organometallics* **1997**, *16*, 5618-5620.

[12] G. E. Southard, M. D. Curtis, *Organometallics* **2001**, *20*, 508-522.

[13] G. M. Brown, T. J. Meyer, D. O. Cowan, C. LeVanda, F. Kaufman, P. V. Roling, M. D. Rausch, *Inorg. Chem.* **1975**, *14*, 506-511.

[14] M. Sato, S. Tanaka, K. Kaeriyama, *J. Chem. Soc., Chem. Commun.* **1986**, 873-874.

[15] T. Shimura, H. Funaki, H. Nishihara, K. Aramaki, T. Ohsawa, K. Yoshino, , *Chem. Lett.* **1992**, *457-460*.

[16] D. A. Foucher, B.-Z. Tang, I. Manners, *J. Am. Chem. Soc.* **1992**, *114*, 6246-6248.

[17] C. M. Casado, M. Moran, J. Losada, I. Cuadrado, *Inorg. Chem.* **1995**, *34*, 1668-1680.

[18] M. Cazacu, A. Vlad, M. Marcu, C. Racles, A. Airinei, G. Munteanu, *Macromolecules* **2006**, *39*, 3786-3793.

[19] D. Chao, X. Lu, J. Chen, X. Liu, W. Zhang, Y. Wei, *Polymer* **2006**, *47*, 2643-2648.

[20] P. A. Deck, M. J. Lane, J. L. Montgomery, C. Slebodnick, F. R. Fronczek, *Organometallics* **2000**, *19*, 1013-1024.

[21] W. Gary Hollis, Jr., T. F. Bonsall, V. L. Cuba, P. A. Deck, F. R. Fronczek, *Transition Met. Chem.* **2006**, *31*, 246-249.

[22] C. B. Hollandsworth, W. G. Hollis, Jr., C. Slebodnick, P. A. Deck, *Organometallics* **1999**, *18*, 3610-3614.

[23] K. A. Mahmoud, H. B. Kraatz, *J. Inorg. Organomet. Polym.* **2006**, *16*, 201-210.

[24] E. E. Bunel, P. Campos, J. Ruz, L. Valle, I. Chadwick, M. S. Ana, G. Gonzalez, J. M. Manriquez, *Organometallics* **1988**, *7*, 474-476.

[25] K. Ma, F. F. d. Biani, M. Bolte, P. Zanello, M. Wagner, *Organometallics* **2002**, *21*, 3979-3989.
[26] S. I. Kirin, H. B. Kraatz, N. Metzler-Nolte, *Chem. Soc. Rev.* **2006**, *35*, 348-354.
[27] R. Jain, H. Choi, C. A. Lalancette, J. B. Sheridan, *Organometallics* **2005**, *24*, 1468-1476.
[28] N. J. Long, A. J. Martin, R. Vilar, A. J. P. White, D. J. Williams, M. Younus, *Organometallics* **1999**, *18*, 4261-4269.
[29] S. S. Zhu, P. J. Carroll, T. M. Swager, *J. Am. Chem. Soc.* **1996**, *118*, 8713-8714.
[30] R. Pyati, R. W. Murray, *J. Phys. Chem.* **1994**, *98*, 11129-11135.
[31] M. T. Nguyen, A. F. Diaz, V. V. Dememnt'ev, K. H. Paennl, *Chem. Mater.* **1994**, *6*, 952-954.
[32] H.-z. Bu, A. M. English, S. R. Mikkelsen, *J.Phys. Chem. B* **1997**, *101*, 9593-9599.
[33] H. Nishihara, Y. Shimano, K. Aramaki, *J. Phys. Chem.* **1987**, *91*, 2918-2921.
[34] C. R. Martin, I. Rubinstein, A. J. Bard, *J. Am. Chem. Soc.* **1982**, *104*, 4817-4824.
[35] P. Daum, J. R. Lenhard, D. Rolison, R. W. Murray, *J. Am. Chem. Soc.* **1980**, *102*, 4649-4653.
[36] S. Chowdhury, K. A. Mahmoud, G. Schatte, H.-B. Kraatz, *Org. Biomol. Chem.* **2005**, *3*, 3018-3023.

CHAPTER 7

GENERAL CONCLUSION

In my present research, I reached my objective of exploring the preparative and structural properties of Fc-peptide conjugates and I successfully explored their applications as biosensors and as polymeric materials. Five scientific questions followed by three major goals listed at the beginning of my research journey were addressed.

7.1. Ferrocene-Peptide Conjugates

Peptide-derived bioconjugates are well recognized potential ligands as part of biomolecular recognition systems for probing of biological processes.[1, 2] These systems are also of a more fundamental interest for the construction of well-defined scaffolds. Fc-peptide conjugates occupy a special position in that they allow for additional control over the structural properties by choosing the appropriate organometallic group. Disubstituted Fc systems, in which both cyclopentadienyl rings are substituted, provide control over the supramolecular structure of the assemblies by controlling the Cp-twist, as well as providing a starting point for the design of electronic biomaterials.[3] This has been demonstrated in the literature and work by Kraatz, Hirao and others have utilized Fc as reliable organometallic scaffolds for constructing self-assembled structures, via intramolecular H-bonding, in which the interaction of the conjugated peptide strands are regulated in appropriate dimension.[4-10] Recently, the artificial amino acid 1'-amino-ferrocene-1-carboxylic acid (Fca) was recognized as a

useful tool in bioorganometallic chemistry. A series of peptides incorporating Fca have been synthesized by using solution phase methods. Initial investigations show that Fca imposes specific secondary-structural elements onto the peptide.[11-13]

I was successful in applying amide-coupling methods to investigate the capability of Fca to conjugate with amino acids and peptides. In Chapter 2, I was able to synthesize and fully characterize a new active ester benzotriazol-1-yl 1-(*tert*-butyloxycarbonylamino) ferrocene-1-carboxylate**,** which is a key intermediate in the coupling of Fca to amino acids and peptides.[14] During the synthesis, I was able to discover a transformation of this active ester into inactive N-oxide derivative, 3-{[1-(*tert*-butyloxycarbonylamino)ferrocen-1-yl]carbonyl}-benzotriazole 1-oxide. Given the importance of Fc-OBt active ester intermediates in the preparation of Fc-bioconjugates and as potential intermediate for the stepwise synthesis of ferrocenamide-based polymers, our finding is significant. Importantly, N-oxide side product is "non-productive" resulting in the loss of the organometallic label.[14]

The next step in my investigation was to properly address the initial investigations by Rapić and Metzler-Nolte who proposed that Fca can induce the formation of a peptide turn,[12] and demonstrate the ability of Fca to impose specific secondary structural elements onto peptides. Thus, Fca was incorporated into oligo-peptides with D- and L-amino acid residues attached to the carboxy and amino terminals of Fca.

In a collaborative study with Rapić and Metzler-Nolte groups, I demonstrated that Fca invariably induces a turn-like structure, which is stable in solution and the solid state.[13] The axial chirality of the Fca group was readily evaluated by CD spectroscopy.

Our result showed different behaviour for Fca peptides depending on the chirality and position of the attached amino acid. The axial chirality of the Fca is completely dependent on the chirality of the first amino acid attached to the amino terminal of the Fca group. Thus, my systematic work described in Chapter 3 lays a solid foundation for the rational design of such unique Fc peptides.[13]

7.2. Applications in Biosensors

In addition to the important consequences of utilizing ferrocene as an organometallic scaffold for building well organized supramolecular structures, this molecule was widely exploited as part of molecular recognition systems because of its reversible redox properties. Fc-peptide conjugates combine the ability of Fc to mediate electron transfer with the molecular recognition potentials of peptides. However, labelling the peptide recognition site in an electrochemical biosensor was potentially problematic since it may interfere with the biomolecular recognition processes.

In an attempt to approach this problem, I was successful in attaching a peptide recognition sequences to a redox probe and exploit the resulting conjugates for the electrochemical detection of papain. The idea was to place a surface-bound redox probe in close proximity to the electrode surface. Diffusive processes will not affect the redox signal. Furthermore, the interaction between the recognition sequence and electrode surface will not be hindered by the interaction with the target protein. In addition, the redox-active Fca label will be part of the recognition site but will not interfere with the recognition process.

In my work, three thiol modified Fca-peptide conjugates Thc-Fca-Gly-Gly-Tyr(Bzl)-Arg(NO_2)-OH, Thc-Fca-Gly-Gly-Arg(Mtr)-Tyr-OH and Thc-Fca-Gly-Gly-Arg-Tyr-OH were synthesized and full characterized.[15] The three peptide sequences were specifically chosen as potential inhibitors for papain.[16-18]

The work described in Chapter 4 clearly shows the utility of this approach, and the system was able to detect papain at low concentrations with good selectivity for the target analyte.

My work represents a truly important proof of concept for establishing this novel bioorganometallic approach for the electrochemical detection of important biological targets. My sensor provides an attractive alternative for the electrochemical detection of non-labelled non-redox active proteins, which under current detection schemes remains a significant challenge.[15]

7.3. Application in Material Science

The idea of incorporating organometallic moieties into polymer structures has been under investigation for almost 50 years. However, in many cases, these polymers are sparingly soluble, which limits their characterization.[10] Pioneering work by Manners allowed for exploiting the ring strain in silaferrocenophanes to develop high molecular weight Fc-backbone polymers by ring-opening metathesis.[10-12] Despite these pioneering efforts by different excellent research groups, oligomers and polymers that have peptide-like characteristics and possess a Fc in their backbone were not known up to date.

The major problem in this research is the difficulty to obtain suitable building blocks. For example, peptide-like organometallic polymers can be obtained by facial

condensation of two active building blocks such as 1,1'-ferrocene dicarboxylic acid chloride $Fc[COCl]_2$ and 1, 1'-ferrocene diamine $Fc[NH_2]_2$. Although $Fc[COCl]_2$ is widely available little efforts have been made to synthesize $Fc[NH_2]_2$.[19-21] None of the existing methods to synthesize $Fc[NH_2]_2$ appeared attractive because of poor overall yield and inconvenient reaction conditions. Furthermore, the explosive nature of diazoferocenes intermediate and the instability of the product were of major challenge.[22]

Having this in mind, I was able recently to develop a very convenient method to synthesize 1,1'-bis(*tert*-butoxycarbonylamino)ferrocene as a stable derivative of $Fc[NH_2]_2$. This new synthetic approach has circumvented the problems encountered with the explosive diazide.[23] The material is stable in solution and in the solid state and does not decompose in solution even after several months.

Building on this successful achievement, I tested the ability of 1,1'-bis(*tert*-butoxycarbonylamino)ferrocene, after acid deprotection of Boc groups, to undergo facial condensation reaction with $Fc[COCl]_2$. This approach was met with success and a series of novel ferrocene-oligomers and polyferrocenyl peptide were obtained.[24]

Preliminary measurements on the polymeric materials indicate a globular structure in aqueous solution. Surprisingly, the electrochemical investigation on these oligomers and polymers showed no evidence of electronic communication between the neighbouring iron centres. Our results are in sharp contrast to results obtained in other oligmeric systems in which separate oxidation waves were observed in the triferrocenes, indicating significant electronic communication.[25, 26]

This unexpected observation inspired me to expand on this study in Chapter 6 and explore the effect of incorporating different linkers having different electronic environments, such as phenylene, cyclohexylene and lysyl groups on the electronic properties of their oligomers and polymers.

Several investigations of Fc-oligomers showed that the linkers between Fc units modulate the interaction between the iron centers by changing the Fc-Fc distances and by tuning through-bond orbital conjugation.[27-31] It was expected that a phenylene spacer enhances the Fc to Fc communication via strong conjugation system.[32, 33] On the other hand a cyclohexyl spacer should give the polymer more flexibility but should reduce the interaction between the Fc groups. In addition, a lysyl spacer may not allow any interactions between the Fc groups. All three systems are linked to the Fc centers via an internal polar amide group which should play a crucial role in influencing the properties of these systems.[34]

More surprisingly, the electrochemical results described in Chapter 6 again suggested unresolved or no interaction between the ferrocene groups in all systems. Only the phenylene polymer displayed some weak electronic interactions. However, it was not possible to evaluate the magnitude of the electronic interactions since the redox peaks are unresolved. These results reveal the influence of the amide groups to suppress the electronic interaction between the iron centers in our polymer.

7.4. Final Remarks and Future Directions

Overall, in my research, I contributed to three major scientific fields: structural design of Fc-peptide conjugates, electrochemical biosensors, and organometallic materials. First, I was successful in demonstrating that Fca is a turn inducer and discovered the ability of this artificial amino acid to impose specific secondary structural elements on peptides. These studies should expand to larger molecules in order to understand naturally occurring biochemical processes such as protein folding. Studies on our novel systems may give important results with relevance to naturally occurring systems.

Second, my efforts for developing a novel biorganometallic-based sensor for proteins have met with a great success. After optimizing the sensor platform and expanding our studies to improve the selectivity, a reliable and cheap electrochemical sensor for proteins could be developed. This may include the multiplexed detection of a series of proteins, making this valuable detection platform for clinical applications.

Finally, my approach of obtaining oligomeric and polymeric ferrocenyl-peptides has met with success. At this point, the electronic properties of these materials are not promising. The next step is to investigate and understand the structure of these polymers in order gain control over their electronic properties. With patient, advanced synthesis and characterization of these materials will open the door for practical and commercially valuable applications.

7.5. References

[1] F. Noor, A. Wuestholz, R. Kinscherf, N. Metzler-Nolte, *Angew. Chem. Int. Ed.* **2005**, *44*, 2429-2432.

[2] J. T. Chantson, M. V. V. Falzacappa, S. Crovella, N. Metzler-Nolte, *J. Organomet. Chem.* **2005**, *690*, 4564-4572.

[3] H.-B. Kraatz, *J. Inorg. Organomet. Polym.* **2005**, *15*, 83-106.

[4] A. Nomoto, T. Moriuchi, S. Yamazaki, A. Ogawa, T. Hirao, *Chem. Commun.* **1998**, 1963-1964.

[5] T. Moriuchi, A. Nomoto, K. Yoshida, A. Ogawa, T. Hirao, *J. Am. Chem. Soc.* **2001**, *123* 68 -75.

[6] T. Moriuchi, A. Nomoto, K. Yoshida, T. Hirao, *J. Organomet. Chem.* **1999**, *589*, 50-58.

[7] R. S. Herrick, R. M. Jarret, T. P. Curran, D. R. Dragoli, M. B. Flaherty, S. E. Lindyberg, R. A. Slate, L. C. Thornton, *Tetrahedron Lett.* **1996**, *37*, 5289-5292.

[8] S. Chowdhury, G. Schatte, H.-B. Kraatz, *Dalton Trans.* **2004**, 1726-1730.

[9] S. Chowdhury, D. A. R. Sanders, G. Schatte, H.-B. Kraatz, *Angew. Chem. Int. Ed.* **2006**, *45*, 751-754.

[10] F. E. Appoh, T. C. Sutherland, H.-B. Kraatz, *J. Organomet. Chem.* **2004**, *689*, 4669-4677.

[11] L. Barišić, V. Rapić, N. Metzler-Nolte, *Eur. J. Inorg. Chem.* **2006**, 4019-4021.

[12] L. Barišić, M. Dropucic, V. Rapić, H. Pritzkow, I. Kirin Srecko, N. Metzler-Nolte, *Chem. Commun.* **2004**, 2004-2005.

[13] L. Barišić, M. Čakić, K. A. Mahmoud, Y. N. Liu, H. B. Kraatz, H. Pritzkow, S. I. Kirin, N. Metzler-Nolte, V. Rapić, *Chem. Eur. J.* **2006**, 4965-4980.

[14] K. A. Mahmoud, Y.-T. Long, G. Schatte, H.-B. Kraatz, *Eur. J. Inorg. Chem.* **2005**, 173-180.

[15] K. A. Mahmoud, H.-B. Kraatz, *Chem. Eur. J.* **2007**, *13,* 5885-5895.

[16] S. Blumberg, I. Schechte, A. Berger, *Eur. J. Biochem.* **1970**, *15*, 97-102.

[17] M. O. Funk, Y. Nakagawa, J. Skochdopole, E. T. Kaiser, *Int. J. Pept. Protein Res.* **1979**, *13*, 296-303.

[18] K. Plumb, H. B. Kraatz, *Bioconj. Chem.* **2003**, *14*, 601-606.

[19] E. M. Acton, R. M. Silverstein, *J. Org. Chem.* **1959**, *24*, 1487-1490.

[20] W. E. Parham, V. J. Traynelis, *J. Am. Chem. Soc.* **1955**, *77*, 68-70.

[21] F. S. Arimoto, A. C. Haven, *J. Am. Chem. Soc.* **1955**, *77*, 6295-6297.

[22] A. Shafir, M. P. Power, G. D. Whitener, J. Arnold, *Organometallics* **2000**, *19*, 3978 -3982.

[23] S. Chowdhury, K. A. Mahmoud, G. Schatte, H.-B. Kraatz, *Org. Biomol. Chem.* **2005**, *3*, 3018-3023.

[24] K. A. Mahmoud, H. B. Kraatz, *J. Inorg. Organomet. Polym.* **2006**, *16*, 201-210.

[25] G. E. Southard, M. D. Curtis, *organometallics* **2001**, *20*, 508-522.

[26] G. E. Southard, M. D. Curtis, *Organometallics* **1997**, *16*, 5618-5620

[27] J. Alvarez, A. E. Kaifer, *Organometallics* **1999**, *18*, 5733-5734.

[28] T. Hirao, M. Kurashina, K. Aramaki, H. Nishihara, *J. Chem. Soc., Dalton Trans.* **1996**, 2929-2933.

[29] A.-C. Ribou, J.-P. Launay, M. L. Sachtleben, H. Li, C. W. Spangler, *Inorg. Chem.* **1996**, *35*, 3735-3740.
[30] T.-Y. Dong, C.-H. Huang, C.-K. Chang, H.-C. Hsieh, S.-M. Peng, G.-H. Lee, *Organometallics* **1995**, *14*, 1776-1785.
[31] R. Rulkens, A. J. Lough, I. Manners, *J. Am. Chem. Soc.* **1994**, *116*, 797-798.
[32] E. E. Bunel, P. Campos, J. Ruz, L. Valle, I. Chadwick, M. S. Ana, G. Gonzalez, J. M. Manriquez, *Organometallics* **1988**, *7*, 474.
[33] K. Ma, F. F. d. Biani, M. Bolte, P. Zanello, M. Wagner, *Organometallics* **2002**, *21*, 3979-3989.
[34] M. Cazacu, A. Vlad, M. Marcu, C. Racles, A. Airinei, G. Munteanu, *Macromolecules* **2006**, *39*, 3786-3793.

APPENDIXES

A. Copyright Permissions from the Journals publishers

A.1. Wiely-VCH

Date: Thu, 24 May 2007 08:40:29 +0200
From: VCH-RIGHTS-and-LICENCES <RIGHTS-and-LICENCES@wiley-vch.de>
To: khaled.mahmoud@usask.ca
Subject: Antwort: permission request

This message was written in a character set other than your own. If it is not displayed correctly, click here to open it in a new window.

Dear Khaled,

Thank you for your email.

We hereby grant permission for the requested use expected that due credit is given to the original source.

With kind regards

Bettina Loycke
****
Bettina Loycke
Copyright & Licensing Manager
Wiley-VCH Verlag GmbH & Co. KGaA
Boschstr. 12
69469 Weinheim
Germany

Phone: +49 (0) 62 01- 606 - 280
Fax: +49 (0) 62 01 - 606 - 332
Email: rights@wiley-vch.de

Wiley Bicentennial: Knowledge for Generations 1807-2007

Wiley-VCH Verlag GmbH & Co. KGaA
Location of the Company: Weinheim, Germany ; Chairman of the Supervisory

Board: John Herbert Jarvis; Trade Register: Mannheim, Abt. B, Nr. 2833 W;General Partner: John Wiley & Sons GmbH, Location: Weinheim; District Court Mannheim,

Abt. B, Nr. 2296 W; Managing Directors: Jim Dicks, William Pesce

Khaled Mahmoud <kha347@mail.usask.ca> An rights@wiley-vch.de 24.05.2007 00:34 Kopie The Bitte antworten permission request an khaled.mahmoud@usask.ca

Dear Wiley-VHS,

I am writing to request for a permission to reproduce all or some of my publication materials (including verbatim text, figures, and drowning)into my PhD thesis. All requested publications have been co-authored by me. The publications will appear in my thesis as the submitted manuscript and will refer to the published paper.

List of publications that need permission to be reproduced in my PhD thesis

1- Mahmoud, K. A.; Kraatz, H.-B. Bioorganometallic Approach for the Electrochemical Detection of Proteins: A Study on the interaction of Ferrocene-Peptide Conjugates with Papain in Solution and on Au Surfaces", /Chem. Eur. J./ 2007, /DOI: 10.1002/chem.200601878, early view.

2-Barisic', L.; Cakic', M.; Mahmoud, K. A.; Liu, Y. N.; Kraatz,H.-B.; Pritzkow, H.; Kirin, S. I.; Metzler-Nolte, N.; Rapic', V., "Helically chiral ferrocene peptides containing 1'-aminoferrocene-1-carboxylic acid subunits as turn inducers", /Chem. Eur. J./ 2006, 12, 4965-4980.

3- Mahmoud, K. A.; Long, Y.-T.; Schatte, G.; Kraatz, H.-B., "Rearrangement of the active ester intermediate during HOBt/EDC amide coupling"/Eur. J. Inorg. Chem., 2005, 173-180.

Sincerely, Khaled

****
Khaled A. Mahmoud
Chemistry Department, Saskatchewan University
110-Science Place, Saskatoon, SK, S7N 5C9
CANADA
PHONE:(+1)306-966-4712 FAX:(+1)306-966-4730
****

A.2. Springer

Date:	Fri, 15 Jun 2007 10:05:20 +0200
From:	"Permissions Heidelberg, Springer DE" <Permissions.Heidelberg@springer.com>
To:	"Khaled A. Mahmoud" <khaled.mahmoud@usask.ca>
Subject:	Khaled A. Mahmoud (->CCC)

Dear Dr. Mahmoud,

Springer is pleased to grant permission for requested journal titles to be republished in doctoral thesis.

For further questions about using our service, please contact Customer Support via phone 877/622-5543(toll free)or 978/777-9929, or email customercare@copyright.com

Sincerely,
Rights Permissions
Springer Heidelberg
Tiergartenstrasse 17
69121 Heidelberg e-mail: Permissions.Heidelberg@Springer.com

-----Ursprüngliche Nachricht-----
Von: Khaled A. Mahmoud [mailto:khaled.mahmoud@usask.ca]
Gesendet: Donnerstag, 14. Juni 2007 19:22
An: Permissions Europe/NL; Permissions Heidelberg, Springer DE Betreff: permission rquest

Dear Springer,
I am writing to request a permission to reproduce one of my publication material in one of your journals <journal of inorganic and organometallic polymers and materials> to use it in my my PhD thesis The published paper is co-authored by me.I may wanna reproduce the whole document verbatim including figures and drownings

The article is: ***Mahmoud, K. A.*; Kraatz, H.-B., "Synthesis and Electrochemical Investigation of Oligomeric Ferrocene Amides: Towards Ferrocene Polyamides", /J Inorg. Organomet.Polym.*2006*, 16, 201-210.**
Best Regards,
Khaled
****
Khaled A. Mahmoud
Chemistry Department, Saskatchewan University 110-Science Place, Saskatoon, SK, S7N 5C9 CANADA
PHONE:(+1)306-966-1636 FAX:(+1)306-966-4730
****

B. Permission of Co-Author

PERMISSION OF CO-AUTHOR

We, the undersigned, hereby grant permission to reproduce any material designated as being coauthored by us in the thesis copyrighted to the person named below:

Khaled A Mahmoud

Name of copyrighted author **Signature of copyrighted author**

Names of co-authors: **Signatures of co-authors:**

Heinz-Bernhard Kraatz

Yi-Tao Long

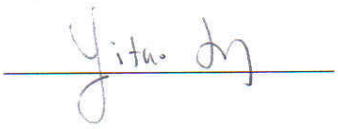

Gabriele Schatte

DATE: May 24, 2007